Targeting myeloid-restricted microRNAs to induce a pro-reparative macrophage phenotype and mucosal healing in the intestine

A thesis submitted to Maynooth University for the degree of Doctor of Philosophy

Caoimhe Cadden, B.A. (Mod.)

Biology Department

January 2026

Supervisor: Dr. Eóin N. McNamee

Head of Department: Prof. Paul Moynagh

TABLE OF CONTENTS

LIST OF FIGURES

LIST OF TABLES

DECLARATION

I have read and understood the Departmental policy on plagiarism.

I declare that this thesis is my own work and has not been submitted in any form for another degree or diploma at any university or other institution of tertiary education.

Information derived from the published or unpublished work of others has been acknowledged in the text and a list of references is given.

Signature: 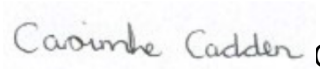 Caoimhe Cadden, B.A. (Mod.)

Date: 30th January 2026

ACKNOWLEDGEMENTS

I feel incredibly lucky to be in a position where there are so many people to thank. Even so, I know that nothing I say can fully capture how grateful I am for everyone who helped me reach the end of this PhD.

First and foremost, I want to thank my supervisor, Dr. Eóin McNamee. You pulled me away from industry (and great money) to the deeply fulfilling world of academia. After first hiring me as a Research Assistant, you proved to be such a great boss that I simply had to commit to a four-year PhD. It has been an absolute pleasure to work with you. You have been consistently supportive and encouraging throughout the years and your advice and mentorship have been invaluable. Thank you for your kindness, your patience, for instilling in me a love of research and for making my PhD such a positive and rewarding experience.

To Prof. Joanne Masterson, I truly could not have chosen a better lab or PI to work alongside. Thank you for all your support and advice – especially for your many questions in joint lab meetings, which have undoubtedly prepared me for the viva. I am also very grateful for the fun you brought to the Gals' nights out, they are a great team building exercise.

To all past members of the MIR and AIRR labs – Lauren, Megan, Gary, Taylor and Gordon. Thank you for making the last four years so enjoyable.

To Dafne, the last PhD student standing in the MIR lab, thank you for your humour, for keeping the MIR lab part of the morning crew and for getting me the duck that now sits on my desk. To Sofia, thank you for your wonderful drawings and your amazing singing in the lab. I am always in awe by your enthusiasm for anything Irish.

To those that have left the reading room but have not left my heart – Sineád and Louise.

Sinead, although you were part of the AIRR lab, you were my first Postdoc, and you set my standards for all future Postdocs impossibly high. Thank you for always being so generous with your help, for never hesitating to share a bottle of wine with me, and for your great laugh, which always let me know that my joke was, in fact, hilarious (you were always laughing).

Louise, the coffee connoisseur, watching your taste for coffee develop was one of my proudest moments. Thank you for your deadly wit, your love of puzzles and riddles, your encyclopaedic knowledge of pop culture, and – most importantly – astrology, which has greatly helped us when sussing out new people and identifying that “the vibes are off because mercury is in retrograde”.

Georgia, you truly are the wellness queen. Thank you for always being so kind, thoughtful, positive, and funny. I will miss hearing “bussssssyyy” echo through the lab or “half day” being shouted when someone leaves before 6 pm. You have been a great person to “lock in” with and have been a ray of sunshine in the lab.

Ciára and Shauna, I don’t know where to start. YISI was the turning point of our friendship. I would not have gotten through this experience without you both.

Ciára, you taught me everything I know. We have been attached at the hip since I joined the MIR lab in 2021. Thank you for your kindness, your support, your patience and your encouragement. Thank you for listening to me rant and for always checking in on me. Even though we are no longer in the same lab – which truly breaks my heart – you are still my first point of call whenever anything happens, and I am so grateful for that.

Shauna, you first joined the AIRR lab as a 4th year undergrad student, and it is crazy to think how our friendship has grown since then. We match each other’s energy and we literally do everything together – work together, drive together, get food together, shop together, gym together, jacuzzi together. You have supported me so much during this PhD, from the late nights in the lab to forcing me to leave my house when I hit a writing block. Thank you for always making me laugh and for being there for me no matter what. You truly are my closest friend.

I am so glad this experience has brought the three of us together. I am so lucky to be able to call you both my best friends.

Now onto those outside my lab circle.

Roisin, thank you so much for your support from our college undergrad days until now. I am so lucky to have met you in Molecular Medicine and to have been able to share these experiences with you.

Niamh, you left for Australia during my PhD, but you came back just in time to support me through the hardest part (clearly just wanted a mention in my acknowledgements). Thank you for surprising me in the lab and making me sob. You have been my best friend for over 20 years and I can't imagine doing any of this without you.

Nanny and Ada, thank you both so much for your endless support and encouragement throughout my life. You have been there for every milestone, big or small. I consider myself incredibly lucky to have you in my life.

Aoife, thank you for always being there for me and for being my biggest supporter. Writing my thesis at home while you studied for your exams, was my favourite part of the writing process. Thank you for always giving me a reason to smile.

Mum, I owe everything I am to you. Thank you for your endless support and encouragement. You have always believed in me, lifted me up when I struggled and celebrated every achievement along the way. I am so grateful for everything you have done to help me get to this point – I couldn't have done it without you.

Prince, the best dog in the world, thank you for never leaving my side and for always providing me comfort.

Michael, you have been my rock (geology reference). From undergrad through to now, you have always been by my side. Thank you for dropping me to the lab on weekends, picking me up late from the lab, for putting up with me when I was stressed and, for attending my oral presentation in Perth, so that there was a

familiar face in the audience. You have done far more than I could ever list here. I could not have asked for a more supportive or caring partner. I hope you get to retire early now!

PUBLICATIONS AND PRESENTATIONS

Publications

- Gallagher, C., MacMahon, J., O'Neill, C., Cassidy, F., Dunbar, H., De Barra, C., Cadden, C. et al. 'Mucosal associated invariant T cells are altered in patients with Hidradenitis Suppurativa and contribute to the inflammatory milieu'. Journal of Investigative Dermatology (2023) 143, 1094 – 1097.

Manuscripts in preparation

- Nguyen, C., Cadden, C. et al. 'CXCR3 blockade limits T cell-driven Paneth cell loss and restores α-defensin expression in experimental Crohn's disease'.
- Cadden, C. et al. '*MiR-223* regulates the cross-talk between macrophages and colonic epithelial cells via STAT3 signalling'.
- Cadden, C. et al. '*MiR-223* regulates the translational control of macrophages through modulation of eIF4E'.

Oral Presentations

- **Australian and New Zealand Society for Immunology (2025)** – Targeting myeloid-restricted microRNAs to induce a pro-reparative macrophage phenotype and mucosal healing in the intestine.
- **All Ireland RNA Club (2024)** – Targeting myeloid-restricted microRNAs to induce a pro-reparative macrophage phenotype and mucosal healing in the intestine.
- **Maynooth University's Biology Annual Research Day (2024)** – Targeting myeloid-restricted microRNAs to induce a pro-reparative macrophage phenotype and mucosal healing in the intestine.
- Ma**ynooth University's Biology Annual Research Day (2023)** – Targeting myeloid-restricted microRNAs to induce a pro-reparative macrophage phenotype and mucosal healing in the intestine.

Poster Presentations

- **Irish Society for Immunology (2025)** – Targeting myeloid-restricted microRNAs to induce a pro-reparative macrophage phenotype and mucosal healing in the intestine.
- **Society for Mucosal Immunology (2024)** – Targeting myeloid-restricted microRNAs to induce a pro-reparative macrophage phenotype and mucosal healing in the intestine.
- **All Ireland RNA Club (2024)** – Targeting myeloid-restricted microRNAs to induce a pro-reparative macrophage phenotype and mucosal healing in the intestine.

ABBREVIATIONS

*223*KD	*miR-223* Knockdown
3′ UTR	3′ untranslated region
5-ASA	5-aminosalicyclic acid
ACK	Ammonium-Chloride-Potassium
AGO	Argonaute
AMPs	Anti-microbial peptides
AOM	Azoxymethane
APS	Ammonium persulfate
BCA	Bicinchoninic acid assay
BM	Bone marrow
BMDM	Bone marrow derived macrophage
BSA	Bovine serum albumin
C/EBP	CCAAT-enhancer-binding proteins
CAC	Colitis-associated colorectal cancer
CD	Crohn’s disease
cDNA	Complementry DNA
cGMP	Cyclic guanosine monophosphate
CRC	Colorectal cancer
DAI	Disease activity index
DNA	Deoxyribonucleic acid
DSS	Dextran sodium sulphate
EDTA	Ethylenediaminetetraacetic acid
FBS	Fetal bovine serum
FFPE	Formalin-fixed and paraffin embedded
GP130	Glycoprotein 130
IBD	Inflammatory bowel diseases
IV	Intravenous
M-CSF	Macrophage colony stimulating factor
Mefc	Myocyte enhancer factor 2C
miRNA	MicroRNA
mRNA	Messenger RNA

NFIA	Nuclear factor 1A
NO	Nitric oxide
NOS	Nitric oxide synthase enzymes
NOS2	Inducible NOS
PBS	Phosphate buffered saline
PCNA	Proliferating cell nuclear antigen
Pre-miRNA	Precursor miRNA
Pri-miRNA	Primary miRNA
RCF	Relative centrifugal force
Rhob	Ras homolog gene family member B
RIPA	Radioimmunoprecipitation assay
RISC	RNA-induced silencing complex
RNA	Ribonucleic acid
RT	Reverse transcription
RT-PCR	Real-time polymerase chain reaction
SDS	Sodium dodecyl sulphate
SDS-PAGE	Sodium dodecyl sulphate polyacrylamide gel electrophoresis
STAT	Signal transducer and activator of transcription
TAMs	Tumour associated macrophage
TEMED	Tetramethylethylenediamine
TME	Tumour microenvironment
TRAF6	TNF receptor-associated Factor 6
TRBP	Trans-activator RNA binding protein
UC	Ulcerative colitis
UNT	Untranslated region
WT	Wild Type

ABSTRACT

Inflammatory bowel diseases (Crohn's Disease and Ulcerative Colitis) are characterised by aberrant myeloid immune activation in the intestine, that damages bowel tissues in genetically susceptible individuals. Globally, approximately 7 million people are currently living with this disease, yet there are few efficacious treatment modalities and no cure. Patients who fail to respond to front-line immunotherapies present with enhanced neutrophil and monocyte inflammatory gene signatures. As such, a dilemma exists in that we cannot block this myeloid arm of the immune response due to the critical need for anti-infection responses and tissue healing. Yet, there are no clear pathways to understand how IBD therapeutics may limit the excessive, tissue destructive inflammation and drive healing processes. To address this challenge, this thesis will focus on understanding myeloid intrinsic control points, namely microRNAs, that have potential to uncover new disease mechanisms and potential therapeutic opportunities.

MicroRNAs (miRNAs) are emerging as important regulators of immunity and are differentially expressed in IBD; however, their mechanistic roles in disease progression remain poorly understood. *MiR-223* is a myeloid-restricted miRNA, and previous research has identified a critical role for *miR-223* in models of infection, colitis and colitis-associated colon cancer. In effect, we propose that *miR-223* can act like a rheostat, shaping the mRNA translator of important inflammation signalling, however we understand little of how this may shape the immune landscape of the inflamed intestine and impact mucosal healing. Functionally, *miR-223* expression was reduced during macrophage differentiation and following activation with inflammatory cytokines or bacterial LPS, coinciding with decreased expression of RISC components and the myeloid transcription factors, C/EBPβ and PU.1. In contrast, supplementation with *miR-223-3p* and *miR-223-5p* mimetics suppressed macrophage inflammatory responses to LPS, reducing expression of pro-inflammatory cytokines and chemokines while promoting a pro-resolving macrophage phenotype.

Using *in situ* hybridization, the dynamic expression of *miR-223* across experimental colitis and recovery was identified. *MiR-223*$^{-/y}$ mice exhibited delayed mucosal healing, increased myeloid infiltration, and disruption of the epithelial stem cell niche. We further mapped the myeloid and macrophage immune compartment along the continuum of inflammation and healing following active colitis, and identified an epithelial stem cell growth differential in *MiR-223*$^{-/y}$ mice. To begin to identify the mechanistic links that *miR-223* can regulate, we showed that STAT3, a key regulator of intestinal regeneration, was hyperactivated in *miR-223*$^{-/y}$ mice following experimentalcolitis. *In vitro* studies using *miR-223KD* macrophages demonstrated regulation of the IL-6 cytokine family and downstream STAT3 signalling. Co-culture experiments with colonic epithelial organoids further revealed that macrophage-derived *miR-223* influences epithelial regeneration via STAT3-dependent pathways.

Collectively, this work identifies *miR-223* as a critical myeloid-derived regulator of intestinal inflammation, epithelial repair, and stem cell niche maintenance.

CHAPTER 1

INTRODUCTION

1.1. Inflammatory bowel disease (IBD)

1.1.1. Ulcerative colitis (UC) and Crohn's disease (CD)

IBD refers to a group of chronic, relapsing inflammatory disorders of the gastrointestinal tract (**Figure 1.1.1.1**), comprising UC and CD (Bai *et al.*, 2024). CD causes transmural inflammation of the intestine, most commonly in the lower part of the small intestine, but can affect any area of the gastrointestinal tract, from the mouth to the anus. Conversely, UC results in inflammation in the mucosal layers of the colon, causing lesions in the large intestine and the rectum (Sairenji, Collins and Evans, 2017). When a definitive diagnosis of UC or CD cannot be established, the condition is classified as indeterminate colitis (Odze, 2015). Symptoms of CD include pain, diarrhoea and fever, whereas UC is associated with blood in stool, intense pain and diarrhoea (Sairenji, Collins and Evans, 2017).

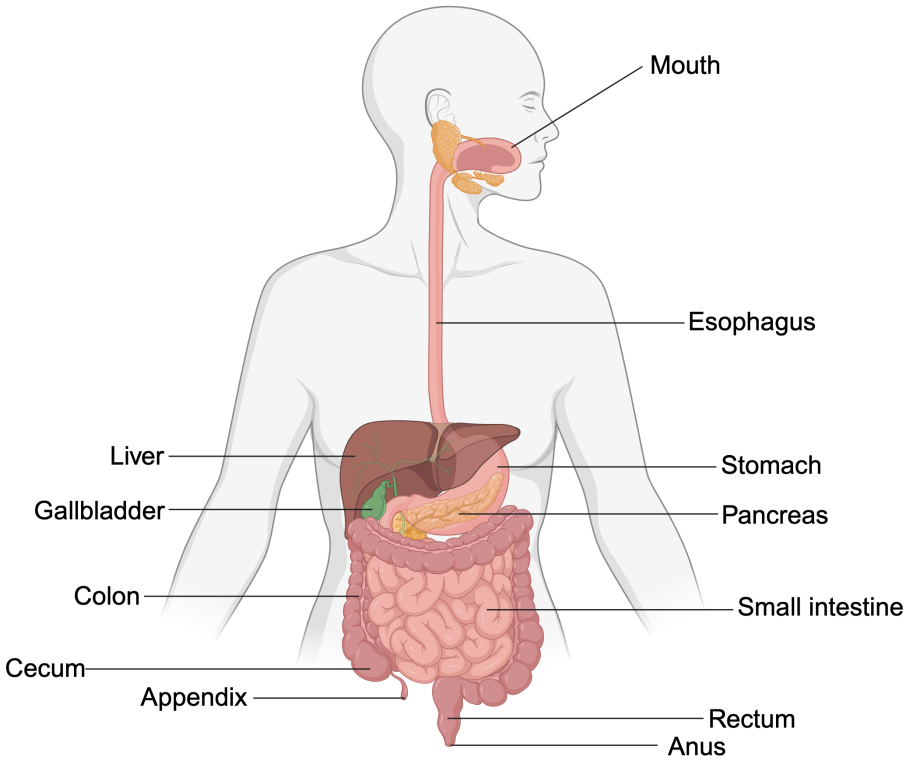

Figure 1.1.1.1. ***Overview of the Gastrointestinal tract.*** The gastrointestinal tract consists of the mouth, esophagus, stomach, liver, pancreas, gallbladder, appendix, small intestine, colon, cecum, rectum, and anus. Adapted from the "Digestive system" on BioRender.com (2026).

1.1.2. Epidemiology of IBD

Initially, during the twentieth century, IBD was considered a disease of early industrialised regions in North America, Europe and Oceania (Kaplan, 2015). However, after the Second World War, the incidence of IBD in early industrialised regions increased rapidly (Molodecky *et al.*, 2012). Evidence suggests that environmental factors linked to Westernization, such as higher smoking rates, Western dietary patterns, and improved hygiene, are thought to contribute to the increasing incidence (Xue *et al.*, 2024; Kaplan and Ng, 2017). During the twenty-first century, IBD incidence stabilized in most early-industrialized regions, except among children, where it continues to rise, whereas prevalence has steadily increased across all age groups (Ng *et al.*, 2017; Kuenzig *et al.*, 2022).

Globally, IBD impacts approximately 7 million individuals, with an annual incidence of 4.97 per 100,000 persons. The highest prevalence of this disease is

observed in North America and Australasia, with an incidence ranging from 350 to 500 cases per 100,000 individuals (**Figure 1.1.2.1**) (Alatab *et al.*, 2020; Vos *et al.*, 2020). In 2019, IBD was responsible for around 41,000 deaths and 1.6 million disability-adjusted life years worldwide (Vos *et al.*, 2020). In Ireland, IBD affects an estimated 40,000 people, with 5.9 new cases of CD and 14.3 new cases of UC per 100,000 persons reported in 2011 (Mallon, Doherty and Burns, 2024). Additionally, between 2009 and 2014, 199 Irish children were diagnosed with early onset IBD (Hussey, 2025).

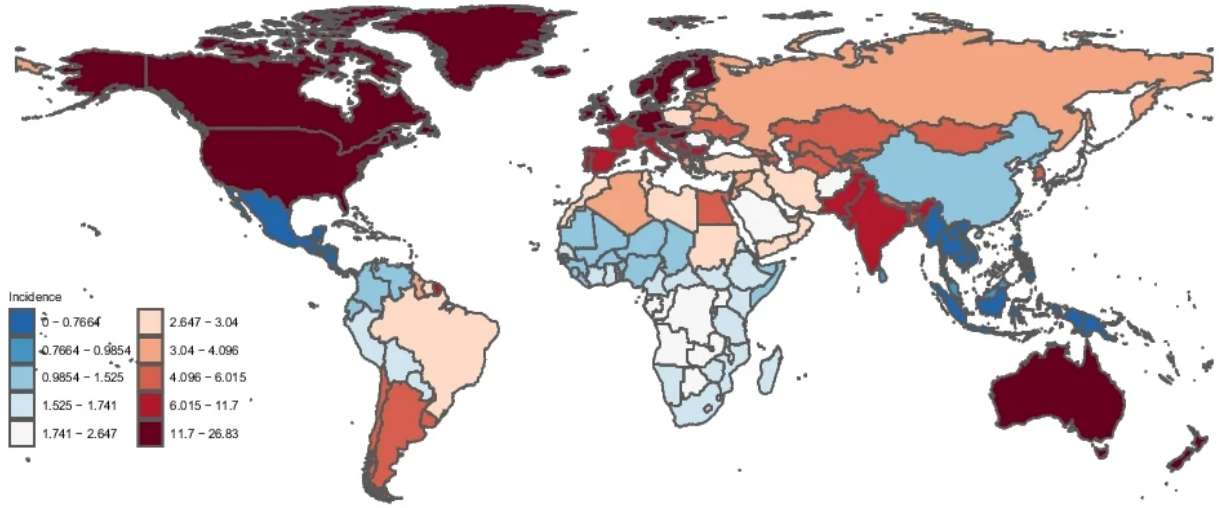

Figure 1.1.2.1. ***Global incidence of IBD.*** The global incidence rate of IBD has been increasing from 1990 to 2021. Figure taken from (Lin et al., 2024).

1.1.3. Aetiology of IBD

IBD is widely acknowledged to have a multifaceted aetiology, with disease initiation and progression influenced by a combination of genetic, environmental and physiological regulatory factors (**Figure 1.1.3.1**) (de Lange *et al.*, 2017; Ng *et al.*, 2013; Yang, Guo and Zou, 2026).

1.1.3.1. Genetic Susceptibility to IBD

Specific genetic variants have been reported to cause immune system dysfunction, thereby contributing to the development of IBD. More than 240 risk loci associated with IBD have been identified, distributed across several key

pathways, including immune regulation, intestinal barrier function, autophagy and cell signalling (Liu *et al.*, 2017; Zhang and Li, 2014). Mutations in the nucleotide-binding oligomerization domain containing 2 (NOD2) gene, were the first genetic variants associated with the onset of CD (Siminovitch, 2006; Rodriguez-Bores *et al.*, 2007). Additionally variants in autophagy-related genes, such as autophagy-related gene-16-like 1 (ATG16L1) affect susceptibility to IBD, particularly in CD (Fuyuno *et al.*, 2016). IBD genetic susceptibility is closely linked to the tissue- and cell type-specific expression of key genes. For example, antimicrobial peptide secretion by Paneth cells is genetically regulated and influenced by the microbiota. Furthermore, loss of the transcription factor EB (TFEB) on the colonic epithelium impairs the antioxidant barrier (Zhou and Zheng, 2023; Zhang *et al.*, 2024). Genetic variation can impact therapeutic outcomes in IBD, with polymorphisms in genes such as interleukin 23 receptor (IL23R) and tumour necrosis factor receptor superfamily member 1A (TNFRSF1A), being associated with responses to anti-tumour necrosis factor (TNF) therapy (Gerich and McGovern, 2014). IBD genetics also vary considerably depending on age of disease onset. Very early-onset IBD is generally monogenic, resulting from a single gene with Mendelian inheritance. In contrast to this, the vast majority of late-onset IBD, occurring in older children through to adulthood, is polygenic in nature (McGovern, Kugathasan and Cho, 2015).

1.1.3.2. Environmental and lifestyle risk factors for IBD

A growing body of evidence indicates that environmental factors such as dietary patterns, lifestyle habit and pollution, influence the risk of IBD onset (Yang, Guo and Zou, 2026). Diet plays a role in IBD development by altering the composition and diversity of intestinal microbiota (David *et al.*, 2014). A high intake of fatty acids and meat were associated with increased risk of UC and CD (Hou, Abraham and El-Serag, 2011; Talebi *et al.*, 2023; Zhao *et al.*, 2022) . Additionally, a Western diet, fast food and ultra-processed foods have been identified as risk factors for IBD (Milajerdi *et al.*, 2021; Zhao *et al.*, 2022; Li *et al.*, 2020; Niewiadomski *et al.*, 2016). Smoking status differentially influences IBD risk. Current smokers have an approximately 2-fold increased risk of developing CD and former smokers are associated with a higher risk of UC in comparison to non-smokers or current smokers (Mahid *et al.*, 2006; Ueno *et al.*, 2014). Residential

exposure to air pollutants has been linked to IBD risk, with nitrogen dioxide exposure in individuals aged 23 years and younger associated with an increased risk of CD, and sulphur dioxide in those aged 25 years or younger associated with a higher risk of UC (Kaplan *et al.*, 2010). With regards to the onset of IBD in infants, breastfeeding has been reported to reduce the risk of developing this disease. This protective effect is attributed to bioactive milk components and maternal microbiota transfer, which collectively support intestinal barrier integrity, microbial diversity and immune homeostasis (Stewart *et al.*, 2018).

1.1.3.3. Impaired regulatory mechanisms in IBD pathogenesis

Pathological manifestations of IBD are attributed to dysfunctions in multiple physiological regulatory systems. At an immunological level, aberrant activation of innate and adaptive immunity, coupled with cytokine network dysregulation, plays a central role in initiating and perpetuating inflammatory responses (Saez *et al.*, 2023; Xu *et al.*, 2014; Silva *et al.*, 2016). At the barrier level, disruption of epithelial barrier integrity, driven by enhanced epithelial cell apoptosis, altered tight junction protein expression and ER stress, compromise the intestinal first line of defence (Hegan *et al.*, 2016; Kim, 2015; Deka *et al.*, 2022). At the microbiological level, altered structure and function of the gut microbiota can trigger and perpetuate inflammation through metabolic and immune-mediated pathways (Sharma *et al.*, 2025; Lavelle and Sokol, 2020; Franzosa *et al.*, 2019; Sultan *et al.*, 2021; Kou *et al.*, 2025). Finally, at an oxidative stress level, reactive oxygen species overproduction and antioxidant imbalance contribute to intestinal mucosal injury and affects immune and barrier functions, creating a vicious cycle that sustains inflammation (Muro *et al.*, 2024; Balmus *et al.*, 2016).

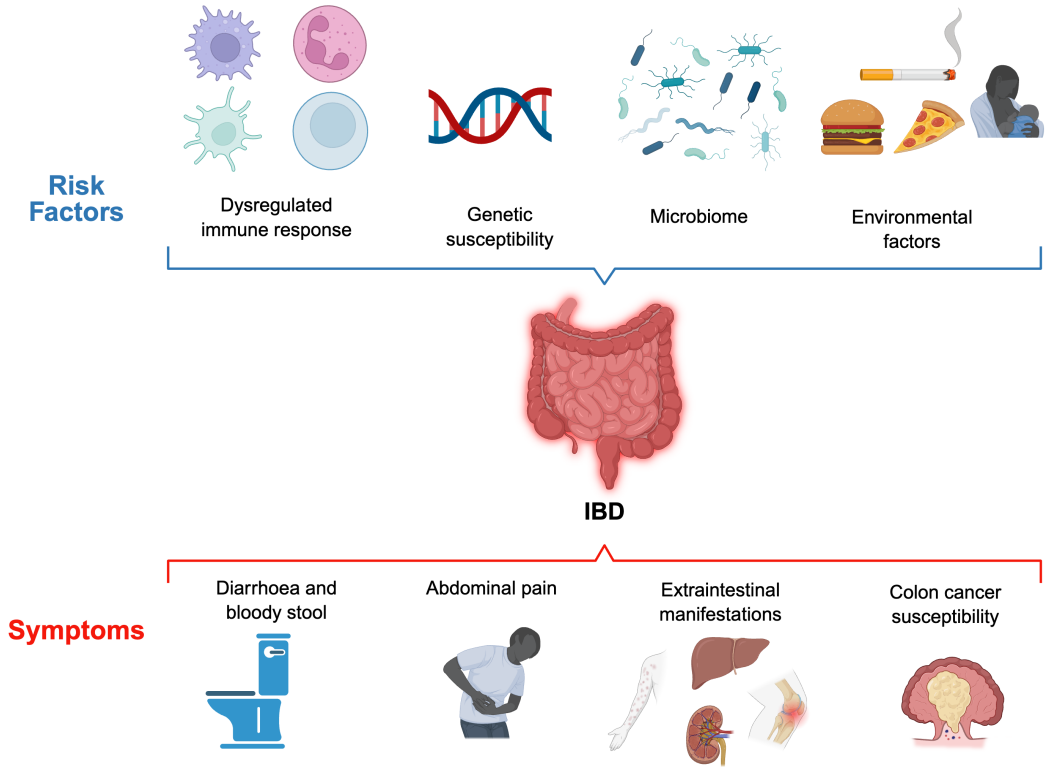

Figure 1.1.3.1. ***Risk factors and clinical manifestations of IBD.*** Initiation and progression of IBD is influenced by a combination of genetic, environmental and physiological regulatory factors. Symptoms of this disease include diarrhoea and bloody stool, abdominal pain, extraintestinal manifestations and colon cancer susceptibility. Created on BioRender.com (2026).

1.1.4. Diagnosis of IBD

IBD exhibits a highly heterogenous clinical presentation. Patients may present with severe symptoms, such as haematochezia, abdominal pain, intestinal obstruction, perforation, or malnutrition. Alternatively, symptoms may be mild and non-specific (Li *et al.*, 2024; Sorrentino, Nguyen and Chitnavis, 2019). The typical presentation of UC includes bloody diarrhoea, with additional symptoms comprising faecal urgency, increased stool frequency, tenesmus and abdominal cramping. Moreover, approximately 30% of UC patients exhibit extraintestinal manifestations, such as arthritis (Ungaro *et al.*, 2017; Vavricka *et al.*, 2011). CD presents variably depending on inflammation location and severity, with abdominal pain, diarrhoea, weight loss and fatigue being common symptoms (Veauthier and Hornecker, 2018). Extraintestinal manifestations are also

observed in CD patients, such as perianal disease, which includes fissures, ulcerations, skin tags and fistulas (Parian *et al.*, 2023).

Endoscopy is a critical diagnostic procedure when IBD is suspected. Ileocolonoscopy and upper endoscopy are employed to assess the location, extent and severity of IBD involvement (Kaz and Venu, 2025; Núñez F *et al.*, 2021). Typical colonic endoscopic features of UC include friable mucosa, ulcerations, erythema, and loss of normal vascular markings (Simpson and Papadakis, 2008). Chronic inflammation can result in loss or distortion of colonic haustra, as well as the formation of strictures, stenoses or inflammatory polyps (**Figure 1.1.4.1**) (Li *et al.*, 2024). In contrast to the continuous mucosal involvement seen in UC, CD typically exhibits segmental, patchy inflammation, referred to as skip lesions. CD ordinarily presents endoscopically with aphthous and serpiginous ulcers and cobblestone-patterned, edematous mucosa (**Figure 1.1.4.2**) (Torres *et al.*, 2017). Mayo endoscopic score (MES) and simple endoscopic score (SES) are scoring systems used by gastroenterologists. MES is commonly used for assessing UC, whereas, SES is used to evaluate CD (Buchner, Farraye and Iacucci, 2024).

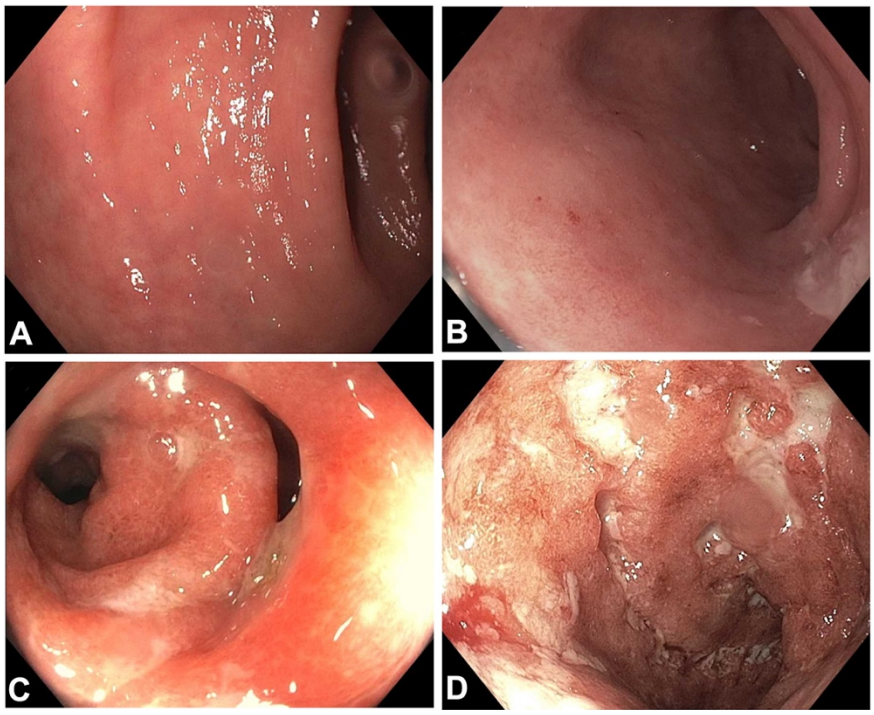

Figure 1.1.4.1. ***Endoscopic images of UC.*** Endoscopic scoring of mucosal inflammation in UC using the mayo endoscopy score (MES). **A.** MES of 0, no friability or granularity, intact vascular pattern. **B.** MES of 1, erythema, diminished vascular markings, and mild granularity. **C.** MES of 2, marked erythema, absent vascular markings, granularity, no ulceration. **D.** MES of 3, marked erythema, absent vascular markings, granularity, friability, spontaneous bleeding in the lumen, and ulcerations. Figure taken from (Shen *et al.*, 2025).

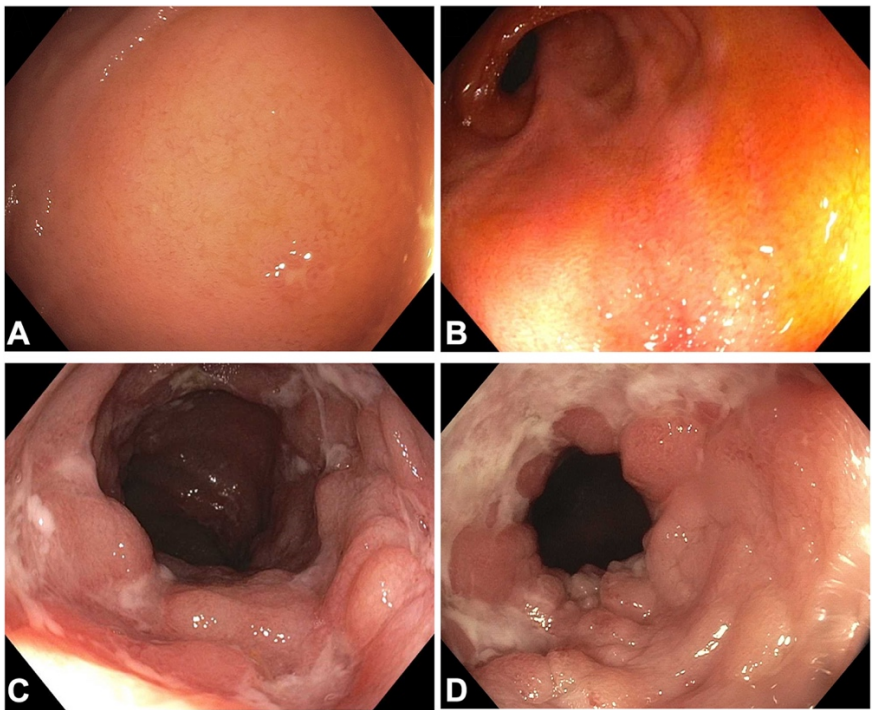

Figure 1.1.4.2. ***Endoscopy images of CD.*** Endoscopic scoring of mucosal inflammation using the simple endoscopy score for CD (SES-CD). **A.** SES-CD ulcer score of 0, no erosions or ulcers. **B.** SES-CD ulcer score of 1, aphthous ulcers 0.1 to 0.5 cm. **C.** SES-CD ulcer score of 2, large ulcers 0.5 cm to 2 cm. **D.** SES-CD ulcer score of 3, very large ulcers >2 cm. Figure taken from (Shen *et al.*, 2025).

During an endoscopy procedure, tissue samples are collected for histopathological analysis. The areas that are typically targeted include the terminal ileum, ascending colon, transverse colon, descending colon, sigmoid colon, and rectum. UC is commonly characterised histologically by crypt abnormalities or abscess, lamina propria inflammation, Paneth cell metaplasia and mucosal erosions (**Figure 1.1.4.3**) (Magro *et al.*, 2013; Kornbluth, Sachar and The Practice Parameters Committee of the American College of Gastroenterology, 2010). Conversely, in cases where CD is suspected, samples are collected from the terminal ileum and various colonic segments. Histology of CD shows focal chronic inflammation, crypt irregularity, and granulomas in the colon, with additional villous architectural abnormalities in the ileum (**Figure 1.1.4.3**) (Magro *et al.*, 2013).

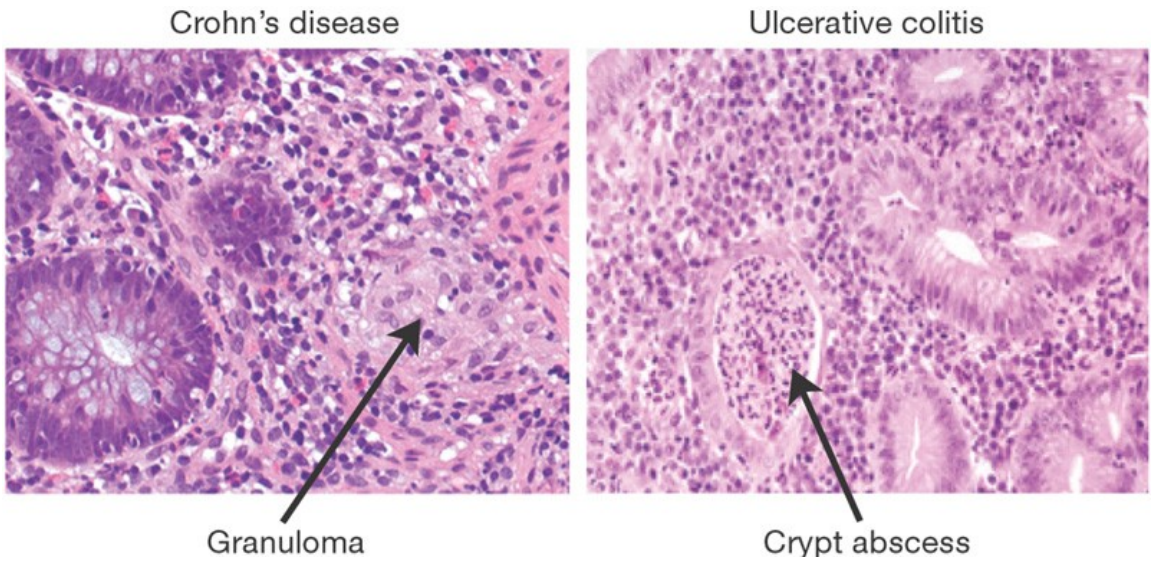

Figure 1.1.4.3. ***Histological hallmarks of IBD.*** **Left panel.** CD – biopsy from a terminal ileum with active disease. A granuloma is composed of compact macrophages, giant cells and epithelioid cells. The nodule is encircled by dense lymphoid, plasma, and other inflammatory cell infiltrates. **Right panel.** UC – colonic mucosal biopsy taken from a patient with active disease. The crypt abscess consists of transmigrated neutrophils and the surrounding epithelium exhibits features of mucosal injury. Figure taken from (Xavier and Podolsky, 2007).

1.1.5. Therapeutic approaches to IBD

Existing treatment options for IBD include anti-inflammatory medications such as aminosalicylates, corticosteroids, immunomodulators, biologics and antibiotics (Kushwaha *et al.*, 2026). The approaches taken by clinicians to treat IBD can vary between a "step-up" approach or "top-down" approach. Under the step-up strategy, which has historically been the preferred approach, treatment begins with aminosalicylates or corticosteroids, with subsequent escalation to immunomodulators and biologics, if response is inadequate or steroid-free remission cannot be achieved (**Figure 1.1.5.1**) (Becker *et al.*, 2023). There is evidence that reports that the step-up approach was preferred in mild-to-moderate UC, whereas, the top-down approach was favoured for the management of CD (You *et al.*, 2025).

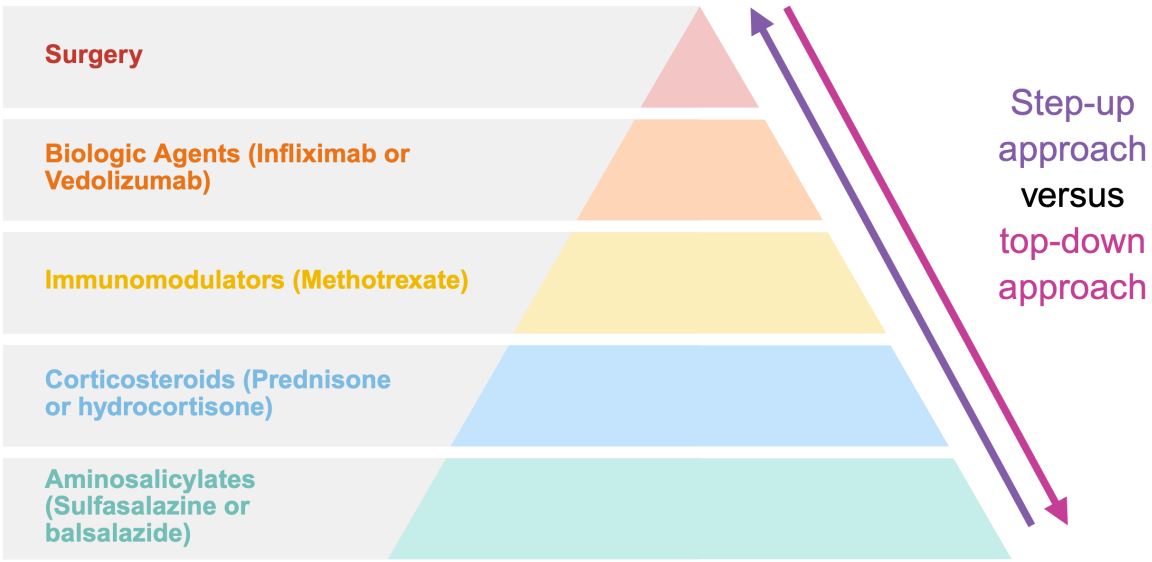

Figure 1.1.5.1. ***Therapeutic pyramid for IBD.*** The step-up approach begins with aminosalicylate or corticosteroid treatment, followed by use of immunomodulators or biological agents, when response is inadequate. In contrast, the "top-down" approach starts aggressively with biological agents or immunomodulators early in the disease course, rather than waiting for failure of first-line therapies. Adapted from (Becker *et al.*, 2023) on BioRender.com (2026).

1.1.5.1. Aminosalicylates

Aminosalicylates are a class of drugs containing 5-aminosalicylic acid (5-ASA) as the active component, including sulfasalazine, balsalazide, mesalamine, and olsalazine. 5-ASA reduces inflammation in the intestinal lining by interfering with the metabolism of arachidonic acid and inhibits the production of prostaglandins and leukotrienes (Kushwaha *et al.*, 2026). In IBD, this group of drugs inhibits downstream MAPK and NF-κB signalling pathways, while activating PPAR-γ, which is expressed by intestinal epithelial cells and immune cells (Kaiser, Yan and Polk, 1999; Rousseaux *et al.*, 2005). During colitis, 5-ASA has been proposed to promote colonic T_{regs} through the aryl hydrocarbon receptor pathway by eliciting TGF-β-dependent signalling (Oh-Oka *et al.*, 2017). Sulfasalazine had traditionally been the standard therapy for UC, however, balsalazide, mesalamine, and olsalazine are derivates that have similar effects to sulfasalazine, but with fewer adverse effects (Baron *et al.*, 1962; Dick *et al.*, 1964; Kushwaha *et al.*, 2026).

1.1.5.2. Corticosteroids

Corticosteroids suppress excessive inflammation that causes damage to the digestive tract. Binding of glucocorticosteroids to their receptors modulates multiple signalling pathways including NF-κB, PI3K/AKT and MAPK, thereby inducing anti-inflammatory effects (Nissen and Yamamoto, 2000; Croxtall, Choudhury and Flower, 2000). It has also been demonstrated that corticosteroids inhibit the migration of immune cells by decreasing the expression of adhesion molecules, including ELAM-1 on endothelial cells and ICAM-1 on both endothelial and immune cells (Cronstein *et al.*, 1992). Prednisone, prednisolone, hydrocortisone and methyl-prednisolone are common corticosteroids that are prescribed to patients with moderate-to-severe IBD (Kushwaha *et al.*, 2026).

1.1.5.3. Immunomodulator – methotrexate

Methotrexate is an example of an immunomodulator that induces apoptosis in T cells by increasing reactive oxygen species (ROS) production and c-Jun N-terminal kinase (JNK) activity (Spurlock *et al.*, 2011). Following rapid intracellular uptake, methotrexate inhibits 5-aminoimidazole-4-carboxamide ribonucleotide (AICAR) transformylase (ATIC), resulting in increased adenosine production and release. Adenosine subsequently activates cell-surface receptors to suppress inflammatory mediator production and reduce intestinal inflammation (Friedman and Cronstein, 2019).

1.1.5.4. Biologics – Anti-TNFα therapy

In 1998, the first class of biological therapies approved for the treatment of IBD focused on inhibiting the pro-inflammatory cytokine TNF (van Deventer, 1999). Anti-TNF biologics, such as infliximab and adalimumab, significantly improved response and remission rates in IBD (Berg, Colombel and Ungaro, 2019). Infliximab, a chimeric IgG1 monoclonal antibody against TNF-α, can activate complement and eliminate TNF-expressing cells, leading to suppression of mucosal inflammation (Poggioli *et al.*, 2007; Jang *et al.*, 2021; Levin, Wildenberg

and van den Brink, 2016). Despite their overall tolerability, a significant number of patients fail to respond adequately to anti-TNF therapy (Sands *et al.*, 2004; Hanauer *et al.*, 2002; Logan and Skelly, 2002; Roda *et al.*, 2016; Gisbert and Panés, 2009). In addition, these agents carry an elevated risk of infection and malignancy, further increasing treatment burden and cost (Galloway *et al.*, 2011).

1.1.5.5. Biologics – Anti-integrin agents

Natalizumab and vedolizumab are anti-integrin therapies that have previously been used for treatment of IBD. Natalizumab targets the α4 subunit of integrins (α4β1 and α4β7), broadly inhibiting leukocyte migration, whereas vedolizumab selectively blocks α4β7-mucosal addressin cell adhesion molecule 1 (MAdCAM-1) interactions, conferring gut-selective immunosuppression (Rudick and Sandrock, 2004; Soler *et al.*, 2009). Natalizumab was approved for treatment of moderate-to-severe CD (Sandborn *et al.*, 2005). However, in 2005, reports of an association between natalizumab and progressive multifocal leukoencephalopathy (PML) emerged (Berger and Koralnik, 2005; Van Assche *et al.*, 2005). Therefore, given these safety concerns, the use of this anti-integrin agent in the treatment of CD is limited (Gubatan *et al.*, 2021). Vedolizumab was approved for induction and maintenance therapy in CD and UC (Feagan *et al.*, 2013). Due to its favourable safety profile, vedolizumab is the most widely used anti-integrin agent in IBD (Gubatan *et al.*, 2021).

1.1.5.6. Surgery

Surgical intervention is often required for IBD when medical therapy fails or complications arise, such as strictures, fistulas, perforations, severe bleeding, and lack of response to conservative treatments (Caprilli, Viscido and Latella, 2007). While it can improve quality of life, surgery carries risks such as stoma complications, bowel dysfunction, and parastomal hernia formation (Kushwaha *et al.*, 2026).

1.2. Immune responses during intestinal inflammation and mucosal healing

Both innate and adaptive immune cells participate in maintaining intestinal homeostasis, mediating inflammation, and promoting tissue repair (**Figure 1.2.1**). Key innate immune cells include monocytes, macrophages, and neutrophils, while T cells, which can proliferate into T_H1, T_H2, T_H17 or T_{reg} cells, are central to adaptive immunity.

1.2.1. Overview of immune responses during intestinal homeostasis

During homeostasis, intestinal macrophages in mice are primarily replenished by blood-circulating monocytes that migrate into the mucosa. Influenced by gut-derived signals – including colony stimulating factor 1 (CSF1), transforming growth factor-beta (TGFβ), interleukin 10 (IL-10) and C-X-C motif chemokine ligand 1 (CXCL1) – as well as environmental cues such as dietary Aryl hydrocarbon receptor (AhR) ligands and microbiota-produced short-chain fatty acids (SCFAs), the recruited monocytes progress through intermediate stages to become fully differentiated lamina propria macrophages (Na *et al.*, 2019).

In the microbe dense intestinal environment, mature lamina propria macrophages become tolerant to microbial stimuli, a state reinforced by factors such as IL-10 and TGFβ. They help maintain tissue homeostasis across the epithelial barrier to sample luminal antigens, delivering these antigens to dendritic cells. By producing immunoregulatory cytokines like IL-10, they also promote the local maintenance and expansion of T_{reg} cells (Na *et al.*, 2019).

Intestinal macrophages support epithelial barrier integrity by secreting factors such as Prostaglandin E2 (PGE2) and wingless-related integration site (WNT) ligands, which stimulate epithelial stem cell renewal (Na *et al.*, 2019).

1.2.2. Overview of immune responses during intestinal inflammation and resolution

During inflammation, the intestinal environment is marked by microbial dysbiosis, mucus layer loss, and increased permeability. Neutrophils and inflammatory

monocytes are recruited sequentially to initiate an appropriate immune response. Neutrophils present with enhanced NETosis and ROS production, while the differentiation of inflammatory monocytes into mature intestinal macrophages is impaired, resulting in the accumulation of pro-inflammatory immature macrophages. In addition, dendritic cells exhibit dysregulated function characterised by heightened antigen presentation. These alterations favour pro-inflammatory T_H1 and T_H17 responses leading to increased epithelial damage (Na *et al.*, 2019; Mousa, Invernizzi and Mousa, 2024).

Once harmful stimuli are cleared, the resolution phase begins. Macrophages clear apoptotic neutrophils via efferocytosis, which triggers their switch from a pro-inflammatory to an anti-inflammatory phenotype. Efferocytosis promotes TGF-β secretion, while intestinal dendritic cells produce retinoic acid (RA); together, these signals drive T_{reg} differentiation. Intestinal macrophages also secrete chemokines, C-C motif chemokine ligand 17 (CCL17) and C-C motif chemokine ligand 22 (CCL22), that are involved in the recruitment of T_{regs}. T_{regs} and macrophages collaborate to suppress inflammation, and these macrophages are also critical for restoring the epithelial barrier (Na *et al.*, 2019; Hine and Loke, 2019).

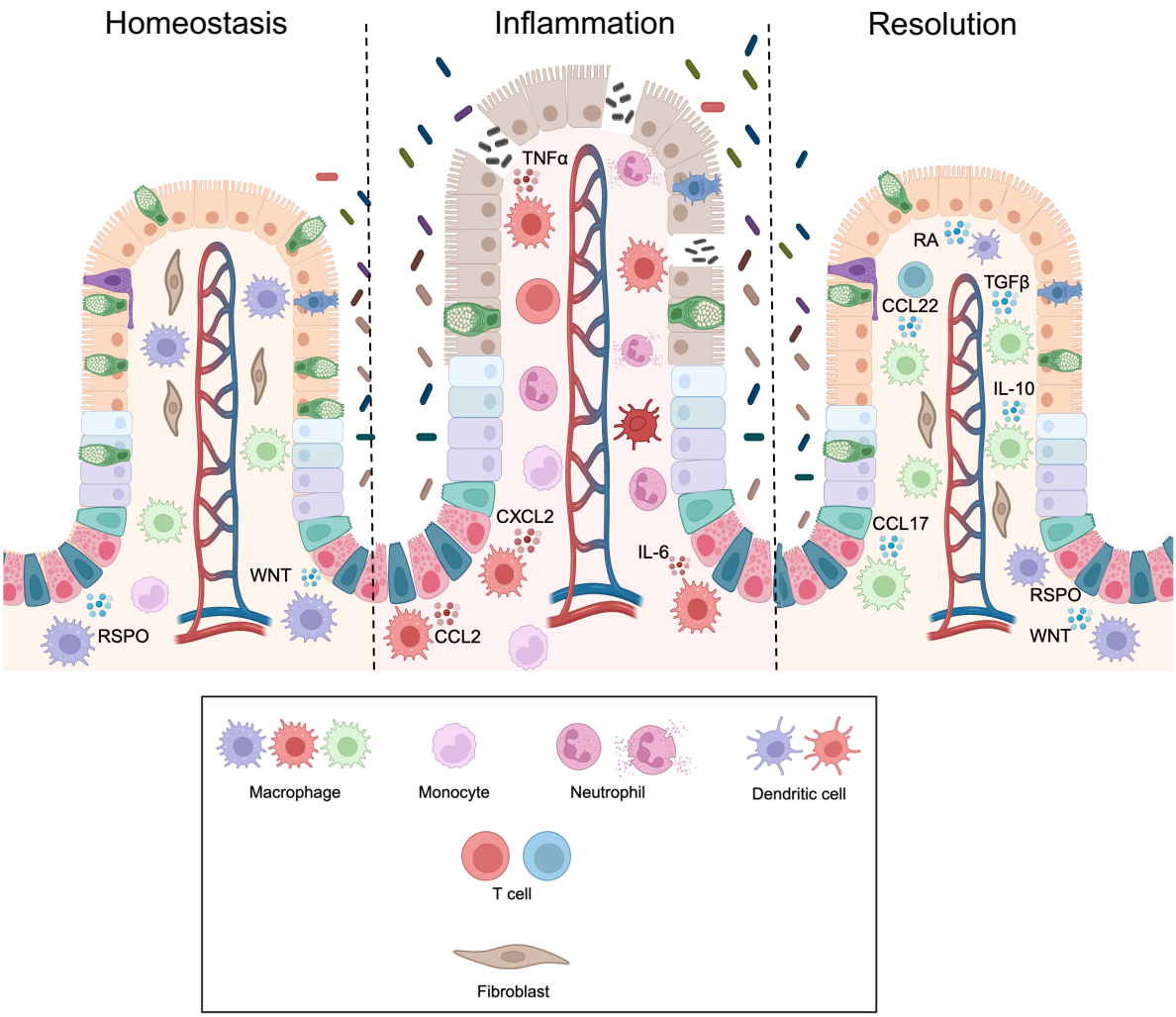

Figure 1.2.1. ***Overview of immune responses during intestinal homeostasis, inflammation and resolution.*** Interaction of innate and adaptive immune cells during intestinal homeostasis, inflammation and resolution. Created on BioRender.com (2026).

1.2.3. Intestinal Macrophages

Mononuclear phagocytes encompass monocytes, macrophages and dendritic cells, and they are the most abundant leukocytes in the intestine (Mowat and Agace, 2014). Macrophages are found along the gastrointestinal tract and throughout all layers of the gut wall. They play essential roles in maintaining intestinal homeostasis, while also driving both inflammation and resolution (Martin *et al.*, 2019). Macrophages are highly plastic cells that readily adapt to

local environmental cues to perform the functions demanded by their tissue of residence.

Intestinal macrophages can be identified from other leukocytes by their expression of cluster of differentiation 68 (CD68), CSF1 receptor and the high-affinity IgG receptor, FcγR1 (Domanska *et al.*, 2022; Tamoutounour *et al.*, 2012). However, a multitude of studies have shown that macrophages do not constitute a homogenous cell population; instead their location within the gut wall profoundly shapes their phenotype, transcriptome and function. For example, macrophages residing in the lamina propria are both transcriptionally distinct from and more abundant than those found in the submucosa and muscularis (Domanska *et al.*, 2022; Gabanyi *et al.*, 2016; Muller *et al.*, 2014; Matheis *et al.*, 2020). Single cell RNA sequencing has identified a range of markers that capture the heterogeneity of intestinal macrophages (**Table 1.1**) (Hegarty, Jones and Bain, 2023).

Table 1.1. ***Intestinal macrophage heterogeneity in distinct compartments of the gut wall.*** (Hegarty, Jones and Bain, 2023).

Subset	Conserved	Human	Mouse
Intestinal monocytes	CD11a, CSF1R, CCR2, CD14, CD62L, TREM1	CD55, CD11c, S100A8, HLA-DR^{int}, *FCN1*, *NLRP3*, *S100A9*	Ly6C, β7 integrin
Mucosal macrophages	CD68, CD64, CSF1R, MerTK, *CD63*, MHCII^{hi}, *DNASE1L3*, *CD9*, CD74, CD11c, ACP5	IL-4I1, *SELENOP*, CD14^{low}, FOLR2, *MRC1*, *SPP1*	CX3CR1, F4/80, CD121b, CD4, CD169, Fcrls, *Cst3*, TIM4
Submucosal or muscularis macrophages	CD68, CD64, CSF1R, MerTK, LYVE1, *MRC1*, *FOLR2*	MARCO, COLEC12	CX3CR1, F4/80, CD11cl^{ow}, CD206, CD169, RELMα, β2AR, TIM4

1.3. MiRNAs (microRNAs)

The first miRNA, *lin-4*, was discovered in 1993 in *Caenorhabditis elegans* (Lee, Feinbaum and Ambros, 1993; Wightman, Ha and Ruvkun, 1993). MiRNAs were classified as a broad class of small RNAs across higher eukaryotes in 2001 (Lau *et al.*, 2001; Lee and Ambros, 2001; Lagos-Quintana *et al.*, 2001). MiRNAs are small non-coding RNAs that are approximately 22 nucleotides in length (O'Brien *et al.*, 2018). They regulate gene expression by binding to the 3' untranslated region (UTR) of mRNA. MiRNAs account for 1-5% of the human genome and refine the expression of nearly 30% of genes (Macfarlane and Murphy, 2010). Approximately 2,300 true human mature miRNAs have been identified (Alles *et al.*, 2019). These small molecules are critical for normal development and are involved in a variety of biological processes including proliferation, apoptosis and immune responses (Fu *et al.*, 2013; Tüfekci, Meuwissen and Genç, 2014).

1.3.1. MiRNAs in disease pathogenesis

Given their important biological roles, any dysregulation in their function can contribute to various diseases, included cancer, infection and inflammatory diseases.

MiRNAs have been observed to be dysregulated in solid tumours and hematological malignancies (Melo and Esteller, 2011; Chen, Su and Hung, 2012). *MiR-21* has been reported to be upregulated in breast, lung, gastric and brain cancers, where it enhances tumour growth metastasis and chemoresistance by inhibiting tumour suppressors like phosphatase and tensin homolog (PTEN), programmed cell death 4 (PDC4) and tropomyosin 1 (TPM1) (Zhang *et al.*, 2020). Similarly, *miR-221* is elevated in hepatocellular carcinoma, melanoma, colon cancer and renal cell carcinoma. Its upregulation results in the repression of cell cycle inhibitors, including p27 and p57, subsequently promoting uncontrolled proliferation (Di Martino *et al.*, 2022; Ali *et al.*, 2024; Di Martino *et al.*, 2016; Fornari *et al.*, 2008).

Conversely, downregulation of miRNAs can also negatively impact cancer progression. For example, *miR-143* and *miR-145* are downregulated in bladder,

breast, lung, colorectal and pancreatic cancers (Wu *et al.*, 2024; Mozammel *et al.*, 2023). Additionally, the expression of *miR-126* and *miR-125b* are decreased in breast, lung and gastric cancers, emphasising their crucial roles in apoptosis and cellular differentiation (Jalil *et al.*, 2023; Huang *et al.*, 2013).

Studies have offered insights into the critical participation of miRNAs in host immune defence against bacterial pathogens. The anti-inflammatory *miR-21*, has been observed to limit host glycolysis during Tuberculosis infection to favour bacterial replication (Hackett *et al.*, 2020). *MiR-146a* is upregulated following *Helicobacter pylori* infection in gastric epithelial cells and gastric mucosal tissues in an NF-κB-dependent manner. In turn, *miR-146a* suppresses the expression of key signalling molecules, including TNF receptor-associated factor 6 (TRAF6) and IL-1 receptor-associated kinase 1 (IRAK1). Additionally, *miR-146a* reduces the production of pro-inflammatory mediators such as interleukin 8 (IL-8), growth-related oncogene-α (GRO-α), macrophage inflammatory protein-3α (MIP-3α), TNF-α, and interleukin 1 beta (IL-1β), by attenuating NF-κB signalling (Liu *et al.*, 2010; Li *et al.*, 2012). In addition, miRNAs have been investigated in the context of Salmonella infection. For instance, virulent *Salmonella enteritidis* alters *miR-128* expression in intestinal epithelial cells, suppressing epithelial M-CSF secretion and thereby impairing macrophage recruitment (Zhang *et al.*, 2014).

Finally, miRNAs have been found to be differentially expressed in IBD. Studies investigating the expression of miRNAs in IBD have revealed differential expression of miRNAs between UC and CD (**Figure 1.3.1.1** and **Figure 1.3.1.2**). MiRNAs have been implicated in the pathogenesis of IBD through alterations in autophagy, intestinal barrier and immune homeostasis (Alfaifi *et al.*, 2023). For example, *miR-21* has been reported to be elevated in the mucosa and serum of UC patients, and this is associated with increased intestinal permeability. *MiR-21* targets ras homologous protein B (RhoB), resulting in tight junction dysfunction in intestinal epithelial cells (Yang *et al.*, 2013). Additionally, it has been demonstrated that *miR-192* suppresses NOD2 expression, which is strongly associated with CD susceptibility and plays a key role in regulating autophagy and NF-κB signalling (Chuang *et al.*, 2014).

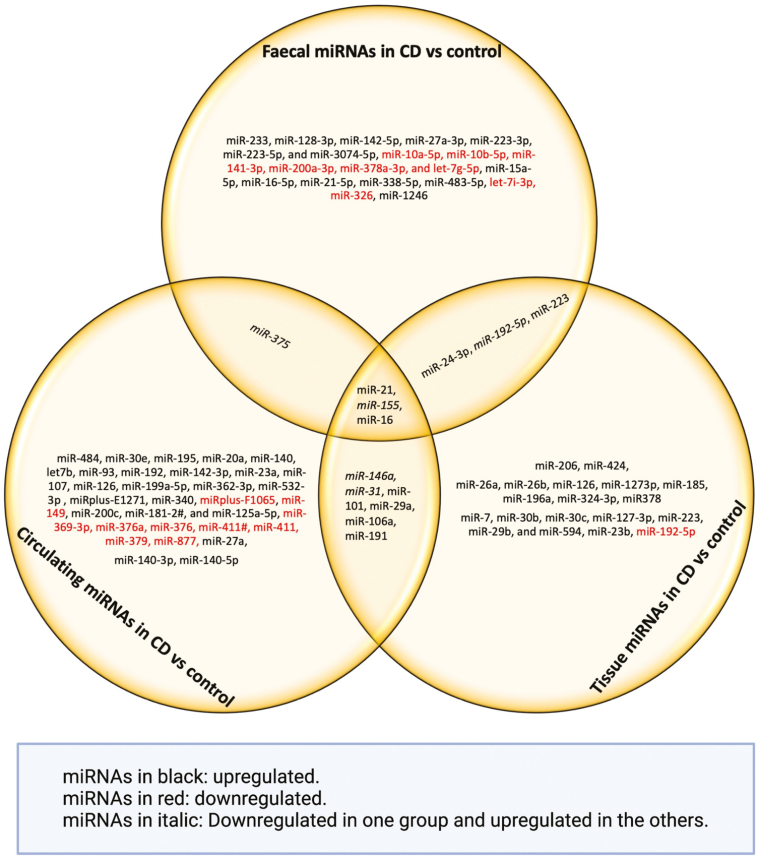

Figure 1.3.1.1. ***Summary of dysregulated miRNAs in CD.*** Figure taken from (Alfaifi *et al.*, 2023).

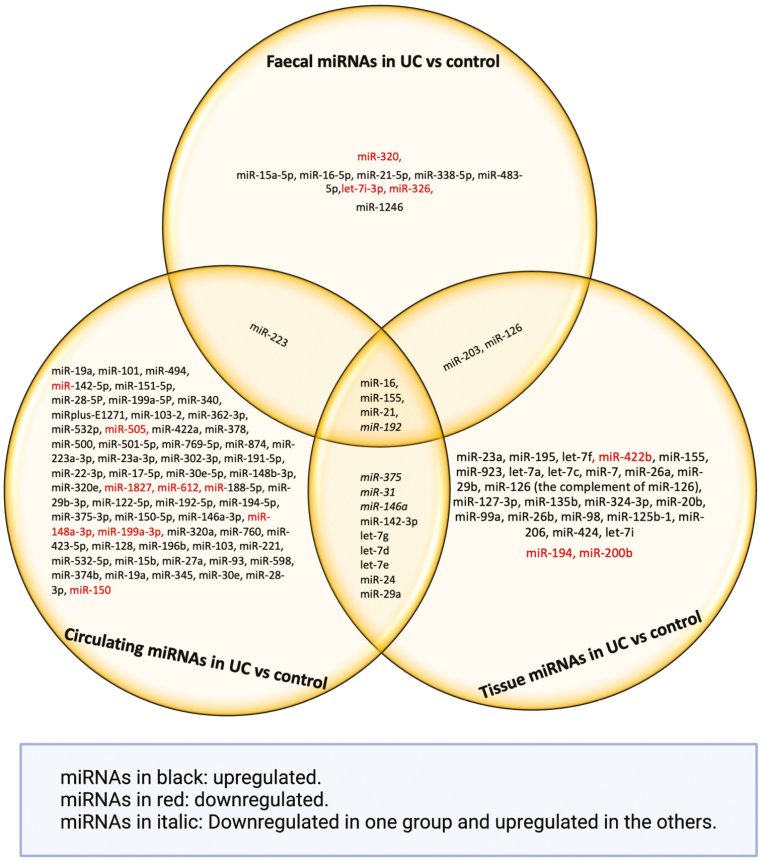

Figure 1.3.1.2. ***Summary of dysregulated miRNAs in UC.*** Figure taken from (Alfaifi *et al.*, 2023).

1.3.2. MiR-223 in the pathogenesis of disease

MiR-223 is a myeloid-restricted miRNA and it has been associated with the pathogenesis of various diseases. Its importance was first demonstrated in granulocytes, where *miR-223*-deficient mice spontaneously developed inflammatory lung pathology and showed exaggerated tissue damage following endotoxin challenge (Johnnidis *et al.*, 2008). Additionally, genetic studies have shown that *miR-223* deficiency is associated with severe lung inflammation, whereas pulmonary overexpression of *miR-223* in mice confers protection against acute lung injury induced by mechanical ventilation or *Staphylococcus aureus* infection (Neudecker *et al.*, 2017a). Furthermore, *miR-223*$^{-/y}$ mice exhibited exacerbated colitis and an increased myeloid inflammatory signature in a DSS-induced experimental colitis model (Neudecker *et al.*, 2017b).

1.3.3. MiR-223 in the pathogenesis of IBD

Given that myeloid cells have been observed to be drivers of intestinal inflammation, *miR-223* has been investigated in the context of IBD. Studies have identified this miRNA as being upregulated in IBD, both during active disease in patients and in DSS-induced murine models of colitis (Neudecker *et al.*, 2017b). Additionally, *miR-223*$^{-/y}$ mice present with exacerbated DSS-colitis (Neudecker *et al.*, 2017b; Zhou *et al.*, 2015).

AIMS OF THIS THESIS

The central hypothesis of this thesis is that *miR-223* promotes mucosal healing during IBD.

Therefore, the specific aims of this project are:

1. Assess the functional role of *miR-223* during macrophage development and activation.
2. Assess the contribution of macrophage-associated *miR-223* in intestinal epithelial repair.
3. To elucidate the role of the IL-6 cytokine family and the STAT3 signalling pathway in regulating intestinal epithelial regeneration.

CHAPTER 2

MATERIALS AND METHODS

Table 2.1. ***Animals and cell culture lines.***

Product	Catalogue number	Company
L929 cell line murine	850111425	Sigma
Lentiviral miR-223KD RAW 264.7 cell line murine	Generated in this thesis	Generated in this thesis
Lentiviral Negative Control miRNA inhibitor RAW 264.7 cell line murine	Generated in this thesis	Generated in this thesis
Murine colon organoids	Generated in this thesis	Generated in this thesis
C57BL/6J mice (female and male)	000664	The Jackson Laboratory
miR-223$^{-/y}$ mice on a C57BL/6J background (male)	N/A	Provided by V. Dawson (John Hopkins University, Baltimore, MD)
RAW 264.7 cell line murine	91062702	ATCC/ETCC

Table 2.2. ***Lentiviral particles used for transduction of RAW 264.7 cells.***

Product	Catalogue number	Company
MISSION Lenti miRNA inhibitor *mmu-miR-223-3p*	MLTUD0341	Sigma
MISSION Lenti miRNA *mmu-miR-223-3p*	MLMIR0341	Sigma
MISSION Lenti miRNA inhibitor Negative Control	HLTUD002C	Sigma

Table 2.3. ***Cell culture reagents.***

Product	Catalogue number	Company
ACK Lysing Buffer	A10492-01	Gibco
CryoStor CS10	210373	Biolife Solutions
Dimethyl Sulfoxide (DMSO)	D2650	Sigma
Dulbecco's Modified Eagle Medium (DMEM)	41965-039	Gibco
Dulbecco's Modified Eagle's Medium: Nutrient Mixture F-12	36254	StemCell Technologies
Dulbecco's Phosphate Buffered Saline (D-PBS)	SH30028.02	Cytiva
Ethanol	E/0650DF/C17	Fisher Scientific
Fetal Bovine Serum (FBS)	F9665	Sigma
Gentle Cell Dissociation Reagent	100-0485	StemCell Technologies
IntestiCult Organoid Growth Medium (OGM) Mouse Basal Medium	0600	StemCell Technologies
IntestiCult OGM Mouse Supplement 1	06002	StemCell Tehnologies
IntestiCult OGM Mouse Supplement 2	06003	StemCell Technologies
Lipofectamine 3000 Transfection Kit	L300-015	Invitrogen
Matrigel Matric Basement Membrane	366231	Corning
OPTI-MEM	4124801	Gibco
Penicillin-Streptomycin solution (Pen-Strep)	SV3010	Cytiva
Polybrene Infection/Transfection Reagent	TR-1003	Merck Millipore
Puromycin dihydrochloride	P9620	Sigma
Reconstitution Buffer 2	RB02	R and D Systems
Trypan Blue solution	93595	Sigma
Trypsin-EDTA solution	T4049	Sigma

Table 2.4. ***Preparation of cell culture media for different cell types.***

Cell culture reagent	Composition	Cell type
Complete DMEM (cDMEM)	500 mL DMEM supplemented with 10% FBS.	Culture of RAW 264.7, L929, *miR-223*KD, and miRNA inhibitor negative control cell lines.
cDMEM supplemented with LCM and penicillin streptomycin	500 mL DMEM supplemented with 10% FBS, 20% LCM and 1% penicillin streptomycin.	Culture of bone marrow-derived macrophages (BMDMs).
IntestiCult organoid growth media	90 mL of IntestiCult OGM mouse basal media supplemented with 5 mL IntestiCult OGM Mouse Supplement 1, 5 mL IntestiCult OGM Mouse Supplement 2 and 1% penicillin streptomycin.	Culture of murine colonic epithelial organoids.

Table 2.5. ***MiRNA mimics used for the transfection of BMDMs.***

Product	Catalogue number	Company
Ambion mirVana miRNA mimic hsa-*miR-223-3p*	4464066	Thermo Fisher Scientific
Ambion mirVana miRNA mimic mmu-*miR-223-5p*	4464066	Thermo Fisher Scientific
Ambion mirVana miRNA mimic Negative Control #1	4464058	Thermo Fisher Scientific

Table 2.6. ***Reagents used for cell and organoid culture stimulation studies.***

Product	Catalogue number	Company
Recombinant mouse Interferonγ (IFNγ)	485-ML	R and D Systems
Recombinant mouse Interleukin 4 (IL-4)	404-ML	R and D Systems
Recombinant mouse Interleukin 6 (IL-6)	216-16	Peprotech
Recombinant mouse Interleukin 11 (IL-11)	220-11	Peprotech
Recombinant mouse Leukemia Inhibitory Factor (LIF)	250-02	Peprotech
Lipopolysaccharide (LPS) (*Escherichia coli* (*E. coli*) O111:B4)	L5293	Sigma

Table 2.7. ***Reagents used for cell and organoid culture inhibitor pre-treatment studies.***

Product	Catalogue number	Company
Actinomycin D	1229	Tocris
Tomivosertib	HY-100022	MedChemExpress
Stattic	HY-13818	MedChemExpress

Table 2.8. ***Reagents used for harvesting cells and organoids for RNA and protein analysis.***

Product	Catalogue number	Company
2-Mercaptoethanol	M3148	Sigma
Phosphatase Inhibitor	ab201113	Abcam
Protease Inhibitor	FGC-402330	Abcam
QIAzol Lysis Reagent	79306	Qiagen
Radioimmunoprecipitation assay (RIPA) Buffer	R0278	Sigma

Table 2.9. ***Commercial kits.***

Product	Catalogue number	Company
EasyPure RNA kit	ER101-01	TransGen Biotech
High Capacity cDNA Reverse Transcription Kit	4368814	Thermo Fisher Scientific
ImmPACT NovaRED Substrate Kit, Peroxidase	SK-4805	Vector Laboratories
LDH Activity Assay Kit	MAK066	Sigma
miRCURY LNA RT kit	339340	Qiagen
miRCURY LNA SYBR PCR kit	339346	Qiagen
miRNAscope HD Detection Reagents - RED	324510	ACD Biotech.
Mouse CXCL2 DuoSet ELISA	DY452	R and D Systems
Mouse IL-1B DuoSet ELISA	DY401	R and D Systems
Mouse IL-6 DuoSet ELISA	DY406	R and D Systems
Pierce BCA Protein Assay kit	23227	Thermo Fisher Scientific
RNAscope H_2O_2 and Protease Reagents	322381	ACD Biotech
RNeasy kit	74034	Qiagen
SuperSignal West Femto Maximum Sensitivity Substrate	34096	Thermo Fisher Scientific
VECTASTAIN Elite ABC Universal Kit, Peroxidase, R.T.U (Horse Anti-Mouse/Rabbit IgG)	PK-7200	Vector Stain Laboratories

Table 2.10. ***Reagents used for RNA analysis.***

Product	Catalogue number	Company
Chloroform	J67241	Alfa Aesar
Molecular Biology Grade Ethanol	BP8202	Fisher Scientific
Nuclease-free water	SH30538.FS	Cytiva
RNaseZap	R2020	Sigma
TaqMan Fast Advanced Master Mix	4444557	Applied Biosystems

Table 2.11. ***TaqMan primers.***

Target	Catalogue number	Company
18s (18S ribosomal RNA)	Hs99999901_s1	Applied Biosystems
Ago2 (Argonaute 2)	Mm00838341_m1	Applied Biosystems
Ago3 (Argonaute 3)	Mm01188534_m1	Applied Biosystems
Alpi (Intestinal alkaline phosphatase)	Mm01285814_g1	Applied Biosystems
Arg1 (Arginase 1)	Mm00475988_m1	Applied Biosystems
Ascl2 (Achaete-schute homolog 2)	Mm01268891_g1	Applied Biosystems
Atoh1 (Atonal homolog 1)	Mm00476035_s1	Applied Biosystems
Axin2 (Axis inhibition protein 2)	Mm00443610_m1	Applied Biosystems
Ccl2 (C-C motif chemokine ligand 2)	Mm00441242_m1	Applied Biosystems
Ccl17 (C-C motif chemokine ligand 17)	Mm01244826_g1	Applied Biosystems
Ccl22 (C-C motif chemokine ligand 22)	Mm00436439_m1	Applied Biosystems
Cebpb (CCAAT/enhancer-binding protein beta)	Mm07294206_s1	Applied Biosystems
Chga (Chromogranin A)	Mm00514341_m1	Applied Biosystems
Cxcl2 (C-X-C motif chemokine ligand 2)	Mm00436450_m1	Applied Biosystems
Dicer1	Mm00521722_m1	Applied Biosystems

Gja1 (Gap junction alpha-1)	Mm00439105_m1	Applied Biosystems
H2-Ab1 (Histocompatibility 2, class II antigen A, beta 1)	Mm004439216_m1	Applied Biosystems
Hspd1 (Heat shock protein family D member 1)	Mm00849835_g1	Applied Biosystems
Il-1β (Interleukin-1 beta)	Mm00434228_m1	Applied Biosystems
Il-6	Mm00446190_m1	Applied Biosystems
Il-10 (Interleukin-10)	Mm01288386_m1	Applied Biosystems
Il-11	Mm00434162_m1	Applied Biosystems
Irf4 (Interferon regulatory factor 4*)*	Mm00516431_m1	Applied Biosystems
Irf5 (Interferon regulatory factor 5*)*	Mm00496477_m1	Applied Biosystems
Itgam (Integrin subunit alpha M)	Mm00434455_m1	Applied Biosystems
Lgr5 (Leucine-rich repeat-containing G-protein coupled receptor 5)	Mm00438890_m1	Applied Biosystems
Lif	Mm00434762_g1	Applied Biosystems
Ly6a (Lymphocyte antigen 6 family member A)	Mm00726565_s1	Applied Biosystems
Mki67 (Marker of proliferation Kiel 67)	Mm01278617_m1	Applied Biosystems
Muc2 (Mucin 2)	Mm01276696_m1	Applied Biosystems
Nos2 (Nitric oxide synthase 2)	Mm00440502_m1	Applied Biosystems
Olfm4 (Olfactomedin 4)	Mm01320260_m1	Applied Biosystems
Osm (Oncostatin M)	Mm01193966_m1	Applied Biosystems
Prkra (Protein kinase, interferon-inducible double-stranded RNA dependent activator)	Mm00478737_m1	Applied Biosystems
Retnla (Resistin-like molecule alpha)	Mm00445109_m1	Applied Biosystems
Rspo1 (R-spondin 1)	Mm00507077_m1	Applied Biosystems
Spib (Spi-B transcription factor)	Mm03048233_m1	Applied Biosystems

Stat6 (Signal transducer and activator of transcription 6)	Mm01160477_m1	Applied Biosystems
Tacstd2 (Tumour-associated calcium signal transducer 2)	Mm00498401_s1	Applied Biosystems
Tarbp2 (TAR RNA-binding protein 2)	Mm00493423_g1	Applied Biosystems
Tgfb1 (Transforming growth factor beta 1)	Mm01178820_m1	Applied Biosystems
Tnfa (Tumour necrosis factor alpha)	Mm00443258_m1	Applied Biosystems
Wls (Wntless)	Mm00509695_m1	Applied Biosystems
Wnt6 (Wnt family member 6)	Mm00437353_m1	Applied Biosystems

Table 2.12. *SYBR Green primers.*

Product	Catalogue number	Company
U6 (U6 small nuclear RNA)	YP00203907	Qiagen
hsa-miR-223-3p	YP00205986	Qiagen
mmu-miR-223-5p	YP02102349	Qiagen

Table 2.13. ***Reagents used for protein analysis.***

Product	Catalogue number	Company
2-Mercaptoethanol	M3148	Sigma
4x Laemmli sample buffer	1610747	Bio-Rad
Ammonium persulfate (APS)	A3678	Sigma
Bovine serum albumin (BSA)	A3733	Sigma
Ethanol	E/0650DF/C17	Fisher Scientific
Glycine	G8898	Sigma
Hydrochloric acid	H1758	Sigma
Methanol	34860	Sigma
N, N, N', N'-Tetramethyl-ethylenediamine (TEMED)	T9281	Sigma
PageRuler Plus Prestained Protein Ladder	26619	Thermo Fisher Scientific
Ponceau solution	P7170	Sigma
Protogel 30% acrylamide	EC-890	National Diagnostics
Skim milk powder	1.15363.0500	Millipore
Sodium chloride	S9888	Sigma
Sodium dodecyl sulfate (SDS)	75746	Sigma
Tris base	BP152-1	Fisher Scientific
TWEEN20	P1379	Sigma

Table 2.14. ***Preparation of reagents used for protein analysis.***

Reagent	Composition
4X Laemmli sample buffer	900 μL 4X Laemmli sample buffer and 100 μL 2-Mercaptoethanol
4X Resolving gel buffer, potential of hydrogen (pH) 8.8	181.7 g Tris base and 4 g SDS in 1 L distilled water (dH_2O). Adjusted to pH with hydrochloric acid (HCl).
4X Stacking gel buffer, pH 6.8	60.6 g Tris base and 5 g SDS in 1 L dH_2O. Adjusted to pH with HCl.
15% Ammonium persulfate (APS)	0.15 g APS in 1 mL dH_2O.
10X Running buffer	30.2 g Tris base, 144 g glycine and 10 g SDS in 1 L dH_2O.
1X Running buffer	100 mL 10X Running buffer and 900 ml dH_2O
10X Transfer buffer	30.2 g Tris base and 144 g glycine in 1 L dH_2O.
1X Transfer buffer	100 mL 10X Transfer buffer, 200 mL Methanol and 700 mL dH_2O.
10X Tris Buffered Saline (TBS)	48.4 g Tris base and 175.3 g in 1L dH_2O.
1X TBS	100 mL 10X TBS and 900 mL dH_2O.
1X TBS-TWEEN20 (TBS-T)	1 mL TWEEN20, 100 mL 10X TBS and 900 mL dH2O.
Mild stripping buffer, pH 2.2	15 g Glycine, 1 g SDS and 10 mL TWEEN20 in 1L dH_2O. Adjusted to pH with HCl.
5% Milk/TBS	12 g Milk in 250 mL 1X TBS.

Table 2.15. ***Primary antibodies use for protein analysis.***

Antibody	Clone	Catalogue number	Company
β-Actin	AC-15	A1978	Sigma
DICER	EPR24104-105	ab259327	Abcam
P-4E-BP1 (Phosphorylated eukaryotic translation initiation factor 4E-binding protein 1)	236B4	2855	Cell Signalling
P-EIF4E (Phosphorylated eukaryotic translation initiation factor 4E)	Ser209	9741	Cell Signalling
P-ERK1/2 (Phosphorylated extracellular signal-regulated kinases 1 and 2)	Thr202/Tyr204	9101	Cell Signalling
P-MNK1 (Phosphorylated MAP kinase-interacting serine/threonine-protein kinase 1)	Thr197/202	2111	Cell Signalling
P-p38 (Phosphorylated p38)	Thr180/Tyr182	9211	Cell Signalling
P-S6 (Phosphorylated ribosomal protein S6)	Ser252/236	4858	Cell Signalling
P-STAT3 (Phosphorylated signal transducer and activator of transcription factor 3)	Tyr705	9145	Cell Signalling
PACT (protein activator of the interferon-induced protein kinase R)	2W2E10	NBP3-16701	Novus biologics
Puromycin	12D10	MABE343	Sigma
STAT3 (Signal transducer and activator of transcription factor 3)	D1B2J	30835	Cell Signalling
TRBP2 (TAR RNA-binding protein 2)	Polyclonal	NBP2-24725SS	Novus Biologics

Table 2.16. ***Secondary antibodies used for protein analysis.***

Antibody	Catalogue number	Company
Goat anti-Mouse IgG (H+L), HRP	A16066	Invitrogen
Goat anti-Rabbit IgG (H+L), HRP	A16096	Invitrogen

Table 2.17. ***Reagents used for enzyme-linked Immunosorbent Assay (ELISA).***

Product	Catalogue number	Company
1-STEP ULTRA TMB-ELISA	34028	Thermo Fisher Scientific
Bovine serum albumin (BSA)	A3733	Sigma
D-PBS	SH30028.02	Cytiva
Stop solution	DY994	R and D Systems
TWEEN20	P1379	Sigma

Table 2.18. ***Preparation of reagents used for ELISA.***

Reagent	Composition
Block buffer	1% BSA in D-PBS
Reagent diluent	1% BSA in D-PBS
Wash buffer	0.05% TWEEN20 in D-PBS

Table 2.19. ***Reagents used for immunohistochemistry (IHC).***

Product	Catalogue number	Company
Antigen Unmasking solution	H-3300	Vector Laboratories
Bovine serum albumin (BSA)	A3733	Sigma
DPX mounting media	06522	Sigma
Ethanol	E/0650DF/C17	Fisher Scientific
Harris Hematoxylin	6765003	Epredia
ImmEdge pen	H-4000	Vector Laboratories
ImmPACT NovaRED	SK-4805	Vector Laboratories
Phosphate buffered saline (PBS) tablets	BR0014G	Oxoid
Triton X 100	X100	Sigma
VECTASTAIN Elite ABC-HRP kit	PK-7200	Vector Laboratories
Xylene	CRTSX0021612	Lennox

Table 2.20. ***Preparation of reagents used for IHC.***

Reagent	Composition
Antigen retrieval solution	2.5 mL antigen unmasking buffer in 225 mL dH_2O
0.2% Triton X 100 in PBS	100 μL Triton X 100 in 50 mL PBS
5% BSA in PBS	2.5 g BSA in 50 mL PBS
10% Harris' Haematoxylin solution	50 mL Harris' Haematoxylin in 450 mL dH_2O

Table 2.21. ***Primary antibodies used for IHC.***

Antibody	Clone	Catalogue number	Company
β-CATENIN	IGX4794R-3	ab223075	Abcam
C-MYC	E5Q6W	18583	Cell Signalling
CCR2 (C-C chemokine receptor type 2)	EPR20844-15	ab273050	Abcam
CD68	E3O7V	97778	Cell Signalling
CD206	E6T5J	24595	Cell Signalling
CYCLIN D1	E3P5S	55506	Cell Signalling
LY6A/E	EPR3355	ab109211	Abcam
MERTK (MER proto-oncogene, tyrosine kinase)	EPR17534-139	ab184086	Abcam
MUC2	Polyclonal	Ab90007	Cell Signalling
OLFM4	D6Y5A	39141	Cell Signalling
P-STAT3	Tyr705 (D347)	9145	Cell Signalling
PCNA (Proliferating cell nuclear antigen)	D3H8P	13110	Cell Signalling
RELMα (Resistin-like molecule alpha)	Polyclonal	NBP2-29355SS	Novus Biologics

Table 2.22. ***Reagents used for in situ hybridization (ISH).***

Product	Catalogue number	Company
Ammonium hydroxide	423305000	Acros organics
DPX mounting media	06522	Sigma
Ethanol	E/0650DF/C17	Fisher Scientific
Gill's Hematoxylin	6765006	Thermo Fisher Scientific
ImmEdge pen	H-4000	Vector Laboratories
10% Neutral buffered formalin (NBF)	HT501128	Sigma
Xylene	CRTSX0021612	Lennox

Table 2.23. ***Preparation of reagents used for ISH.***

Reagent	Composition
1X Target retrieval reagent	20 mL 10X Target retrieval reagent and 180 mL dH_2O
1X Wash buffer	60 mL 50X Wash buffer and 2.94 L dH_2O
50% Gill's Hematoxylin	100 mL Gill's Hematoxylin and 100 mL dH_2O
0.02% (w/v) Ammonia water	179 μL Ammonium hydroxide and 250 mL dH_2O

Table 2.24. ***MiRNAscope probes.***

Target	Catalogue number	Company
miRNAscope Positive Control Probe-SR-RNU6-S1	727871-S1	ACD Biotech
miRNAscope Negative Control Probe-SR-Scramble-S1	727881-S1	ACD Biotech
miRNAsope Singleplex Target Probe-SR-mmu-miR-223-3p-S1	727821-S1	ACD Biotech.

Table 2.25. ***Software.***

Name	Version	Company
BioRender	BioRender 2025	BioRender
GraphPad Prism	10.6.0	GraphPad (USA)
ImageLab	6.1.0	Bio-Rad
Microsoft Excel	16.100	Microsoft Office
Microsoft Word	16.55	Microsoft Office
miRTarBase	10.0	https://awi.cuhk.edu.cn/~miRTarBase/miRTarBase_2025/php/index.php
Motic Images Plus	3.0.19 (124)	Motic
Nanodrop	NPOS 4.2h build 14900	Implen
OrganoSeg	1.0	https://github.com/JanesLab/OrganoSeg
QuPath	0.5.1	https://qupath.github.io
StepOn Plus Real-time Software	2.3	Applied Biosystems
TargetScanHuman	8.0	https://www.targetscan.org/vert_80/
TargetScanMouse	8.0	https://www.targetscan.org/mmu_80/

2.1. Mouse strains

MiR-223$^{-/y}$ mice on a C57BL/6J background are hemizygous for *miR-223*. The *MiR-223* gene is located on the X chromosome, therefore male mice only carry one copy of the gene, in contrast to female mice. Consequently, male mice carrying the deletion are designated *miR-223*$^{-/y}$, whereas female mice are *miR-223*$^{-/-}$ (Neudecker *et al.*, 2017a).

These mice were previously described and bred in-house at the University of Colorado Anschutz Medical Campus (Flynn *et al.*, 2024; Neudecker *et al.*, 2017b). C57BL/6J mice were purchased from The Jackson Laboratory (Maine, USA). After weaning at 21 days, mice were cohoused and experimental colitis was induced at 8 weeks of age. All mice were bred under specific pathogen-free conditions, and faecal samples tested negative for helminth, protozoa, and *Helicobacter* species. Animal procedures were approved by the Institutional Animal Care and Use Committees at the University of Colorado Denver. All animal procedures were carried out by staff at the University of Colorado. Upon completion of all *in vivo* studies, archived colon tissues from the 2 strains were shipped to Maynooth university for down-stream pathology studies.

For bone marrow-derived macrophage (BMDM) studies, C57BL/6J mice (male and female) from Charles Rivers Laboratory, UK, were bred in-house at Maynooth University and were between 10 and 24 weeks of age at the time of experimentation.

2.2. Induction of experimental DSS-colitis

8 week old mice were administered dextran sodium sulphate (DSS) (3% wt/vol, 36,000–50,000 kD; MP Biomedicals) in drinking water *ad libitium* for 6 days. DSS solution was replaced once on day 3. This was followed by a 10-day recovery period where DSS was removed (drinking water only). Mice were examined daily for clinical signs of colitis (i.e. weight loss, stool consistency and faecal blood).

Based on these data, a colitis disease activity index (DAI) was calculated for each mouse. A score of 1-4 was given for each parameter, with a maximum DAI score of 12. The DAI was defined as per **Table 2.26.** Following euthanasia, colons were removed, and washed with cold D-PBS. The tissue was either snap frozen or fixed with 10% buffered formalin.

Table 2.26. ***Colitis DAI.***

Colitis DAI	
0	No weight loss, normal stool, no blood
1	1-3% weight loss
2	3-6% weight loss, loose stool, blood visible in stool
3	6-9% weight loss
4	>9% weight loss, diarrhoea, gross bleeding

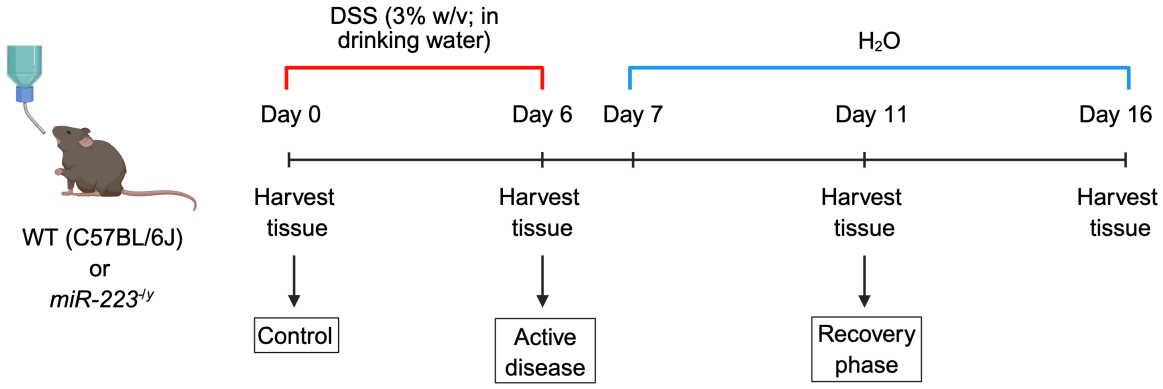

Figure 2.2.1. ***Induction of DSS-induced experimental colitis in mice.*** DSS (3% wt/vol, 36,000–50,000 kD; MP Biomedicals) in drinking water *ad libitium* for 6 days. DSS solution was replaced once on day 3. This was followed by a 10-day recovery period were DSS was removed (drinking water only).

2.3. Cell culture

All cell culture was performed under sterile conditions in a class II biological safety cabinet using aseptic technique. The safety cabinet was cleaned with 70% ethanol before and after use, and all materials introduced into the cabinet were also sprayed with 70% ethanol. UV sterilisation was employed after each session, with only a single cell line handled at one time. All cell lines or primary cells were

cultured in vented cap tissue culture flasks or tissue culture plates, in a humidified incubator maintained at 37°C, 5% CO_2.

2.3.1. Cell counting

Following the resuspension of the cell pellet in growth medium, 10 μL aliquot of the cell suspension was removed and placed into a 1.5 mL tube. 10 μL of trypan blue was added to the aliquot and 10 μL was loaded onto a haemocytometer. Using a light microscope at 10X magnification, viable cells were counted across 4 quadrants, the average was calculated and multiplied by two, in order to account for the dilution factor. This value was then multiplied by 10^4 to determine the number of cells per mL.

2.3.2. Culture of L929 cell line for the production of macrophage colony-stimulating factor (M-CSF)

The murine fibroblast cell line, L929 cells, secrete M-CSF (Weischenfeldt and Porse, 2008; Trouplin *et al.*, 2013). A frozen cryovial of L929 cells was rapidly thawed in a beaded bath at 37°C. The thawed cells were transferred into a 50 mL falcon tube, containing 20 mL of warm cDMEM (without antibiotic). The tube was centrifuged at 1,500 rpm for 5 min and the supernatant was discarded in order to remove the DMSO. The cell pellet was resuspended in 5 mL cDMEM and added to a T25 flask. The cells were incubated at 37°C, 5% CO_2, overnight to grow to 70% confluency.

Cells were washed with 1X D-PBS (Ca^{2+}/Mg^{2+} free) and incubated for 5 min with 3 mL Trypsin. 7 mL cDMEM was then added and cells were detached by pipetting up and down. The cell suspension was transferred to a 50 mL falcon tube and centrifuged at 1,500 rpm for 5 min. The supernatant was discarded, the cell pellet was resuspended in 20 mL cDMEM and transferred to a T75 flask. When the cells had achieved 70% confluency, the above steps were repeated and the cells were split 1:5 into a T175 flask. One week later, the supernatant was collected and centrifuged at 3,000 rpm for 5 min. The L929 conditioned medium containing M-CSF was passed through a 0.45 μm filter and frozen at -20°C in 50 mL aliquots.

The concentration of M-CSF in the L929 conditioned medium was intermittently measured using ELISA (**Figure 2.3.2.1**).

A

	Concentration (pg/ml)	Optical density
Standard 1	1000.0	3.0265
Standard 2	500.0	1.6915
Standard 3	250.0	0.8205
Standard 4	125.0	0.4240
Standard 5	62.5	0.2510
Standard 6	31.3	0.1570
Standard 7	15.6	0.1040
Standard 8	0.0	0.0000
LCM		1.1140

B

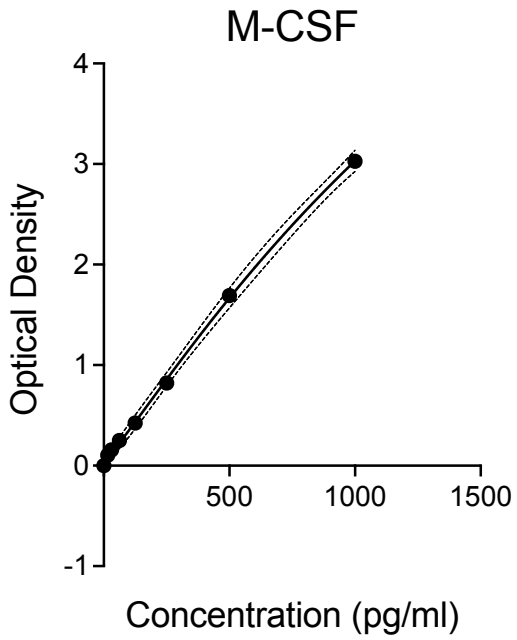

C

	Concentration (pg/mL)	Opitcal density
LCM	326.844	1.114

Figure 2.3.2.1. ***Concentration of M-CSF in L929 conditioned medium (LCM).*** **A.** The table presents the optical density values obtained for each standard used to generate the standard curve, as well as for the LCM sample. **B.** The standard curve was created to measure the concentration of M-CSF in the LCM sample. **C.** The table shows the concentration (pg/mL) of M-CSF in the LCM sample determined by ELISA.

2.3.3. Isolation and culture of murine BMDMs

C57BL/6J mice were euthanized and the femurs were extracted. The muscle, connective tissue and fat were removed and the femur was separated from the hip and the tibia. The joints on either side of the femur were removed in order to reveal the bone marrow (BM). The BM was removed using a 25 G needle containing 10 mL ice-cold D-PBS. BM cells were flushed through a 100 μm cell strainer into a 50 mL tube. Tubes were centrifuged at 1,200 rpm for 5 min. The supernatant was removed and the cell pellet was resuspended in 5 mL ACK lysing buffer. The cells were incubated for 5 min at room temperature to ensure lysis of red blood cells. D-PBS was used to bring the volume of the cell suspension to 50 mL. Again, the cell suspension was passed through a 100 μm cell strainer, into a different 50 mL tube. The tube was centrifuged at 1,200 rpm for 5 min. The supernatant was removed and the pellet was resuspended in 2.6 mL DMEM supplemented with 20% LCM, 10% FBS and 1% Pen-Strep. 200 μL of the cell suspension was added to each well of a tissue culture treated 6-well plate. The plates were placed into the incubator at 37°C with 5% CO_2, for 15 min, to allow the cells to adhere to the plate. After this time, an additional 2 mL of cell culture growth media was added to each well and the plates were placed back into the incubator. The growth media was replaced every 2-3 days.

2.3.4. Transfection of murine BMDMs with synthetic miRNA mimics

Synthetic miRNA mimics are chemically modified double-stranded RNA molecules that are designed to mimic endogenous miRNAs. These mimics have two strands – the mature or guide strand, that is utilised by Argonaute proteins to target mRNAs, and the passenger strand, which is typically degraded. In this case, synthetic *mmu-miR-223-3p* and *mmu-miR-223-5*p mimics were used to overexpress both strands of the miRNA, *miR-223*, resulting in the downregulation of target mRNA translation due to mRNA sequestration or degradation (**Figure 2.3.4.1**).

On day 7 post BMDM isolation, myeloid progenitor cells had differentiated into naïve macrophages and were ready to undergo the transfection procedure.

Culture supernatant was removed from each well, the well was washed with 1 mL warm D-PBS and then replaced with 1 mL OPTI-MEM. The plate was incubated at 37°C, 5% CO_2. Solutions composed of 30% Lipofectamine 3000 in OPTI-MEM were prepared. 5 nmol stock solutions of *mmu-miR-223-3p* mimic, *mmu-miR-223-5p* mimic and miRNA negative control mimic were diluted to a final concentration of 6 nmol/ml in the 30% Lipofectamine 3000 in OPTI-MEM solution. The transfection solutions were incubated at room temperature for 10 min. Following this, 20 μL of each transfection solution was added to the appropriate wells resulting in a final concentration of 120 pmol/mL of each mimic per well. Cells were incubated with the transfection solutions for 24 h at 37°C, with 5% CO_2. The OPTI-MEM and transfection solutions were removed from each well and replaced with 2 mL cDMEM, to allow the cells to rest for 24 h prior to subsequent experiments.

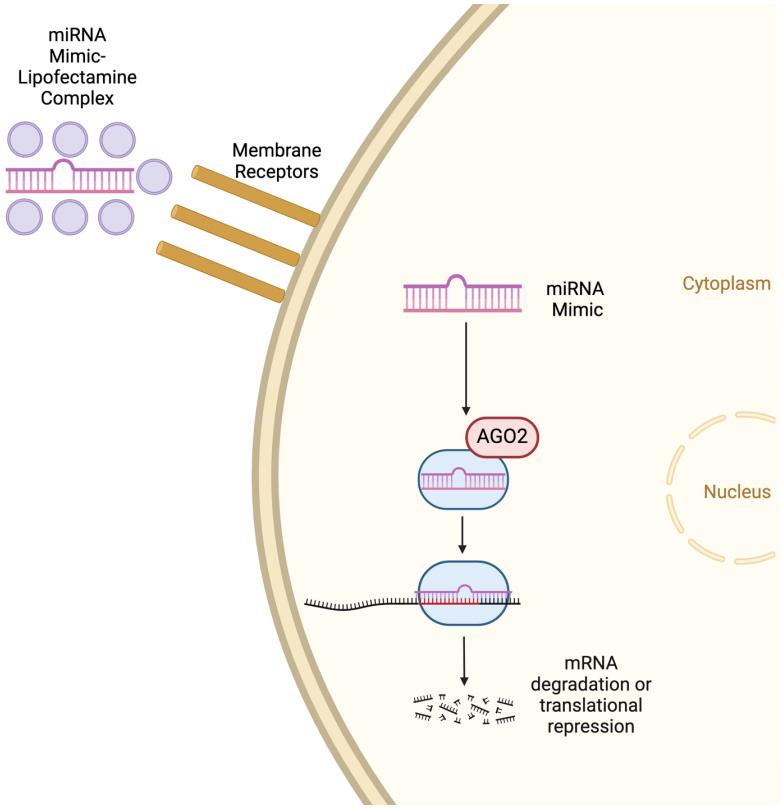

Figure 2.3.4.1. ***Synthetic miRNA mimic transfection.*** Synthetic miRNA mimics are chemically modified double-stranded RNA molecules that are designed to mimic endogenous miRNAs. Similar to native miRNA, these mimics have two strands – the mature, or guide strand, which is functional and utilised by argonaute proteins to target mRNA, and the passenger strand, which is typically degraded. Synthetic mimics result in the down-regulation of target mRNA translation due to mRNA sequestration or degradation.

2.3.5. Pre-treatment of BMDMs with tomivosertib

A 1 h pre-treatment with the small molecule inhibitor tomivosertib, was applied to BMDMs prior to experimental stimulation. The dose used was identified by literature review, with the final concentration indicated in **Table 2.27.**

2.3.6. Stimulation of BMDMs with LPS, IFNγ or IL-4

On day 7, BMDMs were stimulated with cytokines in order to generate distinct activation states. These stimulations included; LPS (100 ng/mL), IFNγ (10 ng/mL)

or IL-4 (10 ng/mL). BMDMs were incubated for 6 h or 24 h before being harvested for further analysis (**Figure 2.3.6.1**).

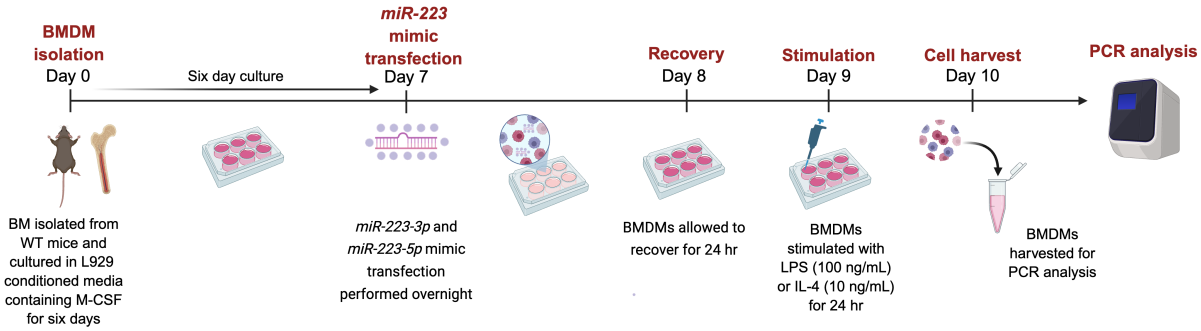

Figure 2.3.6.1. ***Transfection of primary BMDMs with miR-223 synthetic mimics.*** BM was isolated from the femurs of WT mice and cultured in L929 conditioned medium, which contains M-CSF, for six days. This resulted in the differentiation of common myeloid progenitor cells into mature naïve macrophages. On day 7, BMDMs were transfected with *miR-223-3p* and *miR-223-5p* synthetic mimics overnight. On day 8, the cells were allowed to recover for 24 h in cDMEM. BMDMs were stimulated on day 9 with LPS or IL-4 for 24 h before collecting for PCR analysis on day 10.

2.3.7. Culture of RAW 264.7 macrophage cell line

RAW 264.7 is an adherent macrophage cell line that was isolated from a male mouse tumour that was induced by intraperitoneal injection of the Abelson murine leukaemia virus.

A frozen cryovial of RAW 264.7 cells was rapidly thawed in a beaded bath at 37°C. The vial was washed with 1 mL of cDMEM (without antibiotic). The cell suspension was transferred to one 15 mL falcon tube containing 1 mL of warm cDMEM. The tube was centrifuged at 1,500 rpm for 5 min and the supernatant was removed. The cell pellet was resuspended in 5 mL cDMEM and transferred to a T25 flask. The cells were incubated at 37°C, 5% CO_2, overnight to grow to 70% confluency.

Cells were mechanically removed by scraping and placed into a 50 mL tube. The tube was centrifuged at 1,500 rpm for 5 min at room temperature. The supernatant was removed and the pellet was resuspended in cDMEM. For

subculturing, a 1:5 or 1:10 split was performed, and the cells were cultured in a T75 flask. When seeding for an experiment, cells were plated at a density of 0.2 x 10^6 cells per well on a 6-well flat bottom cell culture plate with a final volume of 2 mL cDMEM. For all experiments, the cDMEM was changed prior to stimulations or treatments.

2.3.8. Stimulation RAW 264.7 macrophage cell line with LPS, IFNγ or IL-4

RAW 264.7 cells were stimulated with cytokines in order to generate distinct activation states. These stimulations included; LPS (100 ng/mL), IFNγ (10 ng/mL) or IL-4 (10 ng/mL). These cells were incubated for 30 min, 6 h or 24 h before being harvested for further analysis.

2.3.9. miRNA stability assay using Actinomycin D

RAW 264.7 cells were pre-stimulated with LPS or IL-4 for 30 min. Following this, cells were treated with Actinomycin D for 30 min. The dose used was identified by literature review, with the final concentration indicated in **Table 2.27.**

2.3.10. Puromycin kill curve for the selection of lentiviral transduced RAW 264.7 cells

RAW 264.7 cells were subjected to increasing amounts of puromycin in order to determine the minimum concentration of the antibiotic that can kill all cells during a specific period of time.

Cells were plated at a density of 0.1 x 10^6 cells per well on a 24-well flat bottom cell culture plate with a final volume of 1 mL cDMEM. The cells were incubated at 37°C, 5% CO_2, overnight to grow to 50% confluency.

The cDMEM was replaced with medium containing varying concentrations of puromycin, including 0 μg/mL, 1 μg/mL, 2 μg/mL, 5 μg/mL, 7 μg/mL and 10 μg/mL, with cells being treated with Triton X overnight to act as a positive control for cell death. Each concentration was maintained in triplicates. The medium

containing antibiotic was replaced every 48 h. The cells were maintained for 7 days and then cell viability was determined using a 3-(4,5-dimethylthiazol-2-yl)-5-(3-carboxymethoxyphenyl)-2-(4-sulfophenyl)-2H-tetrazolium (MTS) assay and cell damage was measured using a lactate dehydrogenase (LDH) activity assay.

2.3.11. Determination of cell death using a LDH activity assay

The master reaction mix was prepared by adding 48 μL of the LDH assay buffer and 2 μL of the LDH substrate mix per reaction. 50 μL of the master reaction mix was added to each well of a 96 well flat-bottom plate. After 3 min, the initial absorbance measurement was taken at 450 nm. The plate was incubated at 37°C, 5% CO_2, and absorbance measurements were taken every 5 min. Measurements were taken until the most active sample was greater than the value of the highest standard. The penultimate reading was considered the final measurement. This reading for the 0 mM NADH standard was subtracted from the final measurement for all samples and standards in order to correct for the background.

The NADH standard curve was plotted. The ΔA_{450} was determined for each sample and this was compared to the standard curve in order to ascertain the amount of NADH generated by the assay between the initial time ($T_{initial}$) and the final time (T_{final}).

The LDH activity of each sample was then determined using the following equation:

$$\text{LDH Activity} = \frac{B}{(\text{Reaction Time}) \times V} \times \text{Sample Dilution Factor}$$

B = Amount (nmole) of NADH generated between the $T_{initial}$ and T_{final}.

Reaction Time = $T_{final} - T_{initial}$ (minutes).

V = Sample volume (mL) added to each well.

2.3.12. Determination of cell viability using a MTS assay

The CellTiter 96 AQ_{ueous} One Solution Reagent was thawed in a beaded bath at 37°C. 100 μL of the CellTiter 96 AQ_{ueous} One Solution Reagent was added to

each well of the 24-well cell culture plate. The plate was incubated at 37°C, 5% CO_2, for 4 h. The absorbance was then measured at 490 nm. The absorbance value for the positive control for cell death was subtracted from the value for each puromycin concentration.

2.3.13. Lentiviral transduction of RAW 264.7 macrophage cell line

Lentiviral transduction particles were used to generate *miR-223* knockdown (KD) and negative control (Scramble control) RAW 264.7 macrophage cell lines (**Figure 2.3.13.1**). These cells were utilised as an experimental tool system to assess *miR-223* biology in macrophage.

Cells were plated at a density of 0.2 x 10^6 cells per well on a 6-well flat bottom cell culture plate with a final volume of 2 mL cDMEM. The cells were incubated at 37°C, 5% CO_2, overnight to grow to 70% confluency.

Cells were washed with warm 1X D-PBS (Ca^{2+}/Mg^{2+} free). The lentiviral transduction particles were thawed slowly on ice. 2 mL of cDMEM and 8 μg/mL Polybrene solution was added to each well. 100 μL of MISSION Lenti miRNA Inhibitor *mmu-miR-223-3p* (*miR-223KD*) and miRNA inhibitor Negative control (Scramble control) particles were added to the appropriate wells. The cells were incubated at 37°C, 5% CO_2, overnight.

After 24 h, the transduction solution was removed from each well and was replaced with 2 mL cDMEM. The cells were returned to incubate at 37°C, 5% CO_2, until they achieved 70% confluency.

Once confluency was achieved, antibiotic selection was started by replacing the cDMEM with cDMEM that contained 2 μg/mL puromycin. Growth of cells was monitored. When control cells were near 100% death and lentiviral transduced cells were at 90% confluency, cells were sub-cultured into a T25 flask with puromycin-containing media. Cells were cultured for a number of days and were later seeded for validation experiments.

When seeding for additional experiments, cells were plated at a density of 0.2 x 10^6 cells per well on a 6-well flat bottom cell culture plate with a final volume of 2 mL cDMEM. For all experiments, the cDMEM was changed prior to stimulations or treatments (**Figure 2.3.13.2**).

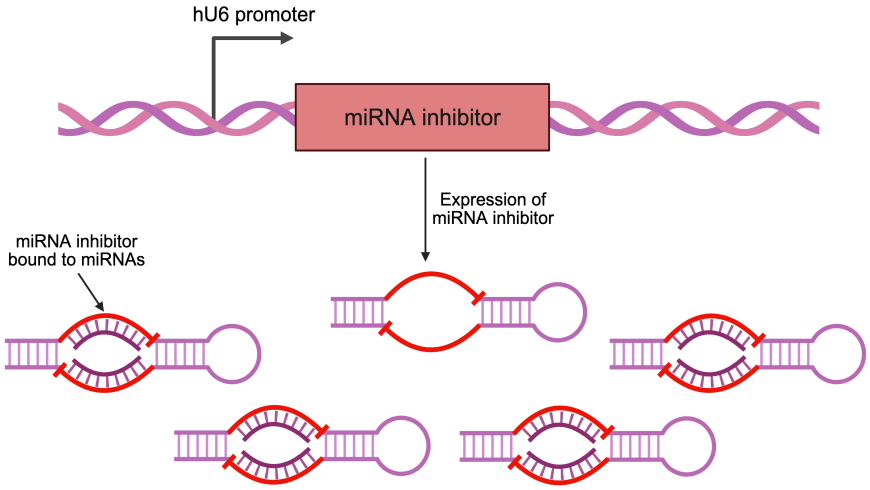

Figure 2.3.13.1. ***Lentiviral transduction of host cell to generate a miRNA knockdown cell line.*** The U6 promoter drives the expression of the miRNA inhibitor upon genomic integration of the lentiviral transfer vector in the host cell post-transduction. miRNA inhibitors have the ability to competitively bind to specific miRNAs in order to prevent them from regulating their endogenous targets.

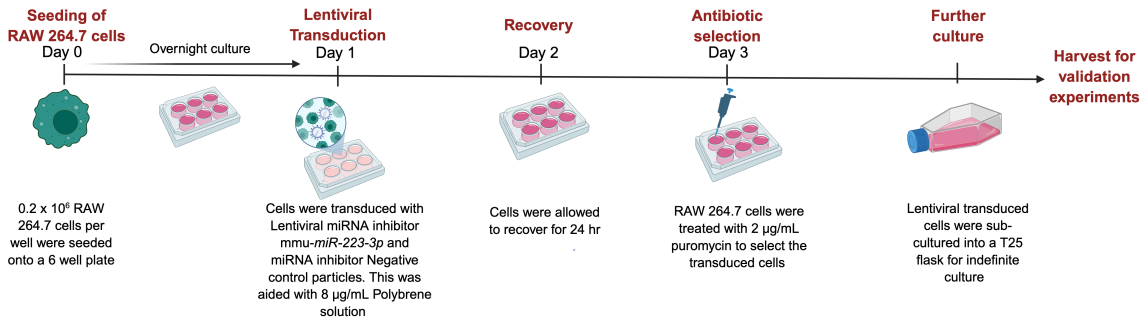

Figure 2.3.13.2. ***Lentiviral transduction of RAW 264.7 macrophage cell line to generate Scramble control and miR-223KD cell lines.*** 0.2 x 10^6 cells were seeded onto a 6 well plate and allowed to grow to 70% confluency overnight. Once confluent, MISSION Lenti miRNA inhibitor *mmu-miR-223-3p* and miRNA inhibitor Negative control particles with 8 µg/mL Polybrene solution were added to the appropriate wells. The cells were left to incubate overnight. The transduction medium was removed and replaced with fresh cDMEM, in order for cells to recover for 24 h. On day 3, antibiotic selection, with 2 µg/mL Puromycin, was started. Cells underwent antibiotic selection for a number of days and then were sub-cultured into a T25 flask. They were cultured indefinitely in puromycin containing medium, so as to create stocks of the lentiviral transduced cell lines and to seed cells for validation experiments.

2.3.14. Inhibitor pre-treatment of miR-223KD and Scramble control cell lines with actinomycin D and tomivosertib

MiR-223KD and Scramble control cell lines were pre-treated with actinomycin D and tomivosertib for 1 h prior to experimental stimulation. The dose used was identified by literature review, with the final concentration indicated in **Table 2.27.**

2.3.15. Stimulation of miR-223KD and Scramble inhibitor cell lines with LPS or IL-4

RAW 264.7, *miR-223KD* and Scramble control cell lines were stimulated with cytokines in order to generate distinct activation states. These stimulations included; LPS (100 ng/mL) or IL-4 (10 ng/mL). These cells were incubated for 6 h or 24 h before being harvested for further analysis.

2.3.16. Determination of protein translation using a Surface Sensing of Translation (SUnSET) assay

BMDMs*, miR-223*KD and Scramble control cell lines were cultured as per sections **2.2.3.3** and **2.2.3.12**. Following 24 h stimulation of cells with cytokines, 10 μg/mL of Puromycin was added to the appropriate wells for 15 min. Following this incubation, cells were harvested for protein analysis, as detailed in section **2.2.5**, and translation was assessed by western immunoblot, through the use of an anti-puromycin antibody.

2.3.17. Generation of murine colonic epithelial organoids

C57BL/6J mice were euthanized and the colons were extracted, ensuring to cut the colon a few millimetres below the cecum and above the rectum. The colonic segment was gently flushed with 1 mL of D-PBS. The intestinal section was cut lengthwise in order to expose the lumen of the intestine, and the intestinal sheet was washed with 1 mL D-PBS three times. The intestinal segment was transferred and cleaned in a petri dish containing cold D-PBS. The intestine was cut in 2 mm pieces and placed in a 50 mL falcon tube containing 15 mL cold D-PBS. These colon pieces were pipetted up and down three times, allowed to settle to the bottom of the tube and the supernatant was carefully removed. This step was repeated 15 times in total. The supernatant was removed, the tissue pieces were resuspended in 25 mL room temperature gentle cell dissociation reagent and incubated at room temperature for 20 min on a rocking platform at 20 rpm. The tissue segments were allowed to settle to the bottom and then the supernatant was removed. The tissue pieces were resuspended in cold 10 mL D-PBS containing 0.1% BSA and pipetted up and down three times. The supernatant was removed and passed through a 70 μm filter. The filtrate was collected in a 50 mL falcon tube, labelled fraction 1 and placed on ice. The generation of fractions was repeated three times. All fractions were centrifuged at 300 *rcf* for 5 min at 4°C and the supernatant was removed. The pellets were resuspended in 10 mL cold D-PBS containing 0.1% BSA. All fractions were centrifuged at 200 *rcf* for 3 min at 4°C to pellet the colonic crypts and the supernatant was removed. Each pellet was resuspended in 1 mL D-PBS. 10 μL of each fraction was placed onto a hemacytometer and the number of crypts were

counted. This number was multiplied by 100 to calculate the number of crypts per mL for each fraction. Samples were centrifuged at 200 *rcf* for 5 min at 4°C, the supernatants were removed and the pellets were resuspended in 150 μL complete IntestiCult Organoid Growth Media. 150 μL undiluted Matrigel Matrix was added to each cell organoid suspension. Using a pre-wet pipette, 50 μL of the suspension was carefully pipetted into the centre of each well on a pre-heated 24-well flat bottom cell culture plate. The samples formed domes and were incubated at 37°C for 20 min. When the domes had solidified, 750 μL complete IntestiCult OGM was added to each well. Sterile D-PBS was added to the unused wells. The organoids were incubated at 37°C, 5% CO_2. The Intesticult OGM was replaced every 2-3 days.

2.3.18. Maintenance of primary murine colonic epithelial organoids

The medium was removed from each well. 500 μL of Gentle Cell Dissociation Reagent was added to the exposed dome in each well and incubated at room temperature for 1 min. The dome was broken up by pipetting the Gentle Cell Dissociation Reagent up and down ten times. The suspension was transferred to a 15 mL falcon tube. This step was repeated an additional time. The culture well was rinsed with an additional 250 μL Gentle Cell Dissociation Reagent and this was added to the 15 mL falcon tube. These steps were repeated for each well to be passaged.

The 15 mL falcon tubes were incubated at room temperature on a rocking platform at 20 rpm for 10 min. The tubes were centrifuged at 300 *rcf* for 5 min at 4°C. The supernatant was removed. The pellets were washed with 10 mL cold DMEM/F12 and then the tubes were centrifuged at 200 *rcf* for 5 min at 4°C. The supernatant was discarded.

Each pellet was resuspended in a 1:1 mix of IntestiCult OGM and Matrigel. 50 μL of this suspension was loaded onto a pre-heated 24-well flat bottom plate to form a dome in each well. The plate was incubated at 37°C, 5% CO_2, for 20 min. Once the domes had solidified, 750 μL complete IntestiCult OGM was added to each

well. The organoids were then incubated at 37°C, 5% CO_2. The IntestiCult OGM was replaced every 2-3 days.

2.3.19. Pharmacological blockade of STAT3 signalling in primary murine colonic epithelial organoids

On day 3 post passage, colonic epithelial organoids were pre-treated with Stattic, a STAT3 inhibitor, for 1 h prior to experimental stimulation. The dose used was identified by literature review, with the final concentration indicated in **Table 2.27.**

2.3.20. Recombinant IL-6, LIF and IL-11 cytokine stimulation of primary murine colonic epithelial organoids

On day 3 post passage, murine colonic epithelial organoids were stimulated with members of the IL-6 family of cytokines. These stimulations included; IL-6 (10 ng/mL), LIF (50 ng/mL) or IL-11 (10 ng/mL). These cells were incubated for 3 days before being harvested for further analysis.

2.3.21. Indirect co-culture of murine colonic epithelial organoids with conditioned media from BMDMs overexpressing miR-223-3p or miR-223KD cell line

Murine colonic epithelial organoids were cultured as previously described. On day 3 and day 5 post-passage, complete medium was removed from each well. This was replaced with a 1:1 mix of complete IntestiCult OGM and conditioned media from BMDMs overexpressing *miR-223-3p* or *miR-223KD* cell line. Organoids were cultured in this media mix for 3 h and 24 h before being harvested for further analysis.

2.3.22. Direct co-culture of murine colonic epithelial organoids with miR-223KD and Scramble control cell lines

*miR-223*KD and Scramble control cell lines were plated at a density of 0.2 x 10^6 cells per well on a 6-well flat bottom cell culture plate with a final volume of 2 mL

cDMEM. The cells were incubated at 37°C, 5% CO_2, to grow to 70% confluency. Once confluency was achieved, cells were stimulated with LPS (100 ng/mL) or IL-4 (10 ng/mL) for 24 h, before being harvested, counted and pelleted for the co-culture experiment.

Murine colonic epithelial organoids were mechanically passaged as previously described, with a 1:8 split. These organoids suspended in organoid complete medium were mixed with the pelleted *miR-223*KD and Scramble control cell lines, to give a final number of 8,000 macrophages per organoid dome. Matrigel was added to this suspension, to give a final ratio of 1:1 organoid/macrophage suspension and Matrigel. 25 μL of this suspension was loaded onto a pre-heated 48-well flat bottom plate to form a dome in each well. The plate was incubated at 37°C, 5% CO_2, for 20 min. Once the domes had solidified, 350 μL complete IntestiCult OGM was added to each well. The organoids were then incubated at 37°C, 5% CO_2. The IntestiCult OGM was replaced every 2-3 days. Organoids were cultured for 6 days before being harvested for further analysis.

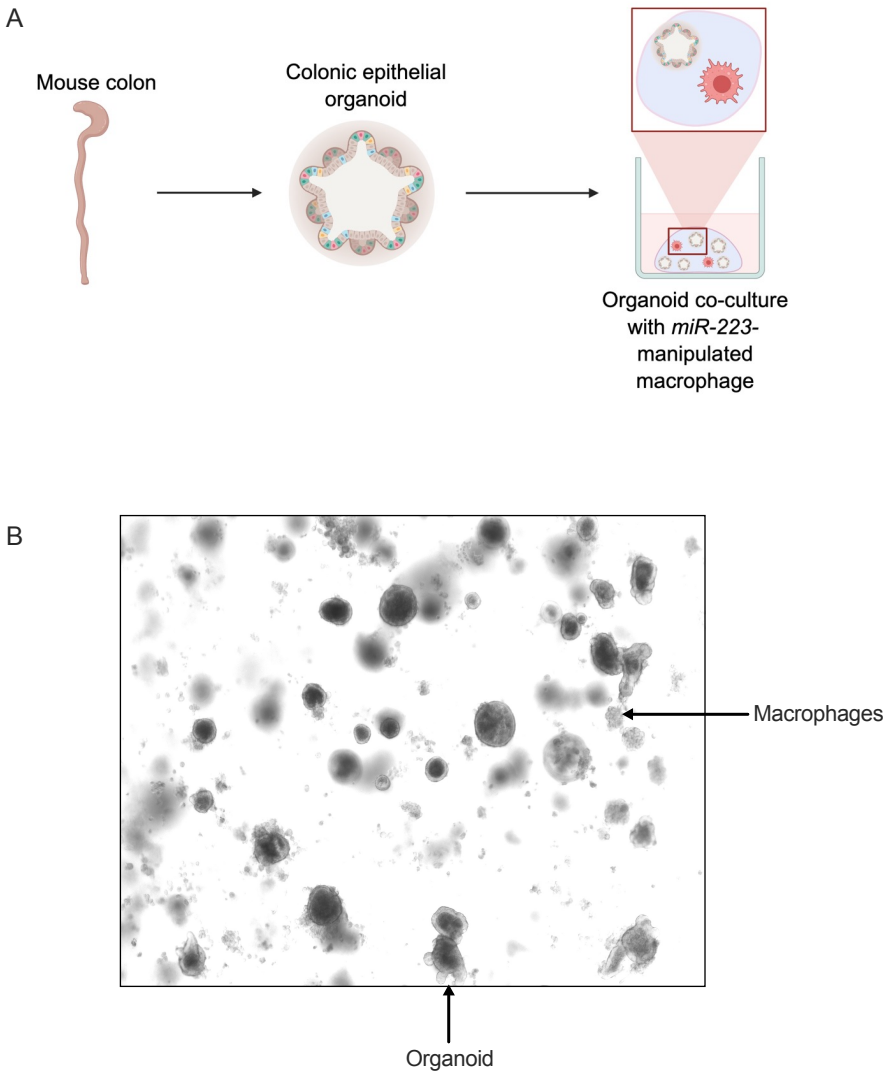

Figure 2.3.22.1. ***Direct co-culture of murine colonic epithelial organoids with miR-223KD and Scramble control cell lines.*** **A.** Diagram depicting the generation of the direct co-culture system of colonic epithelial organoids and *miR-223*-manipulated macrophages. **B.** Representative 4X image of colonic epithelial organoids co-cultured with *miR-223*-manipulated macrophages.

2.3.23. Pharmacological blockade of STAT3 signalling in primary murine colonic epithelial organoids that were co-cultured with miR-223KD and Scramble control cell lines

On day 4 post passage, colonic epithelial organoids were treated with Stattic inhibitor. The dose used was identified by literature review, with the final concentration indicated in **Table 2.27.**

Table 2.27. ***Inhibitors used in cell culture.***

Inhibitor	Target	Concentration
Actinomycin D	Inhibitor of RNA polymerase	5 μg/mL
Tomivosertib	Selective inhibitor of MNK1 and MNK2 activity	1 μM
Stattic	Selective inhibitor of STAT3 activity	500 nM

2.4. Ribonucleic acid (RNA) analysis

2.4.1. Isolation of messenger RNA (mRNA) from cells

Total mRNA was extracted from cell cultures using the EasyPure RNA Kit (Transgen Biotech) as per the manufacturer's instructions. Briefly, medium was removed from each well and the well was rinsed with 1 mL pre-warmed D-PBS. This was removed and replaced with 175 μL of BB4, containing 1% 2-Merceptoethanol, per well. Cells were mechanically removed by scraping and transferred to a 1.5 mL Eppendorf tube.

Equal volume of 70% ethanol was added to the cell suspension, which was then vortexed to disperse any precipitate. The entire mixture was then transferred to a spin column. This was centrifuged at 12,000 *rcf* for 30 s at room temperature and the flow-through was discarded. 500 μL CB4 was added to the spin column and this was centrifuged at 12,000 *rcf* for 30 s at room temperature. The flow-through was discarded. This step was repeated once. 500 μL WB4 was added to the spin column and this was centrifuged at 12,000 *rcf* for 30 s at room temperature. The flow-through was discarded. This step was repeated once. The empty column was centrifuged 20,817 *rcf* (maximum speed) for 2 min at room temperature in order to remove residual ethanol.

The spin column was transferred to a new 1.5 mL Eppendorf tube. 30 μL RNase-free water was added directly onto the centre of the membrane and incubated at room temperature for 1 min. This was centrifuged at 12,000 *rcf* for 2 min at room temperature to elute the mRNA.

2.4.2. Isolation of mRNA from primary murine colonic epithelial organoids

Total RNA was extracted from organoids using a modified protocol from Stem Cell Technologies. Briefly, medium was removed from each well and 500 μL of DMEM/F12 with 1% FBS was added directly on top of the exposed dome. The dome was broken down by pipetting the suspension up and down twenty times and transferred to a 1.5 mL Eppendorf tube. The cell culture well was rinsed with 250 μL DMEM/F12 with 1% FBS and this was added to the Eppendorf tube. The tubes were then centrifuged at 300 *rcf* at room temperature for 5 min. The supernatant was removed and the pellet was resuspended in 175 μL of BB4, containing 1% 2-Merceptoethanol. RNA was extracted as previously described in section **2.4.1.**

2.4.3. Isolation of miRNA from cells

MiRNA was extracted from cell cultures using the RNeasy Kit (Qiagen). Briefly, medium was removed from each well and the well was rinsed with 1 mL pre-warmed D-PBS. This was removed and replaced with 200 μL of QiAzol per sample. Cells were mechanically removed by scraping and transferred to a 1.5 mL Eppendorf tube.

40 μL of chloroform was added to each tube, and these were inverted twenty times. The samples were incubated for 3 min at room temperature. The tubes were then centrifuged at 13,000 rpm for 15 min at 4°C. The clear aqueous layer containing RNA was aspirated off and placed into a 1.5 mL Eppendorf tube. 80 μL of 70% ethanol was added to the tube and this was then transferred to a spin column. The column was centrifuged at 13,000 rpm for 1 min at room temperature. The flow-through was enriched in miRNA.

500 μL of 100% ethanol was added to the flow through. This was loaded into a new spin column and was centrifuged at 13,000 rpm, for 1 min at room temperature. The flow-through was discarded. 500 μL of RPE was added to the column and was centrifuged at 13,000 rpm for 20 s at room temperature. The

flow-through was discarded. 500 μL of 80% ethanol was added to the spin column and was centrifuged at 13,000 rpm for 2 min at room temperature. The flow-through was discarded. The spin column was transferred to a new 1.5 mL Eppendorf tube and was centrifuged at 10,000 rpm for 3 min at room temperature, in order to dry the membrane.

Again, the spin column was transferred to a new 1.5 mL Eppendorf tube. 20 μL RNase-free water was added directly onto the centre of the membrane. This was centrifuged at 13,000 rpm for 1 min at 4°C to elute the miRNA.

2.4.4. RNA quantification

RNA concentration was obtained by nano-drop spectrophotometry, measuring the absorbance at 260 nm. The quality of the samples was determined by a 260/280 ration, which was ≥ 1.8 for pure mRNA or miRNA, and by a 260/230 ration, which was ≥ 2 for uncontaminated RNA. RNA was equalised using nuclease-free water.

2.4.5. Complementary deoxyribonucleic acid (cDNA) synthesis from mRNA

cDNA was synthesized from mRNA isolated from cells and organoids using the High-Capacity cDNA Reverse Transcription kit (Applied Biosystems). The 2X reverse transcription (RT) master mix was prepared as per **Table 2.28.** 10 μL of the master mix was added to each polymerase chain reaction (PCR) tube. 10 μL of the equalised mRNA was added to the PCR tubes. There was a final volume of 20 μL in each tube. The samples were placed into a thermocycler (Applied Biosystems) and the program, as per **Table 2.29**, was used for the cDNA synthesis. cDNA was diluted 1:10 with nuclease-free water.

Table 2.28. ***Components used to make 2X RT master mix for use with mRNA.***

Component	Volume added (μL)
10X RT buffer	2.0
25X deoxynucleotide triphosphates (dNTP) mix (100 nM)	0.8
10X RT random primers	2.0
MultiScribe reverse transcriptase	1.0
Nuclease-free water	4.2

Table 2.29. ***Thermocycler conditions used for cDNA synthesis from mRNA.***

Setting	Step 1	Step 2	Step 3	Step 4
Temperature (°C)	25	37	85	4
Time (min)	10	120	5	Hold

2.4.6. Taqman RT-PCR

Taqman Fast Advanced master mix and primers (Applied Biosystems) were used for RT-PCR. Master mix was prepared as per **Table 2.30.** 5.5 μL of master mix was added to each well of 96-well PCR plate (Applied Biosystems). 5.5 μL of diluted cDNA was added to the appropriate wells. The plate was sealed using adhesive PCR plate seals. The plate was centrifuged at 1,000 *rcf* for 1 min at 4°C, to ensure a homogenous mixture is brought to the bottom of each well. The plate was inserted into a StepOne RT-PCR machine (Applied Biosystems) and the program was run, as described in **Table 2.31**. Changes in gene expression, given as cycle threshold (CT) values, were normalised to 18S expression.

Table 2.30. ***Components used to make Taqman RT-PCR master mix.***

Component	Volume added (μL)
Taqman Fast Advanced master mix	5.0
Taqman primer	0.5

Table 2.31. ***Taqman RT-PCR conditions.***

Uracil-N-glycosylase (UNG) incubation	**Polymerase activation**	**PCR (40 cycles)**	
Hold 50°C	Hold 95°C	Denature 95°C	Anneal/extend 60°C
2 min	2 min	1 s	20 s

2.4.7. cDNA synthesis from miRNA

cDNA was synthesised from miRNA isolated from cells using the miRCURY LNA RT kit (Qiagen). miRNA was equalised to 5 ng/μL. The RT reaction master mix was prepared as per **Table 2.32.** 8 μL of the master mix was added to each PCR tube. 2 μL of the equalised miRNA was added to the PCR tubes. There was a final volume of 10 μL in each tube. The samples were placed into a thermocycler (Applied Biosystems) and the program, as per **Table 2.33**, was used for the cDNA synthesis. cDNA was diluted 1:60 with nuclease-free water.

Table 2.32. ***Components used to make RT master mix for use with miRNA.***

Component	**Volume added (μL)**
5X miRCURY SYBR Green RT reaction buffer	2.0
RNase-free water	5.0
10X miRCURY RT enzyme mix	1.0

Table 2.33. ***Thermocycler conditions for cDNA synthesis from miRNA.***

Step	**Time (min)**	**Temperature (°C)**
RT step	60	42
Inactivation of reaction	5	95
Storage	∞	4

2.4.8. SYBR Green RT-PCR for miRNA targets

The miRCURY LNA SYBR PCR kit (Qiagen) was used for RT-PCR. Master mix was prepared as per **Table 2.34.** 7 μL of master mix was added to each well of 96-well PCR plate (Applied Biosystems). 3 μL of diluted cDNA was added to the appropriate wells. The plate was sealed using adhesive PCR plate seals. The plate was centrifuged at 1,000 *rcf* for 1 min at 4°C, to ensure a homogenous mixture is brought to the bottom of each well. The plate was inserted into a StepOne RT-PCR machine (Applied Biosystems) and the program was run, as described in **Table 2.35**. Changes in gene expression, given as CT values, were normalised to RNU6 expression.

Table 2.34. ***Components used to make SYBR Green RT-PCR master mix.***

Component	Volume added (μL)
2X miRCURY SYBR Green master mix	5.0
ROX Reference Dye	0.5
Primer	1.0
RNase-free water	0.5

Table 2.35. ***SYBR Green RT-PCR cycling conditions.***

Step	Time	Temperature	Ramp rate
PCR initial heat activation	2 min	95°C	Maximal/fast mode
2-step cycling			
Denaturation	10 s	95°C	Maximal/fast mode
Combined annealing/extension	60 s	56°C	Maximal/fast mode
Number of cycles	40		
Melting curve analysis		60-95°C	

2.5. Protein analysis by western immunoblot

2.5.1. Protein extraction from cells

Medium was removed from each well and the well was rinsed with 1 mL pre-warmed D-PBS. This was removed and replaced with 200 μL of RIPA buffer, containing 1% protease and phosphatase inhibitors, per well. Cells were mechanically removed by scraping and transferred to a 1.5 mL Eppendorf tube.

Samples were centrifuged at 20,000 *rcf* for 15 min at room temperature, in order to remove any insoluble material.

2.5.2. Protein extraction from murine colonic epithelial organoids

Medium was removed from each well and 500 μL of DMEM/F12 with 1% FBS was added directly on top of the exposed dome. The dome was broken down by pipetting the suspension up and down twenty times and transferred to a 1.5 mL Eppendorf tube. The cell culture well was rinsed with 250 μL DMEM/F12 with 1% FBS and this was added to the Eppendorf tube. The tubes were then centrifuged at 300 *rcf* at room temperature for 5 min. The supernatant was removed and the pellet was resuspended in 100 μL RIPA buffer, containing 1% protease and phosphatase inhibitors, per sample.

Samples were centrifuged at 20,000 *rcf* for 15 min at room temperature, in order to remove any insoluble material.

2.5.3. Bicinchoninic acid (BCA) assay

Protein concentration was determined by BCA assay (Pierce BCA protein assay kit, ThermoFisher Scientific). Briefly, BSA protein standards ranging from 0 - 2,000 μg/mL were prepared. 10 μL of each standard was added to the appropriate wells of a 96-well plate, in duplicate. 10 μL of each sample was added to the allocated wells, in duplicate. The BCA working reagent was prepared at a ratio of 50:1, reagent A and reagent B. 200 μL of the working reagent was added

into each well. The plate was covered and incubated at 37°C for 20 min. The absorbance of the standards and samples was measured at 562 nm. The readings for the standards were plotted to create a standard curve. The readings for each sample were compared to the standard curve in order to ascertain the protein concentration.

The protein samples were prepared with 4x Laemmli sample buffer to give a final concentration 10 μg. The samples were placed in a thermocycler, and they were boiled at 95°C for 10 min.

2.5.4. SDS-polyacrylamide gel electrophoresis (SDS-PAGE) gel preparation

SDS-PAGE gels were prepared depending on the molecular weight of the protein of interest. The composition for the specific resolving and stacking gels is detailed in **Table 2.36**. The gels were cast in 1.5 mm glass plates. The resolving gel was prepared first, and once poured, it was covered with 70% ethanol to remove bubbles. When it had polymerized, the 70% ethanol was removed and the stacking gel was prepared. The stacking gel was poured directly on top of the resolving gel, and a comb was inserted. 10 well or 15 well combs specified for 1.5 mm casts were used to create protein loading wells. Gels were used immediately or stored at 4°C for a maximum of one week.

2.5.5. Gel electrophoresis

Gels were assembled in an electrophoresis chamber filled with 1X SDS Running buffer. The comb was carefully removed and 8 μL of protein molecular weight ladder was added to a well. 10 μg of protein sample was loaded into the designated wells. The electrophoresis was run at 80V for 20 min and then 110V for the remaining 1 h. Once finished, the gels were removed from the chamber and the stacking gel was discarded.

2.5.6. Semi-dry protein transfer

Extra thick filter paper and 0.2 μm nitrocellulose membrane were pre-soaked in 1X transfer buffer for 10 min before assembly of a transfer sandwich. The sandwich was arranged in the following order; filter paper, nitrocellulose membrane, gel and filter paper. This was placed on a Trans-blot semi-dry transfer rig (Bio-rad) and run for 80 min at 0.2 A.

2.5.7. Primary and secondary antibody staining

The nitrocellulose membrane was rinsed with 1X TBS-T and then blocked in 5% skimmed milk in 1X TBS for 30-60 min. After this incubation, the membrane was washed three times in 1X TBS-T for 5-10 min. The primary antibody was prepared in 5 mL blocking solution and incubated with the membrane overnight at 4°C with rotation. The membrane was washed three times in 1X TBS-T for 10-15 min and incubated with 5 mL of secondary antibody in blocking solution for 1 h at room temperature with rotation. The primary and secondary antibodies used are detailed in **Table 2.37.** The membrane was washed a further three times with 1X TBS-T for 10-15 min. The membrane was then incubated in 1 mL of a 1:1 solution of luminol/enhancer solution and stable peroxide solution (SuperSignal West Femto Maximum Sensitivity Substrate, ThermoFisher Scientific) for 3-5 min. The excess of this solution was removed and the membrane was placed in a ChemiDoc MP Imaging System (Bio-Rad). Membranes were imaged using the auto-exposure feature.

Table 2.36. ***Components used to make resolving and stacking gels.***

8% Resolving gel	**Volume added (μL)**	**10% Resolving gel**	**Volume added (μL)**	**Stacking gel**	**Volume added (μL)**
dH_2O	7.05 mL	dH_2O	15.75 mL	dH_2O	17.4 mL
4X 1.5 M Tris-HCL (pH 8.8)	3.75 mL	4X 1.5 M Tris-HCL (pH 8.8)	9.3 mL	4X 1.5 M Tris-HCL (pH 6.8)	7.5 mL
Acrylamide	4.05 mL	Acrylamide	12.6 mL	Acrylamide	4.95 mL
15% APS	75 μL	15% APS	225 μL	15% APS	90 μL
TEMED	13.5 μL	TEMED	21 μL	TEMED	30 μL

Table 2.37. ***Antibodies used for western immunoblot.***

Primary antibody	Blocking buffer	Working dilution	Secondary antibody	Working dilution
β-Actin	5% Milk/TBS	1:3,000 in 5% Milk/TBS	Goat anti-mouse IgG	1:10,000 in 5% Milk/TBS
DICER	5% Milk/TBS	1:1,000 in 5% Milk/TBS	Goat anti-rabbit IgG	1:5,000 in 5% Milk/TBS
P-4E-BP1	5% Milk/TBS	1:1,000 in 5% Milk/TBS	Goat anti-rabbit IgG	1:5,000 in 5% Milk/TBS
P-EIF4E	5% Milk/TBS	1:1,000 in 5% Milk/TBS	Goat anti-rabbit IgG	1:5,000 in 5% Milk/TBS
P-ERK1/2	5% Milk/TBS	1:1,000 in 5% Milk/TBS	Goat anti-rabbit IgG	1:5,000 in 5% Milk/TBS
P-MNK1	5% Milk/TBS	1:1,000 in 5% Milk/TBS	Goat anti-rabbit IgG	1:5,000 in 5% Milk/TBS
P-p38	5% Milk/TBS	1:1,000 in 5% Milk/TBS	Goat anti-rabbit IgG	1:5,000 in 5% Milk/TBS
P-S6	5% Milk/TBS	1:1,000 in 5% Milk/TBS	Goat anti-rabbit IgG	1:5,000 in 5% Milk/TBS
P-STAT3	5% Milk/TBS	1:500 in 5% Milk/TBS	Goat anti-rabbit IgG	1:5,000 in 5% Milk/TBS
PACT	5% Milk/TBS	1:1,000 in 5% Milk/TBS	Goat anti-rabbit IgG	1:5,000 in 5% Milk/TBS
Puromycin	5% Milk/TBS	1:1,000 in 5% Milk/TBS	Goat anti-mouse IgG	1:10,000 in 5% Milk/TBS
STAT3	5% Milk/TBS	1:500 in 5% Milk/TBS	Goat anti-rabbit IgG	1:5,000 in 5% Milk/TBS
TRBP2	5% Milk/TBS	1:200 in 5% Milk/TBS	Goat anti-rabbit IgG	1:5,000 in 5% Milk/TBS

2.5.8. Analysis of protein expression

Protein expression was analysed by densitometry using Image Lab software (BioRad). The band intensity for each sample was normalised to β-actin, the

housekeeping protein. The fold change is calculated from the resulting data and is used to perform statistical analysis in GraphPad Prism.

2.6. Secreted protein analysis by enzyme-linked immunosorbent assay (ELISA)

2.6.1. ELISA

This technique was performed using mouse DuoSet ELISA kit (R and D Systems), as per the manufacturer's instructions. The concentration of the reagents used are stated in **Table 2.38**. This procedure was performed on the cell culture supernatants.

Briefly, 100 μL of the capture antibody was added to the wells of a 96 well microplate. This was incubated at room temperature overnight. The capture antibody was removed and the wells were rinsed with 300 μL wash buffer three times. 300 μL blocking buffer was added to each well and the plate was incubated for 1 h at room temperature. The blocking buffer was discarded and the washing step was repeated. 100 μL of standards and supernatant samples were placed into the appropriate wells and left to incubate for 2 h at room temperature. The plate was washed, 100 μL of the detection antibody was added to each well and the plate was left to incubate for 2 h at room temperature. The detection antibody was removed from the wells and the wash step was repeated. 100 μL of the Streptavidin-HRP was added to each well. The plate was allowed to incubate for 20 min in the dark at room temperature. The plate was washed for a final time and 100 μL of 1-STEP ULTRA TMB-ELISA was added to the wells. Again, the plate was incubated in the dark for 20 min at room temperature. The enzyme reaction was stopped by adding 100 μL of stop solution to the wells.

The optical density values were measured spectrophotometrically at 450 nm, with wavelength correction being set at 540 nm. Secreted protein concentrations were determined from the standard curve generated using recombinant cytokines of known concentrations.

Table 2.38. ***Concentrations of reagents used for ELISA.***

Target	Capture Antibody	Detection Antibody	Standard
CXCL2	2 μg/mL	75 ng/mL	15.6-1000 pg/mL
IL-1β	4 μg/mL	250 ng/mL	15.6-1000 pg/mL
IL-6	2 μg/mL	75 ng/mL	15.6-1000 pg/mL

2.7. Immunohistochemistry (IHC)

2.7.1. IHC

Formalin-fixed and paraffin embedded (FFPE) tissue was cut into 5 μm sections using a microtome (Lecia), sections were placed onto polarised slides (VWR) and baked overnight at 60°C.

Slides were deparaffinized by sequential immersion as outlined in **Table 2.39.** Antigen retrieval was performed by heating slides in 1% citrate buffer in a pressure cooker at 110°C, 6.0 psi, for 10 min. Following this, slides were rinsed for 5 min in dH_2O and then allowed to re-equilibrate for 5 min in PBS. A hydrophobic barrier was drawn around each section. Sections were placed in a humidified chamber and permeabilised with 200 μL of 0.02% Triton X for 10 min. Slides were blocked for 30 min with 200 μL of 5% BSA/PBS with 2.5% normal horse serum at room temperature. Sections were incubated in the primary antibody overnight at 4°C. Primary antibodies were prepared as per **Table 2.40.**

Slides were washed for 5 min in PBS. Sections were incubated with 200 μL of the Biotinylated Universal Antibody (VECTASTAIN Elite ABC-HRP kit, Vector Laboratories) for 30 min at room temperature. Again, slides were washed in PBS. Sections were incubated with 200 μL of the R.T.U. VECTASTAIN Elite ABC

reagent (VECTASTAIN Elite ABC-HRP kit, Vector Laboratories) for 30 min at room temperature. Slides were washed for 5 min in PBS.

ImmPACT NovaRED was used as the peroxidase substrate solution. The peroxidase substrate working solution was prepared as detailed in **Table 2.41.** The sections were incubated in 200 μL of this working solution for up to 5 min, or until the desired stain intensity developed. Development was monitored using a microscope (Motic). The slides were rinsed in tap water and then counterstained using 10% Harris' Hematoxylin (Merck) for 1 min.

Slides were washed for 5 min in tap water and subsequently dehydrated by sequential immersion, as per **Table 2.42.** Slides were allowed to dry overnight in a fumehood (Astec). 10 μL of DPX mounting media was added to each section and a coverslip was applied. Slides were imaged using a microscope (EVOS).

Table 2.39. ***Sequential immersions for deparaffinizing FFPE slides for IHC.***

Component	Time (min)	Repetitions
100% Xylene	5	2
100% Ethanol	1	2
90% Ethanol	1	2
70% Ethanol	1	2
dH_2O	3	1

Table 2.40. ***Primary antibodies used for IHC.***

Antibody	Working dilution
β-CATENIN	1:14,000 in 5% BSA/PBS
CCR2	1:2,000 in 5% BSA/PBS
CD68	1:2,000 in 5% BSA/PBS
CD206	1:2,000 in 5% BSA/PBS
CYCLIN D1	1:2,000 in 5% BSA/PBS
LY6A	1:1,200 in 5% BSA/PBS
MERTK	1:2,000 in 5% BSA/PBS
MUC2	1:4,000 in 5% BSA/PBS
OLFM4	1:1,200 in 5% BSA/PBS
P-STAT3	1:1,200 in 5% BSA/PBS
PCNA	1:12,000 in 5% BSA/PBS
RELMα	1:4,000 in 5% BSA/PBS

Table 2.41. ***Components used to make ImmPACT NovaRed peroxidase substrate solution for IHC.***

Component	Volume added (μL)
Reagent 1	80.0
Reagent 2	50.0
Reagent 3	50.0
Reagent 4	80.0

Table 2.42. ***Sequential immersions to dehydrate FFPE slides for IHC.***

Component	Time (min)	Repetitions
70% Ethanol	2	1
90% Ethanol	2	1
100% Ethanol	1	1
100% Xylene	5	1

2.7.2. Quantification of IHC

IHC was analysed using QuPath software. Cells were detected based on the optical density. For each image, the number of positive cells was recorded, which was subsequently used for analysis in GraphPad.

2.8. *In situ* hybridization (ISH)

2.8.1. ISH

ISH was performed using miRNAsope HD Assay reagents and probes (ACD), as per the manufacturer's instructions. FFPE tissue was cut into 5 μm sections using a microtome (Lecia), sections were placed onto polarised slides (VWR) and left to air dry overnight at room temperature.

Slides were baked for 1 h at 60°C. Sections were deparaffinized by sequential immersion, as outlined in **Table 2.43.** Slides were left to dry at 60°C for 5 min. Once dry, slides were incubated in 10% NBF overnight at room temperature.

Slides were washed in dH_2O for 2 min and then dried at 60°C for 5 min. Sections were incubated in 200 μL RNAscope Hydrogen Peroxide for 10 min at room temperature. Slides were washed in dH_2O.

Antigen retrieval was performed by heating slides in 1X Target Retrieval reagent in a pressure cooker at 110°C, 6.0 psi for 15 min. Slides were rinsed in dH_2O and transferred to 100% ethanol for 3 min. Slides were then dried at 60°C for 5 min. A hydrophobic barrier was drawn around each section.

Sections were incubated in 200 μL RNAscope Protease III at 40°C for 30 min. Slides were washed in dH_2O. Sections were incubated in 200 μL in the target probe for 2 h at 40°C. Target probe information is detailed in **Table 2.24.** Slides were washed two times in 1X Wash Buffer for 2 min at room temperature.

Sections were incubated with Hybridize Amp 1 – 6 as per **Table 2.44**, with two wash steps, between each Hybridize Amp, in 1X wash buffer for 2 min at room temperature.

Each section was incubated in 120 μL of Fast Red working solution, with a final ratio of 1:60 Fast Red-B and Fast Red-A, for 10 min at room temperature. The slides were then washed two times in 1X wash buffer for 2 min at room temperature.

In order to counterstain the sections, the slides were placed into 50% Gill's Hematoxylin solution for 2 min at room temperature. They were immediately rinsed in tap water and then transferred into 0.02% Ammonia water until the sections turned blue. Again, the slides were rinsed with tap water.

Slides were allowed to dry at 60°C for 15 min. They were briefly dipped in 100% Xylene, 10 μL of DPX mounting media was added to each section and a coverslip was applied. Slides were imaged using a microscope (EVOS).

Table 2.43. ***Sequential immersions to deparaffinize FFPE slides for ISH.***

Component	Time (min)	Repetitions
100% Xylene	5	2
100% Ethanol	2	2

Table 2.44. ***Hybridization of probes to a cascade of signal amplification molecules.***

Component	Temperature (°C)	Time (min)
Hybridize Amp 1	40	30
Hybridize Amp 2	40	15
Hybridize Amp 3	40	30
Hybridize Amp 4	40	15
Hybridize Amp 5	Room temperature	30
Hybridize Amp 6	Room temperature	15

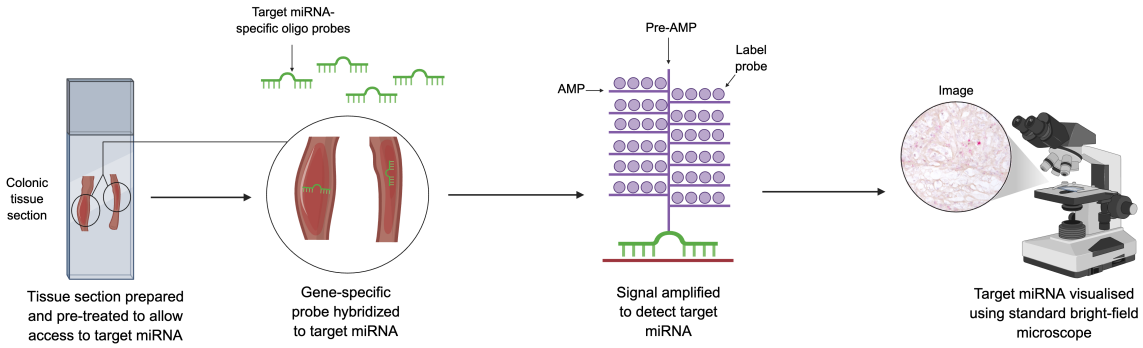

Figure 2.2.6. ***Overview of the ISH procedure.*** Colonic mouse tissue was prepared and pre-treated with RNAscope Hydrogen Peroxide, Protease III and 1X Target Retrieval reagents. Gene-specific probes are hybridized to the target miRNA and this miRNA was detected through the use of signal amplification systems. The tissue was imaged using a standard bright-field microscope and quantified using QuPath (the ISH image included in this schematic is derived from work presented in this thesis).

2.8.2. Quantification of ISH

ISH was analysed using QuPath software. Cells were detected based on the optical density. For each image, the number of positive cells was recorded, which was subsequently used for analysis in GraphPad.

2.9. Identification of *miR-223-3p* mRNA targets

TargetScan and miRTarBase were utilised to identify mRNA targets of *miR-223-3p*. TargetScan uses comparative sequence analysis to predict potential biological targets of specific miRNAs, based on the presence of 6mer, 7mer and 8mer conserved sites that match the seed region of *miR-223-3p*. In contrast to this, miRTarBase provides miRNA-target interactions that have been previously verified by biological experiments.

2.10. Statistical analysis

All statistical analysis was performed using GraphPad Prism software (version 10.6.0). The statistical tests used are detailed in the relevant figure legends. In experiments involving mouse tissues or BMDMs, each individual mouse was

considered a biological replicate. For cell culture studies, biological replicates were defined as independent cultures established and treated on separate occasions. Technical replicates were defined as multiple wells on the same cell culture plates.

CHAPTER 3

INVESTIGATING THE EXPRESSION AND FUNCTIONAL ROLE OF *MIR-223* DURING MACROPHAGE DEVELOPMENT AND ACTIVATION

The intestinal tract is the largest independent immune system in the body, with mononuclear phagocytes, comprising monocytes, macrophages and dendritic cells, representing the most numerous leukocytes in the intestine (Han *et al.*, 2021; Hegarty, Jones and Bain, 2023). Macrophages play a central role in tissue homeostasis, inflammation and resolution (Ginhoux and Guilliams, 2016). Examples of how they perform these roles include, recognising and neutralising foreign pathogens, removing damaged or exhausted cells and facilitating wound healing (Lazarov *et al.*, 2023; Gordon and Plüddemann, 2017).

Macrophages are present in most tissues and account for 10% of immune cells (Sender *et al.*, 2023). The lamina propria of the intestine is the most abundant in macrophage (Guan *et al.*, 2025). Macrophages are crucial cells in a complex environment like the GI tract, due to their ability to constantly respond to signals from their surroundings and modify their phenotype accordingly (Blériot, Chakarov and Ginhoux, 2020). Intestinal macrophages are distinguished from other immune cells by the expression of CSF1R, CD68 and FcγRI (Tamoutounour *et al.*, 2012; Domanska *et al.*, 2022). However, this macrophage pool consists of a heterogeneous mix of diversified and functionally specialised subsets (Viola and Boeckxstaens, 2021). In humans, expression of acid phosphatase 5, complement component 1q and interleukin-4-induced 1 identify subepithelial macrophages in the colonic lamina propria (Matusiak *et al.*, 2023). Additionally, folate receptor expression defines macrophages residing in the lower lamina propria, whereas macrophages expressing LYVE1 and high levels of CD163 and COLEC12, are located in the deeper layers of the human intestine (Matusiak *et al.*, 2023; Domanska *et al.*, 2022). In contrast, lamina propria macrophages are marked by expression of CD11c and CD121b. Crypt-associated, submucosal and muscularis macrophages are identified by expression of CD206 and CD169 (Kang *et al.*, 2020; Asano *et al.*, 2015). Different markers are also associated with functional diversity among macrophages. For example, NRG1, which can promote epithelial differentiation to secretory lineages, was significantly increased in the colonic mucosa of UC patients, and its expression was associated with $CD68^{+}$ macrophages. However, in healthy control, NRG1

expression was restricted to a population underlying the surface epithelium, with little to no colocalization with $CD68^+$ macrophages (Garrido-Trigo *et al.*, 2023). Another study has demonstrated that CSF1R expression is associated with macrophages that are localised around the crypt epithelium. Depletion of these macrophages by CSF1R blockade disturbs intestinal crypt homeostasis, affecting the differentiation of Paneth cells and $Lrg5^+$ intestinal stem cells (Sehgal *et al.*, 2018).

The intestine consists of tissue resident macrophages that derive from embryonic progenitors and the bone marrow, with the majority originating from the latter. Bone marrow derived macrophages are replaced by circulating haematopoietic monocytes (Viola and Boeckxstaens, 2021). In contrast, the small population of macrophages that derive from embryonic precursors are capable of maintaining themselves through in situ self-renewal (De Schepper *et al.*, 2018). However, these cells are progressively replaced by CCR2-dependent influx of $Ly6C^{hi}$ monocytes that differentiate locally into mature, anti-inflammatory macrophages (Bain *et al.*, 2014; De Schepper *et al.*, 2018). Furthermore, in $CCR2^{-/-}$ mice, the recruitment of monocytes to the gut was impaired, and the accumulation of mature macrophages was reduced (Little, Hurst and Else, 2014).

Originally, a M1/M2 polarization paradigm was proposed. This concept was built on the observation that murine macrophages stimulated with LPS and/or IFNγ (M1) produced pro-inflammatory cytokines, whereas, those stimulated with IL-4 (M2) were polarized towards an anti-inflammatory phenotype (Mills *et al.*, 2000; Stein *et al.*, 1992; Murray *et al.*, 2014). Although this paradigm can be recapitulated *in vitro*, it has largely been described as an oversimplification of a highly complex and dynamic continuum of functional states *in vivo* (Katkar and Ghosh, 2023*)*.

Multiple processes are critical for regulating intestinal macrophages, including immunometabolic, epigenetic and environmental mechanisms (Chen *et al.*, 2023). Increasing evidence suggests that miRNAs are important components of the regulatory networks governing macrophage function. MicroRNAs (miRNAs) are small, non-coding RNAs that are approximately 22 nucleotides in length and have the ability to influence posttranscriptional gene expression (Alfaifi *et al.*,

2023). Primary miRNA transcripts (pri-miRNA) are transcribed in the nucleus by RNA polymerase II. Drosha, complexed with DGCR8, process the pri-miRNA in order to produce a precursor miRNA (pre-miRNA), containing the miRNA stem loop structure. The pre-miRNA is transported to the cytoplasm by Exportin-5, where it is cleaved by Dicer, partnered with TRBP and/or PACT, near the terminal loop, yielding a miRNA duplex. The passenger strand is discarded. The mature or guide strand associates with a member of the Argonaute family of proteins and is loaded into the RISC complex, where it can perform its target gene repression (**Figure 3.1**) (Yuan *et al.*, 2018; Shang *et al.*, 2023).

Although, miRNA expression profiles have been extensively studied across different cell types, much less is known about miRNA processing machinery (Faridani *et al.*, 2016; Wang *et al.*, 2019). Their importance in regulating immune cell function has previously been reported. For example, deletion of Dicer results in a developmental block at the pro-B- to pre-B-cell transition (Koralov *et al.*, 2008; Attaway, Chwat-Edelstein and Vuong, 2021). Additionally, deletion or depletion of Dicer in mouse or human $CD8^+$ T cells leads to the upregulation of perforin, granzymes, and effector cytokines (Trifari *et al.*, 2013). In the context of macrophages, deletion of dicer1 has been observed to deplete miRNA levels, consequently decreasing inflammatory cytokines (Gantier *et al.*, 2012). However, the expression and regulation of the miRNA processing machinery has yet to be assessed in macrophages.

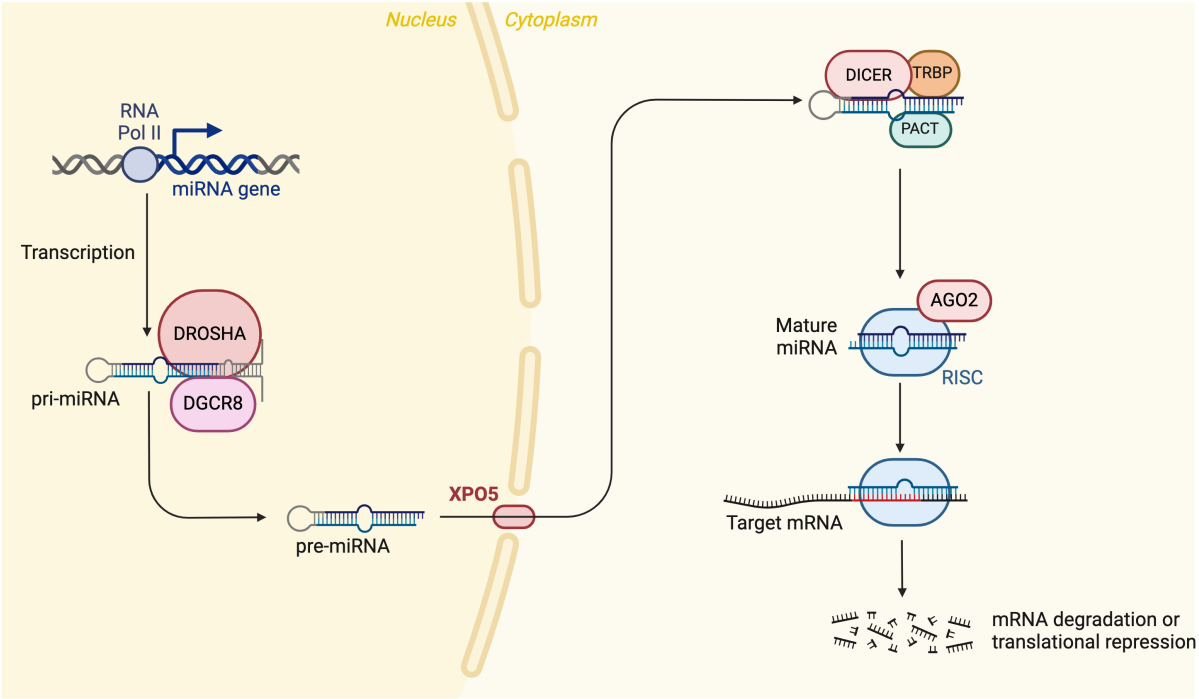

Figure 3.1. ***MiRNA biogenesis pathway.*** In the nucleus, the pri-miRNA is transcribed by RNA polymerase II. Drosha and DGCR8 process the pri-miRNA in order to produce a pre-miRNA. This is transported to the cytoplasm by Exportin-5, where it is cleaved by Dicer, partnered with TRBP and/or PACT, yielding a miRNA duplex. The passenger strand is discarded. The mature or guide strand associates with a member of the Argonaute family of proteins and is loaded into the RISC complex, where it can perform its target gene repression.

MiRNAs are differentially expressed during macrophage polarization (**Figure 3.2**). Using microarray analysis, it was shown that various miRNAs such as *miR-155-5p* and *miR-451* were upregulated and *miR-145-5p* and *miR-143-3p* were downregulated in M1 macrophages (Zhang *et al.*, 2013). Another study illustrated how different miRNAs are expressed in human macrophages polarized towards M1, including *miR-125a-3p* and *miR-26a-2-5p*, and those polarized towards M2, for example *miR-193b* and *miR-27a-5p* (Graff et al., 2012).

MiRNAs have been studied for their ability to alter the phenotypic states of macrophages. *miR-155* has been studied extensively regarding its role in the polarization of macrophages. When *miR-155* in BMDMs was blocked using an oligonucleotide inhibitor, it was found that LPS stimulated macrophages had downregulated expression of *Tnfα* and *Nos2*. This effect was also demonstrated

in BMDMs from *miR-155* KO mice, which again had downregulated expression of *Nos2*, *Il-1β* and *Tnfα* (Jablonski et al., 2016). Additionally, *miR-21* has been reported to mediate macrophage phenotype. Macrophages stimulated with LPS decreased PDC4 via *miR-21* to limit NF-κB activity while promoting IL-10 production (Sheedy *et al.*, 2010). Furthermore, macrophage-specific deletion of *miR-33* resulted in increased oxidative respiration and spare respiratory capacity, accompanied by an induction of a M2 macrophage polarization-associated gene profile (Ouimet *et al.*, 2015).

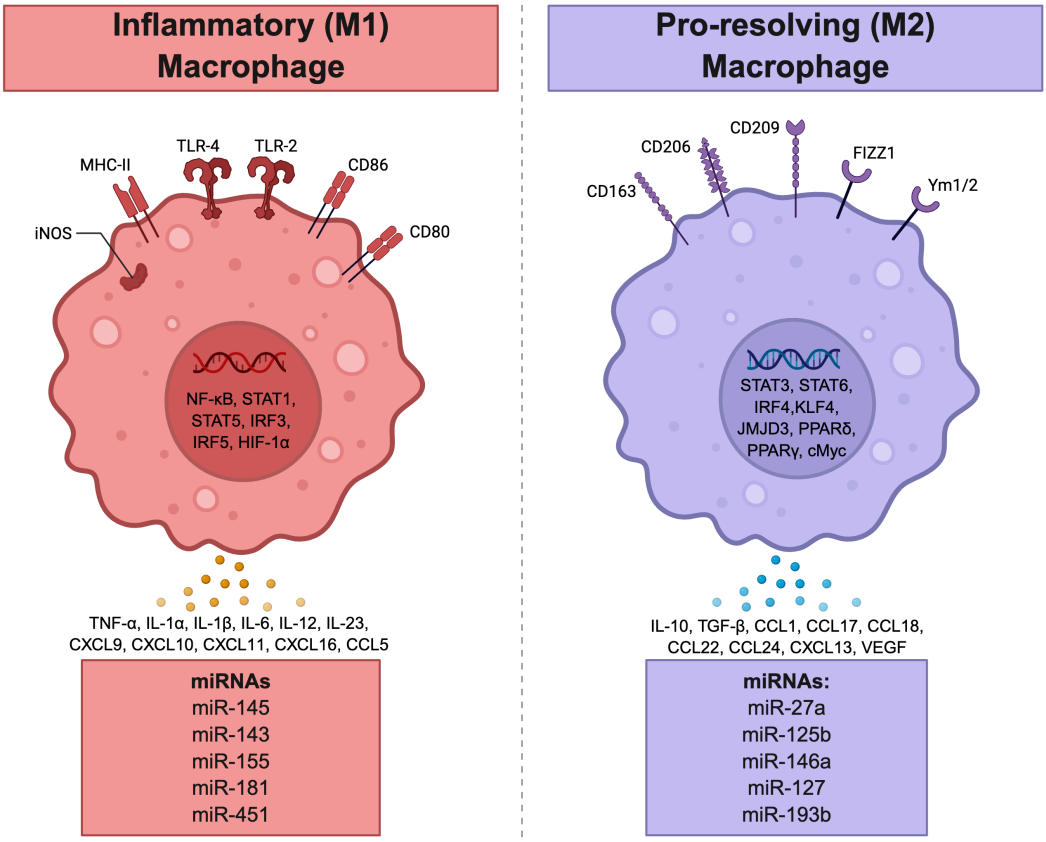

Figure 3.2. ***Differential expression of miRNAs in macrophages polarized towards a pro-inflammatory (M1) or pro-resolving (M2) phenotype.*** Pro-inflammatory (M1) macrophages are associated with anti-microbial activity and tissue damage. In contrast to this, pro-resolving (M2) macrophages are responsible for the resolution of inflammation and tissue repair. These macrophage phenotypes are not only functionally different, but they are also dissimilar in their expression of miRNAs, which likely play a role in their polarization.

MiR-223 is emerging as a critical regulator of innate immunity. Initial studies investigating this miRNA revealed that *miR-223*$^{-/y}$ lungs exhibited inflammatory

lung pathology, characterised by areas of atelectasis, increased cellularity within the parenchyma and inflammatory infiltration of the interstitium (Johnnidis *et al.*, 2008). *MiR-223* is highly expressed in myeloid cells (Chen *et al.*). Work has demonstrated that *miR-223* is lowly expressed in pluripotent haematopoietic stem cells and common myeloid progenitor cells. As granulocytic differentiation proceeds through granulocyte-monocyte progenitors to immature bone marrow neutrophils and terminates in the development of mature peripheral blood granulocytes, *miR-223* expression increases (Johnnidis *et al.*, 2008). In contrast to this, when these myeloid progenitors adopt the monocytic fate, *miR-223* is repressed (Johnnidis *et al.*, 2008). Furthermore, *miR-223* expression is downregulated as monocytes differentiate into mature macrophages (Haneklaus *et al.*, 2012).

MiR-223 has been reported to regulate markers associated with pro-inflammatory macrophages, such as CXCL2, IL-6 and IL-1β, in a wide array of inflammatory conditions such as sepsis, tuberculosis, experimental UC and colitis-associated colorectal cancer (Dorhoi *et al.*, 2013; Johnnidis *et al.*, 2008; Flynn *et al.*, 2024; Neudecker *et al.*, 2017b). However, the role of *miR-223* in modulating inflammatory signalling pathways and in regulating macrophage phenotypes from a pro-inflammatory to a pro-resolving state remains unclear.

AIMS OF THIS CHAPTER

The overall aim of this chapter was to investigate the hypothesis that *miR-223* regulates the phenotype of activated macrophages. In order to address this statement, the following aims were formulated:

1. Evaluate the expression of *miR-223* and the miRNA processing machinery during macrophage development and activation.
2. Assess the functional role of *miR-223* on macrophage activation *in vitro* through the supplementation of primary murine BMDMs with miRNA synthetic mimics.
3. Generation of *miR-223-3p* knockdown cell line, in order to investigate the mRNA circuits controlled by *miR-223* in activated macrophages *in vitro*.

3.1. Macrophage-associated and inflammatory transcription factors are differentially expressed in macrophages during development and activation.

MiR-223 expression is altered during macrophage development and activation. However, the factors responsible for this differential expression are yet to be determined.

To investigate this, BMDMs from WT mice were cultured and harvested at different timepoints (day 0, 2, 4, 6), to represent the development of macrophages from myeloid progenitors in the bone marrow. On day 7, the mature macrophages were stimulated with LPS (100 ng/mL) or IL-4 (10 ng/mL) for 24 h, in order to activate macrophages and polarize them towards either a pro-inflammatory phenotype (LPS) or a pro-resolving phenotype (IL-4), respectively.

The gene expression of different transcription factors associated with macrophage development and activation were examined by RT-PCR. As myeloid progenitor cells (indicated by day 0) differentiate into mature macrophages (represented by day 6), the expression of major histocompatibility complex class II (MHC-II), CD11b, interferon regulatory factor 4 (*Irf4)* and interferon regulatory factor 5 (*Irf5)* is downregulated (**Figure 3.1.1. A – D**). Conversely, these markers were increased in activated macrophages in comparison to naïve macrophages. MHC-II and CD11b were significantly upregulated in LPS stimulated cells, whereas *Irf4* expression was increased in macrophages activated with IL-4 (**Figure 3.1.1. E – G**). There were minimal changes in the expression of *Irf5* (**Figure 3.1.1. H**).

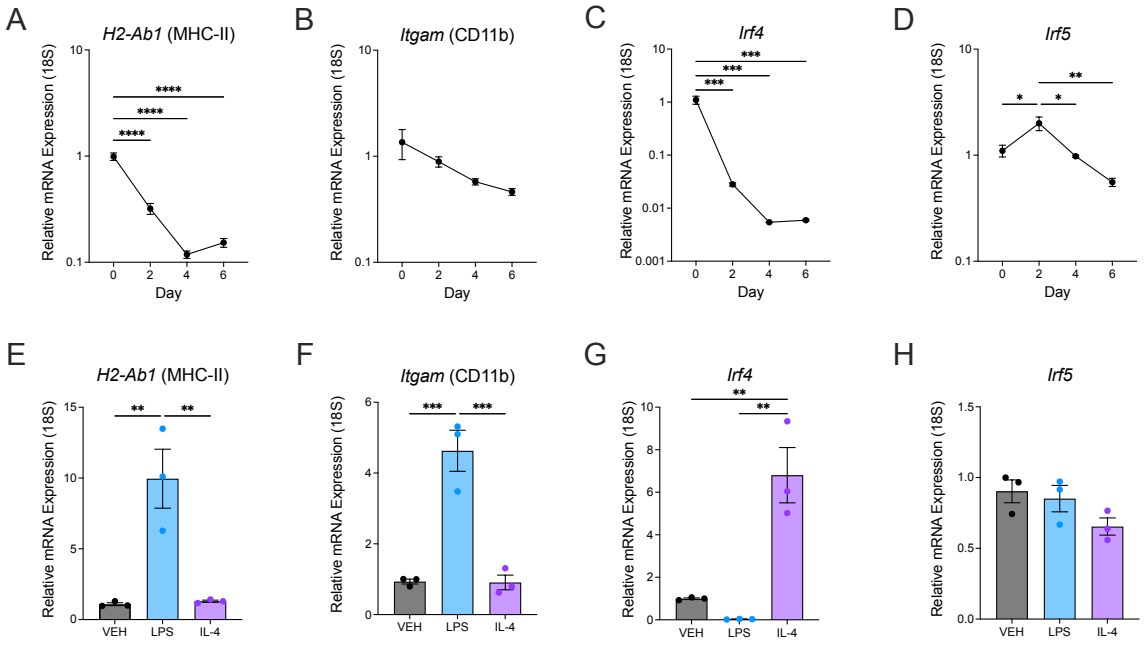

Figure 3.1.1. ***Macrophage-associated and inflammatory transcription factors are differentially expressed during macrophage development and activation.*** Relative mRNA expression of **A.** *H2-Ab1*, **B.** *Itgam*, **C.** *Irf4*, and **D.** *Irf5*, during macrophage development. Relative mRNA expression of **E.** *H2-Ab1*, **F.** *Itgam*, **G.** *Irf4*, and **H.** *Irf5* during macrophage activation, with LPS (100 ng/mL) or IL-4 (10 ng/mL). These were determined by RT-PCR from BMDMs from WT mice. All data is expressed as mean ± SEM; *, P ≤ 0.05; **, P ≤ 0.01, ***, P ≤ 0.001, ****, P ≤ 0.0001, versus the indicated counterpart (one-way ANOVA). n = 3 biological replicates/group.

3.2. Expression of *miR-223* is altered during macrophage development and activation.

Previous studies have provided evidence to show that *miR-223* expression is downregulated in the differentiation of monocytes to macrophage (Haneklaus *et al.*, 2012). However, a mature miRNA is a duplex containing the 3p and the 5p strand, and the expression levels of the specific strands of *miR-223* has not been examined (**Figure 3.2.1. A**).

Therefore, the BMDM time course was used to assess the gene expression of *miR-223-3p* and *miR-223-5p*. Although there is low expression levels of *miR-223-3p* and *miR-223-5p* in myeloid progenitors from the bone marrow, they are

profoundly downregulated as these cell developed into mature macrophages (**Figure 3.2.1. B and C**).

In contrast to this, with macrophage activation, the expression of both strands follows a similar pattern. Polarization of BMDMs to a pro-inflammatory phenotype results in the upregulation of *miR-223-3p* and *miR-223-5p*. However, their expression is decreased following IL-4 induced polarization to a pro-resolving state (**Figure 3.2.1. D and E**). These data suggest that *miR-223* is dynamically regulated and its expression follows macrophage activation in response to stimulation.

To further understand this expression pattern, the stability of these miRNA strands was investigated following LPS or IL-4 stimulation. BMDMs were stimulated for 30 min and treated with Actinomycin D, an inhibitor of mRNA transcription. 30 min post actinomycin D treatment, there was a drastic reduction in the expression of *miR-223-3p* and *miR-223-5p*. Interestingly, there was a greater percentage of miRNA remaining following LPS stimulation compared to naïve and IL-4 stimulated macrophages (**Figure 3.2.1. F and G**). Collectively, this data shows that *miR-223* expression, regardless of the miRNA strand, is decreased during macrophage development, but increased with macrophage activation, particularly following LPS stimulation.

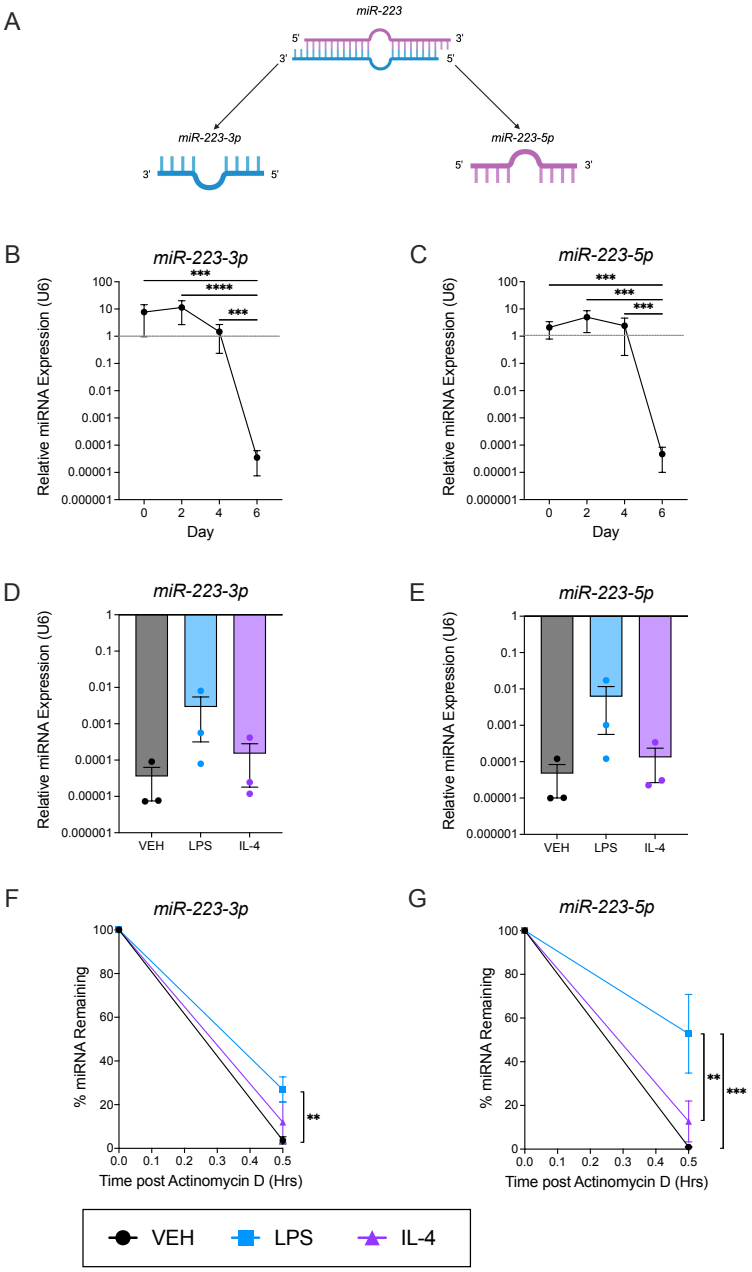

Figure 3.2.1. ***Expression of miR-223-3p and miR-223-5p is altered during macrophage development and activation.*** **A.** Mature *miR-223* consists of the 3p (guide) strand and the 5p (passenger) strand. Relative miRNA expression of **B.** *miR-223-3p* and **C.** *miR-223-5p*, during macrophage development. Relative mRNA expression of **D.** *miR-223-3p* and **E.** *miR-223-5p,* during macrophage activation with LPS (100 ng/mL) or IL-4 (10 ng/mL). These were determined by RT-PCR from BMDMs from WT mice and expressed relative to RNU6. The percentage of **F.** *miR-223-3p* and **G.** *miR-223-5p* remaining in activated macrophages, stimulated with LPS (100 ng/mL) or IL-4 (10 ng/mL), following Actinomycin D treatment. These were determined by RT-PCR from RAW 264.7 cells and expressed relative to RNU6. All data is expressed as mean ± SEM; *, P ≤ 0.05; **, P ≤ 0.01, ***, P ≤ 0.001, ****, P ≤ 0.0001, versus the indicated counterpart (one-way ANOVA). n = 3 biological replicates/group.

3.3. During macrophage development and activation the miRNA-processing machinery is altered.

Dicer, TRBP (*Tarbp2*), PACT (*Prkra*), Argonaute 2 (*Ago2*) and Argonaute 3 (*Ago3*) are essential for the production of mature miRNAs from pre-miRNA, as they are essential for the formation of the RNA-induced silencing complex (**Figure 3.3.1. A**). Therefore, the differential expression of these components has the potential to modulate the production of *miR-223*. To date, the regulatory mechanisms governing the expression of RISC protein constituents in macrophages remain uncharacterised. To address this, the expression levels of mRNA for these proteins were assessed in BMDMs during differentiation of myeloid progenitors to mature macrophages and then following inflammatory stimulation.

Similar to the expression of *miR-223* in macrophages, *Dicer1*, *Tarbp2* and *Ago2* were downregulated during the differentiation to macrophages (**Figure 3.3.1. B**). Conversely*, Prkra* expression was upregulated during the development of mature macrophages (**Figure 3.3.1. B**). Minimal changes were observed in the expression of *Ago3* (**Figure 3.3.1. B**).

In contrast to this, macrophage activation with LPS or IL-4 had little effect on the expression of the *Dicer1*, *Tarbp2*, *Ago2* and *Ago3* (**Figure 3.3.2. A**). However, *Prkra* was significantly decreased following activation with inflammatory stimulation (**Figure 3.3.2. A**). Proteins levels did not correspond to mRNA expression (**Figure 3.3.2. B**). Minimal changes were observed overall. However, Dicer levels increased following activation with either LPS or IL-4, whereas TRBP exhibited the opposite trend, with protein expression decreasing upon inflammatory stimulation (**Figure 3.3.2. B**). PACT protein expression was upregulated in macrophages activated with either LPS or IL-4 (**Figure 3.3.2. B**). Interestingly, a second PACT protein band appeared specifically following LPS stimulation (**Figure 3.3.2. B**)

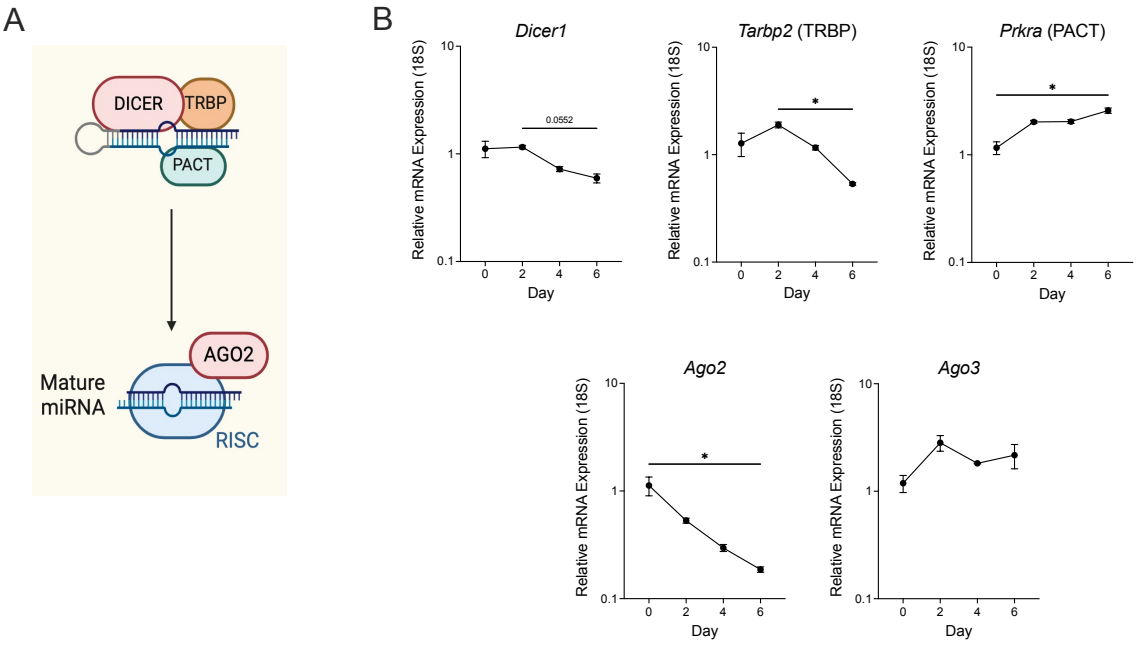

Figure 3.3.1. ***Expression of the miRNA-processing processing machinery is changed during macrophage development.*** **A.** Dicer, bound to TRBP and PACT, processes the pre-miRNA in the cytosol and produces a double-stranded miRNA duplex. The miRNA duplex then associates with the Argonaute proteins and is loaded into the RISC complex. The mature strand is retained and binds to target mRNA through their 3' untranslated region (UTR). Relative mRNA expression of **B.** *Dicer1*, *Tarbp2*, *Prkra*, *Ago2* and *Ago3* was measured by RT-PCR from BMDMs from WT mice. All data is expressed as mean ± SEM; *, P ≤ 0.05; **, P ≤ 0.01, ***, P ≤ 0.001, ****, P ≤ 0.0001, versus the indicated counterpart (one-way ANOVA). n = 3 biological replicates/group.

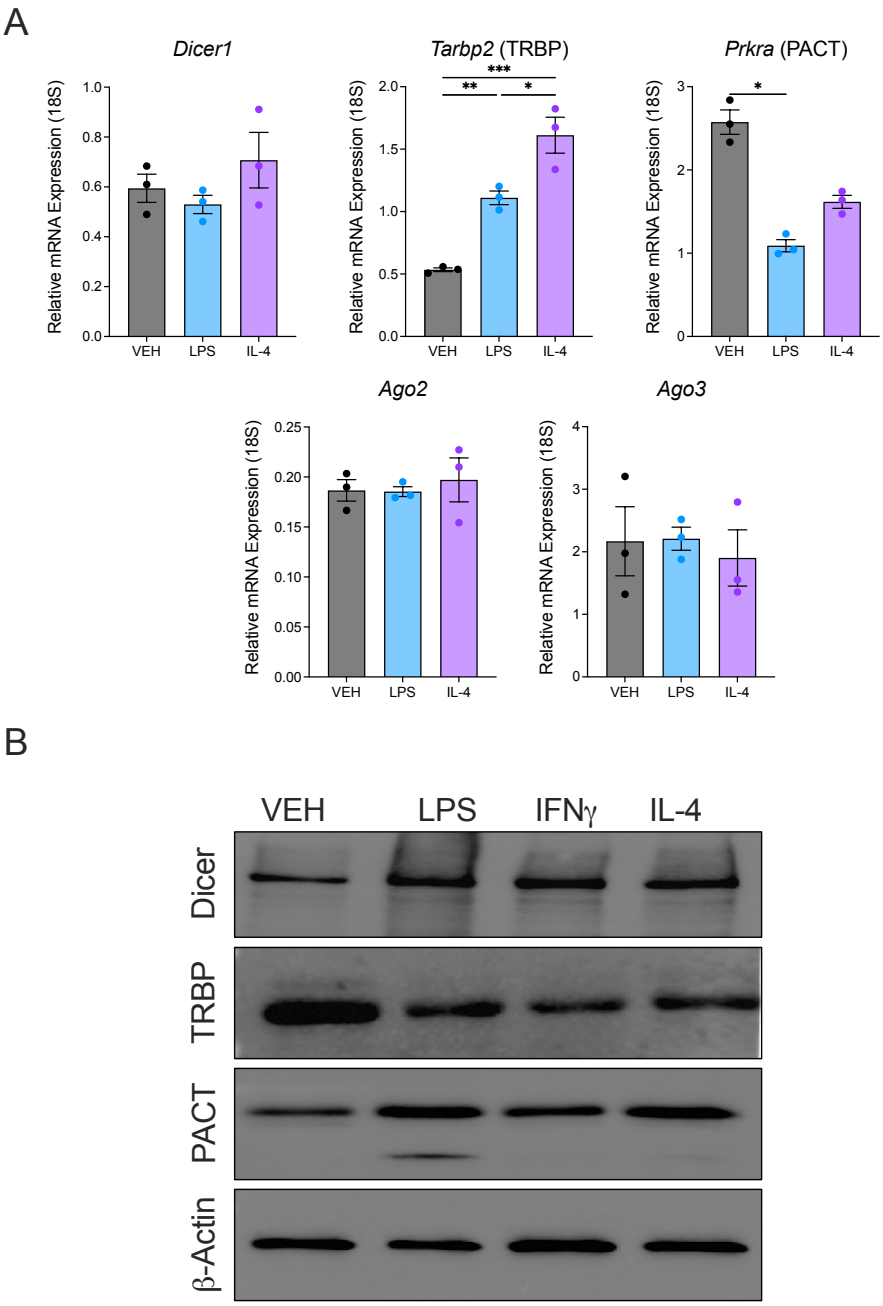

Figure 3.3.2. ***The miRNA processing machinery is differentially expressed during macrophage activation.*** Relative mRNA expression of **A.** *Dicer1*, *Tarbp2*, *Prkra*, *Ago2* and *Ago3* during macrophage activation, with LPS (100 ng/mL) or IL-4 (10 ng/mL). This was measured by RT-PCR from BMDMs from WT mice and expressed relative to 18S. All data is expressed as mean ± SEM; *, P ≤ 0.05; **, P ≤ 0.01, ***, P ≤ 0.001, ****, P ≤ 0.0001, versus the indicated counterpart (one-way ANOVA). n = 3 biological replicates/group. **B.** A western immunoblot assessment of β-Actin, Dicer, TRBP2 and PACT in BMDMs stimulated with LPS (100 ng/ml), IFNγ (10 ng/mL) or IL-4 (10 ng/mL) for 24 h. Representative n1 of n = 3 biological replicates/group.

3.4. Assessment of myeloid-associated transcription factors implicated in the regulation of *miR-223* expression.

As previously stated, the myeloid-associated transcription factors PU.1 and C/EBPβ, have been demonstrated to promote the expression of *miR-223* in granulocytes. Therefore, the gene expression of these transcription factors was examined in BMDMs to assess if they also have the capacity to modulate *miR-223* in macrophages.

Interestingly, the expression of Pu.1 and *Cebpβ* correlates with that of *miR-223-3p* and *miR-223-5p*. These transcription factors were most highly expressed in myeloid progenitor cells and decreased as they differentiated into mature macrophages (**Figure 3.4.1. A, C** and **E**). As observed with *miR-223*, *Cebpβ* and Pu.1 have greater expression in pro-inflammatory macrophages in comparison to pro-resolving macrophages (**Figure 3.4.1. B, D** and **E**).

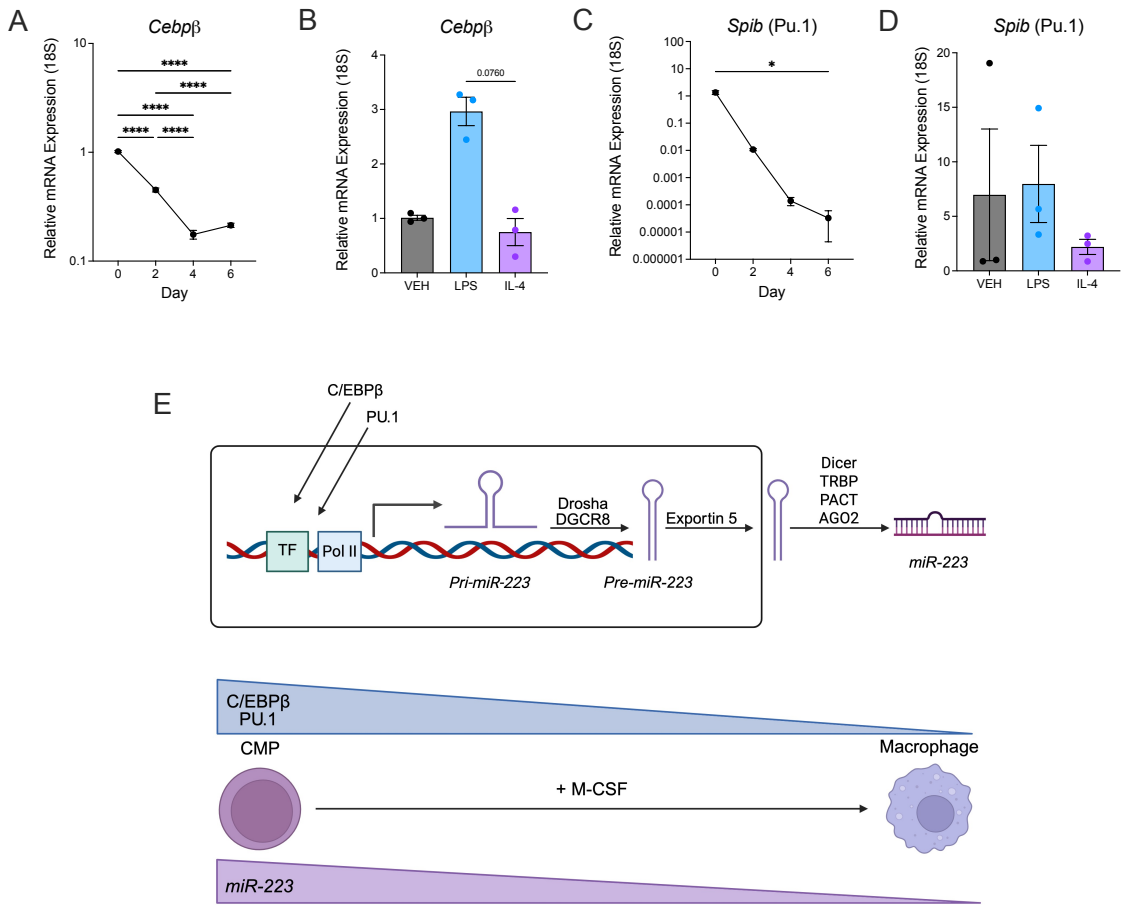

Figure 3.4.1. ***Myeloid-associated transcription factors demonstrate a similar expression pattern as miR-223 during macrophage development and activation.*** Relative mRNA expression of **A-B.** *Cebpβ* and **C-D.** *Spib* during macrophage development and activation, with LPS (100 ng/mL) or IL-4 (10 ng/mL). This was measured by RT-PCR from BMDMs from WT mice and expressed relative to 18S. All data is expressed as mean ± SEM; *, P ≤ 0.05; **, P ≤ 0.01, ***, P ≤ 0.001, ****, P ≤ 0.0001, versus the indicated counterpart (one-way ANOVA). n = 3 biological replicates/group. **E.** C/EBPβ and PU.1 have previously been reported to be promoters of *miR-223* expression. The decrease in expression of *miR-223* during macrophage development correlates with the expression of these transcription factors.

3.5. Supplementation with *miR-223* synthetic mimics alters macrophage phenotype.

The previous data which focused on macrophage development and activation, revealed that *miR-223* was reduced in mature macrophages and differentially expressed in pro-inflammatory and pro-resolving macrophages. Following this,

the functional role of this miRNA in shaping macrophage phenotype was assessed. This was investigated by transfecting BMDMs with synthetic *miR-223-3p* and *miR-223-5p* mimics and stimulating cells with LPS or IL-4.

Initially, common markers associated with pro-inflammatory macrophages were assessed, and this showed that supplementation with either a *miR-223-3p* or a *miR-223-5p* mimic, resulted in the reduction of *Cxcl2*, *Ccl2*, *Il-1β* and *Tnf* following stimulation with LPS (**Figure 3.5.1 A and B**).

The IL-6 family of cytokines, which encompass IL-6, LIF, IL-11 and OSM, are induced by STAT3 signalling and are secreted by pro-inflammatory macrophages. In LPS-induced activated BMDMs, a significant downregulation in the expression of *Il-6*, *Lif* and *Osm* was observed in the presence of both *miR-223-3p* and *miR-223-5p* mimics (**Figure 3.5.1. C**). Although not significant, there was also a decrease in *Il-11* expression (**Figure 3.5.1. C**).

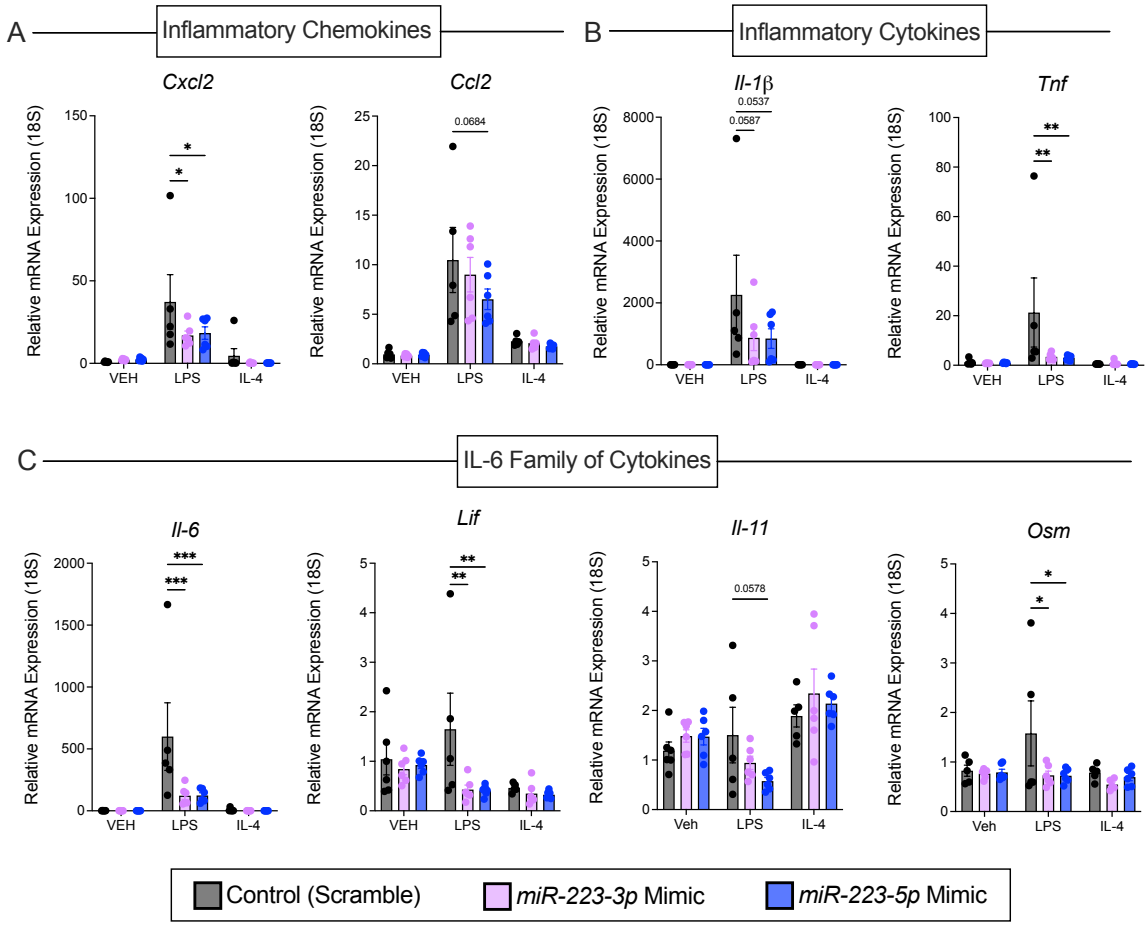

Figure 3.5.1. ***Inflammatory molecules are decreased in activated macrophages following transfection with miR-223-3p and miR-223-5p synthetic mimics.*** Relative mRNA expression of **A.** *Cxcl2* and *Ccl2*, **B.** *Il-1β* and *Tnf*, **C.** *Il-6*, *Lif*, *Il-11* and *Osm* were decreased in macrophages transfected with *miR-223-3p* and *miR-223-5p* synthetic mimics and stimulated with LPS (100 ng/mL) and IL-4 (10 ng/mL) for 24 h. This was measured by RT-PCR from BMDMs from WT mice. All data are expressed as mean ± SEM; *, P ≤ 0.05; **, P ≤ 0.01, ***, P ≤ 0.001, ****, P ≤ 0.0001, versus the indicated counterpart (two-way ANOVA). n = 5-6 biological replicates.

While no significant alteration in cytokine expression was observed at baseline, these data illustrate the ability of *miR-223* to diminish the responses of inflammatory macrophages following LPS challenge. However, the study next aimed to determine whether *miR-223* plays a role in modulating the phenotype of macrophages from a pro-inflammatory to a pro-resolving state.

The gene expression of markers produced by pro-resolving macrophages were assessed. Anti-inflammatory cytokines, *Il-10* and *Tgfb1* were decreased, whereas *Retnla* was increased in BMDMs overexpressing *miR-223-3p* and *miR-*

223-5p following IL-4 stimulation, with little change in *Arg1* expression (**Figure 3.5.2. A**). Immunosuppressive chemokines, *Ccl17* and *Ccl22*, were upregulated in IL-4 stimulated cells with *miR-223-3p* transfection (**Figure 3.5.2. B**). Genes which have been previously demonstrated to directly induce mucosal healing were also examined. Variable changes were observed in Wls (Wnt ligand secretion mediator), Stat6 and Rspo1 (**Figure 3.5.2. C**). However, Wnt6, a ligand secreted by macrophages that activates WNT signalling, was downregulated in macrophage stimulated with LPS in the presence of both *miR-223-3p* and *miR-223-5p* mimics (**Figure 3.5.2. C**). Collectively, these data reveal that *miR-223* not only suppresses the inflammatory responses of macrophages, but also has the ability alter the phenotypic state of macrophages.

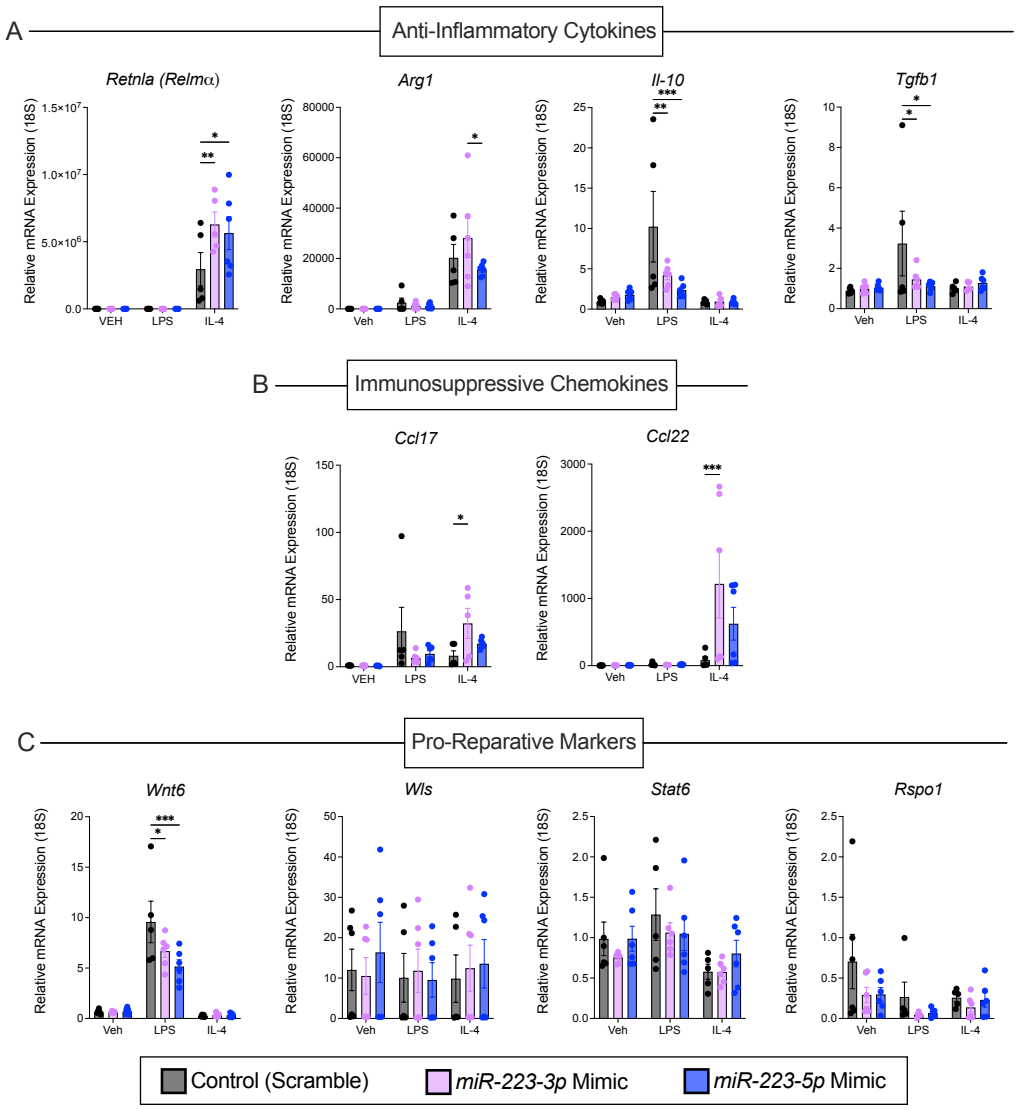

Figure 3.5.2. ***Supplementation of activated macrophages with miR-223-3p and miR-223-5p synthetic mimics results in the upregulation of a selective pro-resolving macrophage gene set.*** Relative mRNA expression of **A.** *Retnla*, *Arg1*, *Il-10*, *Tgfb1*, **B.** *Ccl17*, *Ccl22*, and **C.** *Wnt6*, *Wls*, *Stat6* and *Rspo1* was increased in macrophages transfected with *miR-223-3p* and *miR-223-5p* synthetic mimics and stimulated with LPS (100 ng/mL) and IL-4 (10 ng/mL) for 24 h. This was measured by RT-PCR from BMDMs from WT mice. All data are expressed as mean ± SEM; *, P ≤ 0.05; **, P ≤ 0.01, ***, P ≤ 0.001, ****, P ≤ 0.0001, versus the indicated counterpart (two-way ANOVA). n = 5-6 biological replicates.

3.6. Generation of a *miR-223*KD RAW 264.7 cell line as a tool system to assess *miR-223* biology in macrophages.

Lentiviral transduction particles, produced from sequence-verified plasmid vectors, were used to generate *miR-223* knockdown and a negative control RAW 264.7 macrophage cell lines. These were utilised as an experimental tool system to assess *miR-223* biology in macrophages by providing a robust system to repress *miR-223*. The lentiviral vector carries a puromycin resistance cassette for the selection of successfully transduced cells. Therefore, a puromycin kill curve was used to determine the optimal dose for antibiotic selection.

Initially, RAW 264.7 cells were treated with varying doses of puromycin (0, 1, 2, 5, 7 and 10 μg/mL) and the supernatants were harvested at 48 h and 96 h. An LDH assay measures the amount of lactate dehydrogenase that is released when cells are damaged or dying. 48 h after puromycin treatment, LDH release was highest in cells treated with 10 μg/mL, decreasing at lower doses (**Figure 3.6.1. A**). By 96 h, LDH activity was similar across all concentrations, showing minimal differences (**Figure 3.6.1. B**).

A MTS assay was used as an additional method for determining the optimal concentration of puromycin to use for antibiotic selection. Rather than measuring damage or death, it measures cell viability. The production of formazan is directly proportional to the number of living cells in culture. As before, cells were treated with different concentrations of puromycin (0, 1, 2, 5, 7 and 10 μg/mL) and the percentage cell viability was calculated at 144 h post puromycin treatment (**Figure 3.6.1. C**). There was little difference in the viability of cells between vehicle and cells treated with 1 μg/mL of puromycin (**Figure 3.6.1. D**). However, when cells were cultured in medium containing 2 μg/mL of puromycin, there was a drastic reduction in cell viability, approximately 80% (**Figure 3.6.1 D**). There were minimal differences in the viability of cells between 2 μg/mL – 10 μg/mL of puromycin (**Figure 3.6.1 C and D**).

Based on this data, a concentration of 2 μg/mL of puromycin was chosen as the optimal dose for the antibiotic selection of RAW 264.7 cells.

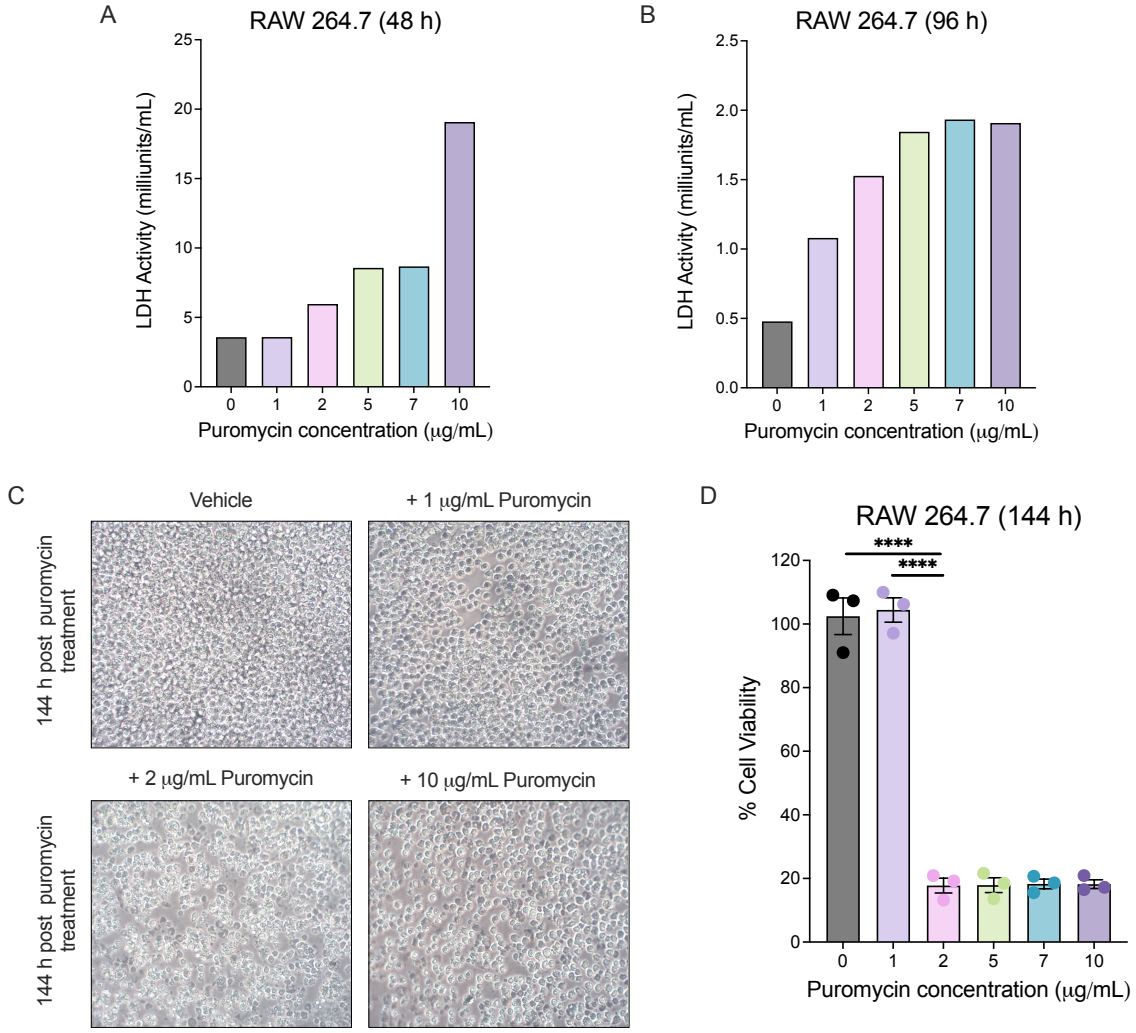

Figure 3.6.1. ***Puromycin (2 μg/mL) is the optimal dose for antibiotic selection of RAW 264.7 cells.*** Cell damage to RAW 264.7 cells was determined by a LDH activity assay, **A.** 48 h and **B.** 96 h, post puromycin treatment at different concentrations. n = 1/group. **C.** Representative images of RAW 264.7 cells 144 h post puromycin treatment at different concentrations. Cell viability was determined by a MTS assay, **D.** 144 h post puromycin treatment at different concentrations. This assay was performed on RAW 264.7 cells. All data are expressed as mean ± SEM; *, P ≤ 0.05; **, P ≤ 0.01, ***, P ≤ 0.001, ****, P ≤ 0.0001, versus the indicated counterpart (one-way ANOVA). n = 3 technical replicates/group.

Following the generation of the Scramble Control inhibitor and *miR-223*KD cell lines, validation experiments were performed to confirm the knockdown of *miR-223*. To begin, the expression of *miR-223-3p* in these cell lines was determined by RT-PCR. Cell lines were stimulated with LPS to induce *miR-223* expression. While the clones exhibited varying levels of *miR-223*, clone 3 was selected for

subsequent experiments in both the Scramble Control inhibitor and *miR-223*KD cell lines (**Figure 3.6.2. A**).

Next, functional read-outs were conducted based on the expression of known *miR-223* targets. Both cell lines were stimulated with LPS and the cells and supernatants were harvested for gene expression and protein production analysis. A trend was observed in which the gene expression of *Cxcl2*, *Il-1*β and *Il-6* were upregulated in the *miR-223*KD cell line (**Figure 3.6.2. A – C**). There was a significant increase in secretion of these proteins in the *miR-223*KD cell line (**Figure 3.6.2. E – G**).

The *miR-223*KD cell line was created to act as an experimental tool system to investigate the functional role of *miR-223* in macrophages. Therefore, markers associated with pro-inflammatory and pro-resolving states were assessed to determine the effect of reduced *miR-223* expression on macrophage phenotype. The *miR-223*KD cell line had an enhanced expression of *Ccl2*, *Tnf* and *Nos2*, following LPS stimulation, however, no significant changes were observed in the *Arg1*, *Il-10* and *Irf4* (**Figure 3.6.3 A**). *Ccl17* and *Ccl22* were upregulated in macrophages that were deficient in *miR-223* (**Figure 3.6.3. B**). Additionally, the expression of the pro-reparative markers, *Wnt6* and *Egf*, that induce mucosal regeneration, were significantly increased in the *miR-223*KD cell line following LPS stimulation (**Figure 3.6.3. C**).

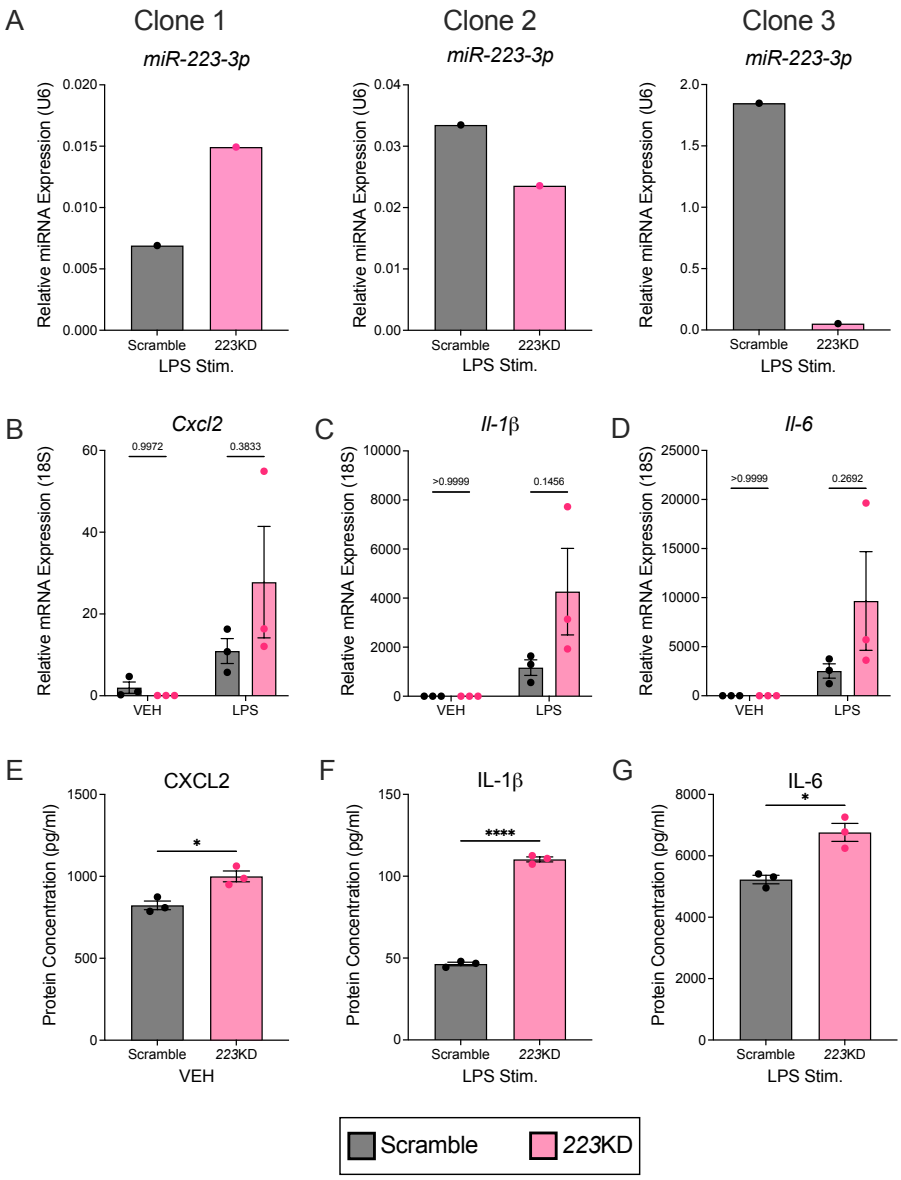

Figure 3.6.2. ***The miR-223KD cell line is functional following lentiviral transduction of RAW 264.7 cell line with a miRNA inhibitor.*** **A.** Relative miRNA expression of *miR-223-3p* in a Scramble inhibitor control (Scramble) cell line versus *miR-223*KD (*223*KD) cell line following LPS (100 ng/mL) stimulation for 24 h. This was expressed relative to RNU6. Relative mRNA expression of **B.** *Cxcl2*, **C.** *Il-1β* and **D.** *Il-6* in a Scramble cell line versus *223*KD cell line following 24 h stimulation with LPS (100 ng/mL). **E.** Supernatants were collected and concentration of CXCL2 secretion was determined by ELISA in non-stimulated cells. The secretion of **F.** IL-1β and **G.** IL-6 was quantified by ELISA. This was performed on supernatants collected from a Scramble cell line versus *223*KD cell line stimulated with LPS (100 ng/mL) for 24 h. All data are expressed as mean ± SEM. Statistical significance was determined by two-way ANOVA for **B, C and D**, and one-way ANOVA for **E, F and G**. *, P ≤ 0.05; **, P ≤ 0.01, ***, P ≤ 0.001, ****, P ≤ 0.0001, versus the indicated counterpart. n = 3 technical replicates/group.

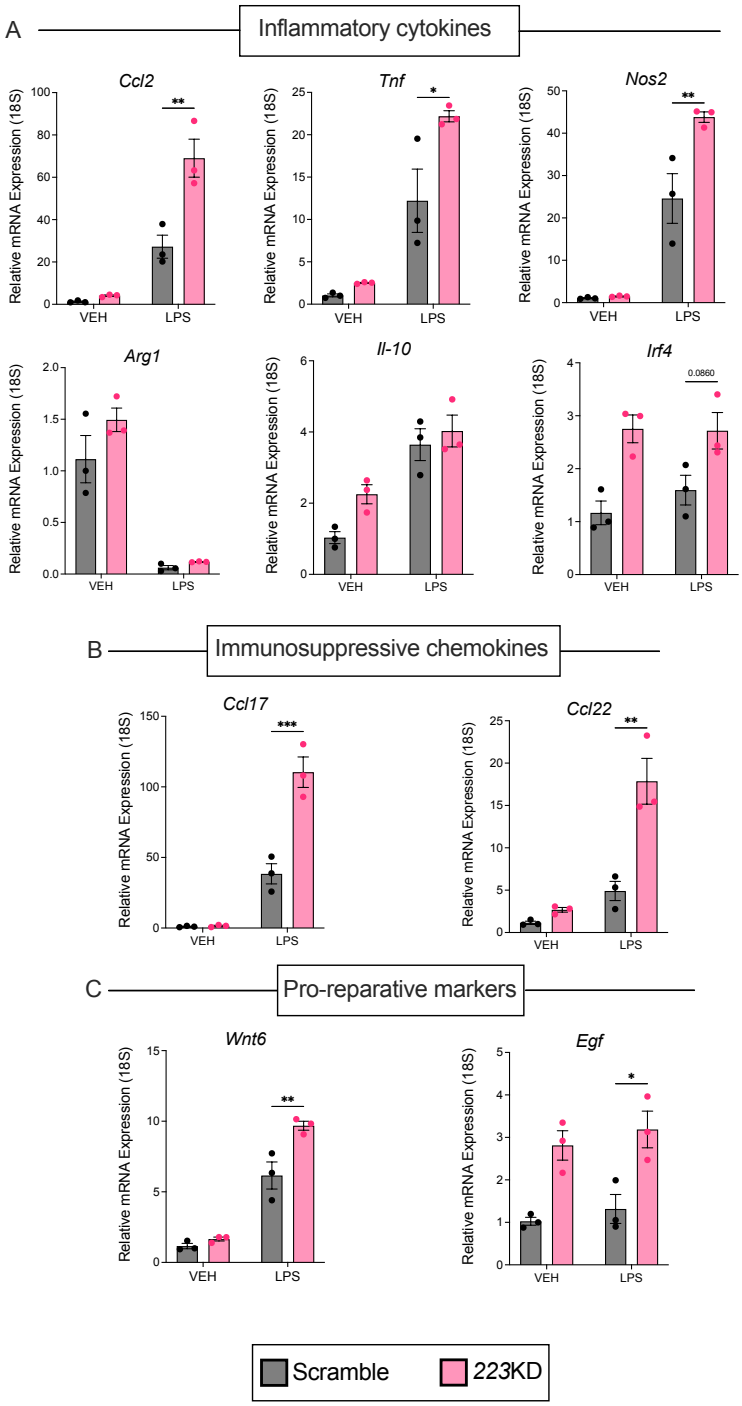

Figure 3.6.3. ***The miR-223KD cell line presents with a dysregulated macrophage phenotype.*** Relative mRNA expression of **A.** *Ccl2, Tnf, Nos2, Arg1, Il-10* and *Irf4*, **B.** *Ccl17* and *Ccl22,* and **C.** *Wnt6* and *Egf* in a Scramble inhibitor control (Scramble) cell line versus *miR-223*KD (*223*KD) cell line following 24 h stimulation with LPS (100 ng/mL). This was expressed relative to 18S. All data are expressed as mean ± SEM. Statistical significance was determined by two-way ANOVA. *, P ≤ 0.05; **, P ≤ 0.01, ***, P ≤ 0.001, ****, P ≤ 0.0001, *, P < 0.05; **, P < 0.01, ***, P ≤ 0.001 versus the indicated counterpart. n = 3 technical replicates/group.

DISCUSSION

Macrophages exist in various tissues and around mucosal surfaces and are critical innate immune cells (Chen *et al.*, 2023). They are highly plastic cells and are known to acquire countless number of states in diverse tissue niches (Katkar and Ghosh, 2023). It is through this phenotype switching, that macrophages have the ability to maintain homeostasis, while also contributing to inflammation and resolution (Hegarty, Jones and Bain, 2023). Polarization of macrophages towards different states is a topic of importance within the field. During inflammatory diseases, whereby disease-associated signals override the homeostatic ones, macrophage function is dysregulated and they are unable to resolve the inflammation resulting in severe tissue damage (Park *et al.*, 2022). Therefore, understanding the mechanisms that modulate the polarization of macrophages towards a pro-inflammatory or pro-resolving phenotype, has the potential to reveal new therapeutic targets for the treatment of various diseases.

Due to their ability to modulate gene expression, including those associated with pro-inflammatory or pro-resolving macrophages, miRNAs are emerging as potential targets to induce phenotype switching in macrophages (Lee, Feinbaum and Ambros, 1993; Wightman, Ha and Ruvkun, 1993). Studies have shown that miRNAs are important in haematopoiesis, for example, the deletion of Ago2 leads to issues in the development of erythroid and B cells (O'Carroll *et al.*, 2007). The global miRNA profile of myeloid progenitors as they differentiate into mature macrophages has previously been investigated and revealed differential expression of 112 miRNAs. Among these miRNAs, 56 miRNAs were decreased and 58 miRNAs were increased on day 3, and 66 miRNAs were downregulated and 48 miRNAs were upregulated on day 5 and day 7 (Zhou *et al.*, 2016). In another study, 249 distinct miRNAs were observed in polarised macrophages with only 13 showing a greater than 2-fold change in expression depending on the polarisation conditions (Graff *et al.*, 2012). miRNAs such as, *miR-155* and *miR-145-5p*, have consistently been shown to be highly expressed in M1 macrophages, and *miR-26a* and *let-7c*, have been expressed at higher levels in M2 macrophages (Lu *et al.*, 2016).

Given the current knowledge gap regarding the regulation of specific miRNAs in macrophages – particularly those restricted to macrophages, or the myeloid lineage – understanding their regulation has the potential to reveal cell-specific mechanisms for controlling macrophage-driven inflammatory diseases. In the present study, the expression of a specific miRNA during macrophage development and activation was investigated in BMDMs. *MiR-223* (both *miR-223-3p* and *miR-223-5p*), was revealed to be among the set of miRNAs that are expressed in BMDMs. Like others, *miR-223* expression was downregulated as myeloid progenitor cells differentiate into mature macrophages. It was also observed to be differentially expressed in polarized macrophages. Cells polarized towards a pro-inflammatory state with LPS, had a trend towards higher expression of *miR-223*, when compared to Vehicle or IL-4 stimulated macrophages. This indicates that pro-inflammatory macrophages activated by LPS, have a greater ability to stabilize *miR-223* in comparison to naïve or pro-resolving macrophages.

Although, the global miRNA signature of macrophages has been investigated in a number studies, very little is known about the expression profile of the miRNA processing machinery in this cell type. The data presented here demonstrated that during macrophage development, the miRNA processing machinery, namely Dicer, TRBP and AGO2 were downregulated. However, following macrophage activation there were minimal differences. Dicer has been reported to play an essential role in hematopoietic stem and progenitor cell (HSPC) maintenance, as its deletion led to greater HSPC apoptosis (Guo *et al.*, 2010). Previous studies have shown that Dicer deletion resulted in the depletion of different miRNAs. Furthermore, this resulted in an increased proportion of TAMs expressing an M1-like phenotype (Baer *et al.*, 2016). Ago2 has also been described to impact macrophage polarization. Macrophages possessing a mutant *Ago2*, which remained bound to miRNAs during macrophage activation, presented with a weakened inflammatory response and failed to prevent parasite invasion (Mazumder *et al.*, 2013).

The miRNA processing machinery (or the RNA-induced silencing complex) has been reported to be of significance in macrophage development and activation, through its impact on miRNAs. However, *miR-223* expression may not be solely dependent on its processing by these components. In naïve $CD4^+$ T cells, *miR-*

223 was the only miRNA that was increased in expression when Ago2 was depleted (Bronevetsky *et al.*, 2013). The work presented here, demonstrated that *miR-223* expression does not directly correlate with the expression of the miRNA processing machinery, suggesting that other factors may be involved.

Importantly to note, *miR-223* is a myeloid restricted miRNA. It is highly expressed in granulocytes and monocytes (Johnnidis *et al.*, 2008). The mechanisms regulating *miR-223* expression have been studied in context of granulocytic differentiation (O'Connell, Zhao and Rao, 2011). Initially, it was shown that C/EBPα activates transcription of *miR-223*, whereas NFI-A represses it (Fazi *et al.*, 2005). Further work hypothesised that due to *miR-223* resembling a "myeloid gene", it is likely driven by myeloid transcription factors, namely PU.1 and C/EBPβ. These are important as they regulate numerous myeloid genes and are specifically required for myeloid differentiation. PU.1 and C/EBPβ had the capacity to activate the core promoter of *miR-223 (Fukao et al., 2007)*. The expression of these transcription factors was examined in BMDMs during differentiation and activation. They had a similar expression pattern to that observed with *miR-223-3p* and *miR-223-5p*. This data suggests that C/EBPβ and PU.1 regulate *miR-223* expression in macrophages.

Thus far, the data has demonstrated how *miR-223* is modulated during macrophage development and activation. The next step was to elucidate the potential functional role of this miRNA. These small molecules have been reported to post-transcriptionally alter macrophages, in order to modify cell fate. Studies have shown that IL-4 and IL-13 induce *miR-142-5p* and reduce *miR-130a-3p*. *In vitro* overexpression of *miR-142-5p* and inhibition of *miR-130a-3p* helped to maintain M2 macrophage polarization. This was caused by their ability to regulate their targets SOCS1 and PPARγ (Su *et al.*, 2015a). This was investigated by transfecting BMDMs with oligonucleotides that overexpress *miR-223-3p* and *miR-223-5p*. Various markers associated with pro-inflammatory molecules have been described or predicted to be targets of *miR-223*, so it was expected that these would be suppressed in the presence of the synthetic mimics (Dorhoi *et al.*, 2013). *miR-223* has previously been investigated in context of modulating macrophage polarization. Work performed with BMDMs from *miR-223*$^{-/-}$ and WT mice has shown that pro-inflammatory cytokines, *Il-1β, Il-6* and

Tnfα were elevated in macrophages deficient in *miR-223*, following LPS stimulation. Conversely, M2-associated genes, *Pparγ* and *Arg1* were decreased in BMDMs from *miR-223*$^{-/-}$ mice (Zhuang *et al.*, 2012; Neudecker *et al.*, 2017b). Therefore, it was interesting to confirm that the opposite effect is observed when *miR-223* is overexpressed in BMDMs. It was also revealed that *miR-223* has the capacity to induce a pro-resolving macrophage phenotype, through its upregulation of *Retnla*, *Ccl17* and *Ccl22*. These findings are significant in the context of disease. RELMα activates the enzyme lysyl hydroxylase 2 (Plod2), which facilitates optimal collagen cross-linking. Moreover, macrophage-derived RELMα has been shown to dampen lung inflammation and promote tissue repair in a model of helminth-induced lung injury caused by the rodent hookworm *Nippostrongylus brasiliensis*. Furthermore, CCL17 and CCL22 are key chemokines that mediate the trafficking of regulatory T cells (T_{regs}) to the intestine, where they contribute to the suppression of inflammation (Kim and Nair, 2019; Guo *et al.*, 2008). This work also uncovered a potential role of *miR-223* to modulate pathways directly involved in regeneration, namely WNT signalling, through its regulation of its ligand, Wnt6 (Cosín-Roger *et al.*, 2016).

Lentiviral transduction particles were used to generate a Scramble Control inhibitor and a *miR-223*KD RAW 264.7 cell lines. They are a robust tool system to investigate the *miR-223* biology in macrophages. *MiR-223-3p* was the strand to be inhibited, as it is recognised as the guide strand and the data presented previously shows that it has greater abundance in macrophages (Zhang *et al.*, 2021b). Although, an overall decrease in the expression was observed in the *miR-223*KD cell line, variability was also present. This is the result of the random nature of lentiviral integration into the host's genome, as the expression level of the gene is dependent on its integration site (Formas-Oliveira, Ferreira and Coroadinha, 2025). A single cell can receive multiple copies of the integrated gene, which can affect its expression levels, leading to variability between clones (Hines and Hines, 2023). As such, multiple clones were generated and the clone achieving over 80% knockdown efficiency – determined by RT-PCR measurement of *miR-223* expression – was selected for subsequent experiments.

The functionality of the *miR-223*KD cell line was validated based on its expression of reported *miR-223* targets. CXCL2, IL-6 and IL-1β have previously been described to be regulated by *miR-223* (Dorhoi *et al.*, 2013; Neudecker *et al.*, 2017b). Inhibition of *miR-223* resulted in the increase of these targets at both a gene expression and a secreted protein level. These results confirmed the successful establishment of a functional *miR-223*KD cell line.

Initial experiments were carried out to explore the effect of *miR-223* inhibition on macrophage phenotype. The data revealed effects that were contrasting to those observed following *miR-223* overexpression. These macrophages appeared to have a dysregulated phenotype rather than merely being in a pro-inflammatory or pro-resolving state. Although there is an upregulation in the expression of pro-inflammatory cytokines, there is also an increase in immunosuppressive chemokines and ligands associated with regeneration (Zhang *et al.*, 2025; Hausmann *et al.*, 2024). This data suggests that *miR-223* may not simply be able to polarise macrophages towards a pro-inflammatory or pro-resolving phenotype, but rather a dysregulated state.

Overall, these findings demonstrate that macrophage-associated *miR-223* is regulated by the myeloid transcription factors, PU.1 and C/EBPβ, and highlight differences in the expression of the miRNA processing machinery in macrophages. Furthermore, this work underscores the importance of *miR-223* in normal macrophage function and its potential to modulate inflammatory responses while promoting tissue repair.

CHAPTER 4

ELUCIDATING THE ROLE OF MACROPHAGE-ASSOCIATED *MIR-223* IN INTESTINAL MUCOSAL HEALING

Macrophages have essential roles in the maintenance of intestinal homeostasis, however, the dysregulation of their normal functions are a central feature of IBD, namely UC, which is a chronic inflammatory condition (Hegarty, Jones and Bain, 2023). Macrophages have been identified as key players in driving inflammation, while also controlling mucosal healing. Previous studies have shown that appropriate regulation of the differentiation from blood-circulating monocytes determines whether macrophages acquire pro-inflammatory, immature phenotype, or mature into cells that support tissue healing and homeostasis (Tamoutounour *et al.*, 2012).

The differentiation continuum of monocytes to macrophages is referred to as the monocyte "waterfall" (**Figure 4.1**) (Tamoutounour *et al.*, 2012). Under steady state conditions, the majority of colonic macrophages are established from CCR2-LY6C^{hi} blood-derived monocytes that express low levels of CX_3CR1. As LY6C^{hi} monocytes infiltrate the intestine, they undergo gradual differentiation by acquiring MHCII and downregulating LY6C expression. This is followed by upregulation in F4/80, CD64 and CX_3CR1, and they become mature macrophages. These macrophages acquire pro-resolving functions such as increased production of anti-inflammatory cytokines, decreased production of pro-inflammatory molecules, such as IL-6 and iNOS, enhanced phagocytic ability, acquisition of scavenger receptors and loss of responsiveness to toll-like receptor (TLR) ligation (Bain *et al.*, 2013; Bain *et al.*, 2014).

During inflammation, the terminal differentiation of LY6C^{hi} monocytes to mature intestinal macrophages is disrupted. It results in the accumulation of LY6C^{int}CX_3CR1^{int} cells that exert pro-inflammatory properties such as secretion of cytokines IL-12, IL-23 and IL-1β, which promote T_H1 and T_H17 responses towards invading microorganisms, and aggravate epithelial damage (Na *et al.*, 2019).

During the resolution of inflammation, efferocytosis of apoptotic neutrophils and epithelial cells by intestinal macrophages induces phenotype switching from a

pro-inflammatory to a pro-resolving state. They dampen the T cell activity that is responsible for the destruction of the epithelial barrier and aid in re-establishing the epithelium. These reparative macrophages localise near the damaged areas of the crypt and induce epithelial cell proliferation through the secretion of regeneration mediators such as WNT and EGF ligands (Na *et al.*, 2019).

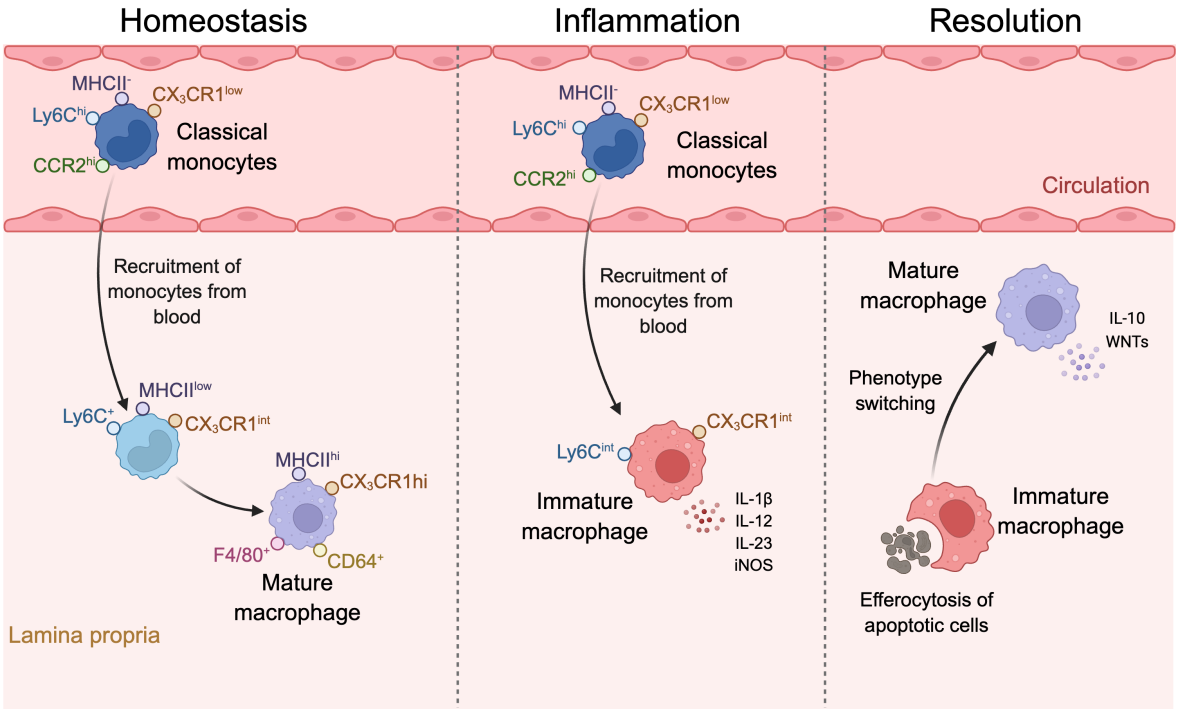

Figure 4.1. ***Differentiation of intestinal macrophages during homeostasis, inflammation and resolution.*** During homeostatic conditions, Ly6C^{hi}CCR2^{hi} classical monocytes are recruited from the blood to the intestine. Once they have infiltrated the lamina propria, they downregulate Ly6C and acquire MHCII and CX_3CR1 expression. This is followed by upregulation of MHCII, CX_3CR1, F4/80 and CD64, and they become mature macrophages. However, during inflammation, this differentiation is disrupted and results in the accumulation of Ly6C^{hi}CX_3CR1^{int} cells, often referred to as immature macrophages. These cells secrete inflammatory cytokines like IL-1β and iNOS. The resolution of inflammation is initiated by the efferocytosis of apoptotic cells by macrophages. This activates phenotype switching of macrophages from a pro-inflammatory to an anti-inflammatory state. These macrophages induce epithelial repair through the production of regeneration mediators such as IL-10 and WNTs.

Mature, pro-reparative macrophages are characterised by the expression of several markers including MERTK, CD206 and Relmα. MERTK, is an efferocytosis receptor that induces phenotype switching in intestinal macrophage

(Cai *et al.*, 2018; Ho *et al.*, 2020). CD206, a mannose receptor, has been reported to distinguish between two distinct macrophage subsets. $CD206^{+}$ macrophages are associated with a mature phenotype, expressing high levels of CD68, CD163, higher transcription of IL-10 and lower expression of TREM1 (Wright *et al.*, 2021). Finally, Relmα, is an anti-parasitic mediator, and has been reported to be effective against intestinal helminth infection (Filbey *et al.*, 2014).

In the context of IBD, macrophages are considered drivers of this disease. Immature, pro-inflammatory macrophages accumulate in the intestine and are potent inducers of inflammatory cytokines, including TNF, IL-1β, IL-6 and IL-23. They have been reported to respond aggressively to commensal bacteria, like *Enterococcus faecalis* (Kamada et al., 2008). A number of IBD susceptibility loci are associated with macrophages, for example risk variants in autophagy can be found in these cells, resulting in the pathogenesis of IBD (Baillie *et al.*, 2017; Lapaquette *et al.*, 2010; Lapaquette, Bringer and Darfeuille-Michaud, 2012). It has also been reported that clinical remission in IBD is associated with reduced pro-inflammatory macrophage activity (Dige *et al.*, 2014; Vos *et al.*, 2011).

Although macrophages have been identified to be involved in the development of IBD, other studies have revealed that they are crucial for the resolution of inflammation and the repair of tissue following injury (Kazemifard *et al.*, 2025). It has been reported that pro-resolving factors (EGF, TGFβ, VEGF) released by macrophages after efferocytosis, promote the resolution of T cell transfer-induced colitis (Martin-Rodriguez *et al.*, 2021). Macrophage-derived Wnt was vital for effective epithelial regeneration following radiation-induced damage (Saha *et al.*, 2016). Insufficient and delayed mucosal wound healing is associated with IBD. Complete mucosal healing is the desired treatment target with the best long-term implication in prognosis (Neurath, 2014). Therefore, macrophages are currently being investigated as potential therapeutic targets (Hegarty, Jones and Bain, 2023).

MiRNAs are important regulators of macrophage function, and offer a novel approach to uncovering the molecular mechanisms underlying macrophage activity during health and disease. *MiR-223* has been investigated in IBD. Previous studies have showed that *miR-223* is significantly higher during active

inflammation from mucosal biopsies of IBD patients. This miRNA was upregulated in DSS-induced experimental colitis. This work showed that the initial source of *miR-223* was from infiltrating neutrophils and monocytes (Neudecker *et al.*, 2017b). It was observed that *miR-223*$^{-/y}$ mice have exacerbated DSS-colitis, implicating its involvement in constraining intestinal inflammation (Zhou *et al.*, 2015; Neudecker *et al.*, 2017b). Studies have also revealed that *miR-223* deficiency in mice led to a significant decrease in the number of intestinal CX_3CR1^{hi} macrophages. Furthermore, CX_3CR1^{hi} macrophages in these mice exhibit a strong inflammatory phenotype, indicating the involvement of macrophage-associated *miR-223* in aggravating intestinal inflammation (Zhou *et al.*, 2015). Thus, *miR-223* appears to act as a molecular control within myeloid cells and its deficiency mimics the pathophysiology of human UC.

However, the role of *miR-223* in mucosal healing remains largely unexplored. Unpublished data indicate that *miR-223*$^{-/y}$ mice exhibit impaired recovery following DSS-induced colitis. Ten days after DSS withdrawal, *miR-223*$^{-/y}$ mice displayed higher DAI and histological scores compared with WT mice. Hematoxylin and eosin (H and E) staining of the colon confirmed delayed epithelial regeneration in *miR-223*$^{-/y}$ mice (**Figure 4.2**) (Gumer and McNamee). Therefore, understanding how *miR-223* regulates intestinal function has therapeutic implications. Specifically, the role of *miR-223* in controlling macrophage cross-talk with the epithelial stem cell niche is unknown.

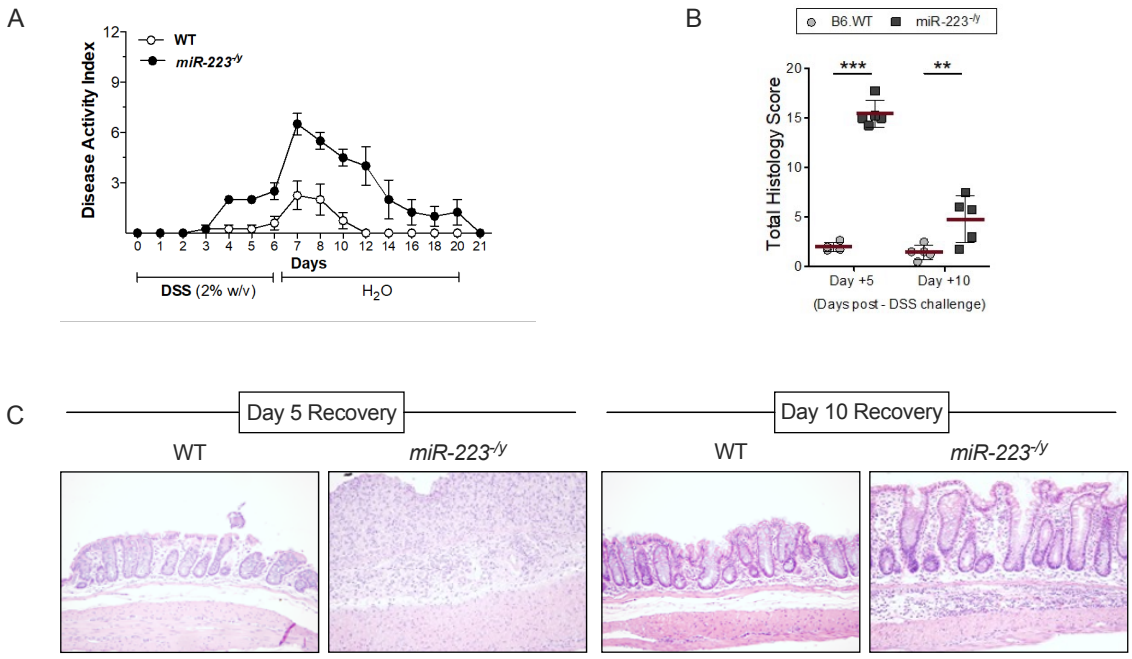

Figure 4.2. *MiR-223$^{-/y}$* have delayed mucosal healing. A. Clinical DAI was a composite of weight change stool score, and occult blood index in WT and *miR-223$^{-/y}$* mice. **B.** Histopathology scores from WT and *miR-223$^{-/y}$* colons during recovery of DSS-colitis. **C.** Representative 10X micrographs of tissue sections from H and E staining. Tissue sections were from WT and *miR-223$^{-/y}$* mice, during recovery in a model of DSS-induced colitis. (Gumer and McNamee).

Leucine-rich repeat-containing G protein-coupled receptor 5 (LGR5^{+}) intestinal stem cells (ISC) are located in the crypt base and they are responsible for the constant renewal and rapid replenishment of all epithelial cell types lining the crypt-villus axis. These adult stem cells give rise to transit-amplifying (TA) progenitor cells which mature into a variety of differentiated cell types namely, tuft cells, goblet cells and intestinal enteroendocrine cells (Meyer *et al.*, 2022; Zheng and Duan, 2023; Hausmann *et al.*, 2024). The microenvironment that regulates the maintenance, self-renewal, proliferation and differentiation of stem cells is referred to as the stem cell niche (Meyer *et al.*, 2022).

There are four signalling pathways that are essential for epithelial proliferation and differentiation in the intestine and they include wingless/integrated (WNT), Notch, bone morphogenetic proteins (BMPs) and epidermal growth factor (EGF) signalling pathways (**Figure 4.3**) (Hausmann *et al.*, 2024).

Briefly, WNT signalling regulates ISC maintenance and differentiation via LRP5/6 and Frizzled receptors, resulting in the stabilisation and nuclear translocation of β-catenin. WNT signalling is augmented by R-spondins, that are ligands for LGR4/5, and stabilize the WNT/LRP/FZ complex. In contrast, notch signalling relies on direct cell-cell contact. Paneth cells express the notch ligands DLL1/4 on their surface and they bind to Notch1-4 receptors through cell-cell contact. This leads to the generation of the Notch intracellular domain, which translocates to the nucleus, interacts with the transcription factor CSL and regulates gene expression. BMP signalling promotes ISC differentiation by inducing phosphorylation of SMAD1/5/8, leading to their translocation into the nucleus, resulting in terminal differentiation. BMP antagonists, such as Gremlin1/2 and Noggin, reside around the crypt bottom and protect stem cells and TA cells from these effects. Finally, EGF receptors are expressed on epithelial cells and they primarily activate the RAS/MAPK signalling pathway, promoting cell fate regulators (Hausmann *et al.*, 2024; Ma *et al.*, 2022).

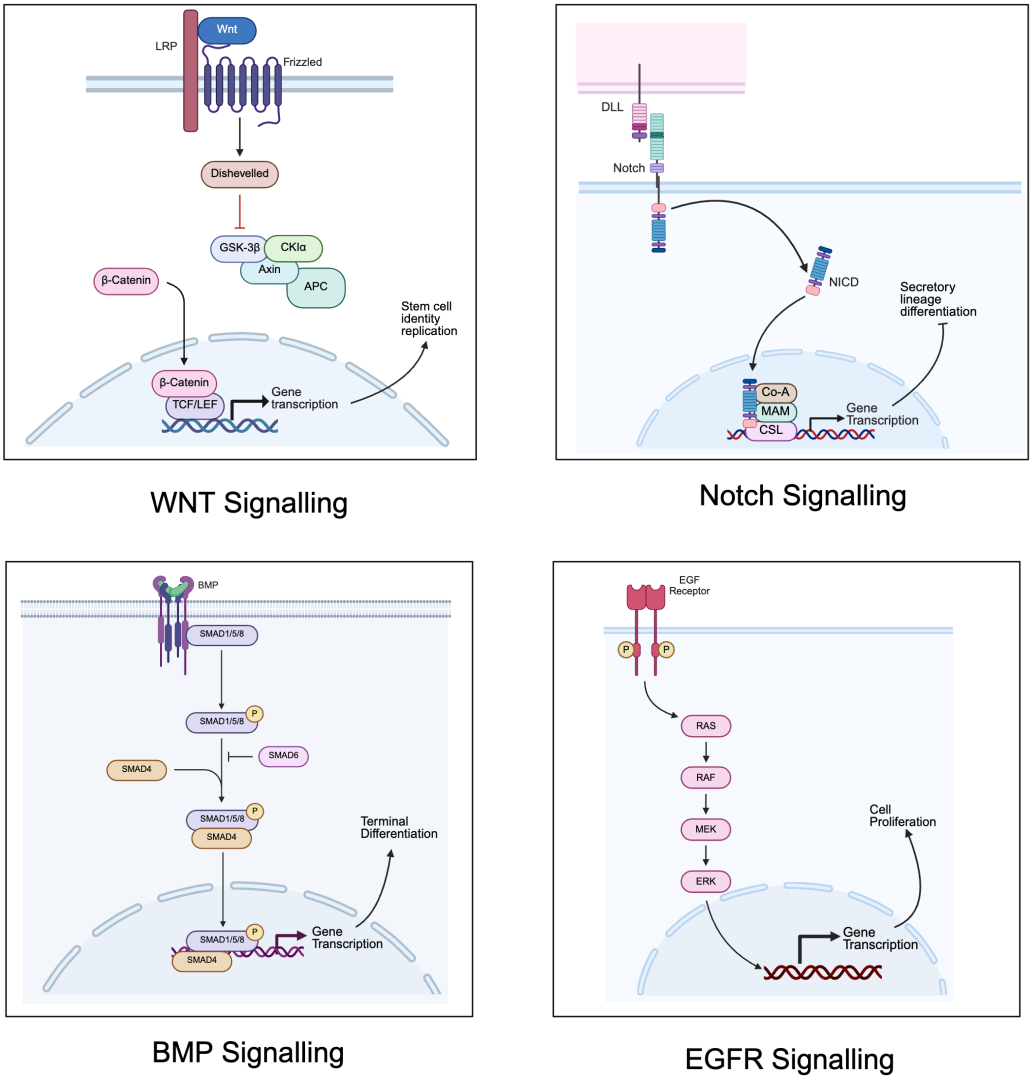

Figure 4.3. ***Signalling pathways involved in the ISC niche maintenance and epithelial cell turnover.*** The four signalling pathways that are essential for epithelial proliferation and differentiation in the intestine are WNT, Notch, BMP and EGFR signalling.

Macrophages have been identified to fulfil stem cell niche-associated roles (**Figure 4.4**). Depletion of macrophages following CSF1R blockade resulted in reversibly reduced numbers of Paneth and LGR5^{+} cells (Sehgal *et al.*, 2018). They have been reported as an emerging source of Wnt ligands. Murine macrophages polarized towards a M2 phenotype, overexpressed Wnt2b, Wnt7b and Wnt10a in a STAT6-dependent manner (Cosín-Roger *et al.*, 2016). Porcupine is required for Wnt signalling. Macrophage-specific deletion of Porcupine resulted in mice being hypersensitive to irradiation-induced injury (Saha *et al.*, 2016). In addition, macrophages produce prostaglandin E2 (PGE2)

and promote ISC proliferation and reduces radiation-induced apoptosis through transactivation of EGFR and enhance activation of AKT (Tessner *et al.*, 2004). Neuregulin 1 (NRG1), is an EGF signalling ligand that is expressed by macrophages. It was reported to drive ISC proliferation and regeneration of damaged epithelium through activation of MAPK and AKT (Jardé *et al.*, 2020). Therefore, macrophages maintain the ISC niche through the secretion of mediators that support Wnt and EGFR signalling (**Figure 4.2**) (Ma *et al.*, 2022).

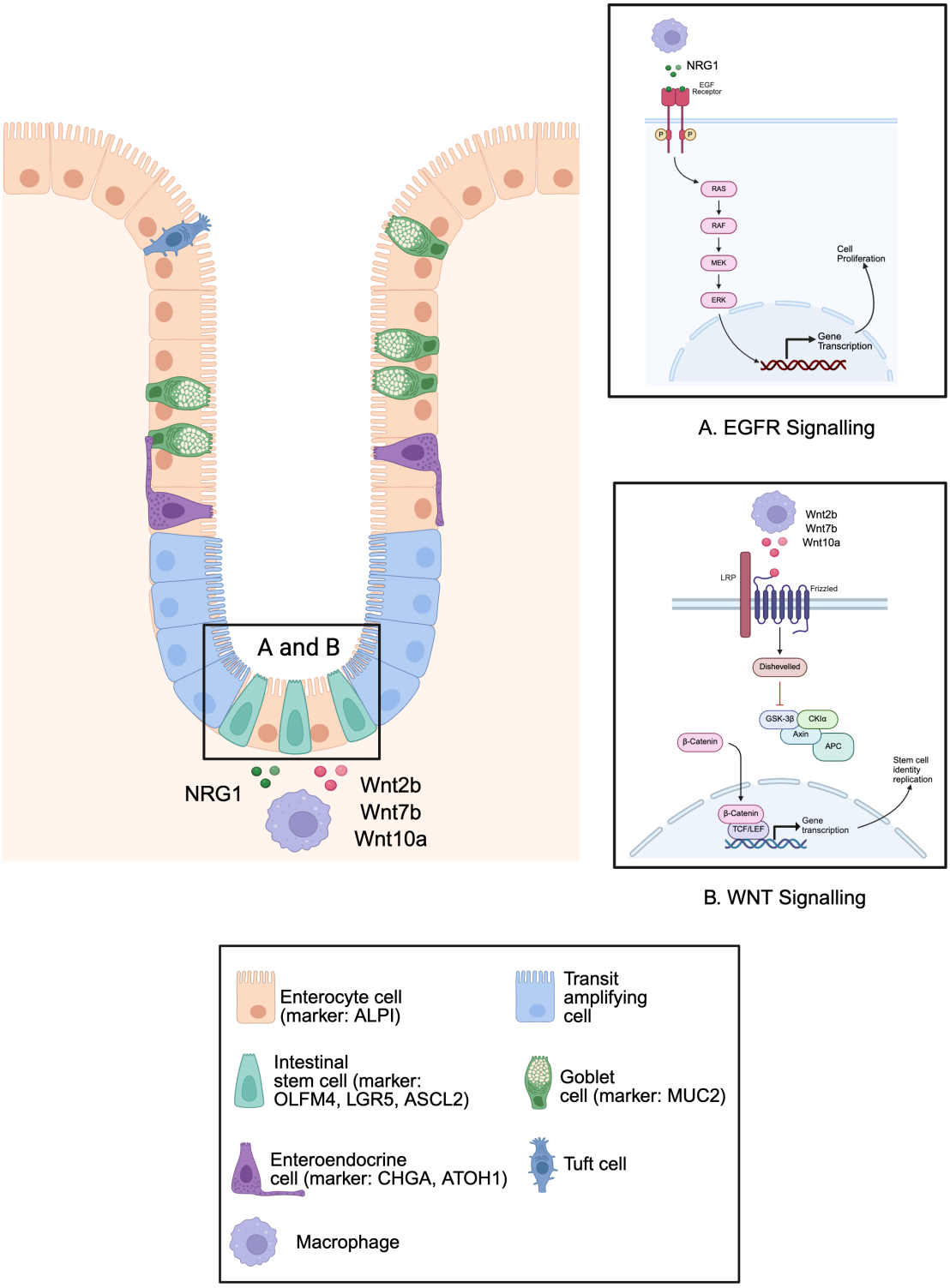

Figure 4.4. ***Macrophage interaction with the stem cell niche.*** Macrophages are involved in maintaining the intestinal stem cell niche. Intestinal macrophages secrete pro-resolving mediators, such as NRG1 and Wnts, that maintain homeostasis and promote mucosal repair following tissue injury.

A newly discovered concept is the remarkable ability of the regenerating intestinal epithelium to acquire a fetal-like transcriptome. The fetal-like regenerative state

has been observed in response to helminth infection, irradiation, ablation of crypt base columnar cells, and DSS-induced colonic damage (Nusse *et al.*, 2018; Yui *et al.*, 2018). Injuries to the small intestine often result in the loss of crypt-based proliferative cells, triggering a fetal-like transcriptional program marked by *Ly6a* (SCA1) expression. This response is driven by immune-, mesenchymal-, ECM-, and epithelial-derived signals and is regulated by mTORC1 and Notch signalling, with activation of YAP/TAZ and SOX9. Resolution of this reprogramming and restoration of tissue homeostasis likely involves suppression of YAP signalling and reactivation of canonical ISC pathways, including Wnt and Notch signalling (**Figure 4.5**) (Mustata *et al.*, 2013; Viragova, Li and Klein, 2024).

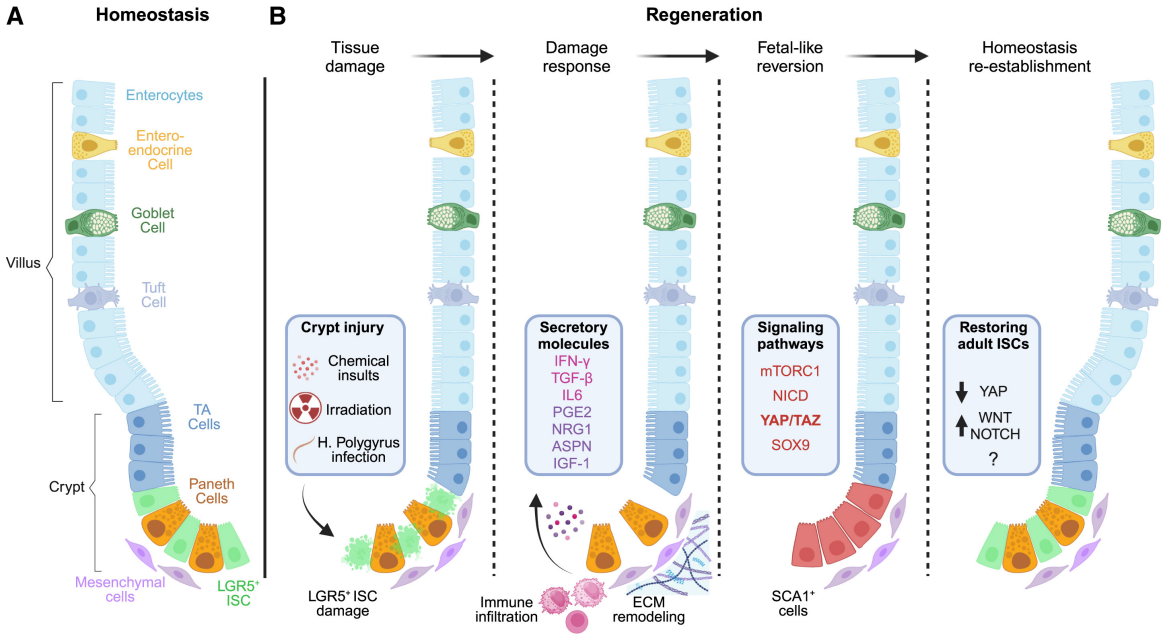

C

Fetal-like Gene Signature

Top 50 genes enriched in fetal intestinal organoids compared to adult organoids (Mustata et al., 2013)

Spp1*	Car2	Msln*	Syt14l	Ly6f	Igfbp7*•	Gkn1	Anxa8*	Eda2r	Ddit4l
Gja1*•	Sftpd*	Vsig1	Crip2*	Sprr1a*	Akap13	Akr1b8	1700007K13Rik	S100a6*°	Pdzk1ip1*
Ctgf*•	Mal*	Expi	Anxa1*†	Lor*†	Sptssb	Cdh13*	Acsm3*	Ldh2	Ly6d*•
Basp1†	Clu*•†	Tubb6*	Col4a1*	Col4a2*	Ecscr°	Slc45a3*°	Ppic•	Ly6c	2310002J15Rik
Tacstd2*•	Wfdc2*	Ly6a†°	Il33°	Krt4*	Ivl*	Efna5*	Anxa3*	Efemp1*•	Cugbp2

Figure 4.5. ***Overview of fetal-like reversion during intestinal regeneration.*** **A.** Small intestinal epithelium under homeostatic conditions. **B.** Following injury, various signalling pathways result in the expression of genes that have previously been characterised as enriched in fetal intestinal spheroids, for example, lymphocyte antigen 6 complex locus A *(Ly6a),* clusterin *(Clu),* gap junction protein alpha 1 *(Gja1)* and tumour-associated calcium signal transducer 2 *(Tacstd2)*. **C.** Fetal-like signature genes; the top 50 differentially expressed genes enriched in fetal intestinal spheroids by Mustata *et al.* (Mustata et al., 2013). Figure taken from (Viragova, Li and Klein, 2024).

Understanding the complex interactions between macrophages and the ISC niche during epithelial repair is emerging as a new research frontier. Furthermore, given its significance in macrophage function in IBD, the involvement of macrophage-associated *miR-223* in regulating mucosal healing offers a novel perspective that is yet to be discovered.

AIMS OF THIS CHAPTER

The overall aim of this chapter was to investigate the hypothesis that macrophage-associated *miR-223* regulates intestinal mucosal healing. The specific aims to address this were as follows:

1. Determine the expression profile of *miR-223* during the continuum of experimental colitis.
2. Evaluate the heterogeneity of macrophages and their impact on mucosal healing in *miR-223*$^{-/y}$ mice during the continuum of experimental colitis.
3. Assess the contribution of macrophage-associated *miR-223* on intestinal epithelial stemness using murine colonic epithelial organoids.

4.1. In a murine model of DSS-induced colitis, *miR-223-3p* is upregulated during active disease.

MiR-223 expression has previously been reported to be increased during active inflammation in IBD and during DSS-induced colitis in mice (Neudecker *et al.*, 2017b). However, the cellular location of this miRNA during disease is yet to be determined. To address this, colonic tissues from WT mice during DSS-induced active colitis and recovery were analysed via *in situ* hybridization. Initially, this procedure was optimised by measuring expression of RNU6 (positive control) and a Scramble sequence (negative control) (**Figure 4.1.1. A**). *MiR-223-3p* is considered the guide strand of *miR-233*, therefore, it was this strand that was investigated. Quantification of this staining revealed that *miR-223-3p* is upregulated during active colitis. Although not significant, during the recovery phase of this mouse model, a slight reduction in *miR-223-3p* expression was observed (**Figure 4.1.1. B** and **C**). It is also important to note, that *miR-223-3p* was most highly expressed in areas of more severe inflammation.

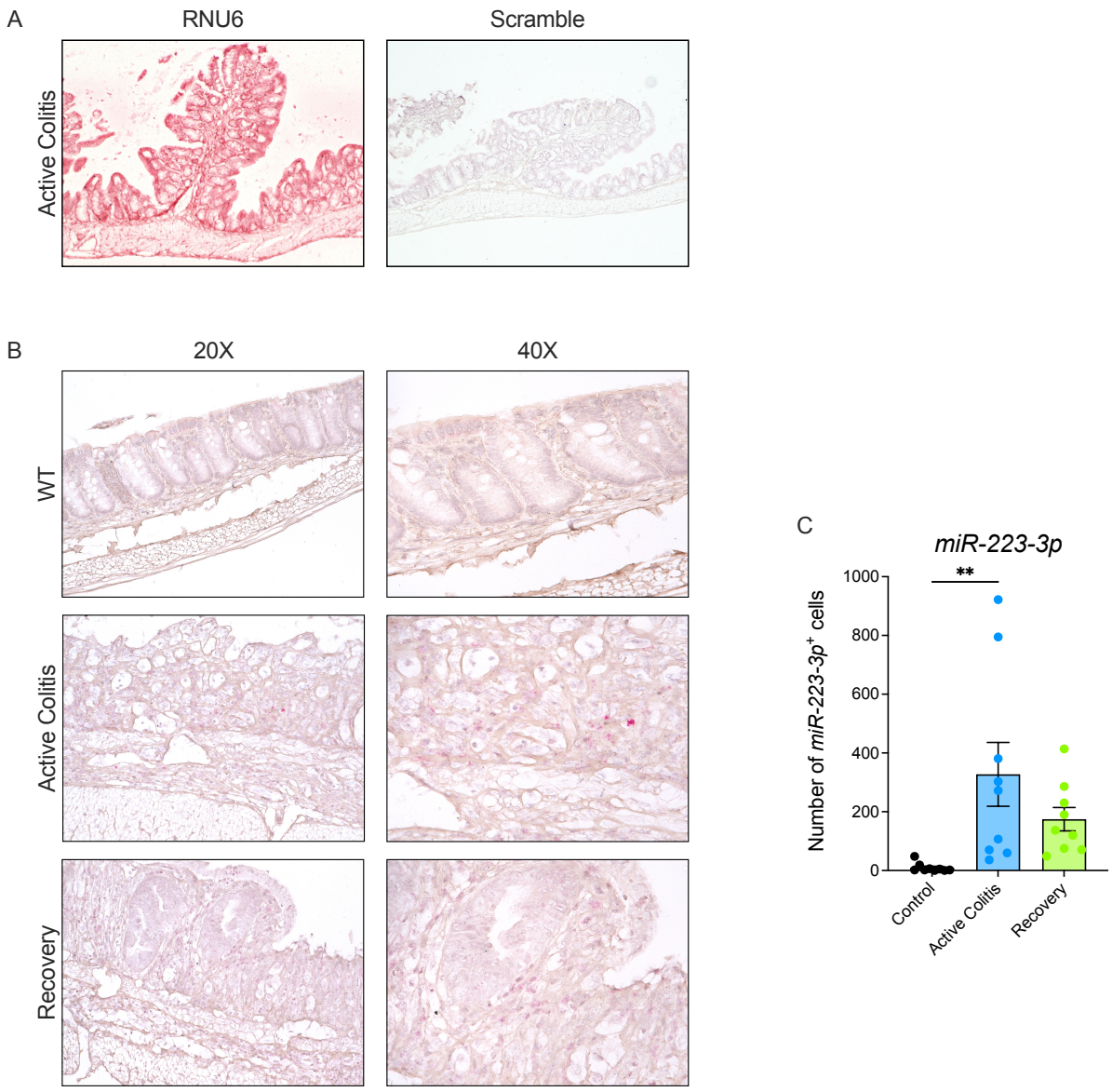

Figure 4.1.1. ***MiR-223-3p is upregulated during active colitis.*** **A.** Representative 10X images of tissue sections following *in situ* hybridization staining for RNU6 and a Scramble sequence. **B.** Representative 20X and 40X micrographs of tissue sections following *in situ* hybridization staining for *miR-223-3p*. Tissue sections were from WT mice, during active inflammation and recovery in a model of DSS-induced colitis. **C.** Quantification of *miR-223-3p*$^{+}$ cells. Data are expressed as mean ± SEM; *, P ≤ 0.05; **, P ≤ 0.01, ***, P ≤ 0.001, ****, P ≤ 0.0001 versus the indicated counterpart (one-way ANOVA). n = 3 biological replicates/group with 3 fields of view presented per animal (total of 9 points on graph).

4.2. *MiR-223*$^{-/y}$ mice have enhanced colonic influx of CCR2^{+} monocytes and CD68^{+} macrophages during active disease and the recovery phase of a DSS-induced colitis model.

MiR-223 deficiency has been reported to lead to exacerbated intestinal inflammation, however, the impact on mucosal healing has scarcely been addressed (Neudecker *et al.*, 2017b). Initially, immunohistochemical staining was carried out on colonic tissues from WT and *miR-223*$^{-/y}$ mice in order to examine the myeloid signature during the continuum of experimental colitis. Quantification of this staining showed a greater number of CCR2^{+} monocytes and CD68^{+} macrophages in *miR-223*$^{-/y}$ mice during active disease, in comparison to control and WT counterparts (**Figure 4.2.1.** and **Figure 4.2.2. A** – **B**). Similar differences in the *miR-223*$^{-/y}$ mice were observed during the recovery phase (**Figure 4.2.1.** and **Figure 4.2.2. C**). In contrast, WT mice presented with minimal differences (**Figure 4.2.1.** and **Figure 4.2.2. A** – **F**).

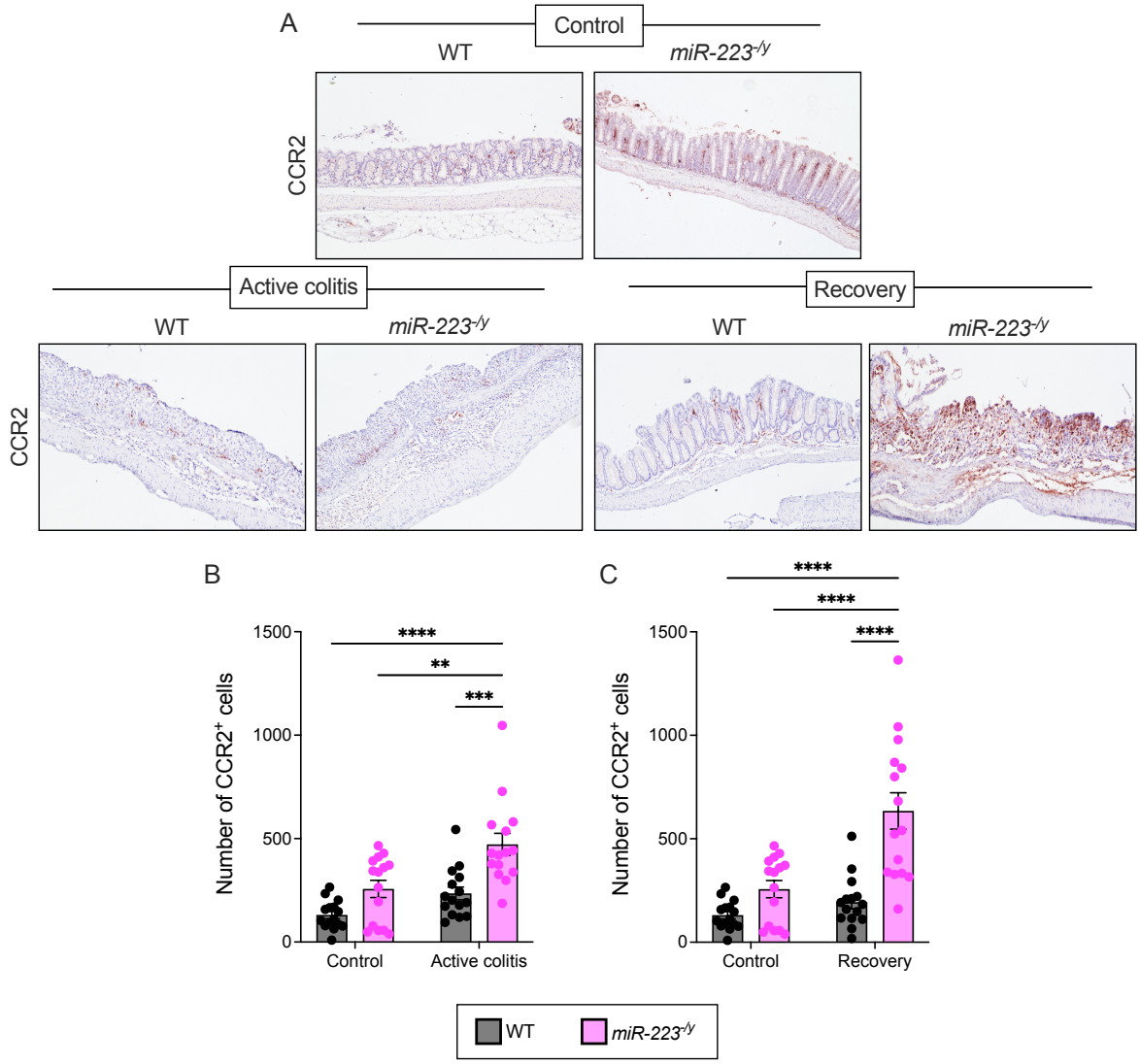

Figure 4.2.1. ***MiR-223$^{-/y}$ mice have enhanced colonic influx of CCR2^{+} monocytes during active disease and the recovery phase of a DSS-induced colitis model.*** **A**. Representative 10X micrographs of tissue sections from immunohistochemical staining for CCR2. Tissue sections were from WT and *miR-223$^{-/y}$* mice, during active inflammation and recovery in a model of DSS-induced colitis. Quantification of **B** – **C**. CCR2^{+} cells. Data are expressed as mean ± SEM; *, P ≤ 0.05; **, P ≤ 0.01, ***, P ≤ 0.001, ****, P ≤ 0.0001 versus the indicated counterpart (two-way ANOVA). Same controls were used in **B** and **C**. n = 3 biological replicates/group with 5 fields of view presented per animal (total of 15 points on graph).

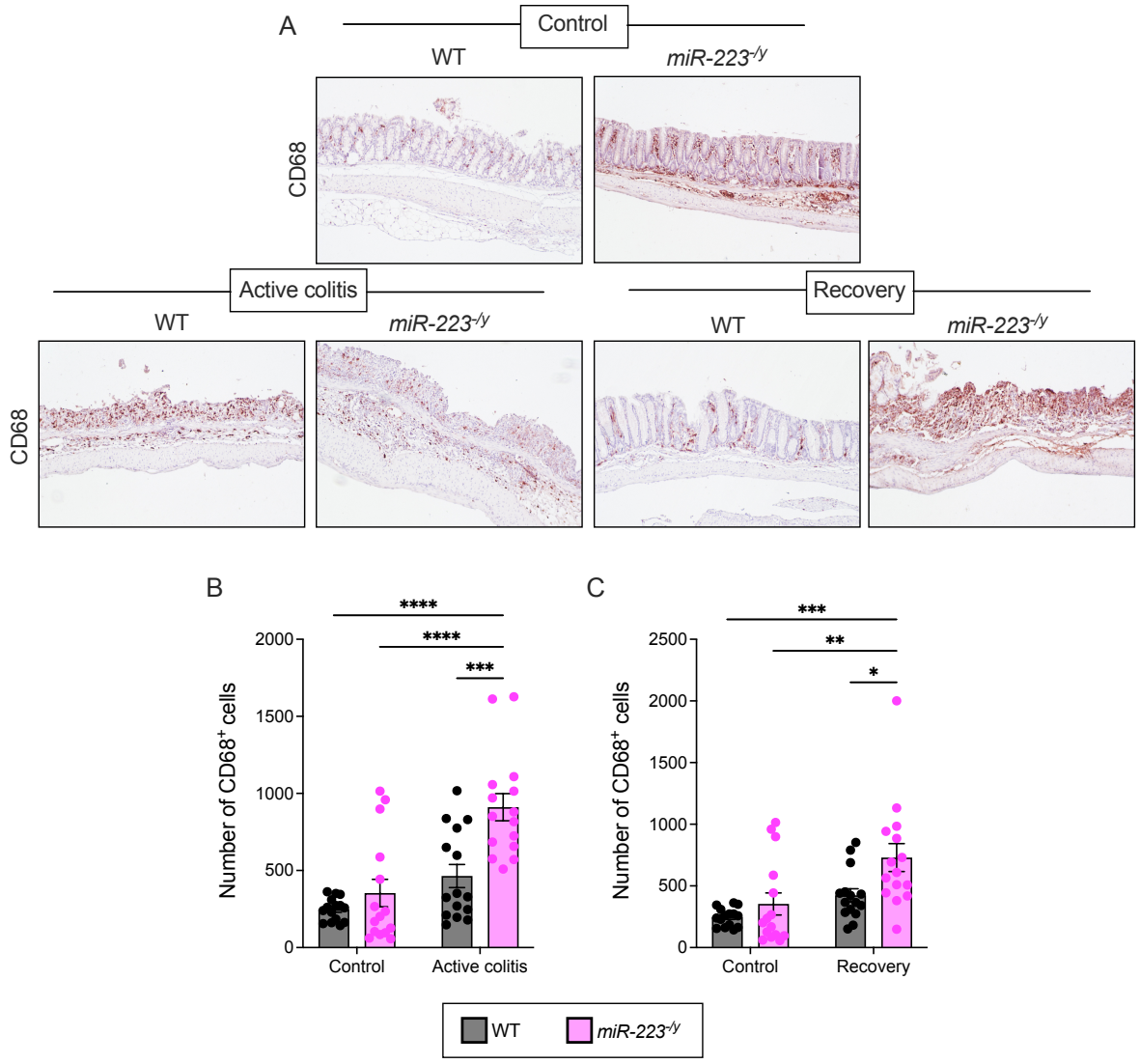

Figure 4.2.2. *MiR-223$^{-/y}$ mice have enhanced colonic influx of CD68^{+} macrophages during active disease and the recovery phase of a DSS-induced colitis model.* **A**. Representative 10X micrographs of tissue sections from immunohistochemical staining for CD68. Tissue sections were from WT and *miR-223$^{-/y}$* mice, during active inflammation and recovery in a model of DSS-induced colitis. Quantification of **B** – **C**. CD68^{+} cells. Data are expressed as mean ± SEM; *, P ≤ 0.05; **, P ≤ 0.01, ***, P ≤ 0.001, ****, P ≤ 0.0001 versus the indicated counterpart (two-way ANOVA). Same controls were used in **B** and **C**. n = 3 biological replicates/group with 5 fields of view presented per animal (total of 15 points on graph).

4.3. *MiR-223*$^{-/y}$ mice present with increased expression of pro-reparative macrophages during active disease and the recovery phase of DSS-induced experimental colitis.

Work has demonstrated that *miR-223*$^{-/y}$ colons present with increased myeloid infiltrate during active disease, which persists into the recovery phase of DSS-induced experimental colitis. To understand how *miR-223* regulates repair mechanisms, colonic tissues from DSS-treated WT and *miR-223*$^{-/y}$ mice were assessed for the presence of pro-reparative macrophage markers, MERTK, CD206 and Relmα. Quantification of this immunohistochemical staining showed minimal differences between WT and *miR-223*$^{-/y}$ mice at baseline (**Figure 4.3.1. A** – **I**). However, the numbers of MERTK^{+}, CD206^{+} and Relmα^{+} cells were consistently higher in *miR-223*$^{-/y}$ mice, in comparison to WT counterparts, during active disease and the recovery phase of DSS-colitis (**Figure 4.3.1. A** – **I**). This indicates that *miR-223* has the capacity to regulate the colonic myeloid signature, both inflammatory and reparative, during the continuum of experimental colitis.

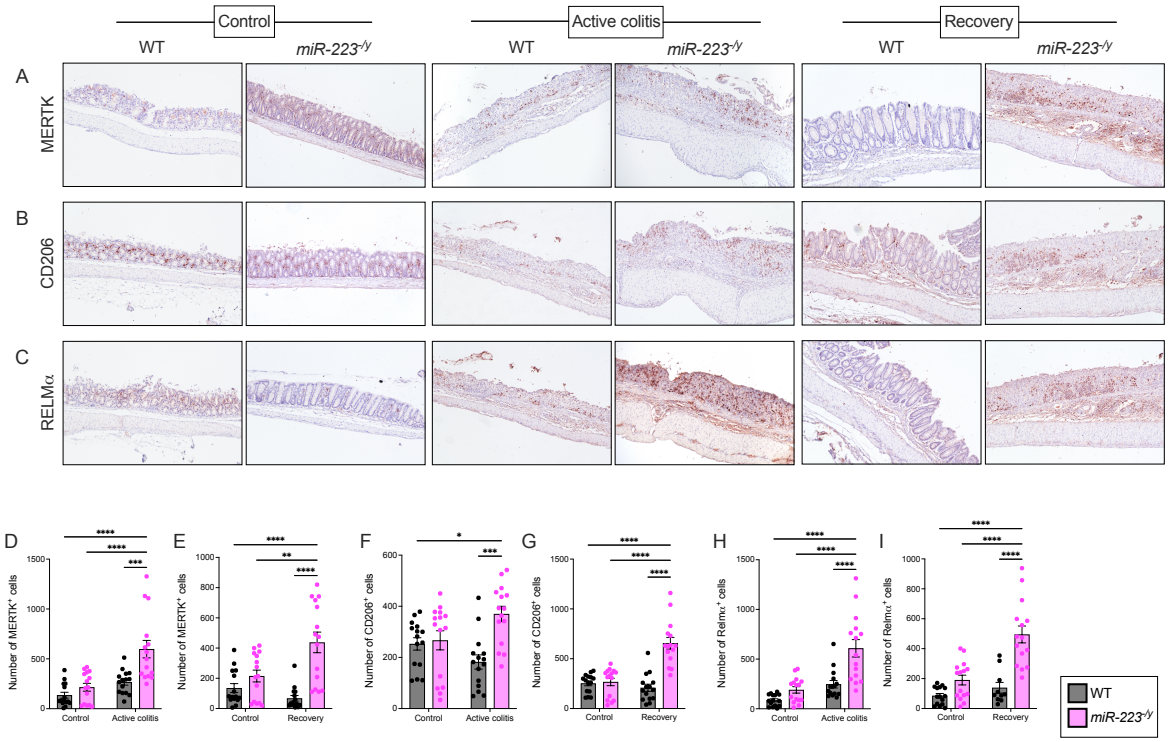

Figure 4.3.1. ***MiR-223$^{-/y}$ colons have increased expression of pro-reparative macrophages during active disease and the recovery phase of DSS-induced experimental colitis.*** **A** – **C**. Representative 10X images of immunohistochemical staining of colonic tissue sections for MERTK, CD206 and Relmα. Tissue sections were from WT and *miR-223$^{-/y}$* mice, during active inflammation and recovery in a model of DSS-induced colitis. Quantification of **D** – **E**. MERTK^{+}, **F** – **G.** CD206^{+}, **H** – **I**. Relmα^{+} cells. Data are expressed as mean ± SEM; *, P ≤ 0.05; **, P ≤ 0.01, ***, P ≤ 0.001, ****, P ≤ 0.0001 versus the indicated counterpart (two-way ANOVA). Same controls were used in **D** and **E**, **F** and **G**, **H** and **I**. n = 3 biological replicates/group with 5 fields of view presented per animal (total of 15 points on graph).

4.4. Dysregulated epithelial stem cell patterning in *miR-223$^{-/y}$* colon during experimental colitis.

Interestingly, the delayed mucosal healing observed in *miR-223$^{-/y}$* mice is not the result of a lack of pro-reparative macrophages in the intestine. Therefore, the next area of investigation was the ISC niche. There is a plethora of evidence that demonstrates the ability of the ISC niche to adapt beyond its homeostatic state to interpret pathogenic stimuli and translate them into regeneration of the epithelium (Santos *et al.*, 2018).

Immunohistochemical analysis of colonic tissues from WT and *miR-223*$^{-/y}$ during DSS-induced colitis showed that the mature stem cell marker olfactomedin 4, OLFM4, was significantly upregulated in *miR-223*$^{-/y}$ mice during active disease, and this persisted into the recovery phase (**Figure 4.4.1. A, C, D)**. Similarly, lymphocyte antigen 6 family member A, or LY6A, a fetal-like stem cell marker was induced in *miR-223*$^{-/y}$ colons (**Figure 4.4.1. B, E, F**).

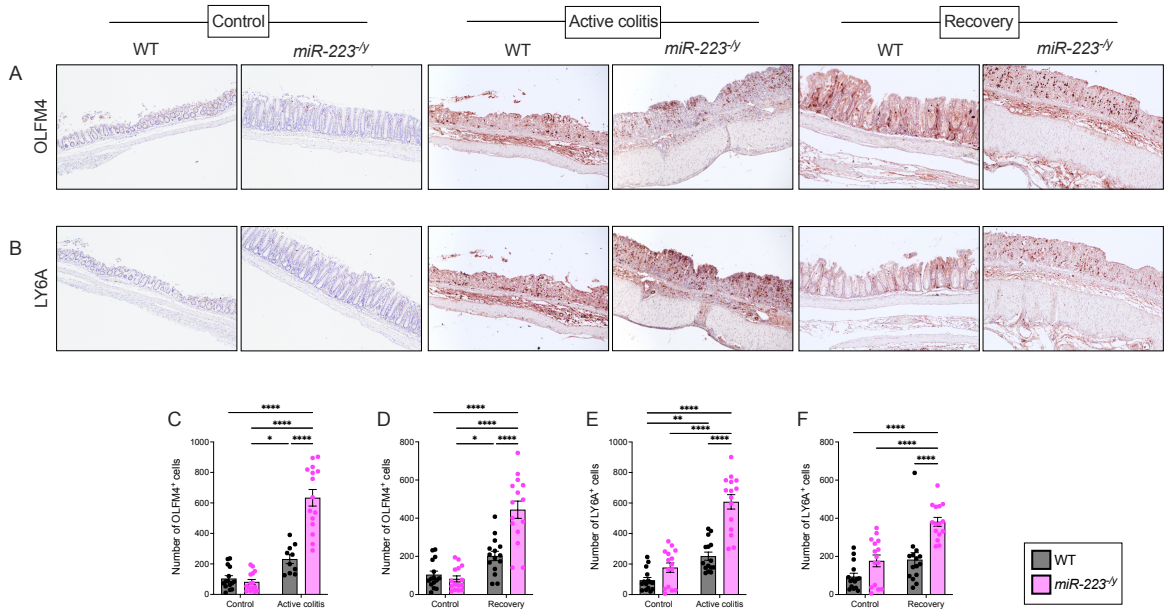

Figure 4.4.1. ***Upregulation of the mature stem cell marker, OLFM4, and the fetal-like stem cell marker, LY6A, were observed in the miR-223*$^{-/y}$ *mice.*** **A** and **B.** Representative 10X images of immunohistochemical staining of colonic tissue sections for OLFM4 and LY6A. Tissue sections were from WT and *miR-223*$^{-/y}$ mice, during active inflammation and recovery in a model of DSS-induced colitis. Quantification of **C** and **D.** OLFM4^{+}, and **E – F**. LY6A^{+} cells. Data are expressed as mean ± SEM; *, P ≤ 0.05; **, P ≤ 0.01, ***, P ≤ 0.001, ****, P ≤ 0.0001 versus the indicated counterpart (two-way ANOVA). Same controls were used in **C** and **D**, **E** and **F**. n = 3 biological replicates/group with 5 fields of view presented per animal (total of 15 points on graph).

ISCs are precursors for differentiated epithelial cells. Following injury, differentiated cells can undergo a process referred to as dedifferentiation, whereby they revert to a stem-like state. To investigate this process in the *miR-223*$^{-/y}$ mice, MUC2, the marker for goblet cells, was assessed via immunohistochemical staining. Alterations in its expression pattern were discovered. In WT animals, MUC2, was confined to the crypts, remaining there

over the course of the DSS-induced colitis model (**Figure 4.4.2. A**). In *miR-223*$^{-/y}$ mice, the staining pattern during active disease and recovery differed considerably. MUC2 was expressed throughout the distorted epithelium and possessed an atypical appearance (**Figure 4.4.2. A**). Unlike differentiated cells, intestinal stem cells are highly proliferative. Proliferation markers, PCNA and Cyclin D1, were predominantly restricted to the epithelium or, during active disease, around crypt abscesses in WT colons (**Figure 4.4.2. B and C**). However, this was not the case in *miR-223*$^{-/y}$ animals. PCNA^{+} and Cyclin D1^{+} cells were identified in the epithelium and the lamina propria during the continuum of experimental colitis (**Figure 4.4.2. B and C**). Collectively, this data suggests a dysregulation in regeneration in *miR-223*$^{-/y}$ mice.

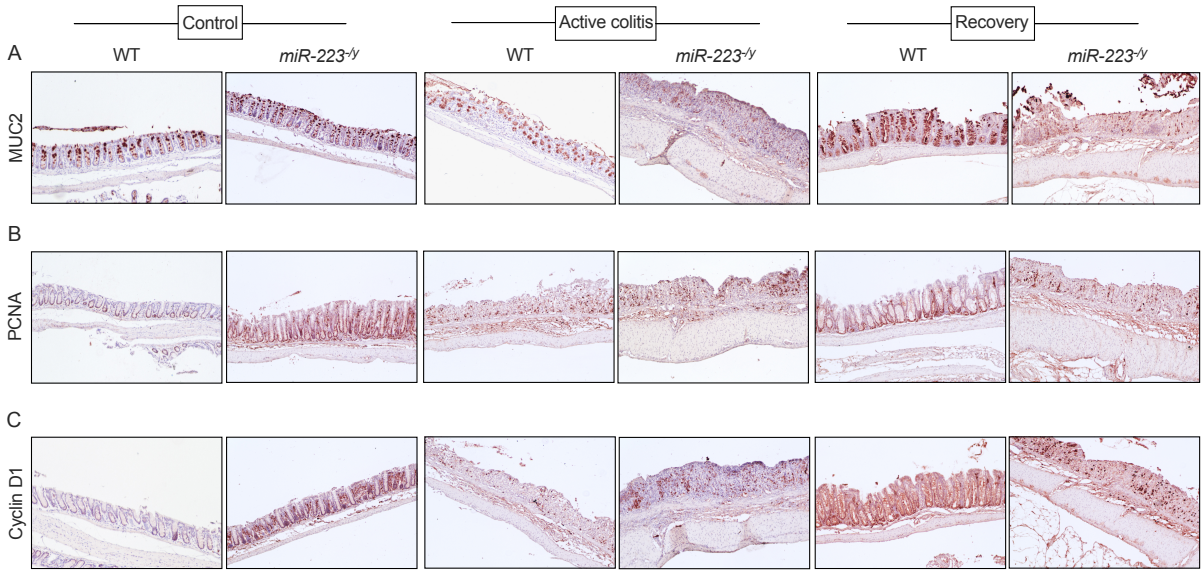

Figure 4.4.2. ***MiR-223*$^{-/y}$ *mice present with alterations in the staining pattern of the differentiation cell marker, MUC2, and the proliferation markers, PCNA and Cyclin D1.*** **A, B** and **C**. Representative 10X images of immunohistochemical staining of colonic tissue sections for MUC2, PCNA and Cyclin D1. Tissue sections were from WT and *miR-223*$^{-/y}$ mice, during active inflammation and recovery in a model of DSS-induced colitis. n = 3 biological replicates/group.

4.5. Utilization of an indirect co-culture system to investigate the role of *miR-223* in regulating the cross-talk between macrophages and colonic epithelial organoids.

To further examine the cross-talk between macrophages and colonic epithelial organoids and how *miR-223* is implicated in this process, an indirect co-culture system was used. On day 3 post-passage, organoids were cultured in conditioned media (CM) from RAW 264.7 cells, *miR-223KD (223KD)* cells, BMDMs and BMDMs transfected with a *miR-223-3p* synthetic mimic (*3p* mimic). Each cell line was stimulated with either LPS (100 ng/mL) or IL-4 (10 ng/mL).

Morphologically, a specific phenotype was not identified. Organoids cultured in the normal growth medium were present in various stages of growth (**Figure 4.5.1**). Fetal-like organoids are typically characterised by a spheroid shape, in contrast to mature organoids, that possess complex, budding structures (**Figure 4.5.1**). All stages of growth were observed in organoids that were cultured in conditioned media (**Figure 4.5.2** – **4.5.5**). However, cell death was more prevalent in these cells, particularly those organoids that were culture with conditioned media from LPS-stimulated macrophages (**Figure 4.5.2** – **4.5.5**).

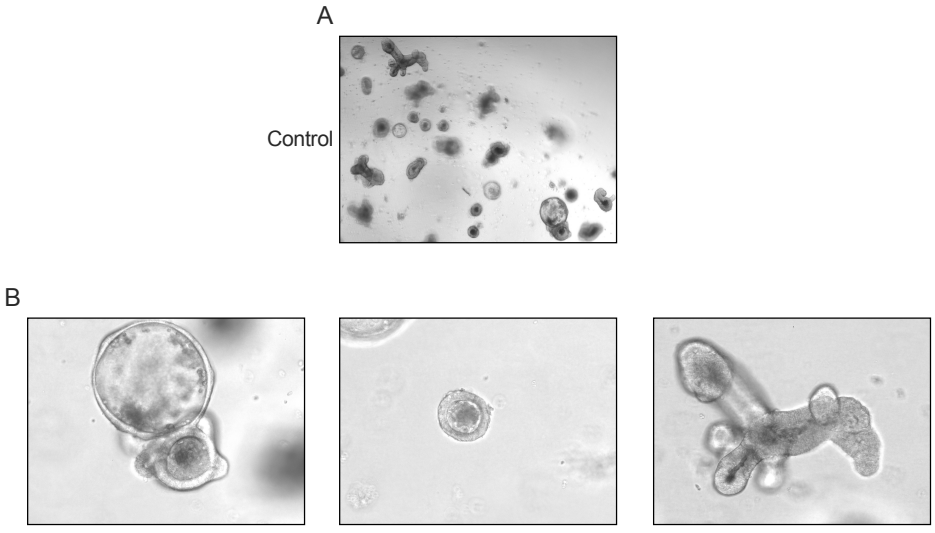

Figure 4.5.1. ***Colonic epithelial organoids cultured in normal growth medium.*** **A.** Representative 4X image of colonic epithelial organoids cultured in normal growth medium. **B.** Representative 20X images of colonic epithelial organoids at various stages of growth – fetal-like organoids to mature organoids. n = 3 biological replicates/group.

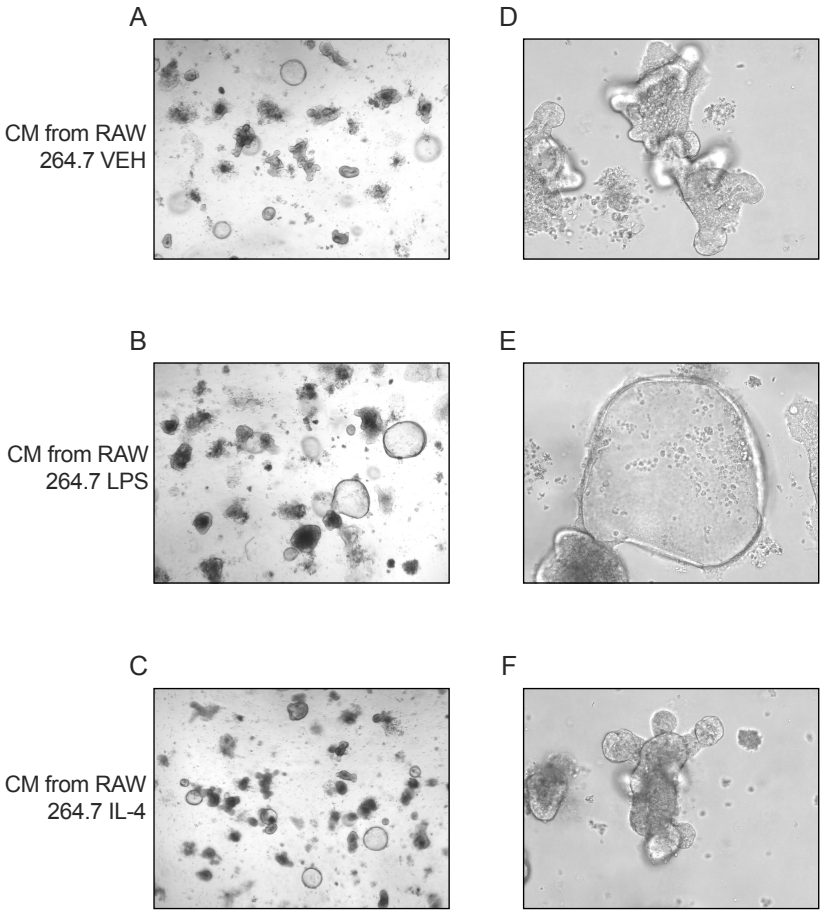

Figure 4.5.2. ***Colonic epithelial organoids cultured in conditioned media (CM) from RAW 264.7 cells on day 3 post-passage.*** **A** and **D.** Organoids cultured in CM from RAW 264.7 cells. **B** and **E.** Organoids cultured in CM from RAW 264.7 cells stimulated with LPS (100 ng/mL) for 24 h. **C** and **F.** Organoids cultured in CM from RAW 264.7 cells stimulated with IL-4 (10 ng/mL) for 24 h. **A** – **C**. Representative 4X images. **D** – **E**. Representative 20X images. n = 3 biological replicates/group.

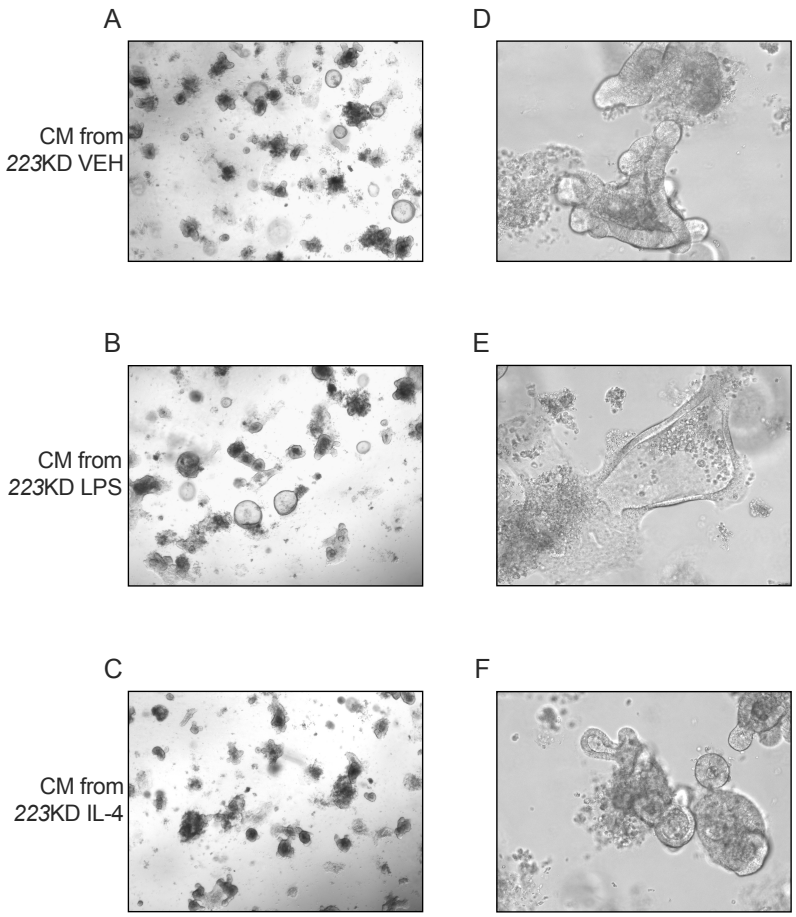

Figure 4.5.3. ***Colonic epithelial organoids cultured in conditioned media (CM) from 223KD cells on day 3 post-passage.*** **A** and **D.** Organoids cultured in CM from 223KD cells. **B** and **E.** Organoids cultured in CM from *223*KD cells stimulated with LPS (100 ng/mL) for 24 h. **C** and **F.** Organoids cultured in CM from *223*KD cells stimulated with IL-4 (10 ng/mL) for 24 h. **A** – **C**. Representative 4X images. **D** – **E**. Representative 20X images. n = 3 biological replicates/group.

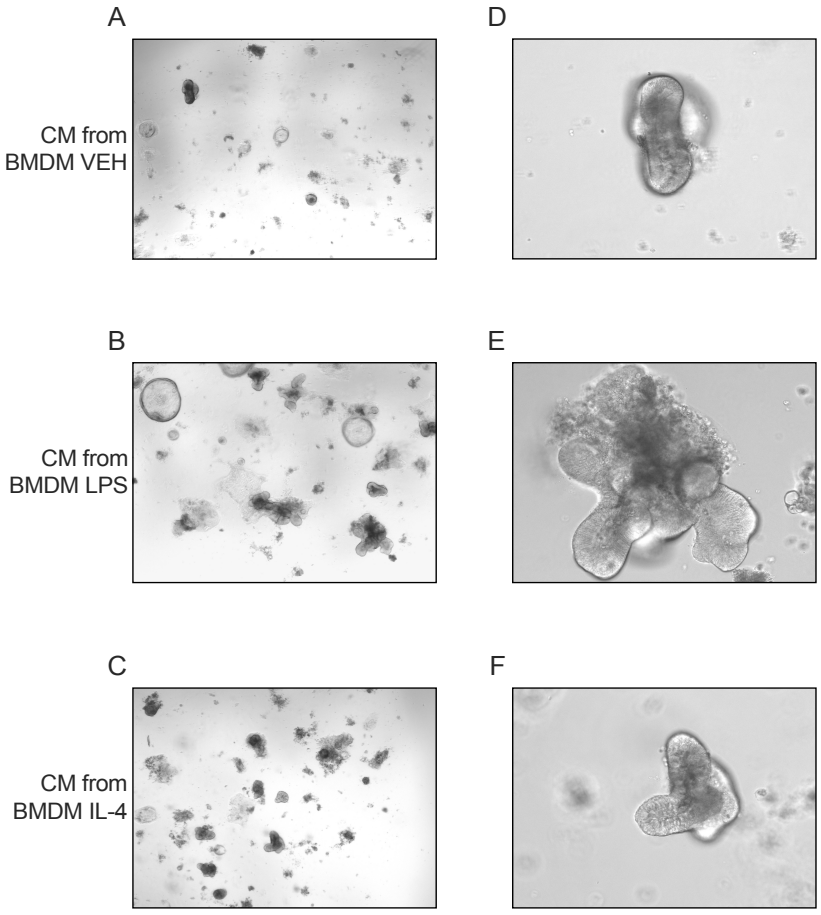

Figure 4.5.4. ***Colonic epithelial organoids cultured in conditioned media (CM) from BMDMs on day 3 post-passage.*** **A** and **D.** Organoids cultured in CM from BMDMs. **B** and **E.** Organoids cultured in CM from BMDMs stimulated with LPS (100 ng/mL) for 24 h. **C** and **F.** Organoids cultured in CM from BMDMs stimulated with IL-4 (10 ng/mL) for 24 h. **A** – **C**. Representative 4X images. **D** – **E**. Representative 20X images. n = 3 biological replicates/group.

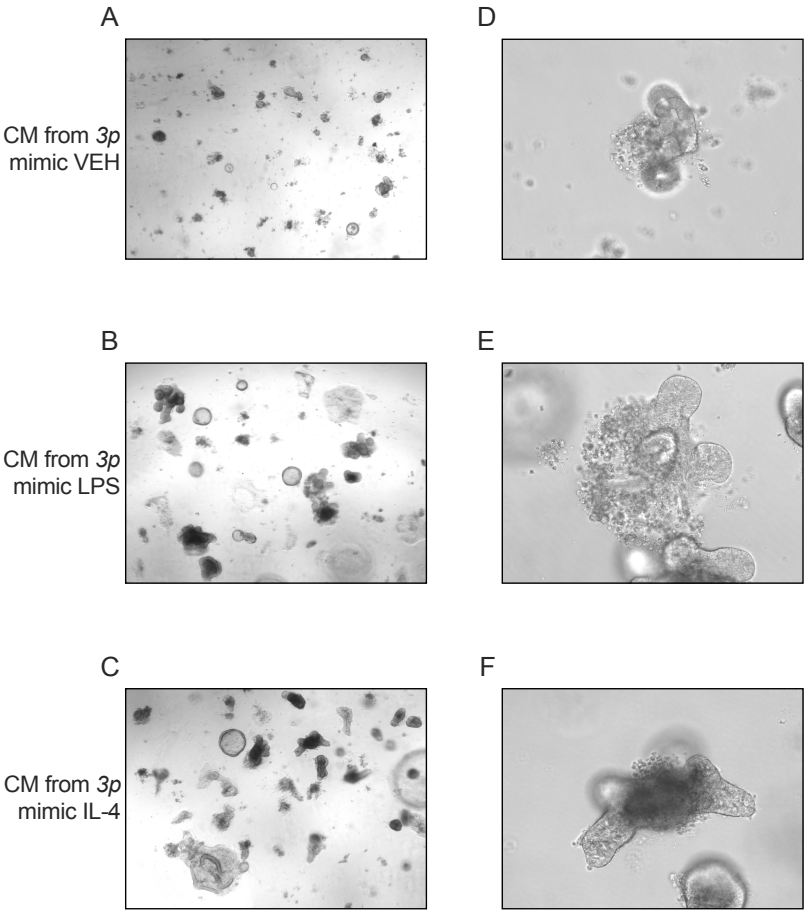

Figure 4.5.5. ***Colonic epithelial organoids cultured in conditioned media (CM) from BMDMs, transfected with a miR-223-3p synthetic mimic, on day 3 post-passage.*** **A** and **D.** Organoids cultured in CM from BMDMs, transfected with a *3p* mimic. **B** and **E.** Organoids cultured in CM from BMDMs, transfected with a *3p* mimic, stimulated with LPS (100 ng/mL) for 24 h. **C** and **F.** Organoids cultured in CM from BMDMs, transfected with a *3p* mimic stimulated with IL-4 (10 ng/mL) for 24 h. **A** – **C**. Representative 4X images. **D** – **E**. Representative 20X images. n = 3 biological replicates/group.

Following co-culture with conditioned media, organoids were harvested and the expression of stem cell and differentiated cell markers were analysed via RT-PCR. Changes were not observed at a transcriptional level between the different conditions (**Figure 4.5.6. A** – **F**, and **Figure 4.5.7. A** – **F**). These data show, that indirect co-culture of colonic epithelial organoids with conditioned media, is not an optimal system for investigating the cross-talk between macrophages and intestinal epithelial cells.

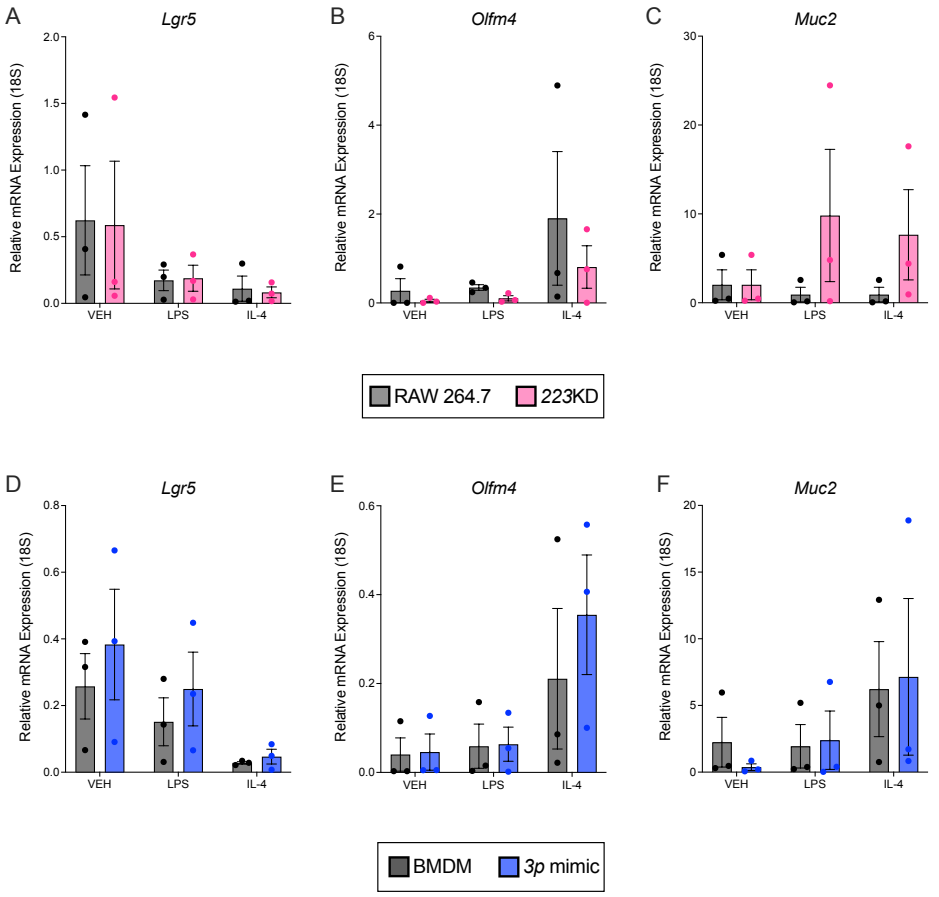

Figure 4.5.6. ***Gene expression levels of stem cell and differentiated cell markers are unchanged following indirect co-culture of colonic epithelial organoids with conditioned media from miR-223-manipulated macrophages.*** Relative mRNA expression of **A.** *Lgr5*, **B.** *Olfm4* and **C.** *Muc2* in colonic organoids following co-culture with CM from RAW 264.7 and *223KD* cells. Relative mRNA expression of **D.** *Lgr5*, **E.** *Olfm4* and **F.** *Muc2* in colonic organoids co-cultured with CM from BMDMs and BMDMs transfected with a *3p* mimic. Data are expressed as mean ± SEM; *, P ≤ 0.05; **, P ≤ 0.01, ***, P ≤ 0.001, ****, P ≤ 0.0001, versus the indicated counterpart (two-way ANOVA). n = 3 biological replicates/group.

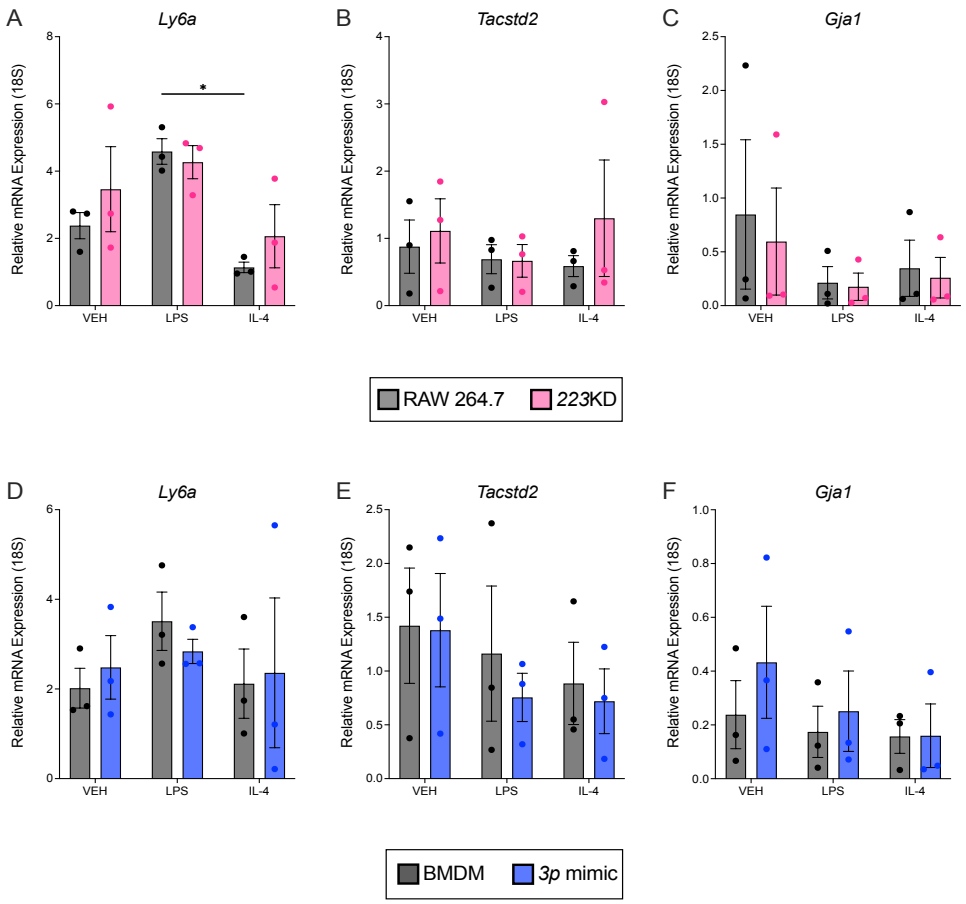

Figure 4.5.7. ***Gene expression levels of fetal-like stem cell markers are unchanged following indirect co-culture of colonic epithelial organoids with conditioned media from miR-223-manipulated macrophages.*** Relative mRNA expression of **A.** *Ly6a*, **B.** *Tacstd2* and **C.** *Gja1* in colonic organoids following co-culture with CM from RAW 264.7 and *223KD* cells. Relative mRNA expression of **D.** *Ly6a*, **E.** *Tacstd2* and **F.** *Gja1* in colonic organoids co-cultured with CM from BMDMs and BMDMs transfected with a *3p* mimic. Data are expressed as mean ± SEM; *, P ≤ 0.05; **, P ≤ 0.01, ***, P ≤ 0.001, ****, P ≤ 0.0001, versus the indicated counterpart (two-way ANOVA). n = 3 biological replicates/group.

DISCUSSION

IBD is characterised by chronic intestinal inflammation, resulting in relapsing and remitting symptoms. The relapsing-remitting feature of IBD involves repeated inflammatory insults to the intestine followed by a healing process in order to return to normal function and attain remission (Villablanca, Selin and Hedin, 2022). Almost all currently available therapies for this disease act by inhibiting inflammation, for example infliximab, a biologic that targets TNF-α (Selinger, Rosiou and Lenti, 2024). However, as these biologics suppress the immune system, there is an increased risk of infections and other malignancies, such as lymphoma (Ford and Peyrin-Biroulet, 2013; Lemaitre *et al.*, 2017). As a result, mucosal healing has become an increasingly acknowledged goal in IBD therapy in order to achieve and maintain long-term remission (Sommer *et al.*, 2021). Unfortunately, few therapeutics attempt to harness the regenerative response (Villablanca, Selin and Hedin, 2022). Therefore, identifying molecular targets and pathways that promote mucosal healing and recovery has the potential to be a therapeutic alternative to treat IBD.

During active disease, *miR-223* has been reported to be upregulated in IBD and in the DSS-induced colitis model (Neudecker *et al.*, 2017b). During the course of colitis induction, this miRNA is abundantly expressed in neutrophils and monocytes, and lowly expressed in dendritic cells and macrophages (Zhou *et al.*, 2015; Neudecker *et al.*, 2017b). Although its restriction to myeloid cells has previously been shown, the expression profile of *miR-223* during recovery and its cellular location during the continuum of experimental colitis is yet to be explored. Here, *in situ* hybridization studies confirmed that *miR-223* was significantly upregulated during active disease. However, only minor decreases in expression were observed during recovery. WT mice were euthanised 5 days after DSS removal from drinking water (recovery) and colon mucosa abnormalities were still present at this stage. It has been demonstrated that the effects of DSS on colon mucosa can persist more than 3 weeks after the removal of DSS from drinking water, potentially explaining the minimal changes in expression observed between active disease and recovery (Vidal-Lletjós *et al.*, 2019). *MiR-223* was also observed to accumulate in areas of severe inflammation, which are

characterised by increased cell infiltration into lamina propria, ulceration and crypt irregularity or loss. The location of *miR-223* correlated with the accumulation of myeloid cells at these sites (Remke *et al.*, 2024).

MiR-223 deficiency results in exacerbated inflammation in DSS-induced colitis. This is accompanied by an influx of monocytes and neutrophils (Zhou *et al.*, 2015; Neudecker *et al.*, 2017b). Furthermore, intestinal macrophages and dendritic cells exhibit a strong pro-inflammatory signature (Zhou *et al.*, 2015). This further demonstrates that *miR-223*-deficient mice possess a pro-inflammatory myeloid signature during active disease. However, little is known about whether these effects persist into the recovery phase of this mouse model.

In conjunction with the "monocyte waterfall" concept, there is considerable evidence to indicate that Ly6C^{hi} monocytes can give rise to intestinal macrophages during inflammation (Tamoutounour *et al.*, 2012; Platt *et al.*, 2010). Further studies have revealed that CCR2 expression, which is commonly used as a marker for inflammatory monocytes in mice, is essential to the recruitment of bone marrow-derived Ly6C^{hi} monocytes into the inflamed colon during acute colitis. Furthermore, ablation of these cells reduces intestinal inflammation (Bain *et al.*, 2014; Zigmond *et al.*, 2012). The work presented here showed that CCR2^{+} monocytes are increased on *miR-223*$^{-/y}$ colons, which has previously been reported in the literature (Neudecker *et al.*, 2017b; Flynn *et al.*, 2024). However, this upregulation was also observed in the recovery phase. As a consequence of this upregulation in CCR2^{+} monocytes, a similar pattern of expression was seen with CD68^{+} macrophages in the colon during the continuum of experimental colitis. These findings suggest that the absence of *miR-223* underlies the excessive myeloid inflammation observed during active disease and its persistence into the recovery phase.

Monocytes recruited from the bone marrow are responsible for the generation of immature, pro-inflammatory macrophages. This process drives inflammation in the context of IBD, causing severe epithelial damage. However, it is also essential for initiating repair, as efferocytosis of apoptotic cells by these macrophages downregulates secretion of pro-inflammatory molecules, while promoting the production of immunoregulatory cytokines, such as TGF-β and IL-10 (Bain *et al.*,

2013; Bain *et al.*, 2014; Ho *et al.*, 2020). This process is predicted to be disrupted in IBD. In a model of T-cell mediated colitis, macrophage differentiation from blood monocytes was blunted, leading to accumulation of immature, pro-inflammatory macrophages that aggravated epithelial damage (Tamoutounour *et al.*, 2012). To determine whether this phenomenon was recapitulated in the DSS-colitis model in *miR-223*$^{-/y}$ mice, mature, pro-reparative macrophage markers, MERTK, CD206 and Relmα, were assessed during the continuum of experimental colitis. These pro-reparative macrophages were increased in the *miR-223*$^{-/y}$ colons during active disease and remained in the recovery phase. Thus, the delayed mucosal healing observed in the mouse model is not attributable to defective monocyte-to-macrophage differentiation or a deficiency of pro-reparative macrophages in the tissue. Although, while present in higher numbers, it cannot be excluded that these macrophages are functionally impaired and fail to provide adequate repair signals to the epithelial stem cell niche.

Mucosal repair relies on intestinal epithelial cell regeneration. Wound healing is initiated when epithelial cells that surround the injury site lose their columnar polarization and then migrate to the lesion. This process is regulated by cytokines such as TGFα, and chemokine receptors, CXCR4 and CCR6, and their respective ligands, CXCL12 and CCL20. This is followed by intestinal epithelial cell proliferation and differentiation to reconstitute the barrier. Cell proliferation is initiated by intestinal stem cells, that are located in the ISC niche at the bottom of the crypt, highlighting the importance of this microenvironment in the regeneration process (Villablanca, Selin and Hedin, 2022). Intestinal macrophages that accumulate at the base of the crypt, have been reported to fulfil stem cell niche-associated roles (Hausmann *et al.*, 2024).

OLFM4 has been used as a specific marker for mature ISCs. Studies have shown that it's expression is increased during inflammation. Moreover, higher levels of OLFM4 expression have been reported in the inflamed mucosa of patients with IBD (Xing *et al.*, 2024). The data presented here revealed that OLFM4 is increased in *miR-223*$^{-/y}$ mice during the continuum of DSS-colitis. This was accompanied by aberrant expression of the proliferation markers, PCNA and Cyclin D1, and MUC2, a differentiated cell marker. Although, the regeneration process has commenced in the *miR-223*$^{-/y}$ mice, these data indicate that the

process is either delayed or dysregulated, as the stem cells continue to proliferate but do not transition into differentiated epithelial cells. These findings suggest that *miR-223* is necessary for precise regulation of the repair process.

A newly described phenomenon indicates that tissue regeneration can be accompanied by reversion to a fetal-like state. This concept was initially proposed as a regenerative mechanism in the small intestine of mice infected with the helminth Heligmosomoides polygyrus (Hp). Epithelial cells in granuloma-associated crypts (GACs) had reduced expression of $Lgr5^+$ ISCs and mature intestinal epithelial cell (IEC) lineages. Regardless of this, the GACs were hyperproliferative and maintained their epithelial integrity. RNA-seq revealed that these GACs had upregulated expression of *Ly6a*, a gene associated with fetal-like intestinal organoids (Nusse *et al.*, 2018). Studies have demonstrated that epithelial damage induced by DSS, resulted in regenerating epithelial cells expressing fetal-like markers, *Ly6a*, *Anxa1* and *Tacstd2*. Tissues samples from UC patients have been reported to express fetal markers (Yui *et al.*, 2018). To investigate whether fetal-like molecular programs are activated during regeneration in *miR-223*$^{-/y}$ mice, LY6A was examined during DSS-induced colitis. LY6A expression was increased during active disease and recovery in *miR-223*$^{-/y}$ colons. These data provide evidence that *miR-223* may play a role in inducing fetal-like reprogramming following intestinal injury.

Colonic epithelial organoids are self-organised, three-dimensional tissue cultures that are derived from intestinal stem cells and recapitulate key features of the colon (Yui *et al.*, 2018). They mimic the ecological niche of ISCs, and precisely regulate the proliferation and differentiation of stem cells (Tian *et al.*, 2023). Organoid cultures have been essential in advancing the understanding of the cross-talk between immune cells and intestinal epithelial cells (Kromann, Cearra and Neves, 2024). Early co-cultures revealed that T cells cluster around enteroids (Rogoz *et al.*, 2015). Co-cultures of small intestinal organoids and $CD4^+$ T cells, showed that pro-inflammatory T_H1, T_H2 and T_H17 cells reduce the ISC populations, while T_{regs} promote stem cell maintenance (Biton *et al.*, 2018). Here, an indirect co-culture of colonic epithelial organoids and conditioned media from *miR-223*-manipulated macrophages was developed. Although, a phenotype was not identified, the various stages of growth, from fetal to mature organoids, were

observed. This was accompanied by increased occurrences of cell death. The organoids were likely subjected to stress due to the 1:1 ratio of normal growth medium to macrophage conditioned medium. The gene expression of various stem cell and differentiated cell markers were analysed by RT-PCR, however, no significant changes were detected. These data indicate that an indirect co-culture system is not optimal for examining macrophage-epithelial cell cross-talk, and a more suitable system should be developed.

Overall, these findings demonstrate that *miR-233* is critical for the precise regulation of intestinal epithelial regeneration throughout inflammation and mucosal repair.

CHAPTER 5

MIR-223 REGULATES THE CROSS-TALK BETWEEN MACROPHAGES AND COLONIC EPITHELIAL ORGANOIDS VIA STAT3 SIGNALLING

The intestinal epithelium is continuously subjected to harsh conditions from the luminal environment, making it susceptible to a number of damaging events including, infection, acute or chronic inflammatory disease and genotoxic stress associated with chemotherapy and radiation therapy. Different approaches can promote epithelial repair. The ability of intestinal epithelial cells to revert to a stem cell state is an essential physiological damage response to regenerate the intestinal epithelium (**Figure 5.1**) (Meyer *et al.*, 2022).

$LGR5^+$ cells are considered the active multipotent intestinal stem cells that give rise to transit-amplifying (TA) cells and all differentiated cell types. OLFM4, a glycoprotein, is used as an additional marker for $LGR5^+$ crypt basal columnar cells in the human and mouse small intestine and colon (Grover, Hardingham and Cummins, 2010; Xing *et al.*, 2024). Additionally, achaete-scute family BHLH transcription factor 2 (ASCL2), is a transcriptional target gene of Wnt signalling, and it is restricted to the $LGR5^+$ basal crypt cells in mice and humans (van der Flier and Clevers, 2009; Jubb *et al.*, 2006; van der Flier *et al.*, 2009). ASCL2 has been observed to control intestinal stem cell fate (van der Flier *et al.*, 2009). A second population of stem cells have been identified, referred to as reserve ISCs, that become mobilised upon injury to repopulate the crypt. They are quiescent, resistant to stress and are located in the +4 cell position. Markers for these cells, B lymphoma Mo-MLV insertion region 1 homolog (BMI1), Hop homeobox (HOPX), telomerase reverse transcriptase (TERT) and leucine-rich repeats and immunoglobulin-like domain 1 (LRIG1), have been postulated (Meyer *et al.*, 2022; Beumer and Clevers, 2021). Reserve stem cells have been reported to proliferate in response to irradiation damage (Tian *et al.*, 2011; Takeda *et al.*, 2011; Montgomery *et al.*, 2011; Powell *et al.*, 2012).

Although, not necessarily a stem cell population, lineage-committed progenitor cells are also present in the intestinal epithelium. These include secretory-progenitors, which can be identified by Atonal bHLH transcription factor 1 (ATOH1), and absorptive progenitors, characterised by intestinal alkaline phosphatase (ALPI) expression. These cell types have the ability to act as

facultative stem cells that are capable of repopulating the crypt following intestinal injury (Tomic *et al.*, 2018; Ishibashi *et al.*, 2018; Meyer *et al.*, 2022). For example, loss of $LGR5^+$ stem cells in response to acute inflammation, resulted in Paneth cells losing their secretory expression signature and acquiring stem-like characteristics, thus promoting tissue regeneration (Schmitt *et al.*, 2018). Similarly, during target $LGR5^+$ stem cell ablation, it was reported that $ALPI^+$ cells promoted the production of functional $LGR5^+$ cells (Tetteh *et al.*, 2016).

Differentiated epithelial cells have been shown to exhibit stem-like properties. Enteroendocrine cells, marked by prospero homeobox 1 (PROX1) expression, possess homeostatic and injury-inducible stem cell activity (Yan *et al.*, 2017). Another study demonstrated that doublecortin-like kinase 1 ($DCLK1^+$) tuft cells, can acquire stemness under homeostatic conditions and showed that ablation of these cells diminished epithelial repair following DSS-induced injury (Westphalen *et al.*, 2014). Recent work has also shown that single mature tuft cells can form organoids that contain all intestinal epithelial cell types. Furthermore, human tuft cells can survive irradiation damage and retain the ability to generate all other epithelial cell types (Huang *et al.*, 2024).

Tissue regeneration can also be accompanied by reversion to a fetal-like state. This process involves cells at the site of mucosal injury, reactivating programs that operate during fetal development, but are typically absent during adult homeostasis (Viragova, Li and Klein, 2024). Genes that were enriched in fetal intestinal organoids include, *Ly6a*, *Gja1*, *Tacstd2* and *Clu* (Mustata et al., 2013; Yui et al., 2018*)*.

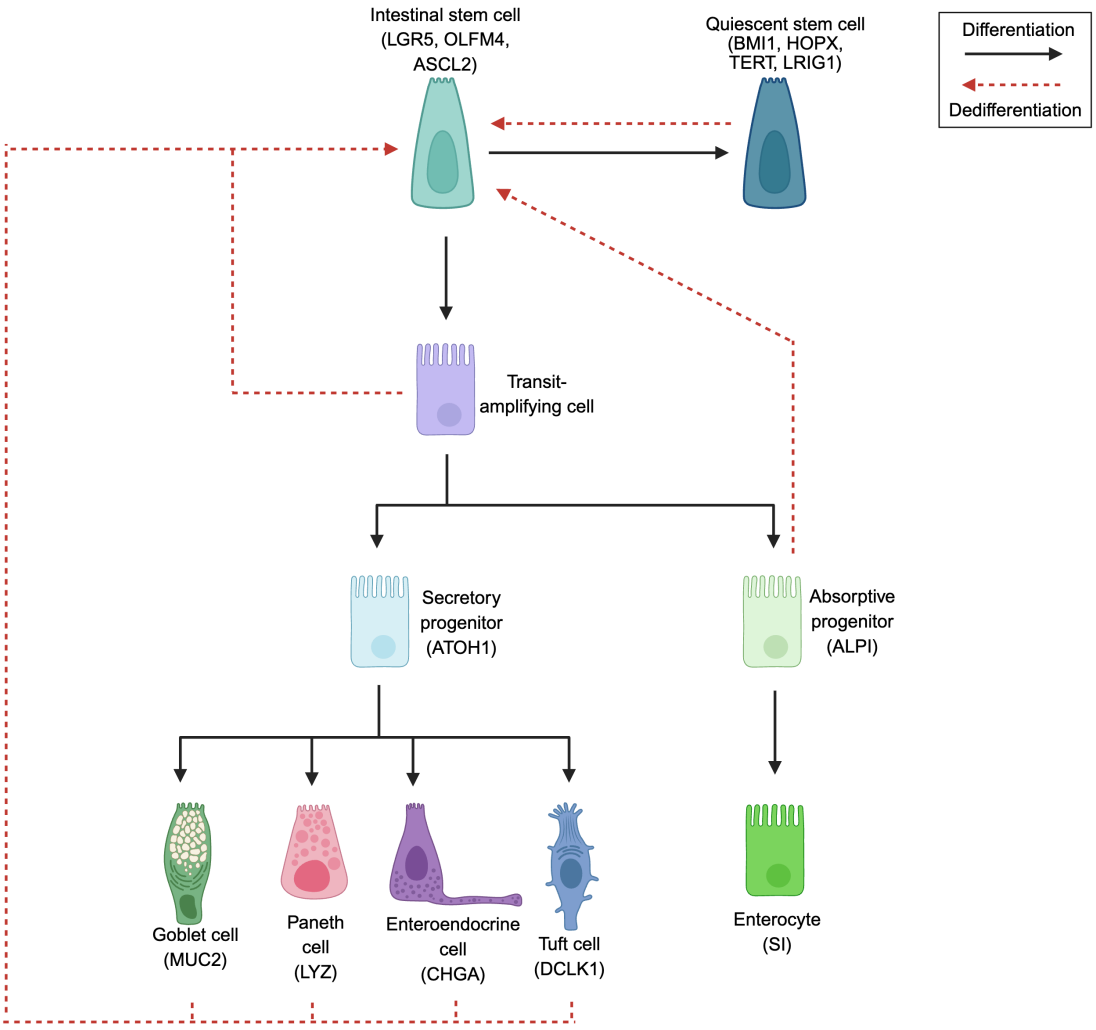

Figure 5.1. ***Schematic illustrating cellular plasticity and dedifferentiation following intestinal injury.*** Cells from reserve stem cells, secretory and absorptive lineages are capable of dedifferentiating to intestinal stem cells in order to repopulate the crypt after damage. Leucine-rich repeat-containing G-protein coupled receptor 5 (LGR5); Olfactomedin 4 (OLFM4); Achaete-scute family BHLH transcription factor 2 (ASCL2); B lymphoma Mo-MLV insertion region 1 homolog (BMI1); Hop homeobox (HOPX); Telomerase reverse transcriptase (TERT); Leucine-rich repeats and immunoglobulin-like domains 1 (LRIG1); Atonal bHLH transcription factor 1 (ATOH1); Intestinal alkaline phosphatase (ALPI); Mucin 2 (MUC2); Lysozyme (LYZ); Chromogranin A (CHGA); Doublecortin-like kinase 1 (DCKL1); Sucrase-isomaltase (SI).

Important pathways that support cellular plasticity and regeneration include, the WNT and HIPPO (YAP/TAZ) pathways (Meyer *et al.*, 2022; Hausmann *et al.*, 2024). With regards to WNT signalling, *Ascl2* is a target gene of this pathways that is restricted to LGR5^{+} cells. This transcription factor coordinates with β-

catenin and TCF4 to induce the transcription of stem cell genes. It has been reported that regenerating cells express *Ascl2* and following ISC injury, ASCL2 is crucial for crypt cell dedifferentiation (Murata *et al.*, 2020). Furthermore, in a DSS-induced colitis model, it was found that the repairing epithelium expresses fetal-associated markers, and this reprogramming is the result of YAP/TAZ activation (Yui *et al.*, 2018).

Moreover, inflammatory mediators, responsible for epithelial damage, also induce epithelial repair (Hausmann *et al.*, 2024). Key among these, are activators of signal transducer and activator of transcription 3 (STAT3) signalling. STAT3-dependent immune activation drives epithelial damage, in contrast, activation of STAT3 signalling in epithelial cells promotes epithelial survival and proliferation (Wittkopf *et al.*, 2015; Pickert *et al.*, 2009; Hausmann *et al.*, 2024). Cytokines associated with IBD pathophysiology, interleukin 6 (IL-6) and interleukin 22 (IL-22), serve as ligands for cell surface receptors on epithelial cells, leading to STAT3 activation (Samad *et al.*, 2025). Briefly, IL-22 binds to its receptor complex interleukin 22 receptor 1/interleukin 10 receptor subunit beta (IL-22R1/IL-10R2), activating Janus kinases (JAKs), resulting in the phosphorylation and activation of STAT3 (**Figure 5.3**) (Naher *et al.*, 2012). IL-22 has been shown to be a strong activator of STAT3 in epithelial cells. Mice lacking IL-22 exhibited more severe colitis, loss of mucosal architecture and delayed healing. Moreover, upon induction of colitis, $STAT3^{IEC\text{-}KO}$ mice exhibited a pronounced defect in epithelial restitution. Gene expression profiling revealed that STAT3 regulated cellular stress responses, apoptosis, and wound healing-associated pathways in intestinal epithelial cells (IEC) (Pickert *et al.*, 2009). Another study, reported that JAK/STAT activation by IL-22 significantly augmented organoid formation and size (Maciag *et al.*, 2024). Another study reported that *Stat3*-deficient organoids demonstrated an impaired response to IL-22 stimulation. Furthermore, expression of the $Lgr5^{+}$ gene signature was significantly reduced in *Stat3*-deficient mice with colitis (Lindemans *et al.*, 2016). These studies demonstrate the importance of IL-22 as a regulator of STAT3 activation in epithelial cells.

IL-6 is a key cytokine that contributes to intestinal inflammation and regeneration, with macrophages serving as a major source of this pro-inflammatory mediator. It is a member of the IL-6 family of cytokines, which is comprised of nine other

members: interleukin 11 (IL-11), ciliary neurotrophic factor (CNTF), cardiotrophin-1 (CT-1), charcot-leyden crystal galectin (CLC), leukemia inhibitory factor (LIF), nucleoprotein (NP), oncostatin M (OSM), interleukin 27 (IL-27) and interleukin 31 (IL-31). These cytokines signal through a complex of non-signalling α-receptors (IL-6Rα, IL-11α, CNTFRα) that permit the interaction with signal-transducing β-receptors (glycoprotein 130 (gp130), LIFR, OSMR, IL-27RA, IL-31RA) (Nguyen, Putoczki and Ernst, 2015). In the context of IL-6/STAT3 signalling, upon binding of IL-6 to the membrane-bound receptor, IL-6R, on epithelial cells, the IL-6 family signal transducer glycoprotein, gp130, is recruited. This triggers autophosphorylation of Janus kinase 1 (JAK1), ultimately leading to STAT3 phosphorylation and activation (Garbers, Aparicio-Siegmund and Rose-John, 2015) (**Figure 5.3**).

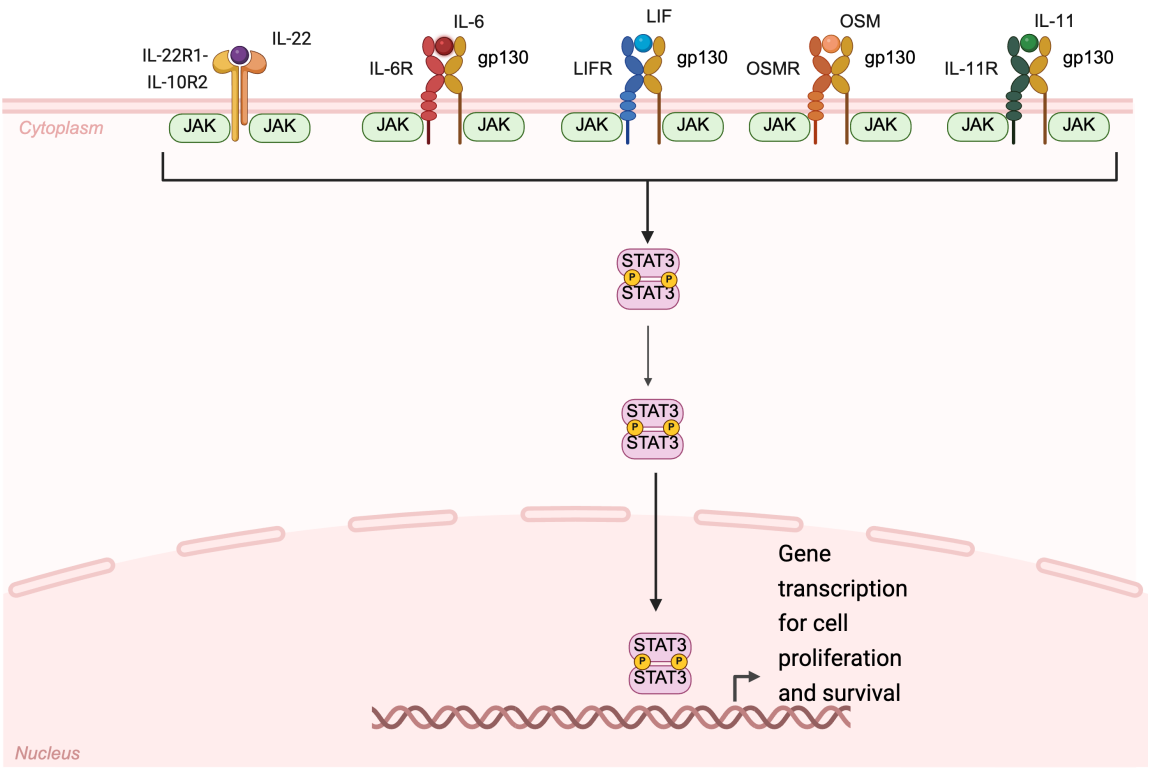

Figure 5.2. ***Overview of STAT3 signalling in intestinal epithelial cells following activation by IBD-associated cytokines, IL-22 and the IL-6 family.*** Engagement of IL-22 with the IL-22R1/IL-10R2 receptor complex, IL-6 with IL-6R/gp130 complex, LIF with LIFR/gp130 complex, OSM with OSMR/gp130, and IL-11 with IL-11R/gp130 complex, induces JAK autophosphorylation and subsequent STAT3 activation.

IL-6/STAT3 signalling has been demonstrated to be essential for the survival and proliferation of intestinal epithelial cells. DSS-exposed *Il6*$^{-/-}$ mice exhibited elevated apoptosis of intestinal epithelial cells, this was accompanied by a decrease in proliferation within the crypts (Grivennikov *et al.*, 2009). Another study, that used two different colonic injury models, wound by biopsy and bacterial triggered colitis, reported similar results. In both models, IL-6 was rapidly induced following injury, and this burst of IL-6 expression was required to stimulate intestinal epithelial cell proliferation (Kuhn *et al.*, 2014).

MiR-223 has been identified as a crucial regulator of innate immunity. Extensive work has demonstrated its ability to limit intestinal inflammation. It has been reported to constrain the myeloid-driven inflammatory response in a model of DSS-induced colitis and in the AOM-DSS model of colitis-associated cancer (CAC) (Flynn *et al.*, 2024; Neudecker *et al.*, 2017b). There is evidence to suggest that *miR-223* regulates IL-6-STAT3 signalling in macrophages. Downregulation of *miR-223* in LPS-activated macrophages promoted IL-6 secretion in a STAT3-dependent manner (Chen *et al.*, 2012). Interaction between *miR-223* and IL-6/STAT3 signalling in an experimental mouse model of IBD has also been examined. Following induction of DSS-colitis, administration of a *miR-223* agomir alleviated colonic inflammation by targeting the IL-6/STAT3 pathway (Zhang *et al.*, 2021a). However, this relationship, in the context of mucosal healing, is yet to be elucidated. Therefore, investigating the interplay between *miR-223* and IL-6/STAT3 signalling during epithelial repair, has the potential to identify novel therapeutic targets.

AIMS OF THIS CHAPTER

The primary objective of this chapter is to evaluate the hypothesis that *miR-223* regulates epithelial repair through the STAT3 signalling pathway. Accordingly, the following aims were developed:

1. To determine whether *miR-223* deficiency leads to enhanced STAT3 activation.
2. To assess whether macrophages deficient in *miR-223-3p* impact epithelial repair, in a STAT3-dependent manner, in colonic epithelial organoids.
3. To elucidate the role of IL-6 family/STAT3 signalling in epithelial repair pathways using colonic epithelial organoids.

5.1. *MiR-223* deficiency promotes STAT3 activation in mouse colons and colonic epithelial organoids.

Although, an increasing body of evidence indicates that *miR-223* modulates STAT3 signalling to attenuate intestinal inflammation, its function in epithelial healing remains poorly understood (Chen *et al.*, 2012; Zhang *et al.*, 2021a). To address this, STAT3 activation was assessed in colonic epithelial organoids and in *miR-223*$^{-/y}$ colons during the continuum of experimental colitis.

Initially, colonic organoids were cultured in conditioned medium (CM) from *miR-223*-manipulated macrophages. Organoids were harvested at an acute timepoint of 3 h, and a prolonged timepoint of 24 h. Expression of active P-STAT3 was examined by immunoblot analysis. At the 3 h timepoint, the most prominent differences were observed in organoids cultured in CM from LPS-activated macrophages. There was a greater expression of P-STAT3 in organoids cultured in LPS-activated BMDM CM in comparison to CM from LPS-activated BMDMs that were transfected with a *miR-223-3p* mimic (*3p* mimic) (**Figure 5.1.1. A**). The opposite was observed in RAW 264.7 cell lines. Protein expression of P-STAT3 was upregulated in organoids that were cultured in CM from LPS-activated RAW *miR*-223KD (RAW *223*KD) cells (**Figure 5.1.1. A**). Interestingly, at the 24 h timepoint, P-STAT3 expression was greater in colonic organoids following culture with CM from IL-4-activated RAW *miR*-223KD cells, in comparison to RAW 264.7 cells (**Figure 5.1.1. B**). Additionally, organoids cultured with CM from either LPS or IL-4-activated macrophages, presented with prolonged STAT3 activation for up to 24 h (**Figure 5.1.1. B**).

Expression and localisation of P-STAT3 protein was assessed in WT and *miR-223*$^{-/y}$ colons during the continuum of DSS-induced colitis. There was an increase in P-STAT3 in *miR-223*$^{-/y}$ mice, in comparison to WT mice (**Figure 5.1.2. A – C**). This enhanced expression of STAT3 signalling was observed prior to DSS-treatment, during active colitis and during the recovery phase (**Figure 5.1.2. A –**

C). Taken together, these findings suggest that *miR-223* regulates STAT3 signalling across the continuum of experimental colitis.

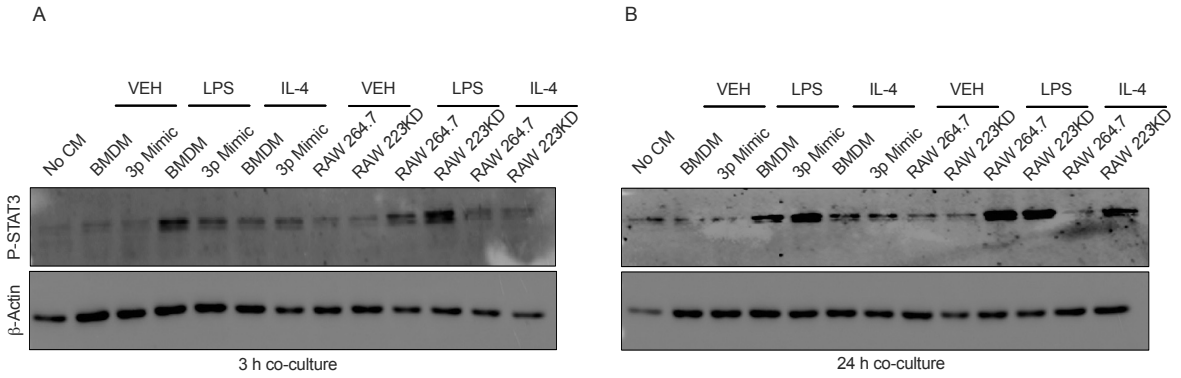

Figure 5.1.1. ***P-STAT3 is differentially expressed in colonic epithelial organoids following co-culture in CM from miR-223-manipulated macrophages.*** A western immunoblot assessment of β-Actin and P-STAT3 in colonic organoids co-cultured in CM for **A.** 3 h, and **B.** 24 h.

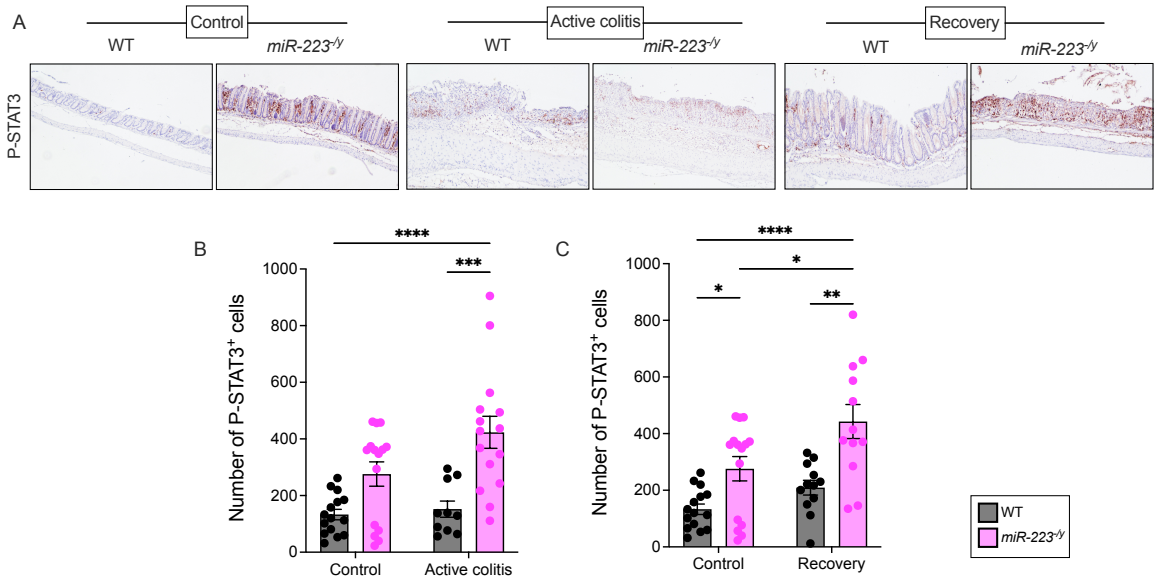

Figure 5.1.2. *P-STAT3 protein expression is upregulated in miR-223$^{-/y}$ mice during the continuum of DSS-induced experimental colitis.* **A.** Representative 10X images of immunohistochemical staining of colonic tissue sections for P-STAT3. Tissue sections were from WT and *miR-223$^{-/y}$* mice, during active inflammation and recovery in a model of DSS-induced colitis. **B** and **C.** Quantification of P-STAT3^{+} cells. Data is expressed as mean ± SEM; *, P ≤ 0.05; **, P ≤ 0.01, ***, P ≤ 0.001, ****, P ≤ 0.0001, versus the indicated counterpart (two-way ANOVA). Same controls used in **B** and **C**. n = 3 biological replicates/group with 3 – 5 fields of view presented per animal (Total of 9 – 15 points on graph).

5.2. A direct co-culture system of colonic epithelial organoids with *miR-223KD* cells did not reveal morphological changes in organoid formation.

In order to further elucidate the role of *miR-223* in regulating the cross-talk between macrophages and colonic epithelial cells, a direct co-culture system was established. The first report of a co-culture system for immune cells revealed that primary T cells survive long-term culture with murine enteroids (Rogoz *et al.*, 2015). In the work presented here, macrophages were embedded next to the colonic epithelial organoids within the ECM-rich gels to allow contact-dependent interactions (**Figure 5.2.1 A and B**) (Kromann, Cearra and Neves, 2024).

Within the direct co-culture system, it was difficult to identify morphological differences between the groups. There were various stages of growth observed within each of the conditions, from fetal-like to mature organoids (**Figure 5.2.2. A**

and **B**). The RAW 264.7 cell lines formed large aggregates within the Matrigel, which is an expected characteristic of this immortalised cell line (**Figure 5.2.2. A** and **B**). Although, equal numbers of macrophages were embedded within the Matrigel, LPS-activated macrophages, including both Scramble and *miR-223KD* cells, exhibited reduced survival (**Figure 5.2.2. A** and **B**). Furthermore, treatment with Stattic, a small molecule selective inhibitor of STAT3, did not induce morphological effects on the organoids (**Figure 5.2.2. B**).

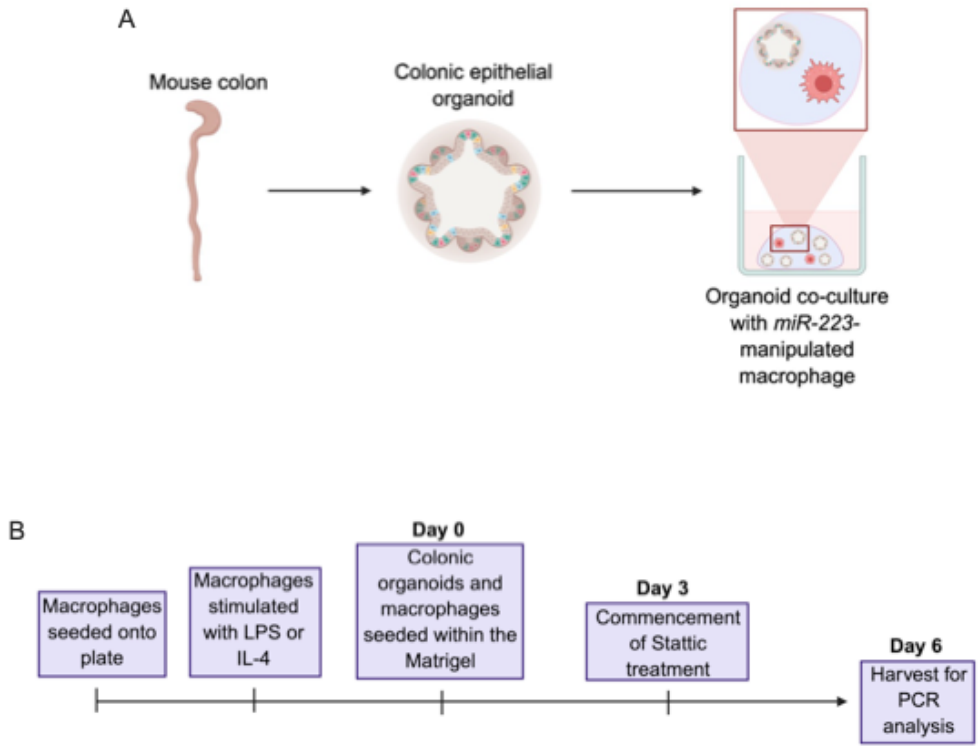

Figure 5.2.1. ***Generation of a direct co-culture system of colonic epithelial organoids with miR-223KD cells.*** **A.** Diagram depicting the generation of the direct co-culture system of colonic organoids and *miR-223*-manipulated macrophages. **B.** Schematic overview of the experimental timeline for the direct co-culture system.

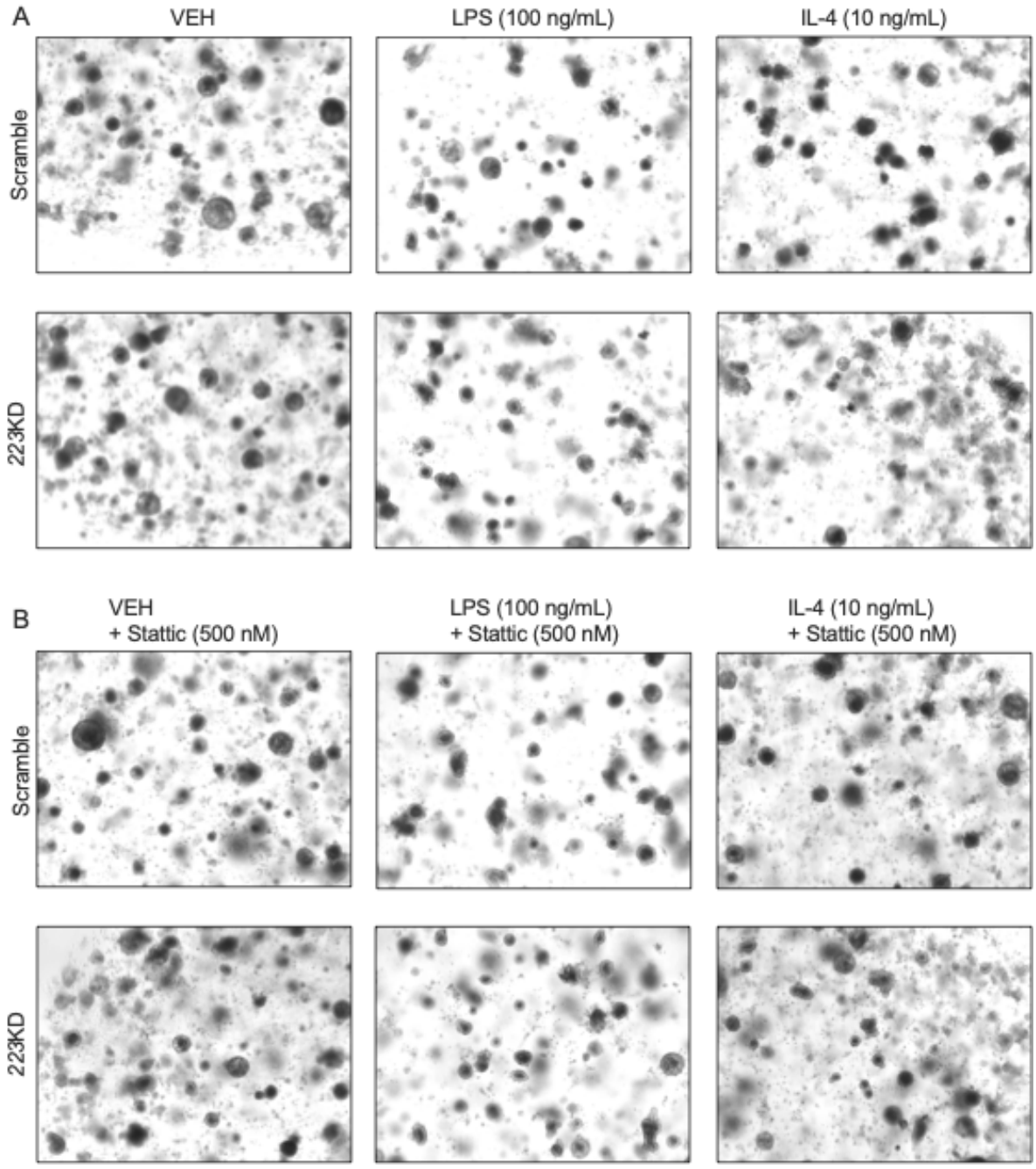

Figure 5.2.2. ***Morphological changes in organoid formation were not observed in the direct co-culture system of colonic epithelial cells and miR-223KD cells.*** **A.** Representative 4X images of colonic organoids co-cultured with Scramble control inhibitor (Scramble) or *miR-223KD* (*223*KD) cells. **B.** Representative 4X images of colonic organoids co-cultured with Scramble or *miR-223KD* cells, following STAT3 inhibition with Stattic.

5.3. *MiR-223* regulates epithelial repair in a STAT3-dependent manner.

Intestinal stem cells and progenitor cells have been demonstrated to be crucial in the epithelial regeneration process (Choi and Augenlicht, 2024). Therefore, examining whether markers of these cell populations are altered in the context of *miR-223* deficiency would provide valuable insight into the role of *miR-223* in epithelial repair.

Organoids were harvested from the direct co-culture system and the relative gene expression levels of various intestinal stem cell, fetal stem cell and progenitor cell markers were analysed. No significant changes were observed in organoids co-cultured with LPS-activated macrophages (**Figure 5.3.1 – E** and **Figure 5.3.2. A – C**). Similarly, Stattic treatment had minimal transcriptional effects on these targets (**Figure 5.3.1 A – E** and **Figure 5.3.2. A – C**).

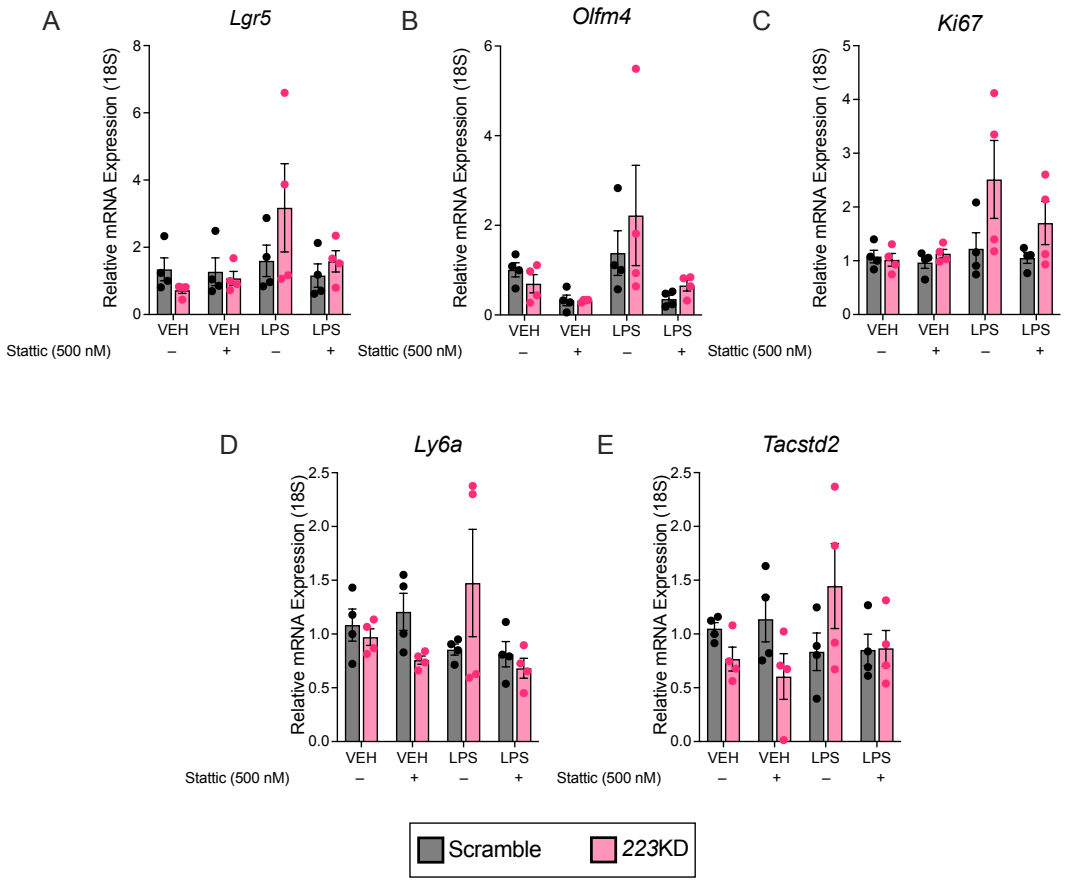

Figure 5.3.1. ***Mature stem cell and fetal stem cell markers are unchanged in colonic epithelial organoids co-cultured with miR-223KD cells and following STAT3 inhibition.*** Relative gene expression of **A.** *Lgr5*, **B.** *Olfm4*, **C.** *Ki67*, **D.** *Ly6a* and **E.** *Tacstd2*. This was measured by RT-PCR and expressed relative to 18S. All data are expressed as mean ± SEM; *, P ≤ 0.05; **, P ≤ 0.01, ***, P ≤ 0.001, ****, P ≤ 0.0001, versus the indicated counterpart (two-way ANOVA). n = 4 technical replicates/group.

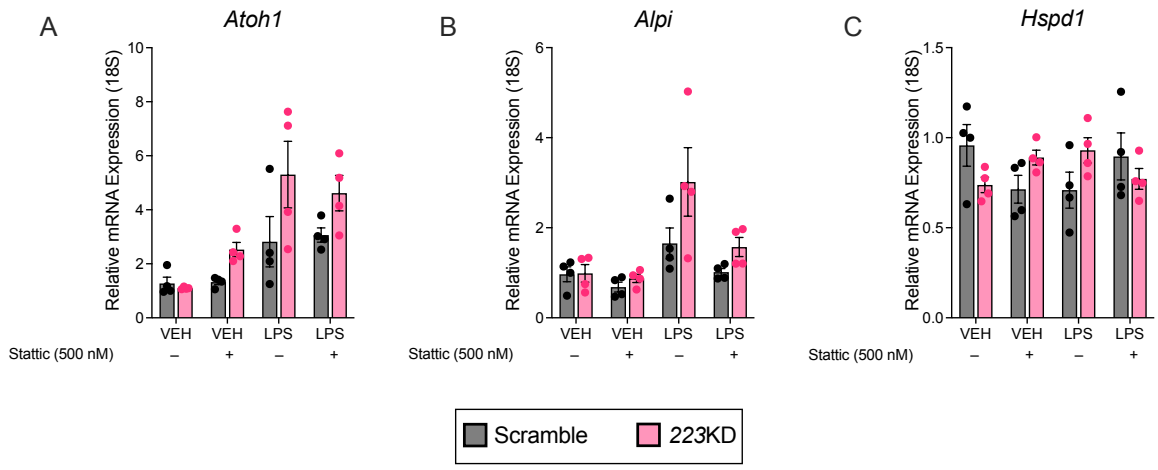

Figure 5.3.2. ***Progenitor cell markers and Hspd1 are unchanged in colonic epithelial organoids co-cultured with miR-223KD cells and following STAT3 inhibition.*** Relative gene expression of **A.** *Atoh1*, **B.** *Alpi*, and **C.** *Hsdp1*. This was measured by RT-PCR and expressed relative to 18S. All data are expressed as mean ± SEM; *, P ≤ 0.05; **, P ≤ 0.01, ***, P ≤ 0.001, ****, P ≤ 0.0001, versus the indicated counterpart (two-way ANOVA). n = 4 technical replicates/group.

Although changes were not observed in organoids co-cultured with LPS-activated macrophages, this was not the case with IL-4-activated macrophage. IL-4-activated *miR-223KD* cells increased the expression of the mature stem cell marker, *Olfm4*, in colonic organoids, compared to Scramble cells (**Figure 5.3.3. B**). However, significant changes were not observed with other stem cell or progenitor cell markers (**Figure 5.3.3. A, C – E**, and **Figure 5.3.4. A – B**).

Furthermore, following Stattic inhibitor treatment, additional changes were observed. There was an increase in the expression of *Ki67*, *Atoh1* and *Alpi* in organoids co-cultured with IL-4-activated *miR-223KD* cells in comparison to Scramble cells (**Figure 5.3.3. C** and **Figure 5.3.4. A** and **B**). In organoids co-cultured with IL-4-activated *miR-223KD* cells, inhibition of STAT3 led to upregulation in the expression of *Tacstd2* and *Atoh1* (**Figure 5.3.3. E** and **Figure 5.3.4. A**).

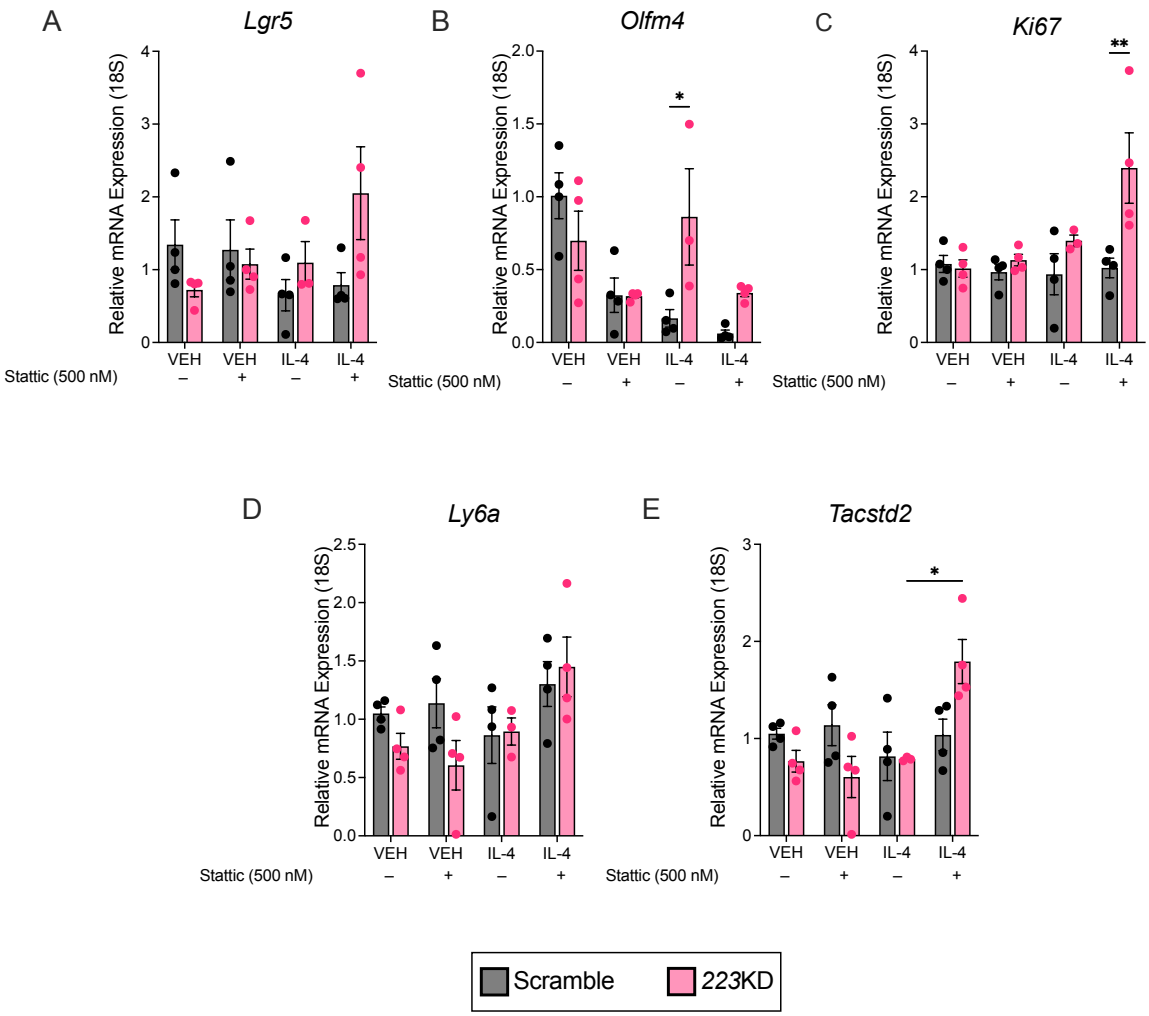

Figure 5.3.3. ***MiR-223 deficiency and STAT3 inhibition increased the expression of specific stem cell markers in colonic epithelial organoids.*** Relative gene expression of **A.** *Lgr5*, **B.** *Olfm4*, **C.** *Ki67*, **D.** *Ly6a* and **E.** *Tacstd2*. This was measured by RT-PCR and expressed relative to 18S. All data are expressed as mean ± SEM; *, P ≤ 0.05; **, P ≤ 0.01, ***, P ≤ 0.001, ****, P ≤ 0.0001, versus the indicated counterpart (two-way ANOVA). n = 4 technical replicates/group.

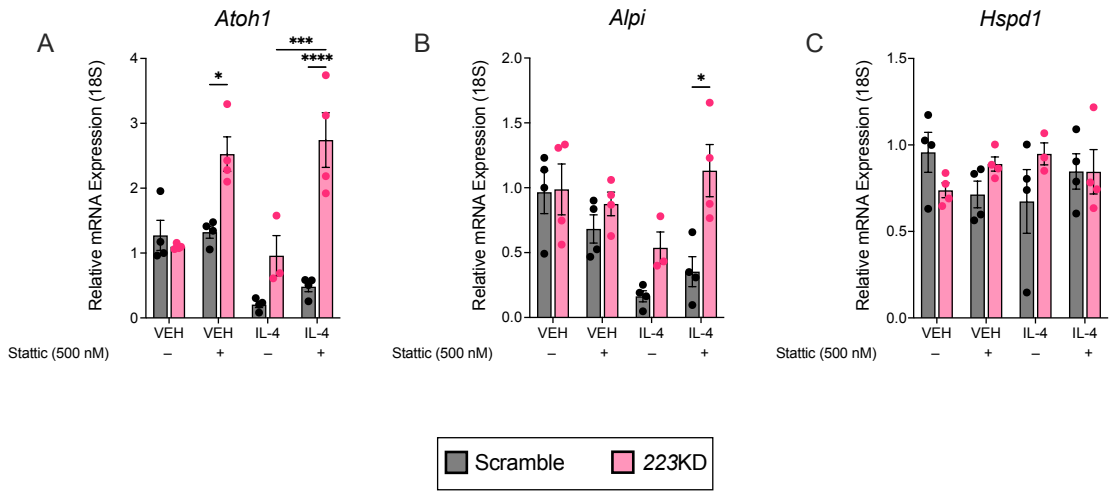

Figure 5.3.4. *MiR-223 deficiency and STAT3 inhibition increased the expression of progenitor cell markers in colonic epithelial organoids.* Relative gene expression of **A.** *Atoh1*, **B.** *Alpi*, and **C.** *Hsdp1*. This was measured by RT-PCR and expressed relative to 18S. All data are expressed as mean ± SEM; *, P ≤ 0.05; **, P ≤ 0.01, ***, P ≤ 0.001, ****, P ≤ 0.0001, versus the indicated counterpart (two-way ANOVA). n = 4 technical replicates/group.

5.4. IL-6 cytokine family and STAT3 signalling orchestrates proliferation and differentiation in colonic epithelial organoids

Upon identifying a potential role for *miR-223* in STAT3-dependent regulation of epithelial repair, subsequent investigations focused on the IL-6 family of cytokines and STAT3 signalling pathway involved in epithelial regeneration.

As previously stated, studies have reported that *miR-223* regulates IL-6/STAT3 signalling (Chen *et al.*, 2012; Zhang *et al.*, 2021a). MiRNA TargetScan was used to identify predicted binding partners of *miR-223-3p* that are involved in this process. *Mmu-miR-223-3p* targets that were identified included *Il-6*, *Lif*, and *Stat3* (**Figure 5.4.1. A – C**). Predicted targets for *hsa-miR-223-3p* were *LIF* and *IL6ST* (**Figure 5.4.2. A and B**).

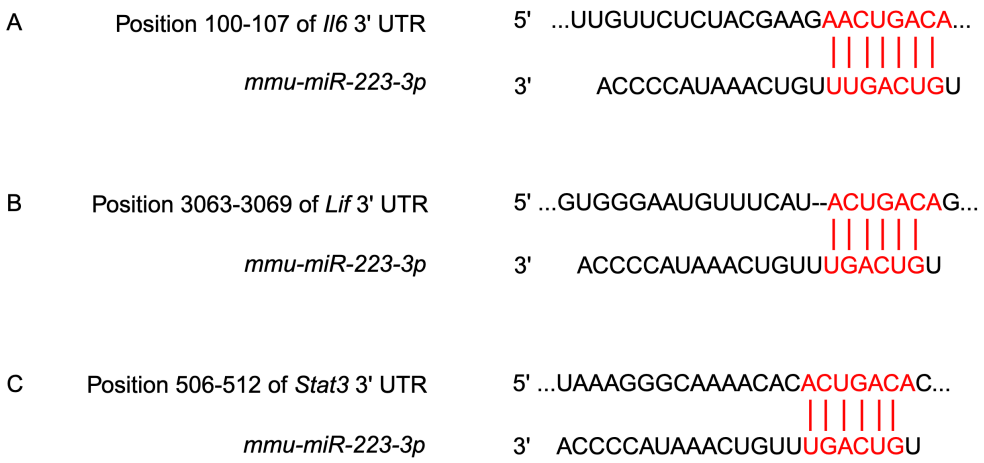

Figure 5.4.1. *Il6, Lif and Stat3 are predicted binding partners of mmu-miR-223-3p.* Predicted consequential pairing of target and *mmu-miR-223-3p*.

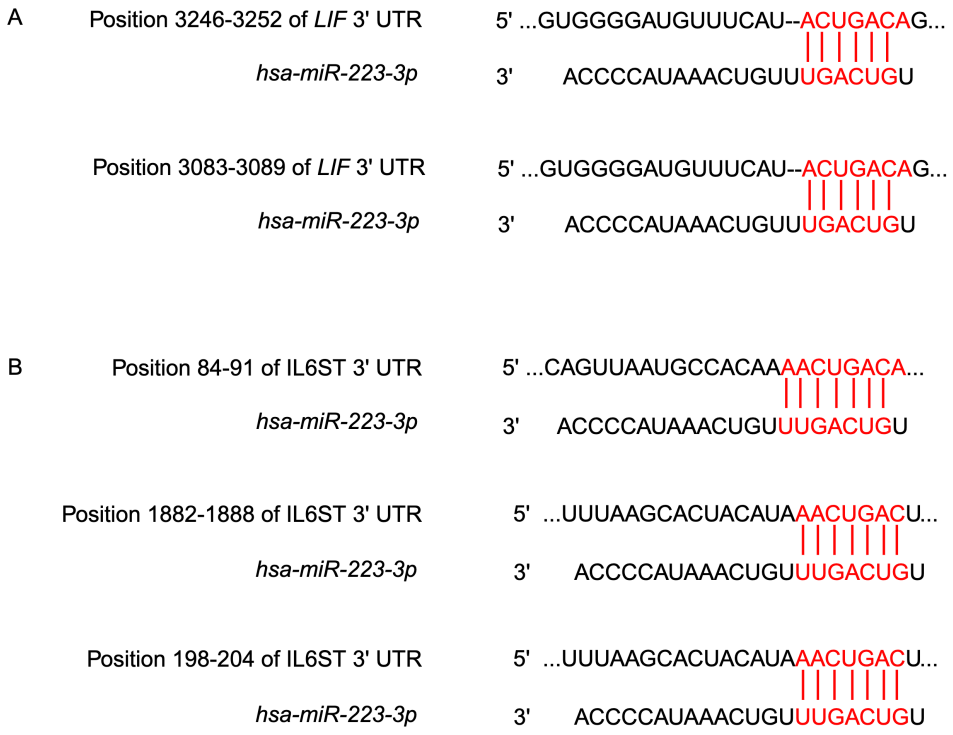

Figure 5.4.2. *LIF and IL6ST are predicted binding partners of hsa-miR-223-3p.* Predicted consequential pairing of target and *hsa-miR-223-3p*.

Initial work involved stimulating colonic organoids with mouse recombinant IL-6, LIF and IL-11. Separately, these cytokines did not induce gene expression changes in differentiated cell, *Muc2* and *Chga*, or progenitor cell, *Atoh1* and *Alpi*, markers (**Figure 5.4.3. A – D**). Similarly, alterations were not observed in mature stem cell or fetal-like stem cell markers (**Figure 5.4.4. A – F**).

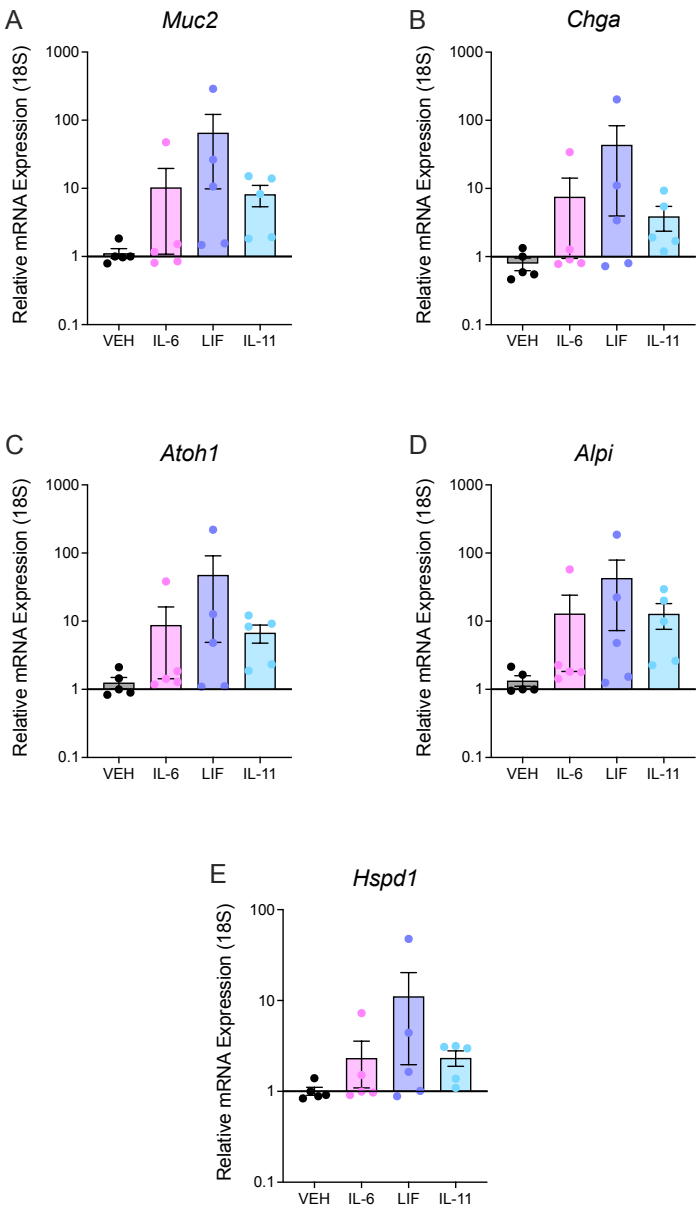

Figure 5.4.3. ***Expression of differentiated cell markers, progenitor cell markers and Hspd1 are unchanged following stimulation with individual IL-6 family of cytokines.*** Relative gene expression of **A.** *Muc2*, **B.** *Chga*, **C.** *Atoh1*, **D.** *Alpi*, and **E.** *Hspd1*. This was measured by RT-PCR and expressed relative to 18S. All data are expressed as mean ± SEM; *, P ≤ 0.05; **, P ≤ 0.01, ***, P ≤ 0.001, ****, P ≤ 0.0001, versus the indicated counterpart (two-way ANOVA). n = 6 technical replicates/group.

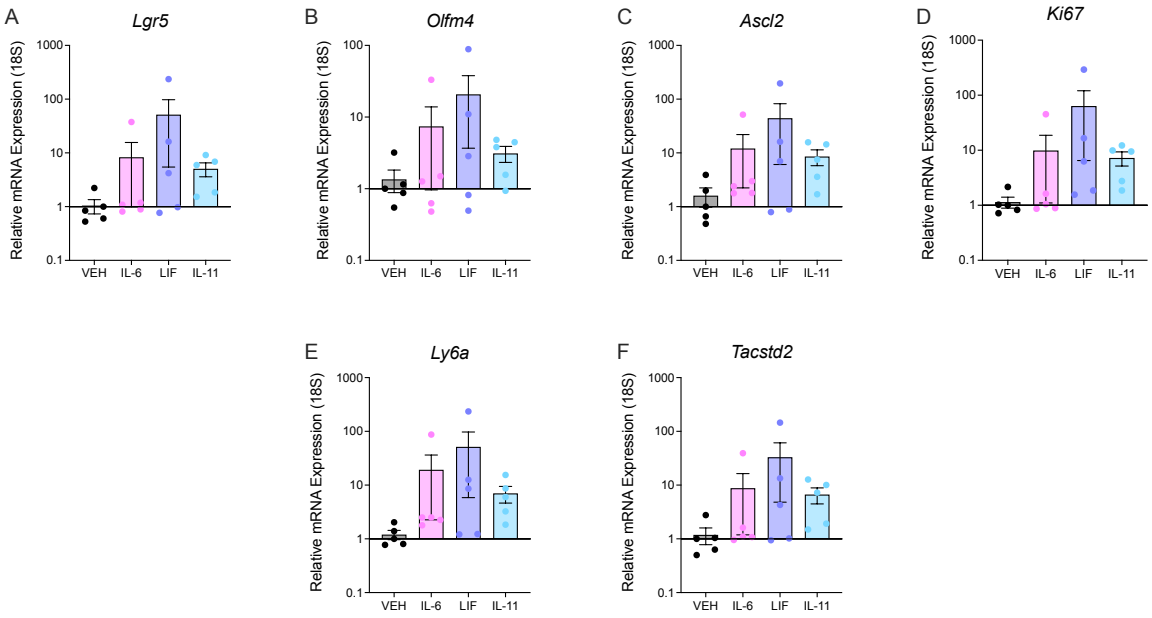

Figure 5.4.4. ***Expression of stem cell and fetal-like stem cell markers are unchanged following stimulation with individual IL-6 family of cytokines.*** Relative gene expression of **A.** *Lgr5*, **B.** *Olfm4*, **C.** *Ascl2*, **D.** *Ki67*, **E.** *Ly6a* and **F.** T*acstd2*. This was measured by RT-PCR and expressed relative to 18S. All data are expressed as mean ± SEM; *, P ≤ 0.05; **, P ≤ 0.01, ***, P ≤ 0.001, ****, P ≤ 0.0001, versus the indicated counterpart (two-way ANOVA). n = 6 technical replicates/group.

In contrast, simultaneous stimulation of colonic organoids with the full panel of cytokines and STAT3 inhibition yielded distinct results. Consistent with previous observations, a specific morphological phenotype was not identified. Using Organoseg software, the circularity of organoids was examined, as this is often used as a measure for fetal-like organoids. There was no differences between the conditions (**Figure 5.4.5. C)**. However, there was a significant decrease in the number of organoids following stimulation with the IL-6 family of cytokines and Stattic treatment (**Figure 5.4.5 A – B**).

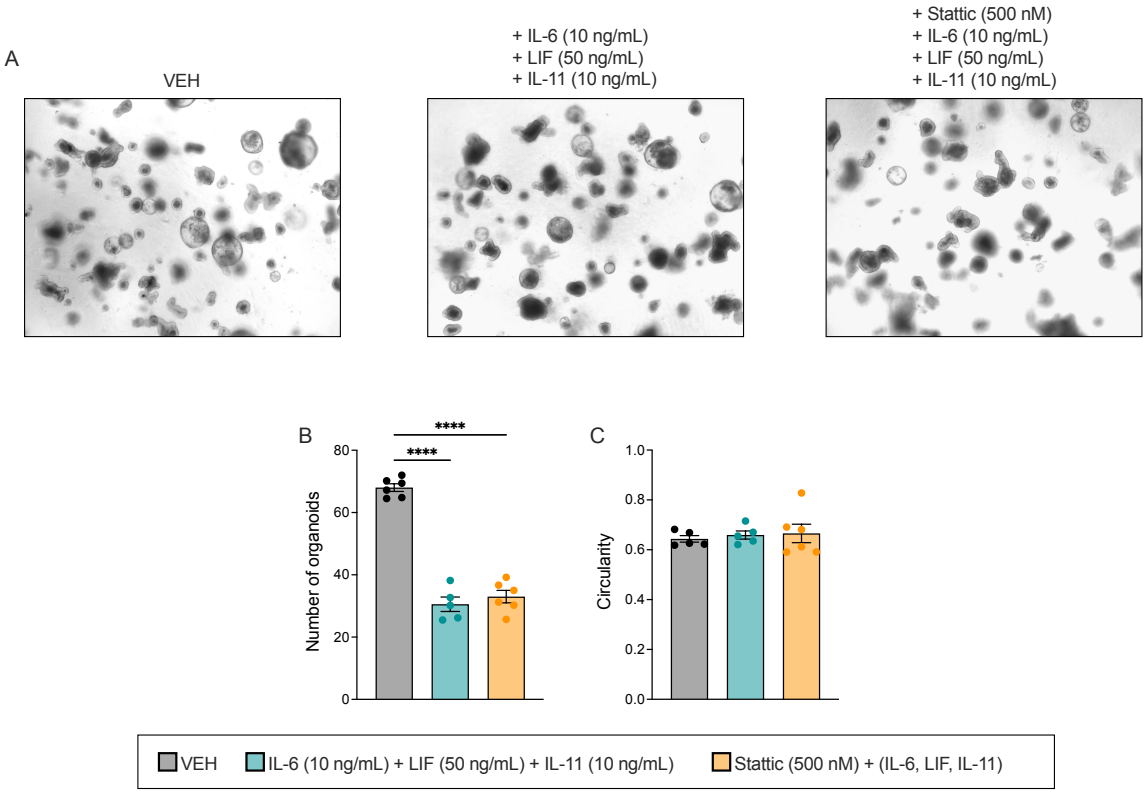

Figure 5.4.5. ***IL-6, LIF and IL-11 stimulation and STAT3 inhibition resulted in a decrease in organoid multiplicity.*** **A.** Representative 4X images of colonic epithelial organoids. **B.** Quantification of organoid multiplicity, which was determined as the average count of organoids per technical replicate. **C.** Quantification of the organoid circularity per technical replicate. All data are expressed as mean ± SEM; *, P ≤ 0.05; **, P ≤ 0.01, ***, P ≤ 0.001, ****, P ≤ 0.0001, versus the indicated counterpart (two-way ANOVA). n = 6 technical replicates/group.

Despite the absence of a distinct morphological phenotype, transcriptional alterations were observed in these colonic epithelial organoids. STAT3 inhibition prevented the transcriptional changes induced by the IL-6 family cytokine stimulation, resulting in reduced expression levels of *Muc2*, *Chga*, *Atoh1* and *Hspd1* (**Figure 5.4.6. A – E**). Similarly, Stattic treatment downregulated the expression of stem cell-associated markers, namely *Olfm4*, *Ascl2*, *Ki67* and *Tacstd2* (**Figure 5.4.7. B, C, D, F**). In contrast to other markers, *Ly6a* expression was significantly upregulated following cytokine stimulation and was subsequently downregulated with STAT3 inhibition (**Figure 5.4.7. E**).

Collectively, these findings support a role for IL-6 family/STAT3 signalling in epithelial dedifferentiation and regeneration.

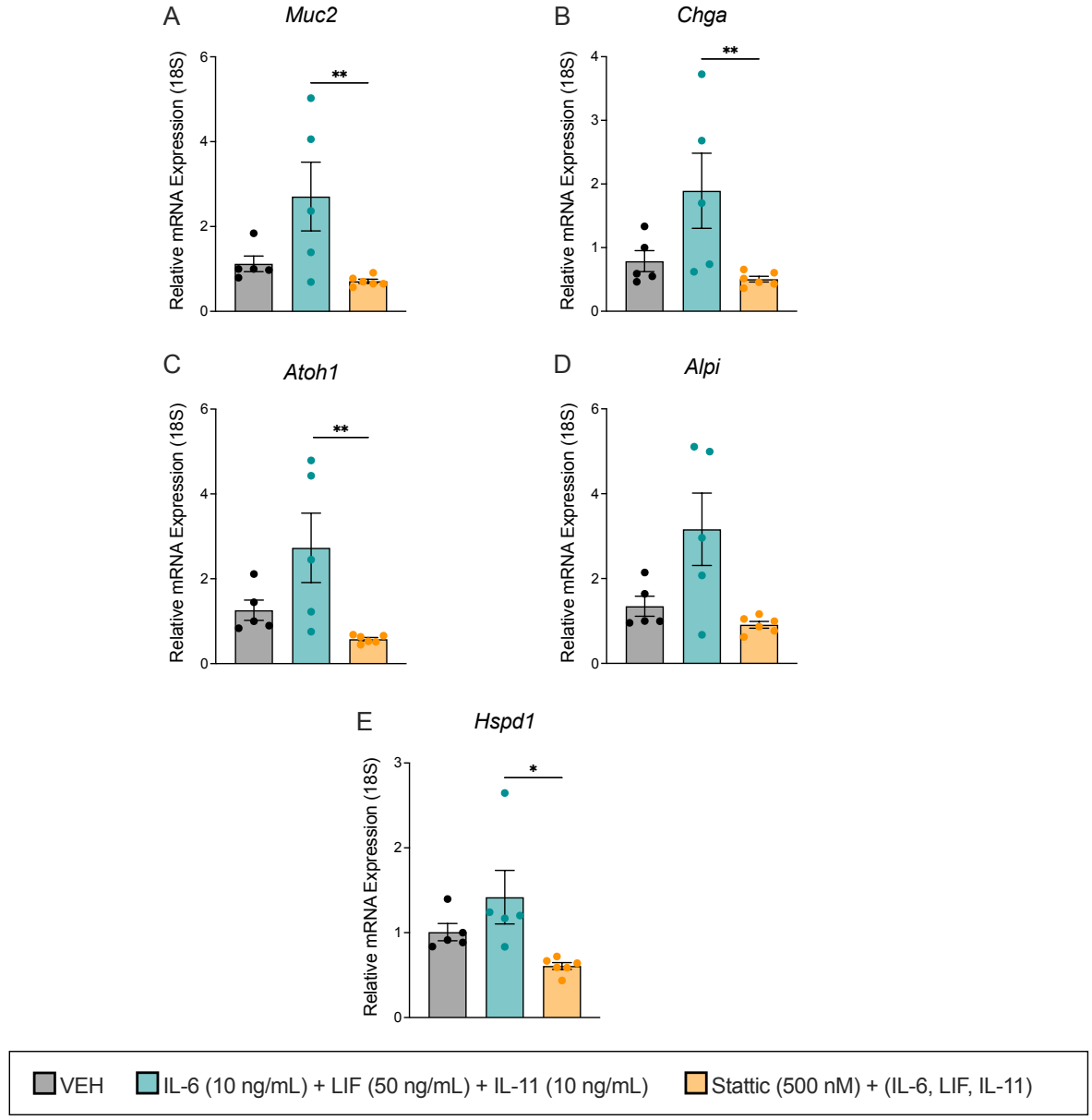

Figure 5.4.6. ***STAT3 inhibition reversed the transcriptional changes induced by the IL-6 family cytokine stimulation, resulting in reduced expression levels of differentiated cell, progenitor cell markers and Hspd1.*** Relative gene expression of **A.** *Muc2*, **B.** *Chga*, **C.** *Atoh1*, **D.** *Alpi*, and **E.** *Hspd1*. This was measured by RT-PCR and expressed relative to 18S. All data are expressed as mean ± SEM; *, P ≤ 0.05; **, P ≤ 0.01, ***, P ≤ 0.001, ****, P ≤ 0.0001,versus the indicated counterpart (two-way ANOVA). n = 6 technical replicates/group.

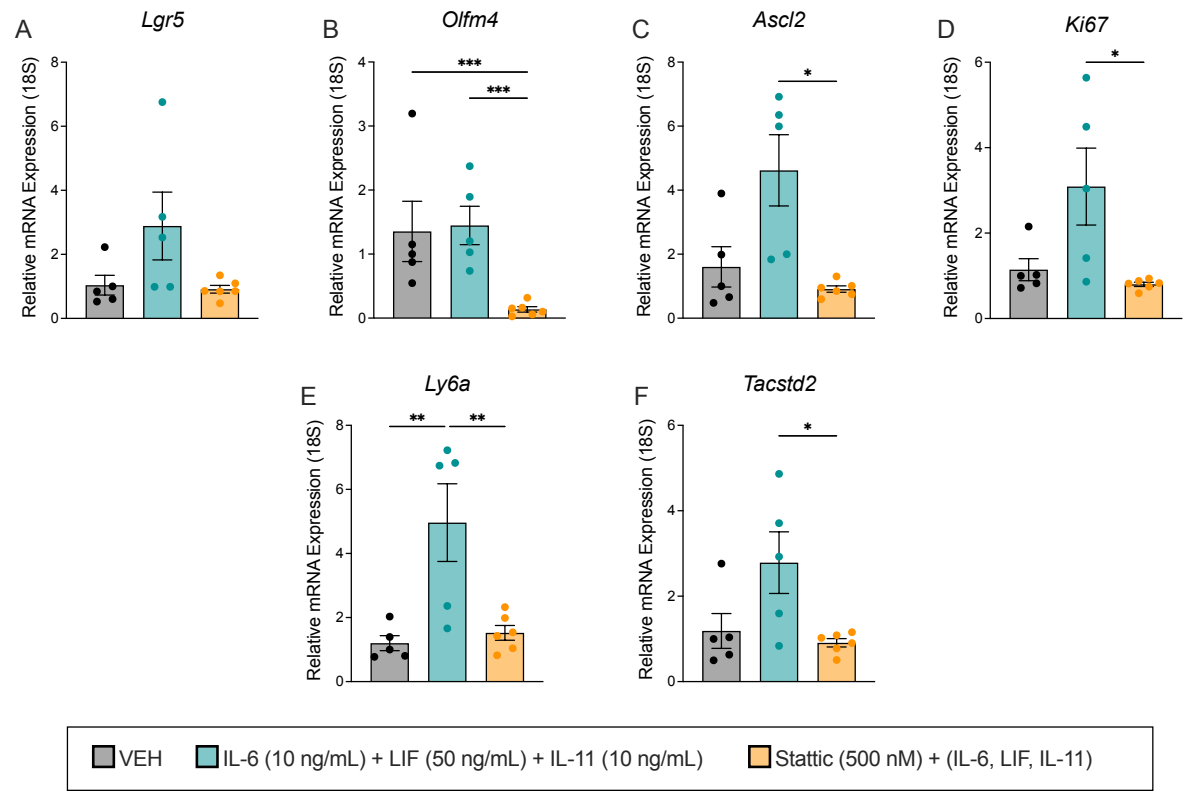

Figure 5.4.7. ***Changes in stem cell marker expression, induced by the IL-6 family of cytokines, were reversed following STAT3 inhibition.*** Relative gene expression of **A.** *Lgr5*, **B.** *Olfm4*, **C.** *Ascl2* **D.** *Ki67*, **E.** *Ly6a*, and **F.** *Tacstd2*. This was measured by RT-PCR and expressed relative to 18S. All data are expressed as mean ± SEM; *, P ≤ 0.05; **, P ≤ 0.01, ***, P ≤ 0.001, ****, P ≤ 0.0001, versus the indicated counterpart (two-way ANOVA). n = 6 technical replicates/group.

The STAT3 signalling pathway and its role in the pathophysiology of IBD has been extensively studied. *STAT3* has been reported to be a susceptibility loci for IBD (Anderson *et al.*, 2011). Persistent or dysregulated activation of STAT3 has been observed in IBD (Shahini, 2023). Excessive accumulation of activated STAT3 has been reported in colonic epithelial cells during active disease in patients with UC (Li *et al.*, 2010). Studies have reported that STAT3 signalling is crucial for maintaining intestinal barrier integrity. *Stat3*$^{+/-}$ mice, or mice carrying a mutant form of gp130, exhibited impaired intestinal regeneration in response to γ-radiation and DSS insult (Tebbutt *et al.*, 2002). Additionally, IEC-specific deficiency in suppressor of cytokine signalling 3 (SOCS3), a negative regulator of STAT3 activation, resulted in susceptibility to IEC injury in a model of DSS-induced colitis (Stuhlmann-Laeisz *et al.*, 2006).

Like in human tissue, active P-STAT3 was upregulated during DSS-induced colitis in *miR-223*$^{-/y}$ colons. These mice have exacerbated inflammation and delayed mucosal healing in comparison to WT mice. These findings suggest, that *miR-223*$^{-/y}$ exhibit overactivation of STAT3 signalling, and suggest a potential role of *miR-223* in modulating this pathway.

The IL-6 family of cytokines are potent activators of STAT3 signalling. The unifying feature of this family is the shared use of the transmembrane β-receptor, gp130 (Nguyen, Putoczki and Ernst, 2015). There is evidence supporting their role in regulating IBD. IL-6 has been reported to be elevated in the serum and mucosa of patients with IBD, and serum IL-6 levels are predictive of disease relapse (Neurath, 2014). Furthermore, IL-6 and soluble IL-6R has been found to be increased in the lamina propria during active IBD (Atreya *et al.*, 2000). LIF, another member of this cytokine family, has also been shown to be upregulated in patients with UC (Wang *et al.*, 2023). Similarly, studies have reported increased serum OSM levels in IBD, as well as in the early post-operative setting of recurrent CD. Moreover, higher colonic OSM levels are observed in a refractory subset of patients requiring biological therapy within the first year after diagnosis, or in the case of anti-TNFα and vedolizumab non-response (Verstockt, Verstockt

and Vermeire, 2019). IL-11 expression has also been observed in a rat model of IBD (Torrence *et al.*, 2008).

miRNAs have been identified as important regulators of STAT3 signalling, particularly in the context of IBD. Various miRNAs have been reported to be increased in IBD patients, including *miR-31*, *miR-106a-5p* and *miR-347b-5p*, and *miR-124* has been observed to be decreased (Ahmed *et al.*, 2025). Studies have revealed that *miR-347b-5p* promotes the differentiation of T_H1/T_H17 cells and modulates the JAK1 and STAT3 pathways in $CD4^+$ T cells through the IL-10/STAT3 axis (Li *et al.*, 2022). In contrast, children suffering with UC present with lower levels of *miR-124* and this is associated with increased expression and activity of STAT3 (Koukos *et al.*, 2013).

As stated previously, *miR-223* is upregulated during active disease in IBD patient biopsies and DSS-induced colitis in mice (Neudecker *et al.*, 2017b). Members of the IL-6 family of cytokines and components involved in STAT3 signalling have predicted *miR-223* binding sites in both mice and humans, namely, *Il-6*, *Lif, Stat3 and* IL6ST. Although not investigated in this work, further research could explore the interaction between *miR-223* and members of the IL-6 family of cytokines. Among the experimental approaches currently available, a luciferase reporter assay is considered the most widely used and reliable method for validating miRNA-target interactions (Jin *et al.*, 2013). This is achieved by inserting a gene segment containing the predicted miRNA binding site into a plasmid downstream of a luciferase reporter gene. Following transfection of this plasmid into cells, binding of the endogenous miRNA to the target site suppresses luciferase expression or promotes mRNA degradation, resulting in a measurable reduction in luminescence and thereby confirming the miRNA-target interaction. This assay has been utilised to confirm the interaction between *miR-485-5p* and flotillin-2 (FLOT2) in SCLC cells, and *miR-422a* and methyl-CpG binding protein 2 (MeCP2) (Gao *et al.*, 2019; Giuliani *et al.*, 2023).

Macrophages are important sources of these cytokines, therefore, when these immune cells are deficient in this miRNA, studies suggest that these IL-6 family members are upregulated, potentially leading to activation of STAT3 signalling (Chen *et al.*, 2012; Zhang *et al.*, 2021a). This was evident when colonic epithelial

organoids exhibited persistent expression of active P-STAT3, following co-culture with *miR-223KD* macrophages. Similar findings were observed in the mouse model, where, *miR-223*$^{-/y}$ colons presented with higher expression of P-STAT3 during the continuum of experimental colitis.

Notably, these findings corroborate the hypothesis that reparative macrophages lacking *miR-223* are functionally dysregulated. Under normal conditions, as seen here with RAW 264.7 cells, IL-4-activated macrophages are not potent activators of STAT3 signalling. However, when *miR-223* is repressed, epithelial organoids demonstrate pro-longed activation of this crucial pathway, alluding to the impaired function of macrophage lacking *miR-223*.

The direct co-culture system used in this study, provided an insight into the functional consequences of *miR-223* deficiency on the STAT3-dependent cross-talk between macrophages and colonic epithelial cells. IL-4 activated-macrophages deficient in *miR-223* drove *Olfm4* expression in epithelial organoids. STAT3 is a known driver of *Olfm4* expression, where studies revealed that treatment of organoids with STAT3 inhibitors ablated the expression of this stem cell marker (Jung *et al.*, 2019). This finding was further supported by the present work, where STAT3 inhibition downregulated *Olfm4* expression in organoids co-cultured with *miR-223KD* cells. The lack of significance could be due to the Stattic treatment not specifically targeting the organoids, and potentially exerting unintended effects on the *miR-223KD* cells. Expression of mature stem cells are vital for maintaining a healthy epithelium, as they are essential for replenishing the intestinal epithelium following injury (Choi and Augenlicht, 2024). However, their persistent expression can often indicate a defect in stem cell differentiation. Numerous studies have reported the consequences of impaired stem cell differentiation in the intestine. Helminth infection in mice has been observed to suppress the ability of intestinal stem cells to differentiate into tuft cells, goblet cells and Paneth cells (Drurey *et al.*, 2022; Karo-Atar *et al.*, 2022). Therefore, the upregulation in expression of *Olfm4* in the work presented here, is potentially indicative of impaired stem cell differentiation, due to overactivation of STAT3 signalling as a result of *miR-223* deficiency.

This was further confirmed with Stattic inhibitor treatment. Intestinal stem cells differentiate into TA cells and then into progenitor cells for secretory and absorptive lineages (Meyer *et al.*, 2022). In this study, STAT3 inhibition promoted the regenerative process, as stem cells differentiated into highly proliferative progenitor cells of both secretory and absorptive lineages, as evidenced by the increased expression of *Ki67*, *Atoh1* and *Alpi*. Thus, *miR-223* deficiency impairs the epithelial regenerative process in a STAT3-dependent manner.

There is extensive evidence that demonstrates the importance of the IL-6 family of cytokines in intestinal regeneration. LIF, a predicted target of *miR-223*, has been reported to be crucial in this process. LIF knockout crypts exhibited a significantly reduced ability to proliferate, expand and form budding organoids. These organoids presented with decreased numbers of Paneth cells, and had a lower survival rate after passage. These effects were reversed by supplementation of recombinant LIF, and resulted in increased $Ki67^+$ and $Olfm4^+$ cells (Wang *et al.*, 2020). Work has shown that OSM promotes the proliferation of epithelial cells (Beigel *et al.*, 2014). OSM orchestrates tissue repair by inducing stromal cell proliferation and migration, drives extracellular matrix remodelling and supports angiogenesis (West, Owens and Hegazy, 2018; Richards and Botelho, 2019). Studies suggest that IL-11 has beneficial functions in the context of epithelial barrier repair. In murine bacterial-induced colitis, administration with recombinant IL-11 prevented the development of mucosal ulcerations (Gibson *et al.*, 2010). Furthermore, IL-11 has been observed to promote intestinal crypt regeneration (Orazi *et al.*, 1996).

The work presented here adds to this body of evidence. Stimulation of colonic epithelial organoids with recombinant IL-6, LIF and IL-11 resulted in upregulation of markers associated with dedifferentiation and regeneration, including stem cells, fetal-like stem cells, progenitor cells and differentiated cells. Although induction of these genes did not reach statistical significance, this may be a consequence of the prolonged 72 h timepoint used. However, these changes can be attributed to STAT3 activation, as inhibition of STAT3 prevented the upregulation of these markers.

Collectively, these findings demonstrate that the IL-6 family of cytokines activates STAT3 signalling in colonic epithelial cells, and that this interplay regulates intestinal epithelial dedifferentiation and regeneration.

CHAPTER 6

DISCUSSION AND FUTURE DIRECTIONS

DISCUSSION

The incidence and prevalence of IBD has increased in numerous countries, notably in Western and newly industrialised nations, with an estimated 7 million individuals globally affected by the disease (Yang, Guo and Zou, 2026; Alatab *et al.*, 2020). According to Crohn's and Colitis Ireland, there are an estimated 40,000 people living with IBD. In 2011, there were 5.9 new cases of CD and 14.9 new cases of UC per 100,000 population in Ireland (Crohn's and Colitis Ireland, 2026). This increase in global burden is linked to various factors including urbanization, westernization, dietary changes, increased antimicrobial exposure and alterations in the host-microbial balance (Kumar, Garand and Al Khodor, 2019).

Initially, treatment options for this inflammatory disease were limited to corticosteroids, aminosalicylates, immunosuppressants and surgery, however, these conventional therapies have numerous side effects and suboptimal efficacy (Yeshi, Jamtsho and Wangchuk, 2024). The therapeutic strategies used for IBD have evolved from non-specific anti-inflammatory approaches to an era of precision-targeted therapy, which is centred on biologics and small molecule inhibitors (Yang, Guo and Zou, 2026). Anti-TNF-α agents are an important class of biologics and represents a first-line treatment option. Chimeric infliximab and fully human adalimumab neutralize TNF-α and induce apoptosis of cells expressing this cytokine, significantly improving symptoms, promoting mucosal healing and reducing surgery/hospitalization rates (Khatana, Qamar and Ashfaq, 2021; Sökmen, Göçmen and Tuncer, 2022; Vulliemoz *et al.*, 2020; Cheah and Huang, 2023). However, approximately 30% of treatment-naïve patients are primary non-responders, and 20-40% experience secondary loss of response (Yashima *et al.*, 2025).

Mucosal healing is an established treatment goal in IBD (Parigi *et al.*, 2024). A key feature of IBD is disruption of the intestinal barrier which permits translocation of microorganisms and other antigens into the intestinal mucosa, resulting in uncontrolled immune activation (Villablanca, Selin and Hedin, 2022). A range of mechanisms are involved in this process, for example, abnormal expression or distribution of tight junction proteins, such as claudin-1 and occludin, have been

observed in patients with IBD, and contribute to increased intestinal permeability (Lan *et al.*, 2021). Impaired mucus barrier function, characterised by a thinner and discontinuous mucus layer, associated with reduced density of goblet cells, has been reported during active UC (Alipour *et al.*, 2016). Furthermore, dysregulated epithelial cell death, namely apoptosis and necroptosis, increased intestinal permeability, enabling pathogen translocation and promoting the inflammation and epithelial erosion seen in IBD (Qiu *et al.*, 2011; Jiang *et al.*, 2025). Therefore, the functional definition of mucosal healing is the re-establishment of barrier function (Rieder *et al.*, 2012; Karin and Clevers, 2016).

Numerous methodologies are used to functionally investigate barrier integrity. Among these techniques includes a FITC-Dextran (FD-4) assay. The FD-4 assay is widely used in pre-clinical studies due to its simplicity, cost-effectiveness and ease of implementation in most laboratory settings (Voetmann *et al.*, 2023). Dextrans are non-digestible polysaccharides (Wang *et al.*, 2015; Woting and Blaut, 2018). FD-4 is primarily used due to its size of 4 kDa, meaning it does not cross the intestinal epithelial barrier in high quantities after oral administration unless the intestinal barrier is compromised (Gilani *et al.*, 2017). In the event of intestinal barrier disruption, FD-4 molecules migrate to the serosa of the intestine and subsequently enter systemic circulation (Yan *et al.*, 2009; Joly Condette *et al.*, 2014). The concentration of serum FD-4 can be measured and serves as an indicator for paracellular permeability, reflecting the degree and severity of intestinal mucosal barrier dysfunction (Liu *et al.*, 2021).

Macrophages are strategically distributed throughout the body, display a high degree of functional plasticity and possess both protective and pathogenic functions in human disease (Chen *et al.*, 2025; Na, Kim and Seok, 2023; Murray and Wynn, 2011). Various mouse models have demonstrated the importance of macrophages in tissue repair and regeneration following colonic injury (Hegarty, Jones and Bain, 2023). For instance, macrophage-deficient *Csf1*$^{op/op}$ mice presented with dysregulated epithelial regeneration following DSS-induced injury (Pull *et al.*, 2005). Additionally, depletion of extracellular vesicle packaged WNTs from macrophage conditioned medium, negates its ability to rescue intestinal stem cells from radiation lethality (Saha *et al.*, 2016). Genetic variants in prostaglandin receptor 4 (*PTGER4*), which has been reported to be necessary

for wound repair in mice, are associated with increased susceptibility to IBD (Duffin *et al.*, 2016; Glas *et al.*, 2012). Furthermore, disruption of TGFβR signalling in macrophages delays the resolution of DSS-induced colitis (Rani *et al.*, 2011).

Macrophages have been observed to be vital for clinical response to infliximab and tofacitinib treatment. A distinct subset of $CD206^+$ macrophages are induced in patients that achieve a clinical response to infliximab, in comparison to patients who failed to respond to the biologic (Vos *et al.*, 2012). Furthermore, following treatment with tofacitinib, a small molecule JAK inhibitor, murine and human macrophages exhibit increased IL-10 secretion alongside inhibited IFNγ signalling (De Vries *et al.*, 2019). Although, most currently available therapies that induce mucosal healing exert their effects through immune inhibition, macrophages represent a potential therapeutic strategy to directly promote mucosal healing (Villablanca, Selin and Hedin, 2022).

Although biologic therapies can be highly effective, a substantial proportion of patients eventually develop therapeutic resistance. With anti-TNFα therapy, patients are susceptible to develop resistance within one year of treatment initiation, driven by the activation of alternative signalling pathways (Neurath, 2019). MiRNAs exhibit crucial and multifaceted roles in regulating mucosal immunity to reinstate and maintain intestinal homeostasis. Therefore, their inherent multi-target nature may implicate miRNAs as a readily available alternative treatment option (Dhuppar and Murugaiyan, 2022).

An increasing body of evidence identifies miRNAs as robust biomarkers in IBD (Dhuppar and Murugaiyan, 2022). In the context of UC, *miR-301a* is upregulated in UC, resulting in the downregulation of E-cadherin expression in a BTG1-dependent manner and reduces epithelial integrity (He *et al.*, 2017). *MiR-143* expression levels are increased in CD. This miRNA directly targets ATG2B mRNA, inhibiting autophagy and enhancing the expression of pro-inflammatory molecules IL-8, TNFα and IFNγ in human intestinal epithelial cells (Lin *et al.*, 2018). In a disease setting, aberrant miRNA expression may be therapeutically modulated either by inhibiting the expression of miRNAs using antagomirs or by

inducing their expression through miRNA mimics (Dhuppar and Murugaiyan, 2022).

MiR-223 has emerged as a putative biomarker for IBD, with serum *miR-223* being increased in CD and UC patients (Wang *et al.*, 2016). This miRNA has anti-inflammatory properties which allow it to limit intestinal inflammation by constraining the NOD-, LRR-, and pyrin domain-containing protein 3 (NLRP3) inflammasome in mice (Neudecker *et al.*, 2017b). *MiR-223*$^{-/-}$ mice experience severe colitis, driven by a potent pro-inflammatory response in intestinal macrophages and dendritic cells (Zhou *et al.*, 2015). *miR-223* also inhibits IL-18-mediated neutrophil extracellular trap formation in human neutrophil cultures (Liao *et al.*, 2021).

Although, there is clinical heterogeneity among UC patients, the initial course of treatment for these individuals are identical, and is only modified when patients do not respond. Two transcriptomic profiles of UC, UC1 and UC2, have been identified in both adult and paediatric patients. Both subpopulations are considered inflamed, however, only UC1 patients present with a higher expression of genes associated with neutrophil degranulation and myeloid cytokine signalling. Furthermore, only 10% of patients within this cohort respond to infliximab therapy (Czarnewski *et al.*, 2019).

miR-223 has the potential to provide insight into this patient cohort, as the molecular phenotype of *miR-223*-deficient mice across multiple mouse models mirrors that observed in UC1 patients. In a model of DSS-induced colitis, *miR-223*$^{-/y}$ mice display enhanced colonic neutrophil infiltration and increased *Il-1*β and *Cxcl1* expression, features also observed in UC1 patients (Czarnewski *et al.*, 2019; Neudecker *et al.*, 2017b). Furthermore, in a model of CAC, mice lacking *miR-223* exhibited elevated levels of *Tnf*, *Il-1*β, *Il-6*, *Il-11* and *Socs3*, consistent with upregulation reported in the UC1 cohort (Flynn *et al.*, 2024; Czarnewski *et al.*, 2019). Taken together, these similarities position *miR-223* as a valuable tool for elucidating molecular pathways that could improve IBD therapy and mitigate primary non-response or secondary loss of response.

During DSS-induced colitis, *miR-223*$^{-/y}$ mice present with delayed mucosal healing (Neudecker *et al.*, 2017b). Given the importance of macrophages in this process, it was hypothesised that their functions are dysregulated in these mice, implicating *miR-223* as a crucial regulator of these immune cells. Although a myeloid-restricted miRNA, *miR-223* is minimally expressed in macrophages (Haneklaus *et al.*, 2012). This is supported by the BMDM time course, whereby *miR-223* is downregulated as myeloid progenitor cells differentiate into mature macrophages. Similar to granulocytes, *miR-223* expression is controlled by the myeloid transcription factors, PU.1 and C/EBPβ, which are repressed during the course of myeloid differentiation (Fukao *et al.*, 2007).

Despite low expression in mature macrophages, changes in *miR-223* levels can have profound functional consequences. Intestinal macrophages deficient in this miRNA exhibit a pro-inflammatory phenotype, resulting in the increase in expression of TNFα and IL-1β (Zhou *et al.*, 2015). Conversely, *miR-223* overexpression in macrophages is associated with reduced NLRP3 protein accumulation and consequent suppression of inflammasome-mediated IL-1β production (Haneklaus *et al.*, 2012; Bauernfeind *et al.*, 2012). Unlike other studies, the work presented here investigates the functional role of both *miR-223-3p* and *miR-223-5p* in mediating inflammatory responses in macrophages. Overexpression of the *miR-223* strands through synthetic mimic transfection, supressed the transcription of various pro-inflammatory molecules, including *Cxcl2*, *Tnfα* and *Il-1β. MiR-223* overexpression also had the capacity to induce pro-resolving genes, including *Retnla*, *Ccl17* and *Ccl22*. This study reveals a novel role of *miR-223* in not only limiting macrophage inflammatory responses but also promoting pro-resolving functions.

MiR-223 has been reported to be upregulated during active inflammation in both IBD patient biopsies and in murine tissue samples with DSS-induced colitis (Neudecker *et al.*, 2017b). These observations were expanded on by *in situ* hybridization studies, which demonstrated elevated expression of *miR-223* during active disease and only modest reduction during the recovery phase. Additionally, *miR-223*$^{-/y}$ mice present with delayed mucosal healing, implicating a role of *miR-223* in disease resolution.

CD206^{+}, RELMα^{+} and MERTK^{+} macrophages are crucial for restoring epithelial barrier integrity. Despite the presence of these pro-reparative macrophages throughout the continuum of DSS-induced colitis, tissue repair remained slow in *miR-223$^{-/y}$* colons, suggesting potential functional deficits. This was accompanied with persistent expression of OLFM4 and aberrant expression of Cyclin D1, PCNA and MUC2. These findings indicate that *miR-223* is necessary for precise regulation of the repair process.

So how is *miR-223* regulating inflammatory signalling in macrophages? *MiR-223*-mediated regulation of mucosal healing has been linked to STAT3 signalling (Nguyen, Putoczki and Ernst, 2015). Various members of the IL-6 family of cytokines, namely *Il-6* and *Lif*, are predicted targets of *miR-223*, and these cytokines are potent activators of the STAT3 signalling pathway. Therefore, *miR-223* deficiency in macrophages, leads to upregulation in these cytokines and overactivation of STAT3 signalling (Chen *et al.*, 2012; Zhang *et al.*, 2021a). Most previous studies have only assessed STAT signalling in the context of immune cells. It remains unknown how this inflammatory cytokine environment may regulate JAK-STAT signalling in epithelial cells specifically and consequences for barrier repair. The data presented here identified persistent expression of P-STAT3 in *miR-223$^{-/y}$* mice and in colonic epithelial organoids following co-culture with *miR-223KD* macrophages.

Previous studies have reported the importance of IL-6 family of cytokines and STAT3 signalling in epithelial regeneration. *Stat3$^{+/-}$* mice exhibit impaired intestinal regeneration following radiation and DSS-induced injury (Tebbutt *et al.*, 2002). However, its overactivation has also been reported in IBD (Shahini, 2023). Furthermore, IL-6, LIF, OSM and IL-11 have been observed to be elevated in IBD (Neurath, 2014; Wang *et al.*, 2023; Verstockt, Verstockt and Vermeire, 2019; Torrence *et al.*, 2008). Additionally, these cytokines have been demonstrated to be indispensable for intestinal stem cell survival and proliferation following injury (Grivennikov *et al.*, 2009; Kuhn *et al.*, 2014; Wang *et al.*, 2020; Beigel *et al.*, 2014; Orazi *et al.*, 1996). The present work further supports these findings, as stimulation of colonic epithelial organoids with members of the IL-6 family of cytokines induced markers of dedifferentiation and regeneration in a STAT3-dependent manner. Collectively, these findings reveal the potential of the IL-6

family of cytokines/STAT3 pathway as a potential therapeutic axis for IBD, capable of directly promoting epithelial regeneration.

Interestingly, STAT signalling has been extensively investigated as a therapeutic target in the context of IBD. Janus kinase inhibitors are a novel class of orally bioavailable small molecule inhibitor drugs. Pan-JAK inhibitors such as Tofacitinib being the first approved for use in IBD, followed by more recent agents such as ruxolitinib, filgotinib and updacitinib, selective JAK1 inhibitors (Honap *et al.*, 2024). Tofacitinib is licensed for the treatment of moderate to severe UC and is considered a pan-JAK inhibitor with preferential selectively for JAK1 and JAK3 (Flanagan *et al.*, 2010). In a US retrospective cohort, approximately half of biologic-refractory UC patients achieved steroid-free clinical remission at weeks 12, 52 and 78 following tofacitinib treatment (Dalal *et al.*, 2024). However, the efficacy of this JAK inhibitor in the treatment of CD needs further study (Chen *et al.*, 2024).

Ruxolitinib is a JAK1 and JAK2 inhibitor that has been approved for use in refractory myelofibrosis, polycythemia vera, and steroid-refractory acute graft-versus-host disease (GVHD) and chronic GVHD after the failure of systemic therapy (Pemmaraju *et al.*, 2023). It is currently in the preclinical phase for UC. In a DSS-induced colitis mouse model, this inhibitor was observed to reverse acute colitis and inhibited the expression of pro-inflammatory cytokines and chemokines. Interestingly, ruxolitinib also improved intestinal epithelial barrier damage in intestinal epithelial cells through STAT3 signalling (Li *et al.*, 2023)

Upadacitinib is a selective JAK1 inhibitor, that has been approved for treatment of UC patients who have failed immunosuppressive and TNF suppressive therapy (Friedberg *et al.*, 2023). Following treatment with this inhibitor, the proportion of UC patients achieving clinical remission is greater than those treated with tofacitinib (Boneschansker and Ananthakrishnan, 2023). Additionally, after 8 weeks of treatment, upadacitinib induced clinical remission in 77.8% of UC patients previously treated with tofacitinib (Friedberg *et al.*, 2023).

Finally, filgotinib is the second-generation first choice JAK1 inhibitor that has been approved for use in the treatment of UC (Namour *et al.*, 2022). It has shown efficacy in inducing and maintaining clinical remission (Feagan *et al.*, 2021).

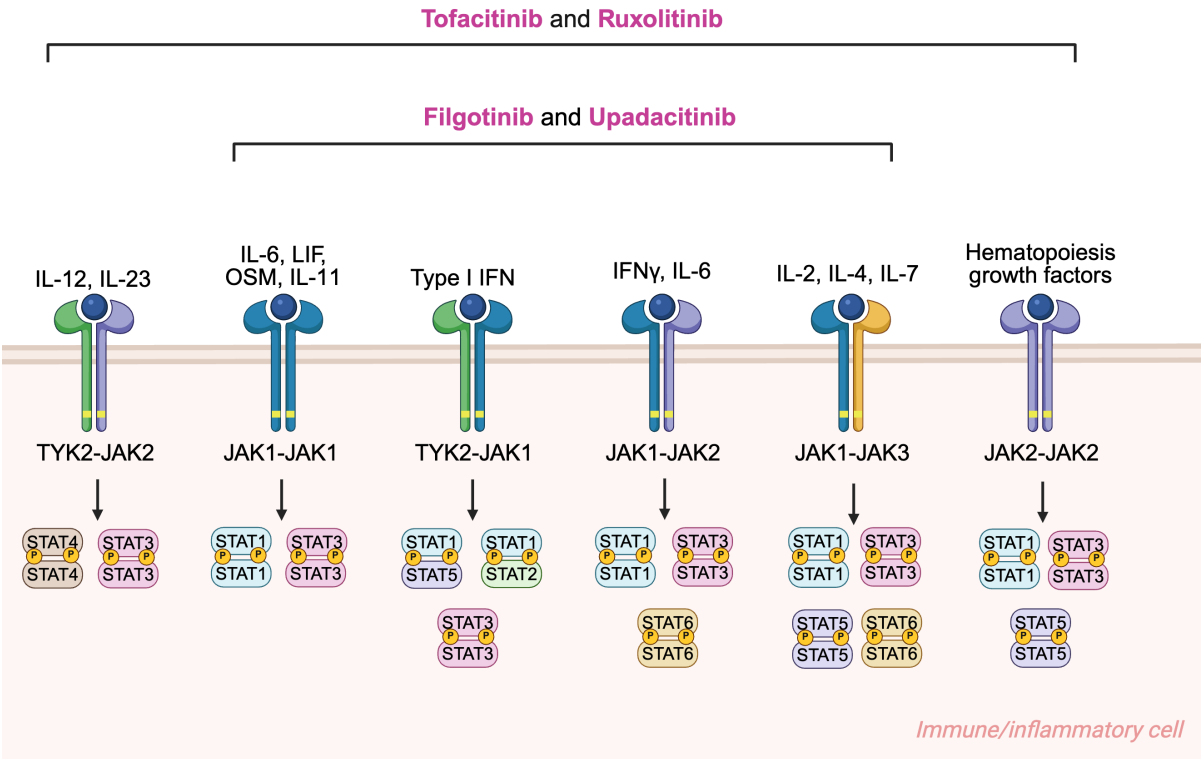

Figure 6.1. ***Overview of JAK inhibitors and targets for the treatment of IBD.*** JAK-STAT pathways inhibited tofacitinib, ruxolitinib, filgotinib and upadactinib.

Despite their relative selectivity, JAK inhibitors at higher doses may engage multiple JAKs via off-target binding, thereby increasing the risk of haematological, metabolic or immunosuppressive adverse effects (Salas *et al.*, 2020). For instance, infections occurred more frequently with tofacitinib treatment than with placebo, namely herpes zoster infection (Sandborn *et al.*, 2019; Sandborn *et al.*, 2017). Conversely, emerging evidence indicates that increased selectivity for specific JAKs is associated with a reduced incidence of adverse effects (Salas *et al.*, 2020). Taken together, while JAK inhibitors are becoming an exciting new treatment option (particularly for patients who are refractory to standard-of-care biologics), the discrete roles of selective JAK-STAT members in epithelial repair and mucosal healing in general, needs further analysis.

Targeting STAT3 signalling represents a potential therapeutic strategy in IBD, with studies investigating its efficacy already underway. TTI-101, a small molecule STAT3 inhibitor, has been examined in the AOM-DSS mouse model of CAC. TTI-101 reduced the adenoma numbers, normalised the transcriptome of the colon, and decreased the expression of STAT3-upregulated genes associated with colorectal cancer (CRC) oncogenesis (Robinson *et al.*, 2025). Moreover, the novel STAT3 inhibitor, TAK875, alleviated weight loss and colon shortening caused by DSS-induced colitis. With respect to the DAI, TAK875 demonstrated a modestly greater therapeutic effect than tofacitinib (He *et al.*, 2024). Additionally, in DSS-induced colitis, TTI-101 has been observed to increase apoptosis of $CD4^+$ T cells, reduce colon infiltration of IL-17 producing cells, and downregulate STAT3-associated genes involved in inflammation, apoptosis resistance and CRC metastases (Robinson *et al.*, 2023).

Although promising, these studies do not assess the impact of STAT3 inhibition on epithelial regeneration. Considering the critical role of STAT3 in stem cell function and post-injury survival, careful consideration is warranted when employing STAT3 inhibitors in IBD therapy (Tebbutt *et al.*, 2002; Shahini, 2023; Stuhlmann-Laeisz *et al.*, 2006). STAT3 inhibition may represent a therapeutic option for patients refractory to anti-TNFα therapy. These patients are characterised by an elevated myeloid inflammatory profile, possible hyperactivation of STAT3 signalling and consequent impairments in epithelial regeneration (Czarnewski *et al.*, 2019). Therefore, targeting this pathway could facilitate mucosal healing in these patients. Thus, small molecule STAT3 inhibitors may serve as promising adjunct therapies for enhancing mucosal healing in IBD.

In addition to small molecule inhibitors, miRNAs are increasingly recognized as both diagnostic biomarkers and therapeutic targets, particularly through the use of miRNA mimics and antimiRs ('What will it take to get miRNA therapies to market?,' 2024; Huang, 2017). MiRNA mimics are synthetic molecules that replicate the function of endogenous miRNAs, thereby restoring or augmenting miRNA activity when expression is reduced. Conversely, antimiRs are designed to bind and silence endogenous miRNAs that are overexpressed ('What will it take to get miRNA therapies to market?,' 2024). A major advantage of miRNA-

based interventions is the ability of a single miRNA to simultaneously regulate multiple target genes. This enables coordinated control of entire cellular pathways, even when the effect on each individual target is relatively modest (Gebert and MacRae, 2019).

Several miRNA-based therapies have advanced to clinical trials. MRX34, an *miR-34a* mimic developed to restore the expression of the tumour suppressor *miR-34a*, was the first miRNA-based cancer therapy to enter a phase 1 clinical trial in 2013; however, the trial was terminated in 2016 due to severe immune-mediated toxicities and patient deaths (Hong *et al.*, 2020). Lademirsen, an antimiR of *miR-21*, was in a phase 2 clinical trial for the treatment of Alpert syndrome, but was terminated in 2022 (Gale *et al.*, 2024). Cobomarsen, an inhibitor for *miR-155*, had entered a Phase 1 clinical trial for the treatment of cutaneous T-cell lymphoma, but was discontinued. Preclinical work had shown that this therapy inhibited multiple survival pathways, including JAK/STAT (Seto *et al.*, 2018). Like other RNA-based therapies, a major obstacle to the clinical application of miRNA therapeutics is the challenge of effective delivery, coupled with the risk of toxicity and immune-mediated adverse effects (Rupaimoole and Slack, 2017). Despite these unsuccessful clinical trials, miRNAs remain promising regulators of STAT3 signalling, as they can target upstream mediators such as IL-6 and JAKs, as well as directly bind to STAT3, with *miR-223* being a notable example (Sajjadi-Dokht *et al.*, 2022; Chen *et al.*, 2012; Zhang *et al.*, 2021a).

Taken together, the findings presented in this thesis indicate that macrophage-associated *miR-223* plays a pivotal role in regulating mucosal healing, while the interaction between the IL-6 family of cytokines and STAT3 signalling is crucial for intestinal epithelial dedifferentiation and regeneration.

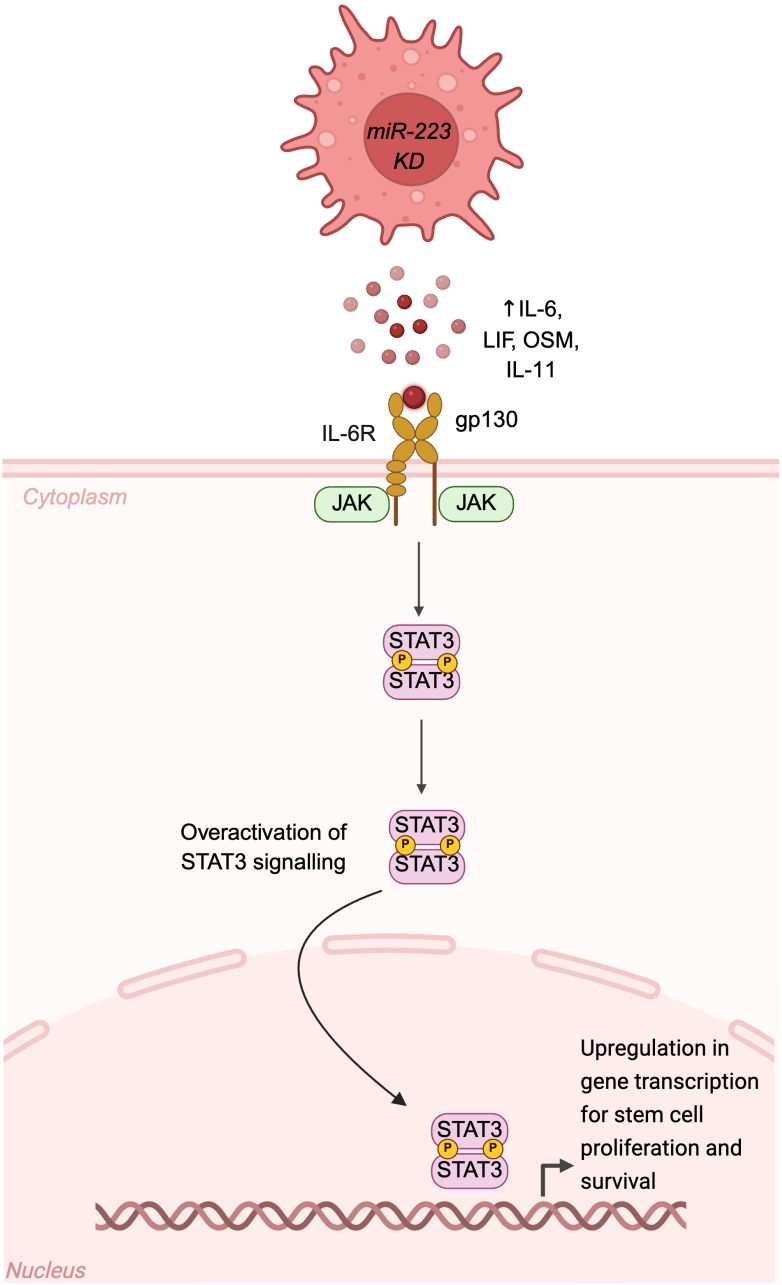

Figure 6.2. ***Overview of the hypothesised STAT3-dependent mechanism through which miR-223 regulates intestinal epithelial regeneration.***

FUTURE DIRECTIONS

Given the increasing global prevalence of IBD, the implementation of effective management strategies is imperative, as the condition adversely affects patient well-being and places substantial financial strain on families. There has been an increase in the number of treatment options available for this inflammatory disease. However, many existing strategies are directed toward resolving inflammation rather than directly promoting mucosal healing, the ultimate therapeutic goal in IBD management. The overall aim of this thesis was to elucidate mechanisms with the potential to serve as therapeutic targets that induce epithelial regeneration. The data presented here demonstrated the importance of *miR-223* in regulating mucosal healing in a STAT3-dependent manner. Moreover, this work revealed that targeting STAT3 signalling represents a promising therapeutic strategy to promote mucosal healing following myeloid-driven inflammation. However, additional experiments are required before these findings can be evaluated in a clinical setting for IBD.

Initially, additional *in vitro* experiments employing the direct co-culture system of colonic epithelial organoids and macrophages would be valuable in further elucidating the therapeutic potential of targeting STAT3 in IBD. However, in contrast to previous work, this approach would involve lentiviral-mediated knockdown of STAT3 in colonic epithelial organoids. Moreover, these organoids would be co-cultured with *miR-223KD* macrophages to further confirm the role of *miR-223* in restricting the epithelial regeneration process in a STAT3-dependent manner. Further studies could involve co-culturing STAT3 knockdown colonic epithelial organoids with LPS or IL-4 activated BMDMs.

Furthermore, examining the interactions of macrophages and intestinal stem cells in human UC biopsies would provide stronger clinical relevance. This could be achieved through IHC analysis of a range of macrophage, intestinal stem cell, and repair-associated markers. In addition, including biopsies from patients who are treatment-responsive or refractory to anti-TNFα or JAKi therapy would offer even deeper insight. These approaches would yield a more detailed and clinically

relevant understanding of macrophage-intestinal epithelial cell interactions and further clarify the role of STAT3 signalling in epithelial regeneration.

Ideally, *in vivo* studies would be conducted to validate the therapeutic potential of these findings. Given the molecular similarities observed between patients in the UC1 cohort and *miR-223*$^{-/y}$ mice following DSS-induced injury, this mouse model would be repeated. These mice could be treated with the STAT3 inhibitor, TTI-101, rather than STATTIC, as this is a first-in-class, orally bioavailable, selective small molecule that binds to STAT3 and prevents STAT3-mediated transcriptional activity (Tsimberidou *et al.*, 2025). Previous studies have investigated this inhibitor in the context of experimental colitis, however, they fail to investigate the direct effect on mucosal healing (Robinson *et al.*, 2025). Consequently, administering TTI-101 to mice during the recovery phase of DSS-induced colitis would provide insight into its potential to enhance epithelial regeneration. Ideally, STAT3 inhibition would be accomplished in a cell-type specific manner, targeting intestinal epithelial cells exclusively. Comparable strategies have been employed in prior studies. For example, myeloid cell-selective STAT3 antisense oligonucleotide (CpG-STAT3ASO) has been utilized to target neutrophils in vivo in tumour-bearing mice. Neutrophil-specific STAT3 knockdown impaired tumour growth and enhanced cytotoxic T cell activity in the tumours and tumour draining lymph nodes (Ozel *et al.*, 2025). Although not specific to STAT3 signalling, selective JAK inhibition has been investigated in a Phase 1b study in patients with UC. TD-143 is a novel, orally administered, gut-selective JAK inhibitor used in patients with UC. Treatment with this inhibitor was associated with numerical trends indicative of potential clinical efficacy (Sandborn *et al.*, 2020). These studies confirm the therapeutic potential of selective STAT3 or JAK inhibition *in vivo* and in a clinical setting.

Although, *in vitro* and *in vivo* studies using murine organoids and DSS-induced murine models of experimental colitis are essential before translating novel findings to a clinical setting, they do have inherent limitations. Organoids are powerful research tools, however, challenges remain including incomplete immune system simulation, limitations in drug sensitivity testing and standardization and reproducibility issues (Wang *et al.*, 2025). Although organoid-immune cell co-culture models have advanced the study of immune-

tissue interactions, most are restricted to a single immune cell type, such as T cells or macrophages (Cattaneo *et al.*, 2020; Jiang *et al.*, 2023). Consequently, they do not adequately reflect the intricate cellular interactions and immune networks found in vivo, limiting their ability to predict long-term responses to immunotherapies (Vitale *et al.*, 2021). Moreover, the absence of vascular endothelial cells and extracellular matrix (ECM) components further constrains their physiological relevance, as these elements are essential for regulating immune function, drug delivery, and microenvironmental conditions, including oxygen availability, pH gradients, and mechanical stress (Hofer and Lutolf, 2021). Evaluating the efficacy of drugs involves monitoring immune cell activity, vascular integrity and cytokine release, all of which impact therapeutic outcomes (Wang *et al.*, 2024). However, the inability of current organoid models to fully recapitulate these complex interactions limits their predictive value (Wang *et al.*, 2025). Finally, challenges in standardization and reproducibility remain major barriers to the broader application of organoid models in preclinical and clinical settings. Differences in tissue sources, culture protocols, and extracellular matrices contribute to inter-laboratory variability, while even patient-derived organoids can display heterogeneous gene expression patterns, microenvironmental features, and drug responses (Hughes, Postovit and Lajoie, 2010; Reed *et al.*, 2009; Wang *et al.*, 2025). This variability limits the reliability, comparability, and clinical translatability of organoid research findings (Wang *et al.*, 2025).

The DSS-induced model of colitis is the most widely used tool for investigating the mechanisms underlying UC and for assessing novel therapeutic strategies. This model has several strengths, including high reproducibility, ease of implementation and maintenance, and the ability to reproduce many of the pathological features observed in human IBD (Yang and Merlin, 2024). Despite its usefulness, the DSS-induced colitis model has limitations in modelling human IBD. It does not capture the complex interplay of genetic, environmental, and immunological factors underlying the disease (Eichele and Kharbanda, 2017; Mizoguchi *et al.*, 2020). DSS causes rapid, severe inflammation with widespread epithelial damage and microbial invasion – features less typical of human IBD (Loddo and Romano, 2015). Unlike human disease, T and B cells are not required for the development of colitis in this mouse model (Chassaing *et al.*, 2014). The model mainly reflects UC, which affects the colon and rectum, and is less

representative of CD, which can involve any part of the gastrointestinal tract (Palnaes Hansen *et al.*, 1990). Moreover, outcomes are highly strain-dependent, with different mouse strains showing variable susceptibility to inflammation and responses to interventions (Yang and Merlin, 2024).

CHAPTER 7

APPENDIX

Table 7.1. MiR-223-3p target genes in mice identified using TargetScan

***MiR-223-3p* targets in mice**
Hipk2, Pak3, Igf1r, Nfat5, Fbxw7, Phf20l1, Fgf6, Gm9938, Fam199x, Ndnf, Pura, Ago3, Kpna3, Spata13, Fat1, POU2F1, Gpr155, Acsl3, Fam120c, Tspan7, Rasa1, Sacs, Fam46d, Rhob, Atp7a, Slc23a2, Tnfrsf19, Acvr2a, Arvcf, Lelp1, Fam46a, 4732440D04Rik, Purb, Rabep1, Tmprss11e, Mef2c, Mmp16, F3, Tnfsf15, Tnrc6b, Cbfb, Sept8, Wdr62, Hlf, Plekhh1, Sp3, Lmln, Cdk17, Adcy7, Sox6, Scn3a, Slc24a2, Gna13, Rc3h1, Rabgap1, Pik3c2a, Olfm1, Alcam, Cers6, Usp6nl, Sh3pxd2b, Brpf3, Pou2f1, Dusp2, Gpm6b, Inpp4a, Rcn2, Nfia, Ccnt2, Slc4a4, Siah1a, Celf1, Crim1, Mbnl1, Kmt2c, Pds5b, Phip, Cep68, Mkln1, Treml2, Dpf3, Ptbp2, Slc39a8, Hsp90b1, Map4, Pkp4, Lcor, Dennd5b, Fbxo8, Kat6a, Rdh10, Elk1, Syncrip, Srek1, Fbxo25, Armcx1, Frmd4a, Snai2, Trpv2, Scn2a1, Nfib, Rap2a, Arfip1, Rprd1b, Eva1a, Zcchc14, Rps6kb1, Scn1a, Mga, Anks1b, Tgfbr3, Vamp2, Ulk2, Slc8a1, Pknox1, Fgfr2, Myh10, Derl1, Cux1, Rnf34, Fnbp1l, Ppp1r12b, Ankrd40, Tshz3, Foxo3, Cpeb3, Usp40, Btbd1, Tmc3, Naa30, Apool, Tmem64, Golga1, Cpne4, Adamts18, Spred1, 2310035C23Rik, Gtpbp8, Ppp1r3a, Plce1, Agmo, 2210018M11Rik, Zfx, Lmo2, Brinp3, Gm9887, Ralgps2, Neto1, Aco1, Smarcd1, Zfhx3, Flrt1, Tmem229a, Rnpc3, Dennd6a, 5031414D18Rik, Mybl1, Kcnq1, Tcerg1, Atp2b1, Rbm20, Tmem170, Clvs1, Inpp5b, Actr1a, Zbtb10, Cdh12, Casq2, Slc37a3, Gpr22, Napepld, Atp1b1, Kif21b, Sft2d2, Fubp3, Atxn1, Fam168a, Rab8b, Rorb, Aebp2, Slc26a7, Fam96b, Xpo4, Arhgap5, Celf2, Smurf2, Naa50, Mon2, Jmy, Slco1a1, Dlgap1, Prpf39, Otud4, Zeb1, Ttc9, Mtpn, Wwtr1, Nefh, Mamld1, Hist1h1a, Frk, Scaf8, Csnk1g1, Pag1, Prdm1, Phlpp1, Plagl2, Cnep1r1, Trim3, Styx, Stam, Crebzf, Map2k6, Uhmk1, Pde4d, Wbp1l, Inip, Lif, Hhex, Cbx5, Dnaja1, Dera, Cops2, Tmem47, Bet1l, Stk39, Tnni3k, Ube2q2, Rnf145, Srgap3, Arid1a, Eif5b, Bai3, Ankrd17, Slain2, Sept11, Cd2ap, Vmp1, G3bp1, Ss18, Nlrp3, Elp4, Pkn2, Ctsl, Gm10300, Gpr126, Mpz, Gpr62, Foxp1, Rab22a, Ebf3, Wasl, Tbx5, Zbtb9, March3, Slc35f1, Cnot2, Rras2, Sgms2, Phactr4, Papolg, Abhd13, Mafb, Tet3, Uqcc1, Eif1ad, G0s2, Xcr1, Fignl2, Smoc1, Fa2h, Sox11, Mboat2, Itgb1, Cenpm, Ube2a, Map1b, Baz1a, Sept6, Snx12, Efna1, Wdr26, Calb1, Fbxo46, Polr3e, Dmrt2, Kdm1b, Vti1a, Mcmbp, Carm1, Maf, Zbtb18, Cdyl, Msi2, 5830473C10Rik, Armc1, Orc4, Zc3h14, Nelfa, Hs3st1, Myo5b, Prdx2, Mpv17l2, Gstz1, Srpk2, Pdzd8, Ypel1, Atp5s, St3gal6, Hspa1b, Dcn, Trmt5, Atxn10, Prpf38a, Arpp19, Trpm4, Zfand5, Srp19, Ppp2r3a, Gmpr, Edc3, Ccne1, Smlr1, Cyb5rl, Calml4.

Table 7.2. MiR-223-3p target genes in humans identified using TargetScan

***MiR-223-3p* targets in humans**
FBXW7, RHOB, LELP1, PTS, TBC1D17, RP11-192H23.4, WDR62, LACC1, GTSF1, GALNT18, GTPBP8, CCDC149, C18orf54, SNX24, FBXO8, IL6ST, PDZD11, ATP7A, FOXO1, ARMCX1, CYTIP, ECT2, SLC4A4, SLC37A3, LMO2, LAYN, INPP5B, RNF145, ACSL3, HSP90B1, NFIA, FAM199X, HLF, SP3, DNAJB13, SIAH1, RGS1, ACVR2A, SYAP1, USP16, PHF19, ARMC1, SLC25A32, NDP, ATP10D, PEX16, TNNI3K, MID1IP1, SEPT8, ARPC5L, FPGT-TNNI3K, RWDD1, RCN2, PURB, CDK17, MEF2C, APC, LYPD6, RASA1, SLC39A1, PROKR2, BRMS1L, TMEM178B, KIAA0226L, SLC8A1, CRIM1, VAMP2, SEPT6, SREK1, CTSV, SRSF10, PRDM1, SEPT4, CBLB, RNF34, NUCKS1, ST3GAL1, SORBS1, NFIB, RERG, WDR77, SSRP1, CTNNA2, XPR1, DESI2, SHOX2, ATP1B1, ARPP19, SCAF8, POMP, NXF1, ADCYAP1, PTBP2, KLF7, PAX5, F3, NUP210, ULK2, CLSTN1, PURA, KAT6A, NLRP3, SLCO1A2, GPM6B, KPNA3, GFPT1, MBNL3, NUTF2, SLC23A2, MSMO1, CSPG5, TMEM64, COPS8, HHEX, INPP4A, UBXN1, NDNF, USP42, SGMS2, RAB8B, SRP19, PFN2, XKR6, POU2F1, ERO1LB, SCARB1, SMARCD1, MMP16, RYBP, SLC24A2, ATP2B1, PLAGL2, LRRC19, FAM46A, SPRED1, C10orf11, ACTRT3, RASSF4, VHL, NAA50, RFTN2, ANKRD17, MMP19, STIM1, KLF12, COPS2, KLK15, FOXO3, ST8SIA3, DOCK2, ITPR3, ARID1A, SYNCRIP, KANSL1L, ELP4, EYA3, AKAP1, BRPF3, SMOC1, KIAA0226, MAP4, PHF20L1, MPZ, MARCH3, MYBL1, EIF4E3, RPS6KB1, CCT3, LHX8, SCN1A, KBTBD6, G3BP1, ZEB1, ZFHX3, PDS5B, RAP2A, METAP1, ZZZ3, BRINP3, CNOT1, NF2, MFSD6, FAM98A, WASL, GABPB2, DNAJC6, FZD4, PHIP, STK39, APOBEC4, ZC3H6, MSI2, ZBTB4, OTUD4, SCN2A, FAT1, TCERG1, ZSWIM7, TMC5, POLR3E, TMEM47, EPSTI1, PKP4, SOX11, PDE4D, RALGPS2, USP6NL, BAI3, FGFR2, PDE3B, CCNT2, SPATA13, OPCML, HMGCS1, LIF, PRKACB, ZXDB, RPS15A, TXLNG, ZBTB10, TBC1D4, RBPJ, TAOK3, LONP2, KIF4A, UBE2W, FNBP1L, ZCCHC14, SCN3A, GNA13, C14orf142, UCP3, NFASC, UQCC1, CEP41, ZSCAN12, MYH10, TMEM170A, ATXN7L1, RBM20, PRKCE, NRF1, CNOT2, ERC1, VAV3, KIAA1468, MTMR2, MAFB, VMP1, PLEKHH1, TSHZ3, GPR155, WBP1L, SDC2, MTSS1, PLCE1, TSC22D1, IGF1R, CSNK1G1, PA2G4, DCUN1D3, PAPD5, NFIC, EPOR, CREBZF, RNF217, ZXDA, ELF2, AEBP2, GRAMD4, ENPP5, FBXL4, MAP1B, TSPAN5, SPTLC2, FDX1L, MOSPD1, GLIPR1, ELK4, SPPL2A, TGFBR3, ZBTB41, JMY, PLEKHA3, CNDP1, ATL2, TRPV2, RNF4, SECISBP2L, KIAA1755, ZFX, DENND5B, GTDC1, AGO3, FBXO28,

ANKFY1, ZNF395, PIK3C2A, FAM168A, CPEB3, NUDT3, SP1, RC3H1, SH2B3, MAT2B, SETBP1, SELT, C11orf30, UHMK1, ZBTB18, KIAA0355, ABCG4, PDS5A, PHLPP1, CBX5, ZFP3, FUBP3, AIFM1, ABI2, CHUK, RBBP4, LRP12, RORB, SLC35F1, PFKFB3, C8orf46, MBNL1, FOXP1, HEY2, NRXN3, TOP2B, KMT2C, CARM1, FRMD4A, POLR1C, WDR43, PDPK1, PSMA5, ZNF706, ELL2, E2F1, RP11-10A14.4, TGFBR2, ABHD13, MGA, TIAL1, HIPK2, TMED7, VPS39, EBF3, FAM46C, ZNF207, MYCBP, SRPK2, MBOAT2, PCDH12, CDYL, FBXO30, TWIST1, FAM160B1, STYX, RRAS2, SH3D19, SOX6, RAB10, CALML4, RIMS3, DLEU1, HNMT, IFNLR1, NCOA1, RSBN1L, PRR14L, SRGAP3, TRMT2B, HDAC4, GLUL, ZBTB40, C17orf75, UBE2A, MAP2K6, CCDC85C, TET3, NOVA2, CLPB, WDR26, SNCA, VTI1A, RP11-315D16.2, ZNF507, KCNMB4, GRHPR, RGS9BP, PAX6, U2SURP, CAND1, EIF5B, RBMS2, PKNOX1, NLE1, SESN3, PSD3, TNRC6B, ZIC1, TBC1D15, ATG7, FAM83D, MEF2D, PHKG2, GPR22, MCMBP, PPP1R15A, WDR7, LRRC40, AGMO.

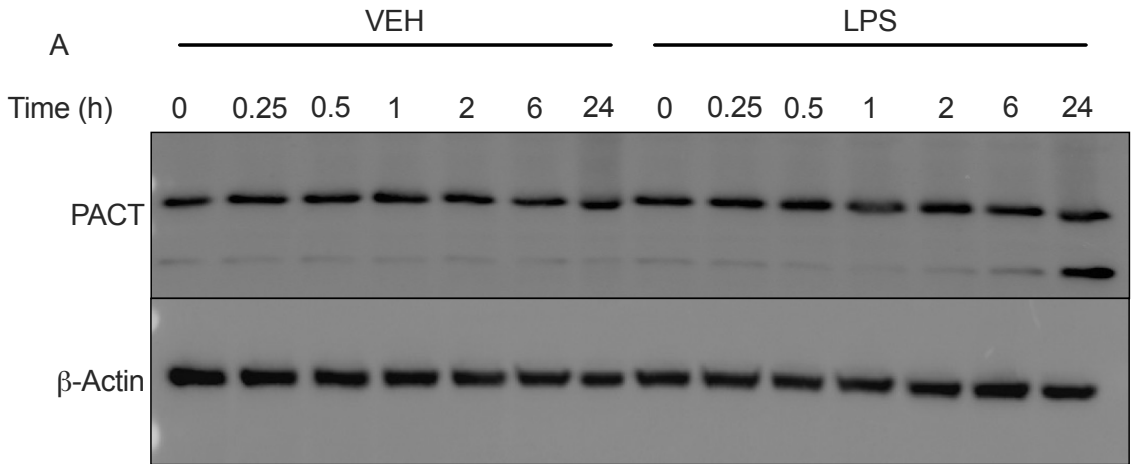

Figure 7.1. ***Stimulation with LPS for 24 h resulted in the appearance of an additional PACT protein band.*** **A.** A western immunoblot assessment of β-Actin and PACT in RAW 264.7 cells following stimulation with LPS (100 ng/mL) for 24 h. Representative n1 of n = 3 biological replicates/group.

A

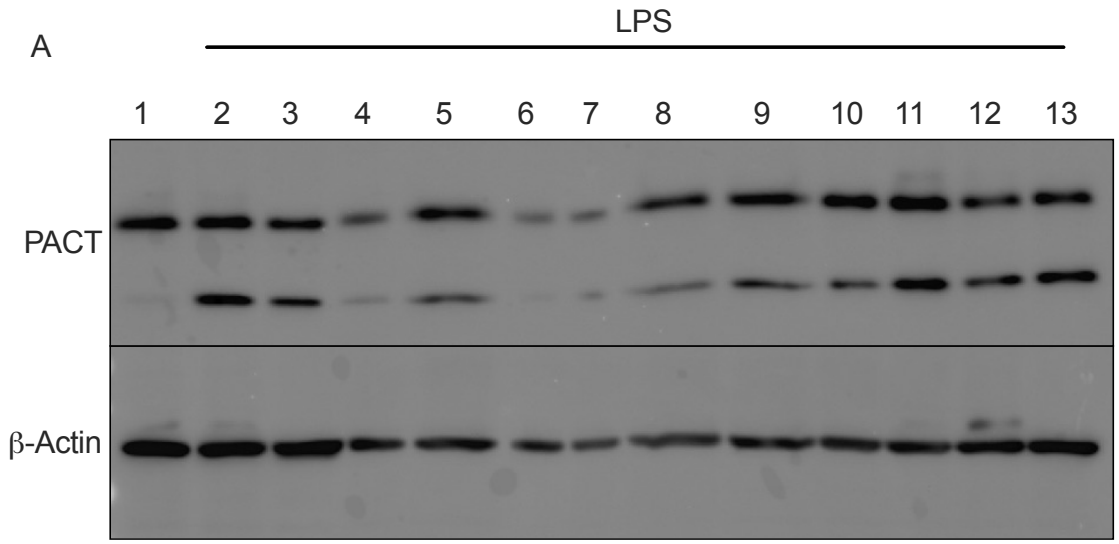

B

1 – VEH
2 – LPS
3 – LPS*
4 – O-Glycosidase & Neuraminidase
5 – O-Glycosidase & Neuraminidase#
6 – PNGase F
7 – PNGase F Ctrl
8 – PNGase F#
9 – PNGase F Ctrl#
10 – Tunicamycin
11 – GSK8612
12 – ST2825
13 – MG132
*No phosphatase and protease inhibitors
#Equal volume of sample and 4X Laemmli buffer loaded into well

Figure 7.2. ***Inhibiting glycosylation resulted in alterations in the appearance of the additional PACT band .*** **A.** A western immunoblot assessment of β-Actin and PACT in RAW 264.7 cells following inhibitor treatment and stimulation with LPS (100 ng/mL) for 24 h. Representative n1 of n = 3 biological replicates/group. **B.** Figure legend for the inhibitor treatment study.

Through modulation of eIF4E, the MNK1/MNK2 and mTOR signalling pathways control selective mRNA translation, allowing proteomic changes to occur without alterations in transcript levels (Bartish *et al.*, 2020). The eIF4F complex is a central regulator of translation initiation and is primarily controlled through its cap-binding subunit eIF4E. The mTOR signalling pathway promotes eIF4F assembly by phosphorylating eIF4E-binding proteins, while MNK1/2-mediated phosphorylation of eIF4E further modulates its activity and has been linked to tumour progression. Together, these mechanisms selectively regulate the translation of specific mRNA subsets, altering protein expression without changes in transcript abundance (**Figure 7.3**) (Sonenberg and Hinnebusch, 2009; Konicek *et al.*, 2011; Robichaud *et al.*, 2015; Robichaud *et al.*, 2018; Zhan *et al.*, 2017).

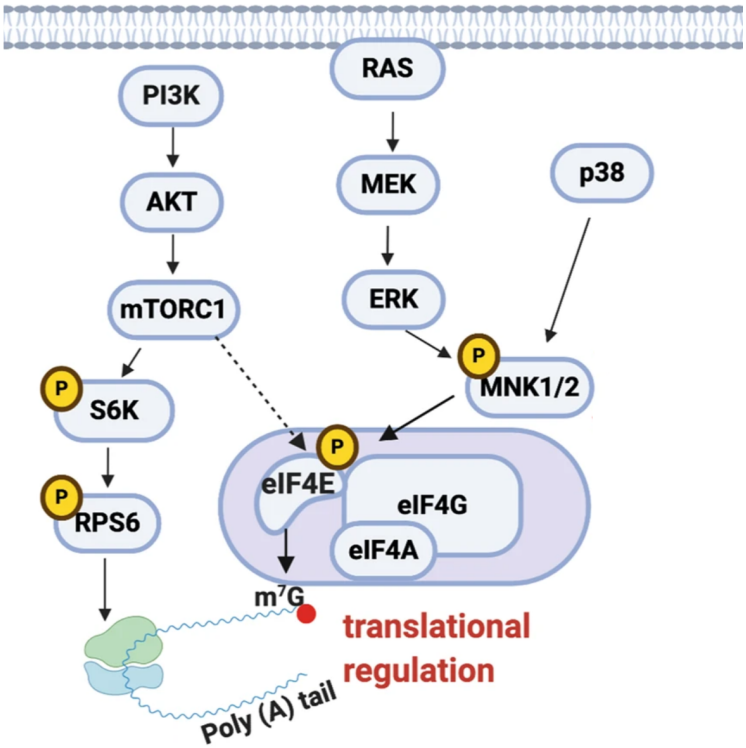

Figure 7.3. ***Overview of MNK1/2 signalling.***

Studies have reported selective changes in mRNA translation in pro-inflammatory macrophages following LPS and IFN stimulation. These have been attributed to mTOR- and MNK1/2-dependent signalling (Xu *et al.*, 2012; Schott *et al.*, 2014; William *et al.*, 2019; Su *et al.*, 2015b).

Moreover, tumour-associated macrophages (TAMs) have been observed to utilise this pathway to adopt their pro-tumour phenotype. During tumour growth, gene expression in TAMs is predominantly regulated through selective mRNA translation and is associated with increased eIF4E phosphorylation. Inhibition of MNK2, but not mTOR signalling, reprograms anti-inflammatory macrophages toward a pro-inflammatory phenotype, with the ability to activate $CD8^+$ T cells (Bartish *et al.*, 2020). In human pancreatic and thyroid tumours, it was shown that MNK inhibitors promote the immunosuppressive functions of TAMs, resulting in a $CD8^+$ T cell exhaustion phenotype (Pham *et al.*, 2022). Furthermore, MNK1 knockout macrophages exhibited increased capacity for phagocytosis and clearance of *Vibrio vulnificus* (Lou et al., 2024).

MiRNAs play a significant role in regulating gene expression by targeting mRNA. However, their ability to control eIF4E and its phosphorylation remain relatively unclear. Work has shown that eIF4E and its binding proteins, 4E-BPs, are targets of *miR-483-5p*. This miRNA reduced ERK1, MKNK1 and the level of phosphorylated eIF4E (Nagaraj *et al.*, 2024). Similarly, *miR-223* possess binding partners that are associated with translational control, namely eIF4E3 and MKNK2 (**Figure 7.4**). This suggests a potential role for *miR-223* in regulating translation.

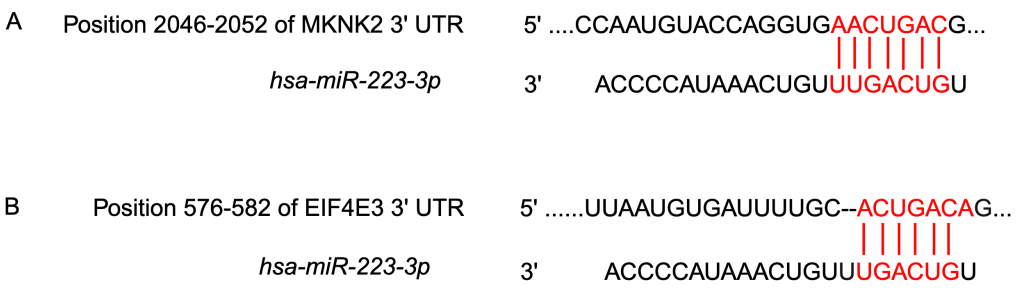

Figure 7.4. MKNK2 and EIF4E3 are binding partners of hsa-miR-223-3p. Predicted consequential pairing of target and *hsa-miR-223-3p.*

Tomivosertib (eFT508) is a highly selective MNK1 and MNK2 inhibitor, that leads to a reduction in eIF4E phosphorylation at serine 209. It has be reported to decrease p-eIF4E levels in mouse pancreatic and thyroid tumours *in vivo*. Combination therapy of tomivosertib and anti-PD-1 immunotherapy increased specific intratumoral T cell subsets *in vivo* (Pham *et al.*, 2022). Additionally, tomivosertib downregulated the expression of PD-L1 and attenuated immunosuppressive effects of macrophages (Hu *et al.*, 2024).

Therefore, the overall aim of this work was to investigate the functional role of *miR-223* in the translational control of macrophages.

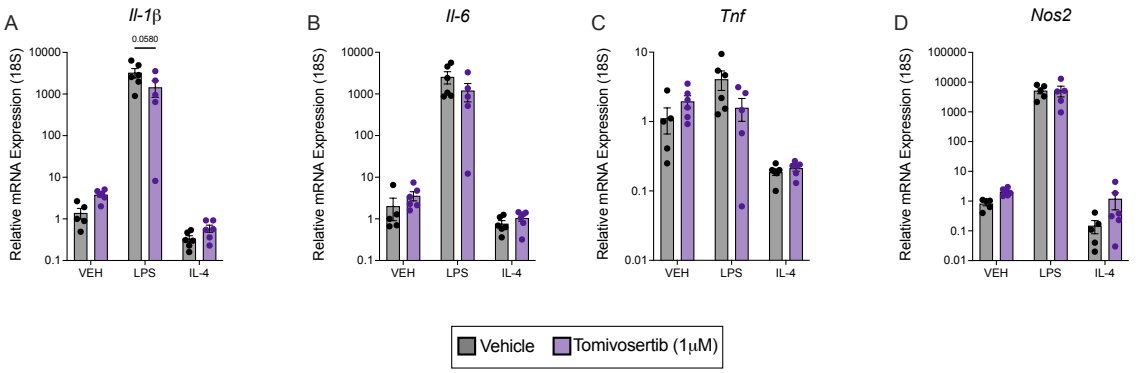

Figure 7.5. ***The effect of Tomivosertib treatment on pro-inflammatory cytokine production by activated macrophages.*** Relative mRNA expression of **A.** *Il-1β*, **B.** *Il-6*, **C.** *Tnf*, and **D.** *Nos2* in BMDMs, following 1 h pre-treatment with Tomivosertib (1 μM) and activation with LPS (100 ng/mL) or IL-4 (10 ng/mL) for 24 h. These were determined by RT-PCR from BMDMs from WT mice. All data is expressed as mean ± SEM; *, P ≤ 0.05; **, P ≤ 0.01, ***, P ≤ 0.001, ****, P ≤ 0.0001, versus the indicated counterpart (two-way ANOVA). n = 5-6 biological replicates/group.

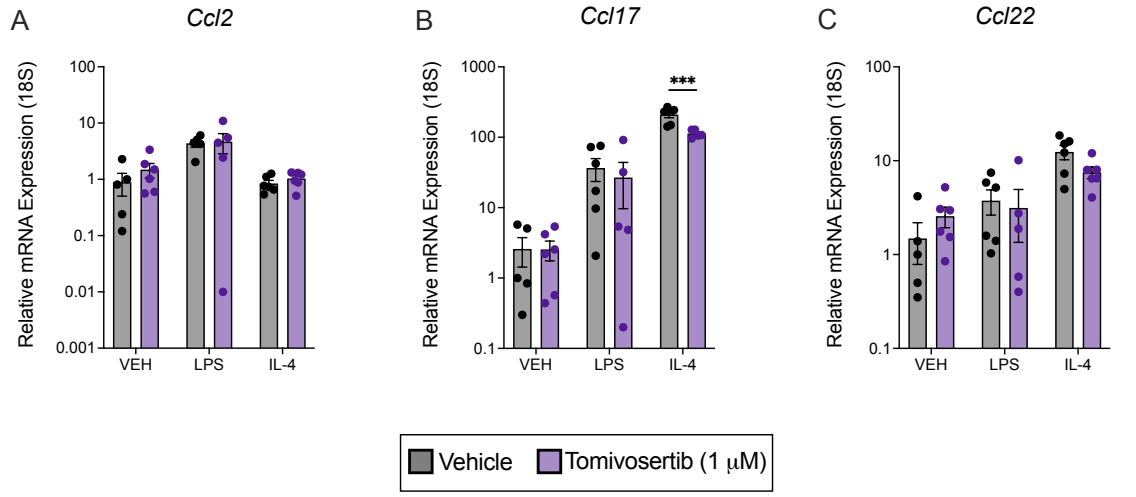

Figure 7.6. ***The effect of Tomivosertib treatment on immunosuppressive chemokine production by activated macrophages.*** Relative mRNA expression of **A.** *Ccl2*, **B.** *Tnf and* **C.** *Ccl22* in BMDMs, following 1 h pre-treatment with Tomivosertib (1 μM) and activation with LPS (100 ng/mL) or IL-4 (10 ng/mL) for 24 h. These were determined by RT-PCR from BMDMs from WT mice. All data is expressed as mean ± SEM; *, P ≤ 0.05; **, P ≤ 0.01, ***, P ≤ 0.001, ****, P ≤ 0.0001, versus the indicated counterpart (two-way ANOVA). n = 5-6 biological replicates/group.

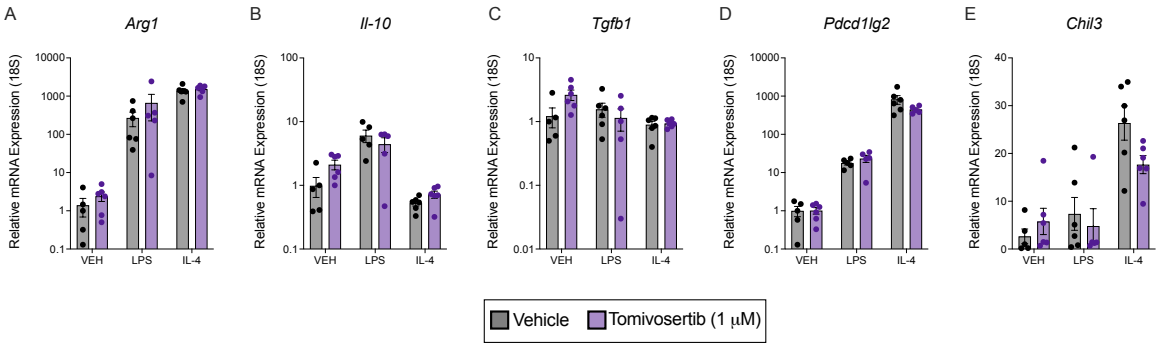

Figure 7.7. ***The effect of Tomivosertib treatment on anti-inflammatory cytokine production by activated macrophages.*** Relative mRNA expression of **A.** *Arg1*, **B.** *Il-10,* **C.** *Tgfb1*, **D.** *Pdcd1lg2* and **E.** *Chil3* in BMDMs, following 1 h pre-treatment with Tomivosertib (1 μM) and activation with LPS (100 ng/mL) or IL-4 (10 ng/mL) for 24 h. These were determined by RT-PCR from BMDMs from WT mice. All data is expressed as mean ± SEM; *, P ≤ 0.05; **, P ≤ 0.01, ***, P ≤ 0.001, ****, P ≤ 0.0001, versus the indicated counterpart (two-way ANOVA). n = 5-6 biological replicates/group.

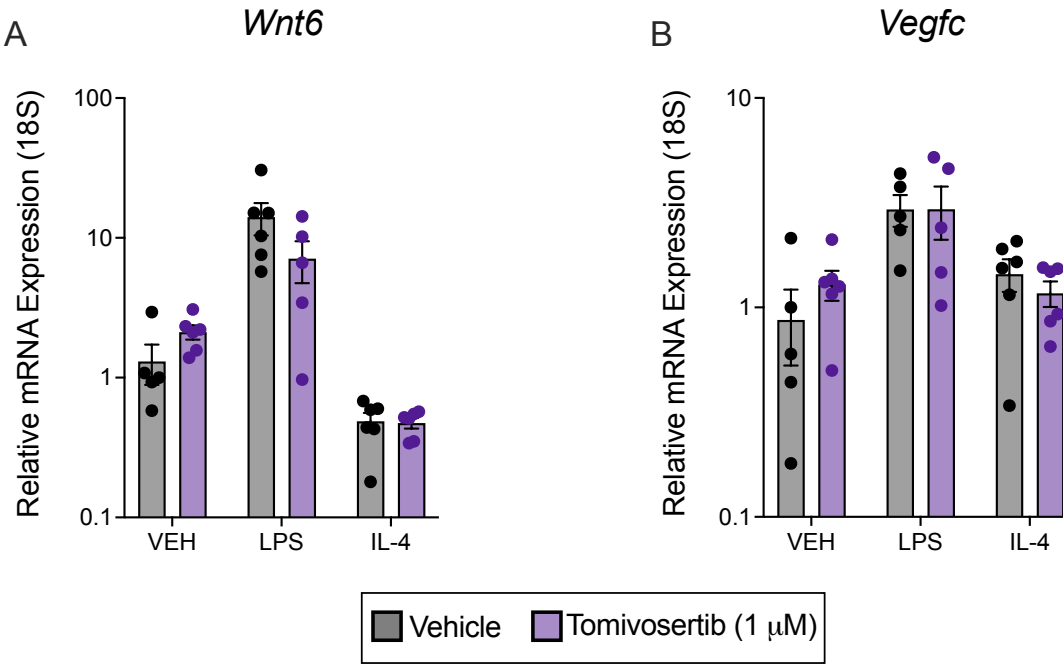

Figure 7.8. ***The effect of Tomivosertib treatment on growth factor production by activated macrophages.*** Relative mRNA expression of **A.** *Wnt6*, and **B.** *Vegfc* in BMDMs, following 1 h pre-treatment with Tomivosertib (1 μM) and activation with LPS (100 ng/mL) or IL-4 (10 ng/mL) for 24 h. These were determined by RT-PCR from BMDMs from WT mice. All data is expressed as mean ± SEM; *, P ≤ 0.05; **, P ≤ 0.01, ***, P ≤ 0.001, ****, P ≤ 0.0001, versus the indicated counterpart (two-way ANOVA). n = 5-6 biological replicates/group.

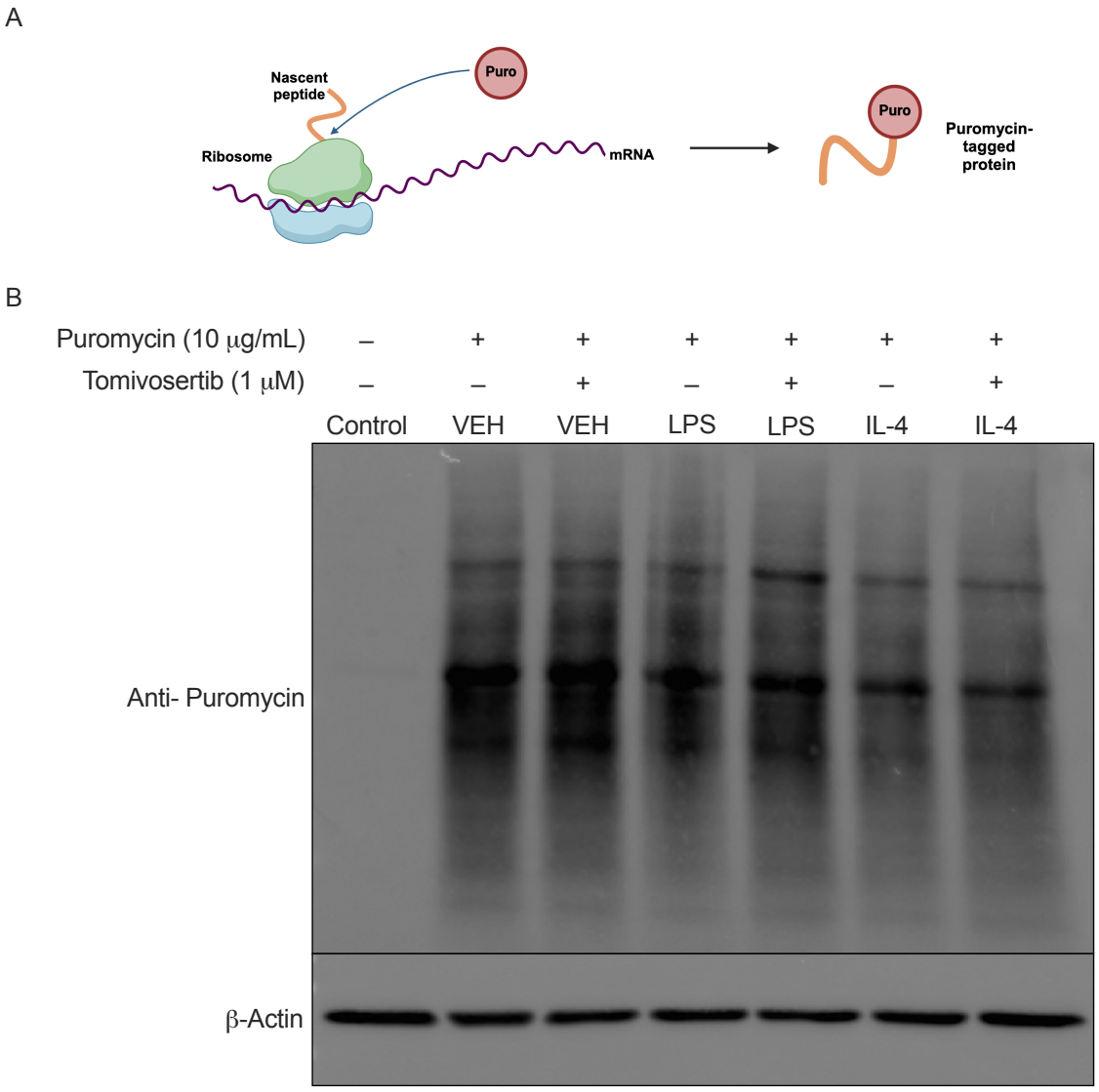

Figure 7.9. ***Treatment with Tomivosertib alters protein translation in LPS-induced activated macrophage.*** **A.** Overview of Surface Sensing of Translation (SUnSET) assay used to measure mRNA translation. **B.** A western immunoblot assessment of β-Actin and anti-puromycin in BMDMs following 1 h pre-treatment with Tomivosertib (1 μM) and stimulation with LPS (100 ng/mL) or IL-4 (10 ng/mL) for 24 h. Representative n1 of n = 5 biological replicates/group.

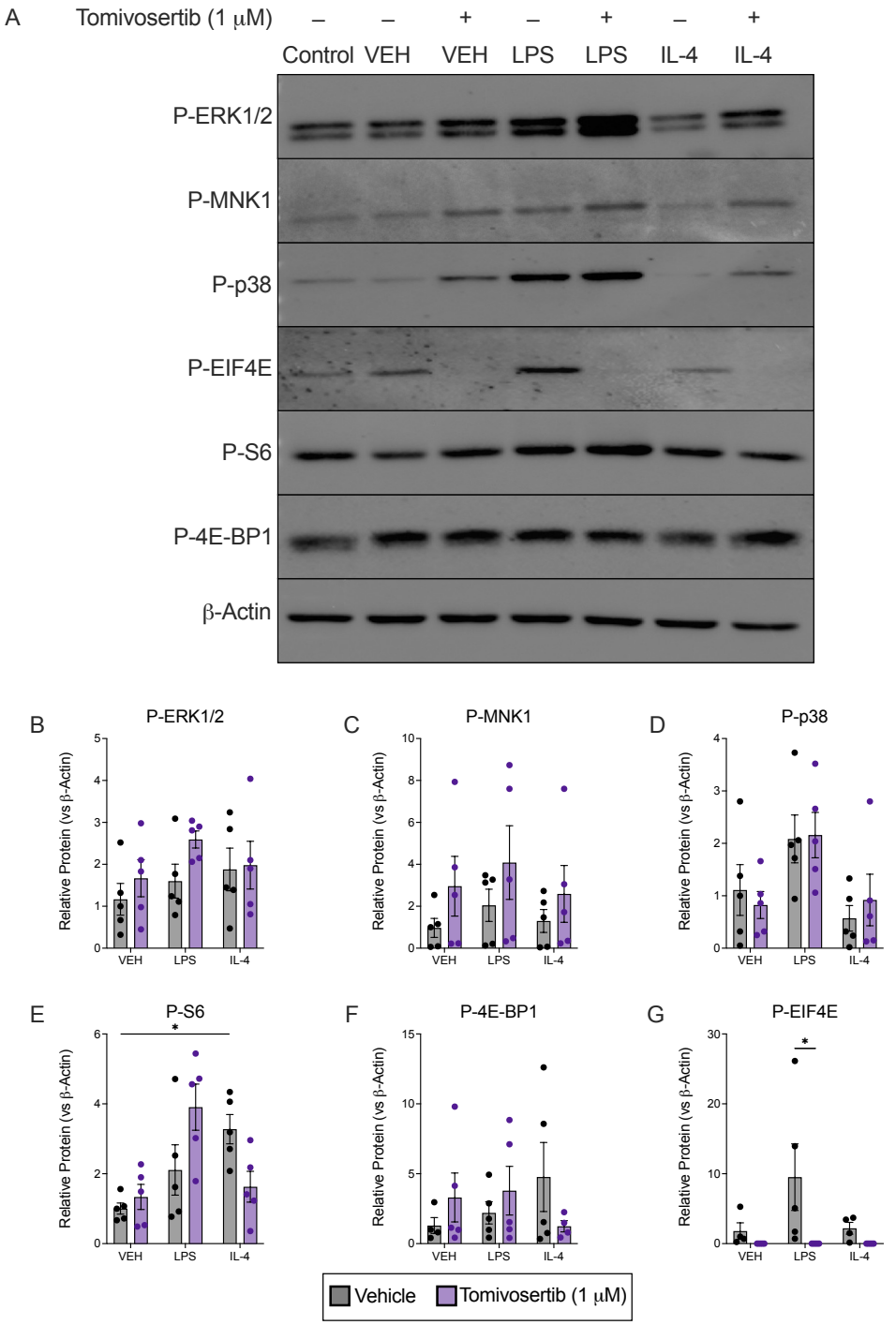

Figure 7.10. *P-EIF4E, a mediator of protein translation, is decreased in LPS-activated macrophages following inhibition of MNK1 and MNK2 with Tomivosertib.* **A.** A western immunoblot assessment of β-Actin, P-4E-BP1, P-S6, P-EIF4E, P-p38, P-MNK1 and P-ERK1/2 in BMDMs following 1 h pre-treatment with Tomivosertib (1 μM) and stimulation with LPS (100 ng/mL) or IL-4 (10 ng/mL) for 24 h. Representative n1 of n = 5 biological replicates/group. Western immunoblots were analysed via densitometry for **B.** P-ERK1/2, **C.** P-MNK1, **D.** P-p38, E. P-S6, **F.** P-4EBP1 and **G.** P-EIF4E. All data is expressed as mean ± SEM; *, P ≤ 0.05; **, P ≤ 0.01, ***, P ≤ 0.001, ****, P ≤ 0.0001, versus the indicated counterpart (two-way ANOVA). n = 5 biological replicates/group.

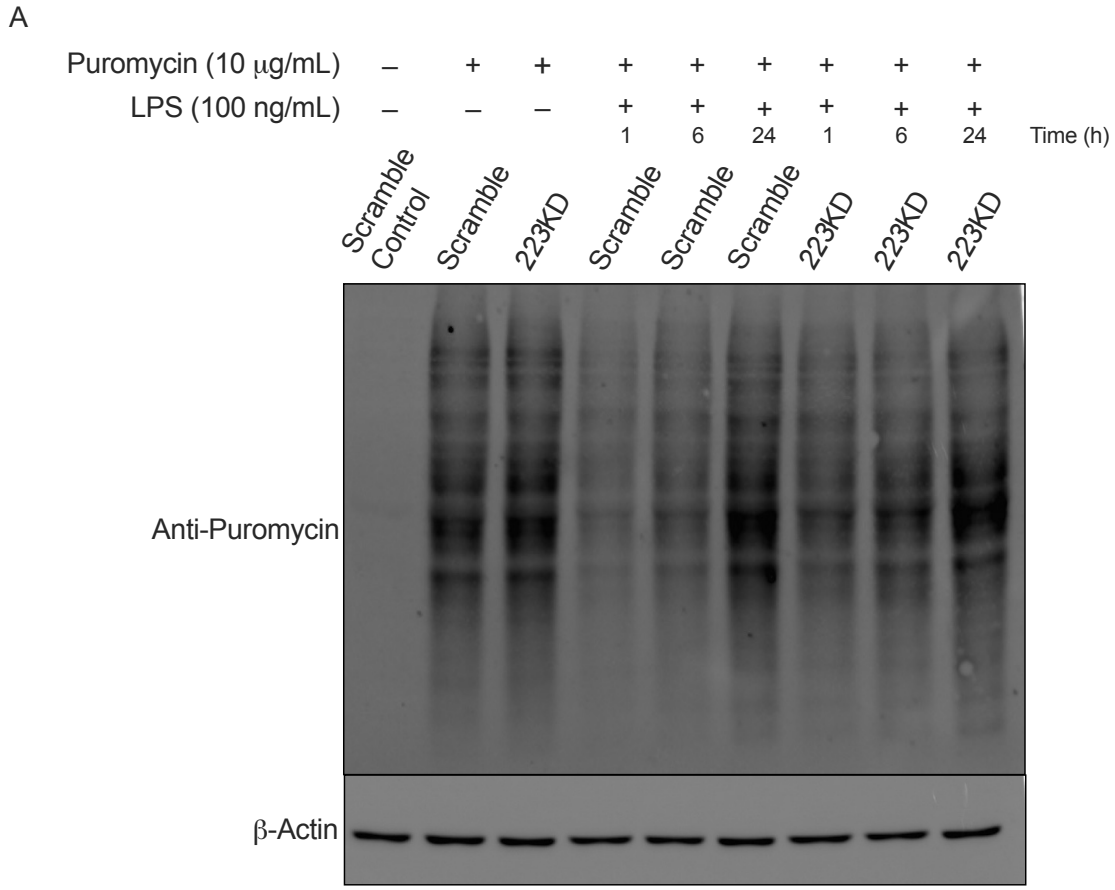

Figure 7.11. ***Protein translation is higher in activated miR-223KD macrophage following acute and pro-longed stimulation with LPS.*** **A.** A western immunoblot assessment of β-Actin and anti-puromycin in Scramble inhibitor versus *miR-223KD* RAW 264.7 cell lines following stimulation with LPS (100 ng/mL) for 1 h, 6 h and 24 h. Representative n1 of n = 3 biological replicates/group.

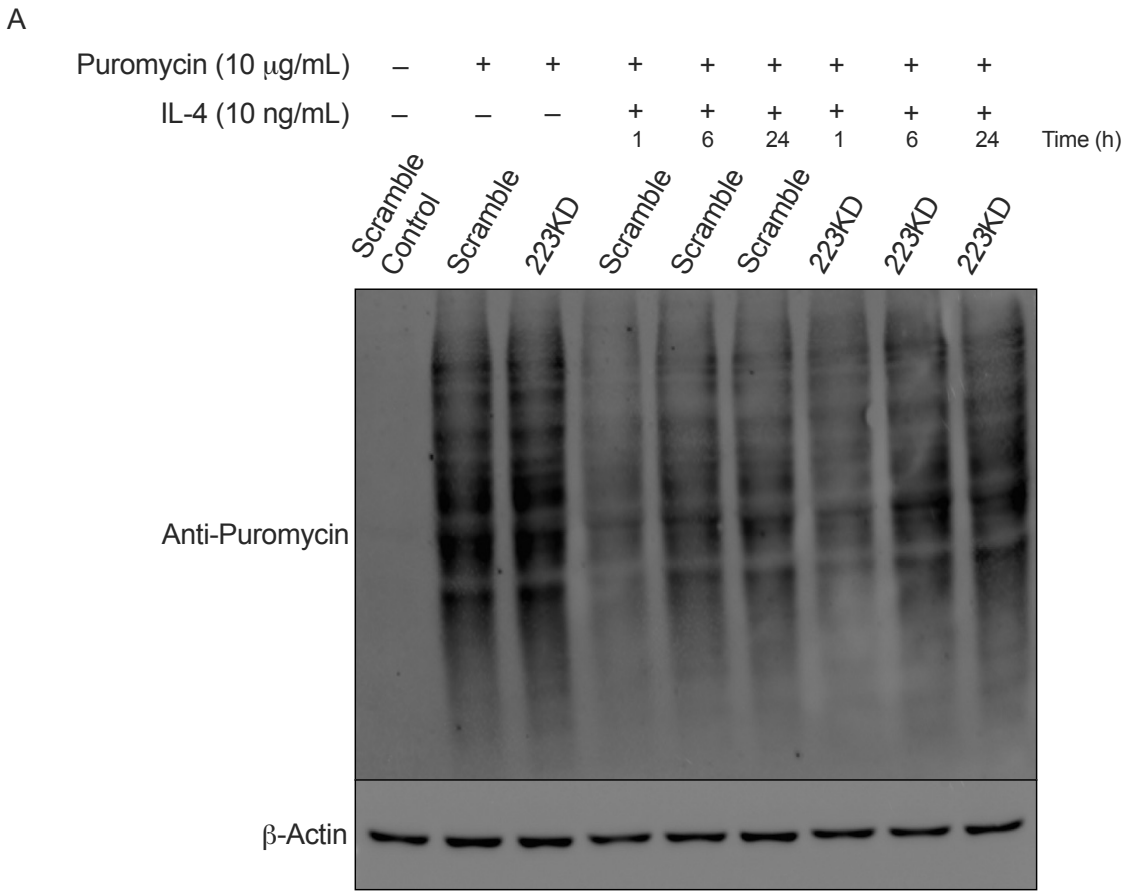

Figure 7.12. ***Protein translation is higher in activated miR-223KD macrophage following acute and pro-longed stimulation with IL-4.*** **A.** A western immunoblot assessment of β-Actin and anti-puromycin in Scramble inhibitor versus *miR-223KD* RAW 264.7 cell lines following stimulation with IL-4 (10 ng/mL) for 1 h, 6 h and 24 h. Representative n1 of n = 3 biological replicates/group.

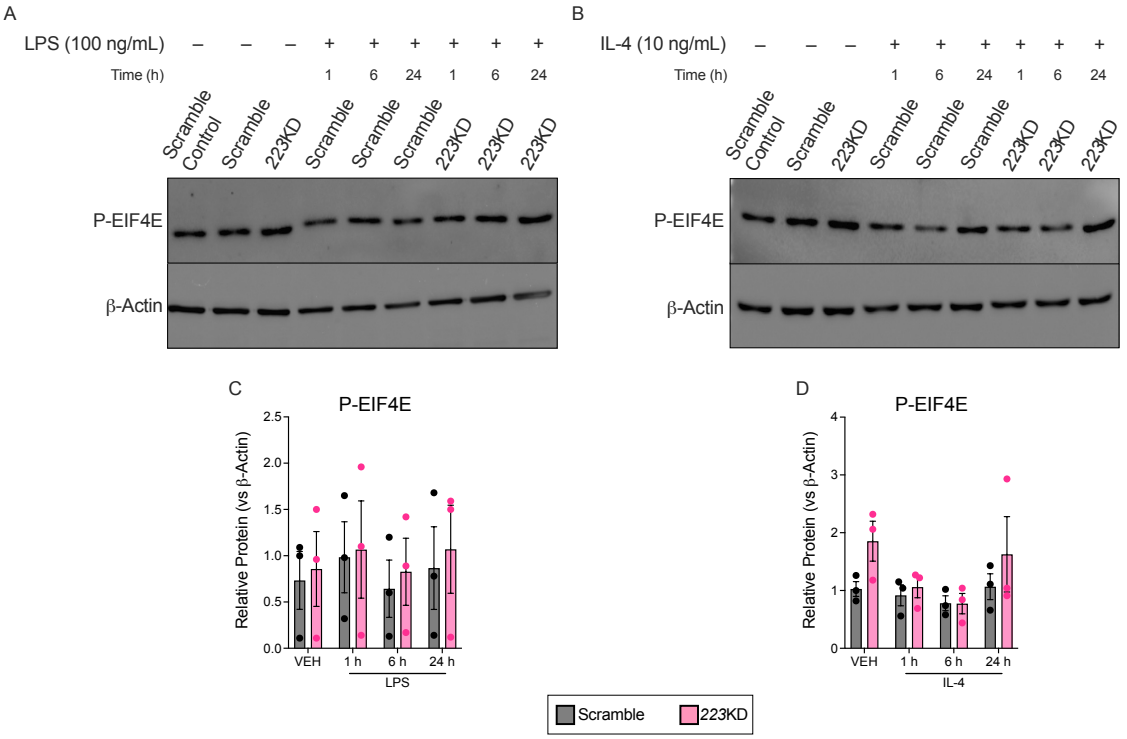

Figure 7.13. ***Protein expression of P-EIF4E is higher in activated miR-223KD macrophage following acute and pro-longed stimulation with LPS or IL-4.*** **A.** A western immunoblot assessment of β-Actin and P-EIF4E in Scramble inhibitor control cell line versus miR-223KD cell line following stimulation with LPS (100 ng/mL) for 1 h, 6 h and 24 h. **B.** A western immunoblot assessment of β-Actin and P-EIF4E in Scramble inhibitor versus *miR-223KD* RAW 264.7 cell lines following stimulation with IL-4 (10 ng/mL) for 1 h, 6 h and 24 h. Representative n1 of n = 3 biological replicates/group. Western immunoblots were analysed via densitometry for **C.** P-EIF4E following stimulation with LPS (100 ng/mL) for 1 h, 6 h and 24 h and **D.** P-EIF4E following stimulation with IL-4 (10 ng/mL for 1h, 6 h and 24 h. All data is expressed as mean ± SEM; *, P ≤ 0.05; **, P ≤ 0.01, ***, P ≤ 0.001, ****, P ≤ 0.0001, versus the indicated counterpart (two-way ANOVA). n = 3 biological replicates/group.

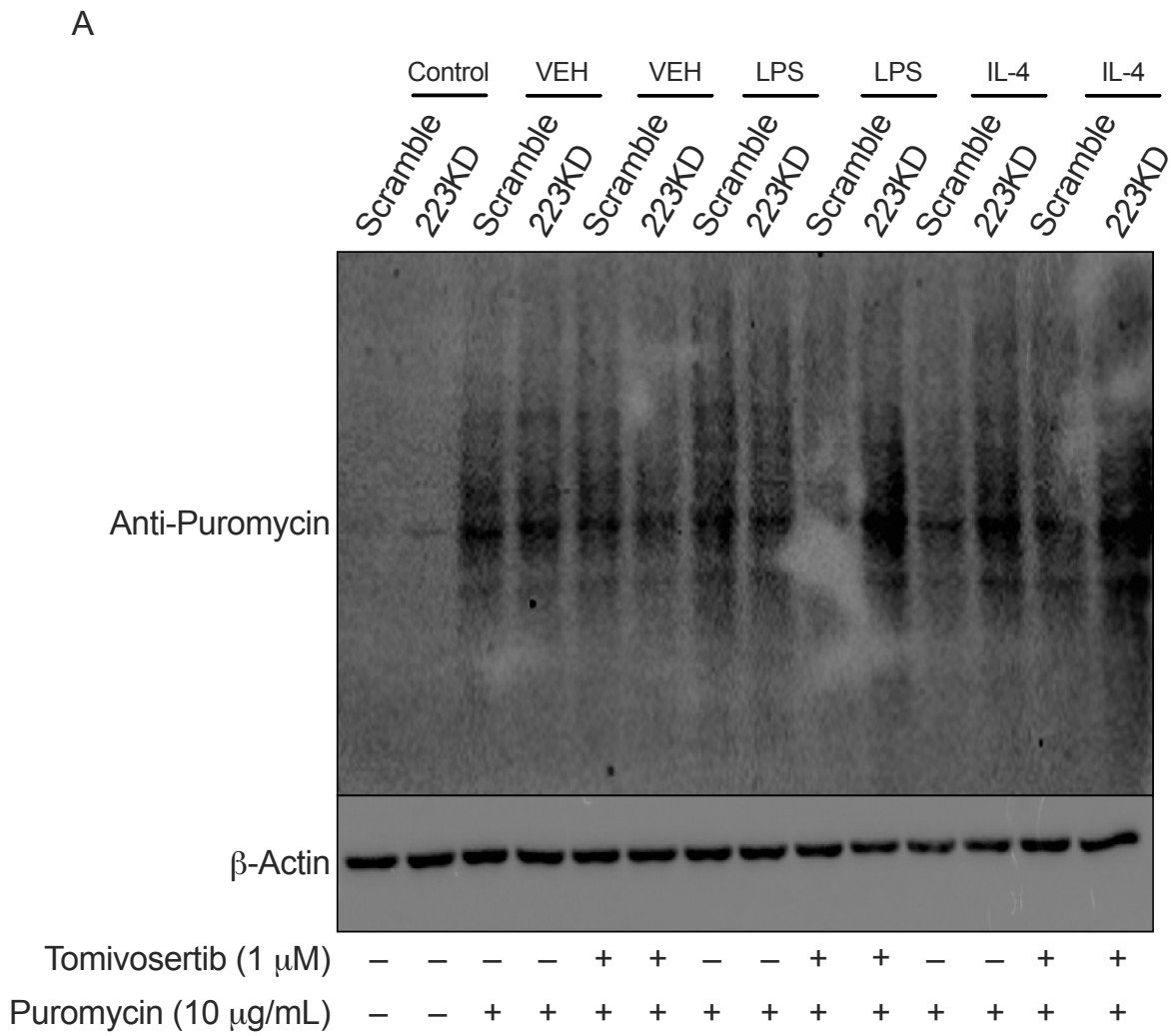

Figure 7.14. ***Inhibition of MNK1 and MNK2 with Tomivosertib, alters protein translation in activated miR-223KD macrophage.*** **A.** A western immunoblot assessment of β-Actin and anti-puromycin in Scramble inhibitor versus *miR-223KD* RAW 264.7 cell lines following 1 h pre-treatment with Tomivosertib (1 μM) and stimulation with LPS (100 ng/mL) or IL-4 (10 ng/mL) for 6 h. Representative n1 of n = 3 biological replicates/group.

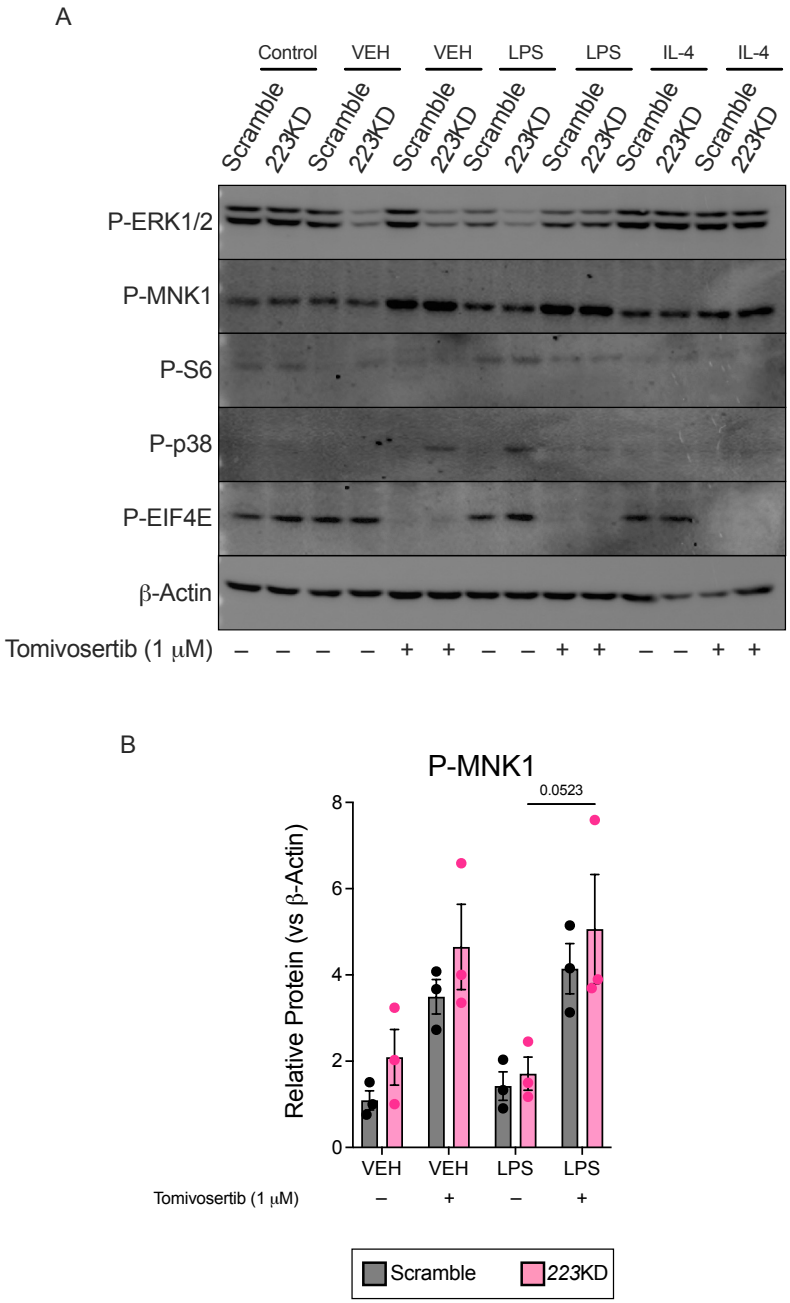

Figure 7.15. ***Targets associated with mediating protein translation are altered in activated miR-223KD macrophage, following inhibition of MNK1 and MNK2 with Tomivosertib.*** **A.** A western immunoblot assessment of β-Actin, P-EIF4E, P-S6, P-EIF4E, P-p38, P-MNK1 and P-ERK1/2 in Scramble inhibitor versus *miR-223KD* RAW 264.7 cell lines following 1 h pre-treatment with Tomivosertib (1 μM) and stimulation with LPS (100 ng/mL) or IL-4 (10 ng/mL) for 6 h. Representative n1 of n = 2-3 biological replicates/group. Western immunoblot was analysed via densitometry for **B.** P-MNK1. All data is expressed as mean ± SEM; *, P ≤ 0.05; **, P ≤ 0.01, ***, P ≤ 0.001, ****, P ≤ 0.0001, versus the indicated counterpart (two-way ANOVA). n = 3 biological replicates/group.

CHAPTER 8

BIBLIOGRAPHY

BIBLIOGRAPHY

Ahmed, A. T., Oghenemaro, E. F., Hjazi, A., Jain, V., Ahmad, I., Roopashree, R., Soothwal, P., Goswami, M., Zwamel, A. H. and Kdhim, K. (2025) 'The Significance of STAT3 in Colonic Diseases: A Comprehensive Study of Pathological Roles and Therapeutic Implications', *Cell Biochem Biophys,* 83(4), pp. 4097-4120.

Alatab, S., Sepanlou, S. G., Ikuta, K., Vahedi, H., Bisignano, C., Safiri, S., Sadeghi, A., Nixon, M. R., Abdoli, A., Abolhassani, H., Alipour, V., Almadi, M. A. H., Almasi-Hashiani, A., Anushiravani, A., Arabloo, J., Atique, S., Awasthi, A., Badawi, A., Baig, A. A. A., ... and Naghavi, M. (2020) 'The global, regional, and national burden of inflammatory bowel disease in 195 countries and territories, 1990–2017: a systematic analysis for the Global Burden of Disease Study 2017', *The Lancet Gastroenterology & Hepatology,* 5(1), pp. 17-30.

Alfaifi, J., Germain, A., Heba, A.-C., Arnone, D., Gailly, L., Ndiaye, N. C., Viennois, E., Caron, B., Peyrin-Biroulet, L. and Dreumont, N. (2023) 'Deep Dive Into MicroRNAs in Inflammatory Bowel Disease', *Inflammatory Bowel Diseases,* 29(6), pp. 986-999.

Ali, A., Grillone, K., Ascrizzi, S., Caridà, G., Fiorillo, L., Ciliberto, D., Staropoli, N., Tagliaferri, P., Tassone, P. and Di Martino, M. T. (2024) 'LNA-i-miR-221 activity in colorectal cancer: A reverse translational investigation', *Mol Ther Nucleic Acids,* 35(2), pp. 102221.

Alipour, M., Zaidi, D., Valcheva, R., Jovel, J., Martínez, I., Sergi, C., Walter, J., Mason, A. L., Wong, G. K., Dieleman, L. A., Carroll, M. W., Huynh, H. Q. and Wine, E. (2016) 'Mucosal Barrier Depletion and Loss of Bacterial Diversity are Primary Abnormalities in Paediatric Ulcerative Colitis', *J Crohns Colitis,* 10(4), pp. 462-71.

Alles, J., Fehlmann, T., Fischer, U., Backes, C., Galata, V., Minet, M., Hart, M., Abu-Halima, M., Grässer, F. A., Lenhof, H. P., Keller, A. and Meese, E. (2019) 'An estimate of the total number of true human miRNAs', *Nucleic Acids Res,* 47(7), pp. 3353-3364.

Anderson, C. A., Boucher, G., Lees, C. W., Franke, A., D'Amato, M., Taylor, K. D., Lee, J. C., Goyette, P., Imielinski, M., Latiano, A., Lagacé, C., Scott, R., Amininejad, L., Bumpstead, S., Baidoo, L., Baldassano, R. N., Barclay, M., Bayless, T. M., Brand, S., ... and Rioux, J. D. (2011) 'Meta-analysis identifies 29 additional ulcerative colitis risk loci, increasing the number of confirmed associations to 47', *Nature Genetics,* 43(3), pp. 246-252.

Asano, K., Takahashi, N., Ushiki, M., Monya, M., Aihara, F., Kuboki, E., Moriyama, S., Iida, M., Kitamura, H., Qiu, C. H., Watanabe, T. and Tanaka, M. (2015) 'Intestinal CD169(+) macrophages initiate mucosal inflammation by secreting CCL8 that recruits inflammatory monocytes', *Nat Commun,* 6, pp. 7802.

Atreya, R., Mudter, J., Finotto, S., Müllberg, J., Jostock, T., Wirtz, S., Schütz, M., Bartsch, B., Holtmann, M., Becker, C., Strand, D., Czaja, J., Schlaak, J. F., Lehr, H. A., Autschbach, F., Schürmann, G., Nishimoto, N., Yoshizaki, K., Ito, H., ... and Neurath, M. F. (2000) 'Blockade of interleukin 6 trans signaling suppresses T-cell resistance against apoptosis in chronic intestinal inflammation: evidence in crohn disease and experimental colitis in vivo', *Nat Med,* 6(5), pp. 583-8.

Attaway, M., Chwat-Edelstein, T. and Vuong, B. Q. (2021) 'Regulatory Non-Coding RNAs Modulate Transcriptional Activation During B Cell Development', *Front Genet,* 12, pp. 678084.

Baer, C., Squadrito, M. L., Laoui, D., Thompson, D., Hansen, S. K., Kiialainen, A., Hoves, S., Ries, C. H., Ooi, C.-H. and De Palma, M. (2016) 'Suppression of microRNA activity amplifies IFN-γ-induced macrophage activation and promotes anti-tumour immunity', *Nature Cell Biology,* 18(7), pp. 790-802.

Bai, J., Wang, Y., Li, F., Wu, Y., Chen, J., Li, M., Wang, X. and Lv, B. (2024) 'Research advancements and perspectives of inflammatory bowel disease: A comprehensive review', *Sci Prog,* 107(2), pp. 368504241253709.

Baillie, J. K., Arner, E., Daub, C., De Hoon, M., Itoh, M., Kawaji, H., Lassmann, T., Carninci, P., Forrest, A. R. R., Hayashizaki, Y., Faulkner, G. J., Wells, C. A., Rehli, M., Pavli, P., Summers, K. M. and Hume, D. A. (2017) 'Analysis of the human monocyte-derived macrophage transcriptome and response to lipopolysaccharide provides new insights into genetic aetiology of inflammatory bowel disease', *PLOS Genetics,* 13(3), pp. e1006641.

Bain, C. C., Bravo-Blas, A., Scott, C. L., Gomez Perdiguero, E., Geissmann, F., Henri, S., Malissen, B., Osborne, L. C., Artis, D. and Mowat, A. M. (2014) 'Constant replenishment from circulating monocytes maintains the macrophage pool in the intestine of adult mice', *Nature Immunology,* 15(10), pp. 929-937.

Bain, C. C., Scott, C. L., Uronen-Hansson, H., Gudjonsson, S., Jansson, O., Grip, O., Guilliams, M., Malissen, B., Agace, W. W. and Mowat, A. M. (2013) 'Resident and pro-inflammatory macrophages in the colon represent alternative context-dependent fates of the same Ly6Chi monocyte precursors', *Mucosal Immunology,* 6(3), pp. 498-510.

Balmus, I. M., Ciobica, A., Trifan, A. and Stanciu, C. (2016) 'The implications of oxidative stress and antioxidant therapies in Inflammatory Bowel Disease: Clinical aspects and animal models', *Saudi J Gastroenterol,* 22(1), pp. 3-17.

Baron, J. H., Connell, A. M., Lennard-Jones, J. E. and Jones, F. A. (1962) 'Sulphasalazine and salicylazosulphadimidine in ulcerative colitis', *Lancet,* 1(7239), pp. 1094-6.

Bartish, M., Tong, D., Pan, Y., Wallerius, M., Liu, H., Ristau, J., de Souza Ferreira, S., Wallmann, T., van Hoef, V., Masvidal, L., Kerzel, T., Joly, A.-L., Goncalves, C., Preston, S. E. J., Ebrahimian, T., Seitz, C., Bergh, J., Pietras, K., Lehoux, S., ... and Rolny, C. (2020) 'MNK2 governs the macrophage antiinflammatory phenotype', *Proceedings of the National Academy of Sciences,* 117(44), pp. 27556-27565.

Bauernfeind, F., Rieger, A., Schildberg, F. A., Knolle, P. A., Schmid-Burgk, J. L. and Hornung, V. (2012) 'NLRP3 Inflammasome Activity Is Negatively Controlled by miR-223', *The Journal of Immunology,* 189(8), pp. 4175-4181.

Becker, H. E. F., Demers, K., Derijks, L. J. J., Jonkers, D. M. A. E. and Penders, J. (2023) 'Current evidence and clinical relevance of drug-microbiota interactions in inflammatory bowel disease', *Frontiers in Microbiology,* Volume 14 - 2023.

Beigel, F., Friedrich, M., Probst, C., Sotlar, K., Göke, B., Diegelmann, J. and Brand, S. (2014) 'Oncostatin M Mediates STAT3-Dependent Intestinal Epithelial Restitution via Increased Cell Proliferation, Decreased Apoptosis and Upregulation of SERPIN Family Members', *PLOS ONE,* 9(4), pp. e93498.

Berg, D. R., Colombel, J. F. and Ungaro, R. (2019) 'The Role of Early Biologic Therapy in Inflammatory Bowel Disease', *Inflamm Bowel Dis,* 25(12), pp. 1896-1905.

Berger, J. R. and Koralnik, I. J. (2005) 'Progressive multifocal leukoencephalopathy and natalizumab--unforeseen consequences', *N Engl J Med: Vol. 4*. United States, pp. 414-6.

Beumer, J. and Clevers, H. (2021) 'Cell fate specification and differentiation in the adult mammalian intestine', *Nature Reviews Molecular Cell Biology,* 22(1), pp. 39-53.

Biton, M., Haber, A. L., Rogel, N., Burgin, G., Beyaz, S., Schnell, A., Ashenberg, O., Su, C. W., Smillie, C., Shekhar, K., Chen, Z., Wu, C., Ordovas-Montanes, J., Alvarez, D., Herbst, R. H., Zhang, M., Tirosh, I., Dionne, D., Nguyen, L. T., ... and Xavier, R. J. (2018) 'T Helper Cell Cytokines Modulate Intestinal Stem Cell Renewal and Differentiation', *Cell,* 175(5), pp. 1307-1320.e22.

Blériot, C., Chakarov, S. and Ginhoux, F. (2020) 'Determinants of Resident Tissue Macrophage Identity and Function', *Immunity,* 52(6), pp. 957-970.

Boneschansker, L. and Ananthakrishnan, A. N. (2023) 'Comparative Effectiveness of Upadacitinib and Tofacitinib in Inducing Remission in Ulcerative Colitis: Real-World Data', *Clin Gastroenterol Hepatol,* 21(9), pp. 2427-2429.e1.

Bronevetsky, Y., Villarino, A. V., Eisley, C. J., Barbeau, R., Barczak, A. J., Heinz, G. A., Kremmer, E., Heissmeyer, V., Mcmanus, M. T., Erle, D. J., Rao, A. and Ansel, K. M. (2013) 'T cell activation induces proteasomal degradation of Argonaute and rapid remodeling of the microRNA repertoire', *Journal of Experimental Medicine,* 210(2), pp. 417-432.

Buchner, A. M., Farraye, F. A. and Iacucci, M. (2024) 'AGA Clinical Practice Update on Endoscopic Scoring Systems in Inflammatory Bowel Disease: Commentary', *Clinical Gastroenterology and Hepatology,* 22(11), pp. 2188-2196.

Cai, B., Kasikara, C., Doran, A. C., Ramakrishnan, R., Birge, R. B. and Tabas, I. (2018) 'MerTK signaling in macrophages promotes the synthesis of inflammation

resolution mediators by suppressing CaMKII activity', *Science Signaling,* 11(549), pp. eaar3721.

Caprilli, R., Viscido, A. and Latella, G. (2007) 'Current management of severe ulcerative colitis', *Nat Clin Pract Gastroenterol Hepatol,* 4(2), pp. 92-101.

Cattaneo, C. M., Dijkstra, K. K., Fanchi, L. F., Kelderman, S., Kaing, S., Van Rooij, N., Van Den Brink, S., Schumacher, T. N. and Voest, E. E. (2020) 'Tumor organoid–T-cell coculture systems', *Nature Protocols,* 15(1), pp. 15-39.

Chassaing, B., Aitken, J. D., Malleshappa, M. and Vijay-Kumar, M. (2014) 'Dextran sulfate sodium (DSS)-induced colitis in mice', *Curr Protoc Immunol,* 104, pp. 15.25.1-15.25.14.

Cheah, E. and Huang, J. G. (2023) 'Precision medicine in inflammatory bowel disease: Individualizing the use of biologics and small molecule therapies', *World J Gastroenterol,* 29(10), pp. 1539-1550.

Chen, C. Z., Li L Fau - Lodish, H. F., Lodish Hf Fau - Bartel, D. P. and Bartel, D. P. 'MicroRNAs modulate hematopoietic lineage differentiation', (1095-9203 (Electronic)).

Chen, P. S., Su, J. L. and Hung, M. C. (2012) 'Dysregulation of microRNAs in cancer', *J Biomed Sci,* 19(1), pp. 90.

Chen, Q., Wang, H., Liu, Y., Song, Y., Lai, L., Han, Q., Cao, X. and Wang, Q. (2012) 'Inducible microRNA-223 down-regulation promotes TLR-triggered IL-6 and IL-1β production in macrophages by targeting STAT3', *PLoS One,* 7(8), pp. e42971.

Chen, S., Qin, Z., Lin, X., Zhou, S., Xu, Y. and Zhu, Y. (2025) 'Macrophages: emerging targets for ulcerative colitis', *Frontiers in Immunology,* Volume 16 - 2025.

Chen, S., Saeed, A. F. U. H., Liu, Q., Jiang, Q., Xu, H., Xiao, G. G., Rao, L. and Duo, Y. (2023) 'Macrophages in immunoregulation and therapeutics', *Signal Transduction and Targeted Therapy,* 8(1).

Chen, Z., Jiang, P., Su, D., Zhao, Y. and Zhang, M. (2024) 'Therapeutic inhibition of the JAK-STAT pathway in the treatment of inflammatory bowel disease', *Cytokine & Growth Factor Reviews,* 79, pp. 1-15.

Choi, J. and Augenlicht, L. H. (2024) 'Intestinal stem cells: guardians of homeostasis in health and aging amid environmental challenges', *Experimental & Molecular Medicine,* 56(3), pp. 495-500.

Chuang, A. Y., Chuang, J. C., Zhai, Z., Wu, F. and Kwon, J. H. (2014) 'NOD2 expression is regulated by microRNAs in colonic epithelial HCT116 cells', *Inflamm Bowel Dis,* 20(1), pp. 126-35.

Cosín-Roger, J., Ortiz-Masiá, D., Calatayud, S., Hernández, C., Esplugues, J. V. and Barrachina, M. D. (2016) 'The activation of Wnt signaling by a STAT6-dependent macrophage phenotype promotes mucosal repair in murine IBD', *Mucosal Immunology,* 9(4), pp. 986-998.

Crohn's and Colitis Ireland (2026) *Inflammatory Bowel Disease explained.* Available at: https://crohnscolitis.ie/support/diagnosis/explanation/.

Cronstein, B. N., Kimmel, S. C., Levin, R. I., Martiniuk, F. and Weissmann, G. (1992) 'A mechanism for the antiinflammatory effects of corticosteroids: the glucocorticoid receptor regulates leukocyte adhesion to endothelial cells and expression of endothelial-leukocyte adhesion molecule 1 and intercellular adhesion molecule 1', *Proceedings of the National Academy of Sciences,* 89(21), pp. 9991-9995.

Croxtall, J. D., Choudhury, Q. and Flower, R. J. (2000) 'Glucocorticoids act within minutes to inhibit recruitment of signalling factors to activated EGF receptors through a receptor-dependent, transcription-independent mechanism', *Br J Pharmacol,* 130(2), pp. 289-98.

Czarnewski, P., Parigi, S. M., Sorini, C., Diaz, O. E., Das, S., Gagliani, N. and Villablanca, E. J. (2019) 'Conserved transcriptomic profile between mouse and human colitis allows unsupervised patient stratification', *Nature Communications,* 10(1), pp. 2892.

Dalal, R. S., Sharma, P. P., Bains, K., Pruce, J. C. and Allegretti, J. R. (2024) 'Clinical and Endoscopic Outcomes Through 78 Weeks of Tofacitinib Therapy for Ulcerative Colitis in a US Cohort', *Inflamm Bowel Dis,* 30(10), pp. 1707-1713.

David, L. A., Maurice, C. F., Carmody, R. N., Gootenberg, D. B., Button, J. E., Wolfe, B. E., Ling, A. V., Devlin, A. S., Varma, Y., Fischbach, M. A., Biddinger, S. B., Dutton, R. J. and Turnbaugh, P. J. (2014) 'Diet rapidly and reproducibly alters the human gut microbiome', *Nature,* 505(7484), pp. 559-563.

de Lange, K. M., Moutsianas, L., Lee, J. C., Lamb, C. A., Luo, Y., Kennedy, N. A., Jostins, L., Rice, D. L., Gutierrez-Achury, J., Ji, S.-G., Heap, G., Nimmo, E. R., Edwards, C., Henderson, P., Mowat, C., Sanderson, J., Satsangi, J., Simmons, A., Wilson, D. C., ... and Barrett, J. C. (2017) 'Genome-wide association study implicates immune activation of multiple integrin genes in inflammatory bowel disease', *Nature Genetics,* 49(2), pp. 256-261.

De Schepper, S., Verheijden, S., Aguilera-Lizarraga, J., Viola, M. F., Boesmans, W., Stakenborg, N., Voytyuk, I., Schmidt, I., Boeckx, B., Dierckx de Casterlé, I., Baekelandt, V., Gonzalez Dominguez, E., Mack, M., Depoortere, I., De Strooper, B., Sprangers, B., Himmelreich, U., Soenen, S., Guilliams, M., ... and Boeckxstaens, G. (2018) 'Self-Maintaining Gut Macrophages Are Essential for Intestinal Homeostasis', *Cell,* 175(2), pp. 400-415.e13.

De Vries, L. C. S., Duarte, J. M., De Krijger, M., Welting, O., Van Hamersveld, P. H. P., Van Leeuwen-Hilbers, F. W. M., Moerland, P. D., Jongejan, A., D'Haens, G. R., De Jonge, W. J. and Wildenberg, M. E. (2019) 'A JAK1 Selective Kinase Inhibitor and Tofacitinib Affect Macrophage Activation and Function', *Inflamm Bowel Dis,* 25(4), pp. 647-660.

Deka, D., D'Incà, R., Sturniolo, G. C., Das, A., Pathak, S. and Banerjee, A. (2022) 'Role of ER Stress Mediated Unfolded Protein Responses and ER Stress Inhibitors in the Pathogenesis of Inflammatory Bowel Disease', *Dig Dis Sci,* 67(12), pp. 5392-5406.

Dhuppar, S. and Murugaiyan, G. (2022) 'miRNA effects on gut homeostasis: therapeutic implications for inflammatory bowel disease', *Trends in Immunology,* 43(11), pp. 917-931.

Di Martino, M. T., Arbitrio, M., Caracciolo, D., Cordua, A., Cuomo, O., Grillone, K., Riillo, C., Caridà, G., Scionti, F., Labanca, C., Romeo, C., Siciliano, M. A., D'Apolito, M., Napoli, C., Montesano, M., Farenza, V., Uppolo, V., Tafuni, M., Falcone, F., ... and Tassone, P. (2022) 'miR-221/222 as biomarkers and targets for therapeutic intervention on cancer and other diseases: A systematic review', *Mol Ther Nucleic Acids,* 27, pp. 1191-1224.

Di Martino, M. T., Rossi, M., Caracciolo, D., Gullà, A., Tagliaferri, P. and Tassone, P. (2016) 'Mir-221/222 are promising targets for innovative anticancer therapy', *Expert Opin Ther Targets,* 20(9), pp. 1099-108.

Dick, A. P., Grayson, M. J., Carpenter, R. G. and Petrie, A. (1964) 'Controlled trial of sulphasalazine in the treatment of ulcerative colitis', *Gut,* 5(5), pp. 437.

Dige, A., Støy, S., Thomsen, K. L., Hvas, C. L., Agnholt, J., Dahlerup, J. F., Møller, H. J. and Grønbæk, H. (2014) 'Soluble <scp>CD</scp>163, a Specific Macrophage Activation Marker, is Decreased by Anti-<scp>TNF</scp>-α Antibody Treatment in Active Inflammatory Bowel Disease', *Scandinavian Journal of Immunology,* 80(6), pp. 417-423.

Domanska, D., Majid, U., Karlsen, V. T., Merok, M. A., Beitnes, A.-C. R., Yaqub, S., Bækkevold, E. S. and Jahnsen, F. L. (2022) 'Single-cell transcriptomic analysis of human colonic macrophages reveals niche-specific subsets', *Journal of Experimental Medicine,* 219(3).

Dorhoi, A., Iannaccone, M., Farinacci, M., Faé, K. C., Schreiber, J., Moura-Alves, P., Nouailles, G., Mollenkopf, H.-J., Oberbeck-Müller, D., Jörg, S., Heinemann, E., Hahnke, K., Löwe, D., Del Nonno, F., Goletti, D., Capparelli, R. and Kaufmann, S. H. E. (2013) 'MicroRNA-223 controls susceptibility to tuberculosis by regulating lung neutrophil recruitment', *Journal of Clinical Investigation,* 123(11), pp. 4836-4848.

Drurey, C., Lindholm, H. T., Coakley, G., Poveda, M. C., Löser, S., Doolan, R., Gerbe, F., Jay, P., Harris, N., Oudhoff, M. J. and Maizels, R. M. (2022) 'Intestinal epithelial tuft cell induction is negated by a murine helminth and its secreted products', *J Exp Med,* 219(1).

Duffin, R., O'Connor, R. A., Crittenden, S., Forster, T., Yu, C., Zheng, X., Smyth, D., Robb, C. T., Rossi, F., Skouras, C., Tang, S., Richards, J., Pellicoro, A., Weller, R. B., Breyer, R. M., Mole, D. J., Iredale, J. P., Anderton, S. M., Narumiya, S., ... and Yao, C. (2016) 'Prostaglandin E_2 constrains systemic inflammation through an innate lymphoid cell-IL-22 axis', *Science,* 351(6279), pp. 1333-8.

Eichele, D. D. and Kharbanda, K. K. (2017) 'Dextran sodium sulfate colitis murine model: An indispensable tool for advancing our understanding of inflammatory bowel diseases pathogenesis', *World J Gastroenterol,* 23(33), pp. 6016-6029.

Faridani, O. R., Abdullayev, I., Hagemann-Jensen, M., Schell, J. P., Lanner, F. and Sandberg, R. (2016) 'Single-cell sequencing of the small-RNA transcriptome', *Nature Biotechnology,* 34(12), pp. 1264-1266.

Fazi, F., Rosa, A., Fatica, A., Gelmetti, V., De Marchis, M. L., Nervi, C. and Bozzoni, I. (2005) 'A Minicircuitry Comprised of MicroRNA-223 and Transcription Factors NFI-A and C/EBPα Regulates Human Granulopoiesis', *Cell,* 123(5), pp. 819-831.

Feagan, B. G., Danese, S., Loftus, E. V., Jr., Vermeire, S., Schreiber, S., Ritter, T., Fogel, R., Mehta, R., Nijhawan, S., Kempiński, R., Filip, R., Hospodarskyy, I., Seidler, U., Seibold, F., Beales, I. L. P., Kim, H. J., McNally, J., Yun, C., Zhao, S., ... and Peyrin-Biroulet, L. (2021) 'Filgotinib as induction and maintenance therapy for ulcerative colitis (SELECTION): a phase 2b/3 double-blind, randomised, placebo-controlled trial', *Lancet,* 397(10292), pp. 2372-2384.

Feagan, B. G., Rutgeerts, P., Sands, B. E., Hanauer, S., Colombel, J. F., Sandborn, W. J., Van Assche, G., Axler, J., Kim, H. J., Danese, S., Fox, I., Milch, C., Sankoh, S., Wyant, T., Xu, J. and Parikh, A. (2013) 'Vedolizumab as induction and maintenance therapy for ulcerative colitis', *N Engl J Med,* 369(8), pp. 699-710.

Filbey, K. J., Grainger, J. R., Smith, K. A., Boon, L., Van Rooijen, N., Harcus, Y., Jenkins, S., Hewitson, J. P. and Maizels, R. M. (2014) 'Innate and adaptive type 2 immune cell responses in genetically controlled resistance to intestinal helminth infection', *Immunology & Cell Biology,* 92(5), pp. 436-448.

Flanagan, M. E., Blumenkopf, T. A., Brissette, W. H., Brown, M. F., Casavant, J. M., Shang-Poa, C., Doty, J. L., Elliott, E. A., Fisher, M. B., Hines, M., Kent, C., Kudlacz, E. M., Lillie, B. M., Magnuson, K. S., McCurdy, S. P., Munchhof, M. J., Perry, B. D., Sawyer, P. S., Strelevitz, T. J., ... and Changelian, P. S. (2010) 'Discovery of CP-690,550: a potent and selective Janus kinase (JAK) inhibitor for the treatment of autoimmune diseases and organ transplant rejection', *J Med Chem,* 53(24), pp. 8468-84.

Flynn, C. L., Markey, G. E., Neudecker, V., Farrelly, C., Furuta, G. T., Eltzschig, H. K., Masterson, J. C. and McNamee, E. N. (2024) 'The MicroRNA miR-223 Constrains Colitis-associated Tumorigenesis by Limiting Myeloid Cell Infiltration and Chemokine Expression', *J Immunol,* 213(12), pp. 1869-1883.

Ford, A. C. and Peyrin-Biroulet, L. (2013) 'Opportunistic Infections With Anti-Tumor Necrosis Factor-α Therapy in Inflammatory Bowel Disease: Meta-Analysis of Randomized Controlled Trials', *Official journal of the American College of Gastroenterology | ACG,* 108(8), pp. 1268-1276.

Formas-Oliveira, A. S., Ferreira, M. V. and Coroadinha, A. S. (2025) 'Deciphering key parameters enhancing lentiviral vector producer cells yields: Vector components copy number and expression', *Molecular Therapy Methods & Clinical Development,* 33(1), pp. 101431.

Fornari, F., Gramantieri, L., Ferracin, M., Veronese, A., Sabbioni, S., Calin, G. A., Grazi, G. L., Giovannini, C., Croce, C. M., Bolondi, L. and Negrini, M. (2008) 'MiR-221 controls CDKN1C/p57 and CDKN1B/p27 expression in human hepatocellular carcinoma', *Oncogene,* 27(43), pp. 5651-61.

Franzosa, E. A., Sirota-Madi, A., Avila-Pacheco, J., Fornelos, N., Haiser, H. J., Reinker, S., Vatanen, T., Hall, A. B., Mallick, H., McIver, L. J., Sauk, J. S., Wilson, R. G., Stevens, B. W., Scott, J. M., Pierce, K., Deik, A. A., Bullock, K., Imhann, F., Porter, J. A., ... and Xavier, R. J. (2019) 'Gut microbiome structure and metabolic activity in inflammatory bowel disease', *Nat Microbiol,* 4(2), pp. 293-305.

Friedberg, S., Choi, D., Hunold, T., Choi, N. K., Garcia, N. M., Picker, E. A., Cohen, N. A., Cohen, R. D., Dalal, S. R., Pekow, J., Sakuraba, A., Krugliak Cleveland, N. and Rubin, D. T. (2023) 'Upadacitinib Is Effective and Safe in Both

Ulcerative Colitis and Crohn's Disease: Prospective Real-World Experience', *Clin Gastroenterol Hepatol,* 21(7), pp. 1913-1923.e2.

Friedman, B. and Cronstein, B. (2019) 'Methotrexate mechanism in treatment of rheumatoid arthritis', *Joint Bone Spine,* 86(3), pp. 301-307.

Fu, G., Brkić, J., Hayder, H. and Peng, C. (2013) 'MicroRNAs in Human Placental Development and Pregnancy Complications', *Int J Mol Sci,* 14(3), pp. 5519-44.

Fukao, T., Fukuda, Y., Kiga, K., Sharif, J., Hino, K., Enomoto, Y., Kawamura, A., Nakamura, K., Takeuchi, T. and Tanabe, M. (2007) 'An Evolutionarily Conserved Mechanism for MicroRNA-223 Expression Revealed by MicroRNA Gene Profiling', *Cell,* 129(3), pp. 617-631.

Fuyuno, Y., Yamazaki, K., Takahashi, A., Esaki, M., Kawaguchi, T., Takazoe, M., Matsumoto, T., Matsui, T., Tanaka, H., Motoya, S., Suzuki, Y., Kiyohara, Y., Kitazono, T. and Kubo, M. (2016) 'Genetic characteristics of inflammatory bowel disease in a Japanese population', *J Gastroenterol,* 51(7), pp. 672-81.

Gabanyi, I., Muller, P. A., Feighery, L., Oliveira, T. Y., Costa-Pinto, F. A. and Mucida, D. (2016) 'Neuro-immune Interactions Drive Tissue Programming in Intestinal Macrophages', *Cell,* 164(3), pp. 378-91.

Gale, D. P., Gross, O., Wang, F., Esteban de la Rosa, R. J., Hall, M., Sayer, J. A., Appel, G., Hariri, A., Liu, S., Maski, M., Shen, Y., Zhang, Q., Iqbal, S., Kowthalam, M. U., Lin, J., Ding, J. and on behalf of the, H. C. T. G. (2024) 'A Randomized Controlled Clinical Trial Testing Effects of Lademirsen on Kidney Function Decline in Adults with Alport Syndrome', *Clinical Journal of the American Society of Nephrology,* 19(8).

Galloway, J. B., Hyrich, K. L., Mercer, L. K., Dixon, W. G., Fu, B., Ustianowski, A. P., Watson, K. D., Lunt, M. and Symmons, D. P. (2011) 'Anti-TNF therapy is associated with an increased risk of serious infections in patients with rheumatoid arthritis especially in the first 6 months of treatment: updated results from the British Society for Rheumatology Biologics Register with special emphasis on risks in the elderly', *Rheumatology (Oxford),* 50(1), pp. 124-31.

Gantier, M. P., Stunden, H. J., McCoy, C. E., Behlke, M. A., Wang, D., Kaparakis-Liaskos, M., Sarvestani, S. T., Yang, Y. H., Xu, D., Corr, S. C., Morand, E. F. and Williams, B. R. (2012) 'A miR-19 regulon that controls NF-κB signaling', *Nucleic Acids Res,* 40(16), pp. 8048-58.

Gao, F., Wu, H., Wang, R., Guo, Y., Zhang, Z., Wang, T., Zhang, G., Liu, C. and Liu, J. (2019) 'MicroRNA-485-5p suppresses the proliferation, migration and invasion of small cell lung cancer cells by targeting flotillin-2', *Bioengineered,* 10(1), pp. 1-12.

Garbers, C., Aparicio-Siegmund, S. and Rose-John, S. (2015) 'The IL-6/gp130/STAT3 signaling axis: recent advances towards specific inhibition', *Curr Opin Immunol,* 34, pp. 75-82.

Garrido-Trigo, A., Corraliza, A. M., Veny, M., Dotti, I., Melón-Ardanaz, E., Rill, A., Crowell, H. L., Corbí, Á., Gudiño, V., Esteller, M., Álvarez-Teubel, I., Aguilar, D., Masamunt, M. C., Killingbeck, E., Kim, Y., Leon, M., Visvanathan, S., Marchese, D., Caratù, G., ... and Salas, A. (2023) 'Macrophage and neutrophil heterogeneity at single-cell spatial resolution in human inflammatory bowel disease', *Nat Commun,* 14(1), pp. 4506.

Gebert, L. F. R. and MacRae, I. J. (2019) 'Regulation of microRNA function in animals', *Nat Rev Mol Cell Biol,* 20(1), pp. 21-37.

Gerich, M. E. and McGovern, D. P. (2014) 'Towards personalized care in IBD', *Nat Rev Gastroenterol Hepatol,* 11(5), pp. 287-99.

Gibson, D. L., Montero, M., Ropeleski, M. J., Bergstrom, K. S., Ma, C., Ghosh, S., Merkens, H., Huang, J., Månsson, L. E., Sham, H. P., McNagny, K. M. and Vallance, B. A. (2010) 'Interleukin-11 reduces TLR4-induced colitis in TLR2-deficient mice and restores intestinal STAT3 signaling', *Gastroenterology,* 139(4), pp. 1277-88.

Gilani, S., Howarth, G. S., Kitessa, S. M., Tran, C. D., Forder, R. E. A. and Hughes, R. J. (2017) 'New biomarkers for increased intestinal permeability induced by dextran sodium sulphate and fasting in chickens', *Journal of Animal Physiology and Animal Nutrition,* 101(5), pp. e237-e245.

Ginhoux, F. and Guilliams, M. (2016) 'Tissue-Resident Macrophage Ontogeny and Homeostasis', *Immunity,* 44(3), pp. 439-449.

Gisbert, J. P. and Panés, J. (2009) 'Loss of response and requirement of infliximab dose intensification in Crohn's disease: a review', *Am J Gastroenterol,* 104(3), pp. 760-7.

Giuliani, A., Sabbatinelli, J., Amatori, S., Graciotti, L., Silvestrini, A., Matacchione, G., Ramini, D., Mensà, E., Prattichizzo, F., Babini, L., Mattiucci, D., Busilacchi, E. M., Bacalini, M. G., Espinosa, E., Lattanzio, F., Procopio, A. D., Olivieri, F., Poloni, A., Fanelli, M. and Rippo, M. R. (2023) 'MiR-422a promotes adipogenesis via MeCP2 downregulation in human bone marrow mesenchymal stem cells', *Cellular and Molecular Life Sciences,* 80(3).

Glas, J., Seiderer, J., Czamara, D., Pasciuto, G., Diegelmann, J., Wetzke, M., Olszak, T., Wolf, C., Müller-Myhsok, B., Balschun, T., Achkar, J.-P., Kamboh, M. I., Franke, A., Duerr, R. H. and Brand, S. (2012) 'PTGER4 Expression-Modulating Polymorphisms in the 5p13.1 Region Predispose to Crohn's Disease and Affect NF-κB and XBP1 Binding Sites', *PLOS ONE,* 7(12), pp. e52873.

Gordon, S. and Plüddemann, A. (2017) 'Tissue macrophages: heterogeneity and functions', *BMC Biology,* 15(1).

Graff, J. W., Dickson, A. M., Clay, G., Mccaffrey, A. P. and Wilson, M. E. (2012) 'Identifying Functional MicroRNAs in Macrophages with Polarized Phenotypes', *Journal of Biological Chemistry,* 287(26), pp. 21816-21825.

Grivennikov, S., Karin, E., Terzic, J., Mucida, D., Yu, G.-Y., Vallabhapurapu, S., Scheller, J., Rose-John, S., Cheroutre, H., Eckmann, L. and Karin, M. (2009) 'IL-6 and Stat3 Are Required for Survival of Intestinal Epithelial Cells and Development of Colitis-Associated Cancer', *Cancer Cell,* 15(2), pp. 103-113.

Grover, P. K., Hardingham, J. E. and Cummins, A. G. (2010) 'Stem cell marker olfactomedin 4: critical appraisal of its characteristics and role in tumorigenesis', *Cancer Metastasis Rev,* 29(4), pp. 761-75.

Guan, F., Wang, R., Yi, Z., Luo, P., Liu, W., Xie, Y., Liu, Z., Xia, Z., Zhang, H. and Cheng, Q. (2025) 'Tissue macrophages: origin, heterogenity, biological functions,

diseases and therapeutic targets', *Signal Transduction and Targeted Therapy,* 10(1).

Gubatan, J., Keyashian, K., Rubin, S. J. S., Wang, J., Buckman, C. A. and Sinha, S. (2021) 'Anti-Integrins for the Treatment of Inflammatory Bowel Disease: Current Evidence and Perspectives', *CLINICAL AND EXPERIMENTAL GASTROENTEROLOGY,* 14, pp. 333-342.

Gumer, L. and McNamee, E.

Guo, S., Lu, J., Schlanger, R., Zhang, H., Wang, J. Y., Fox, M. C., Purton, L. E., Fleming, H. H., Cobb, B., Merkenschlager, M., Golub, T. R. and Scadden, D. T. (2010) 'MicroRNA miR-125a controls hematopoietic stem cell number', *Proceedings of the National Academy of Sciences,* 107(32), pp. 14229-14234.

Guo, Z., Jang, M. H., Otani, K., Bai, Z., Umemoto, E., Matsumoto, M., Nishiyama, M., Yamasaki, M., Ueha, S., Matsushima, K., Hirata, T. and Miyasaka, M. (2008) 'CD4+CD25+ regulatory T cells in the small intestinal lamina propria show an effector/memory phenotype', *International Immunology,* 20(3), pp. 307-315.

Hackett, E. E., Charles-Messance, H., O'Leary, S. M., Gleeson, L. E., Muñoz-Wolf, N., Case, S., Wedderburn, A., Johnston, D. G. W., Williams, M. A., Smyth, A., Ouimet, M., Moore, K. J., Lavelle, E. C., Corr, S. C., Gordon, S. V., Keane, J. and Sheedy, F. J. (2020) 'Mycobacterium tuberculosis Limits Host Glycolysis and IL-1β by Restriction of PFK-M via MicroRNA-21', *Cell Rep,* 30(1), pp. 124-136.e4.

Han, X., Ding, S., Jiang, H. and Liu, G. (2021) 'Roles of Macrophages in the Development and Treatment of Gut Inflammation', *Frontiers in Cell and Developmental Biology,* 9.

Hanauer, S. B., Feagan, B. G., Lichtenstein, G. R., Mayer, L. F., Schreiber, S., Colombel, J. F., Rachmilewitz, D., Wolf, D. C., Olson, A., Bao, W. and Rutgeerts, P. (2002) 'Maintenance infliximab for Crohn's disease: the ACCENT I randomised trial', *Lancet,* 359(9317), pp. 1541-9.

Haneklaus, M., Gerlic, M., Kurowska-Stolarska, M., Rainey, A.-A., Pich, D., McInnes, I. B., Hammerschmidt, W., O'Neill, L. A. J. and Masters, S. L. (2012) 'Cutting Edge: miR-223 and EBV miR-BART15 Regulate the NLRP3

Inflammasome and IL-1β Production', *The Journal of Immunology,* 189(8), pp. 3795-3799.

Hausmann, A., Steenholdt, C., Nielsen, O. H. and Jensen, K. B. (2024) 'Immune cell-derived signals governing epithelial phenotypes in homeostasis and inflammation', *Trends in Molecular Medicine,* 30(3), pp. 239-251.

He, C., Yu, T., Shi, Y., Ma, C., Yang, W., Fang, L., Sun, M., Wu, W., Xiao, F., Guo, F., Chen, M., Yang, H., Qian, J., Cong, Y. and Liu, Z. (2017) 'MicroRNA 301A Promotes Intestinal Inflammation and Colitis-Associated Cancer Development by Inhibiting BTG1', *Gastroenterology,* 152(6), pp. 1434-1448.e15.

He, X., Gou, X., Fan, D., Yang, J., Fu, X., Luo, Y. and Yang, T. (2024) 'Repurposing TAK875 as a novel STAT3 inhibitor for treating inflammatory bowel disease', *Biochemical Pharmacology,* 219, pp. 115957.

Hegan, P. S., Chandhoke, S. K., Barone, C., Egan, M., Bähler, M. and Mooseker, M. S. (2016) 'Mice lacking myosin IXb, an inflammatory bowel disease susceptibility gene, have impaired intestinal barrier function and superficial ulceration in the ileum', *Cytoskeleton (Hoboken),* 73(4), pp. 163-79.

Hegarty, L. M., Jones, G.-R. and Bain, C. C. (2023) 'Macrophages in intestinal homeostasis and inflammatory bowel disease', *Nature Reviews Gastroenterology & Hepatology,* 20(8), pp. 538-553.

Hine, A. M. and Loke, P. (2019) 'Intestinal Macrophages in Resolving Inflammation', *J Immunol,* 203(3), pp. 593-599.

Hines, W. C. and Hines, W. C. (2023) 'Lost in transduction: Critical considerations when using viral vectors', *Frontiers in Cell and Developmental Biology,* 10.

Ho, G.-T., Cartwright, J. A., Thompson, E. J., Bain, C. C. and Rossi, A. G. (2020) 'Resolution of Inflammation and Gut Repair in IBD: Translational Steps Towards Complete Mucosal Healing', *Inflammatory Bowel Diseases,* 26(8), pp. 1131-1143.

Hofer, M. and Lutolf, M. P. (2021) 'Engineering organoids', *Nat Rev Mater,* 6(5), pp. 402-420.

Honap, S., Agorogianni, A., Colwill, M. J., Mehta, S. K., Donovan, F., Pollok, R., Poullis, A. and Patel, K. (2024) 'JAK inhibitors for inflammatory bowel disease: recent advances', *Frontline Gastroenterology,* 15(1), pp. 59.

Hong, D. S., Kang, Y.-K., Borad, M., Sachdev, J., Ejadi, S., Lim, H. Y., Brenner, A. J., Park, K., Lee, J.-L., Kim, T.-Y., Shin, S., Becerra, C. R., Falchook, G., Stoudemire, J., Martin, D., Kelnar, K., Peltier, H., Bonato, V., Bader, A. G., ... and Beg, M. S. (2020) 'Phase 1 study of MRX34, a liposomal miR-34a mimic, in patients with advanced solid tumours', *British Journal of Cancer,* 122(11), pp. 1630-1637.

Hou, J. K., Abraham, B. and El-Serag, H. (2011) 'Dietary intake and risk of developing inflammatory bowel disease: a systematic review of the literature', *Am J Gastroenterol,* 106(4), pp. 563-73.

Hu, Y., Zhang, M., He, K., Lv, L., Yu, H., Li, S., Liu, W., Li, H., Yi, S., Yang, Y. and Ye, L. (2024) 'Novel engineered regulatory macrophages combined with ICIs for post-transplant recurrence after liver transplantation for HCC', *Journal of Clinical Oncology,* 42(16_suppl), pp. e14582-e14582.

Huang, K., Dong, S., Li, W. and Xie, Z. (2013) 'The expression and regulation of microRNA-125b in cancers', *Acta Biochim Biophys Sin (Shanghai),* 45(10), pp. 803-5.

Huang, L., Bernink, J. H., Giladi, A., Krueger, D., Van Son, G. J. F., Geurts, M. H., Busslinger, G., Lin, L., Begthel, H., Zandvliet, M., Buskens, C. J., Bemelman, W. A., López-Iglesias, C., Peters, P. J. and Clevers, H. (2024) 'Tuft cells act as regenerative stem cells in the human intestine', *Nature,* 634(8035), pp. 929-935.

Huang, W. (2017) 'MicroRNAs: Biomarkers, Diagnostics, and Therapeutics', *Methods Mol Biol,* 1617, pp. 57-67.

Hughes, C. S., Postovit, L. M. and Lajoie, G. A. (2010) 'Matrigel: A complex protein mixture required for optimal growth of cell culture', *PROTEOMICS,* 10(9), pp. 1886-1890.

Hussey, S. (2025) *Epidemiology and Outcomes in Paediatric Inflammatory Bowel Disease.* Royal College of Surgeons in Ireland [Online]. Available at:

https://repository.rcsi.com/articles/thesis/Epidemiology_and_Outcomes_in_Paediatric_Inflammatory_Bowel_Disease/24064512.

Ishibashi, F., Shimizu, H., Nakata, T., Fujii, S., Suzuki, K., Kawamoto, A., Anzai, S., Kuno, R., Nagata, S., Ito, G., Murano, T., Mizutani, T., Oshima, S., Tsuchiya, K., Nakamura, T., Watanabe, M. and Okamoto, R. (2018) 'Contribution of ATOH1(+) Cells to the Homeostasis, Repair, and Tumorigenesis of the Colonic Epithelium', *Stem Cell Reports,* 10(1), pp. 27-42.

Jablonski, K. A., Gaudet, A. D., Amici, S. A., Popovich, P. G. and Guerau-De-Arellano, M. (2016) 'Control of the Inflammatory Macrophage Transcriptional Signature by miR-155', *PLOS ONE,* 11(7), pp. e0159724.

Jalil, A. T., Abdulhadi, M. A., Al-Ameer, L. R., Abbas, H. A., Merza, M. S., Zabibah, R. S. and Fadhil, A. A. (2023) 'The emerging role of microRNA-126 as a potential therapeutic target in cancer: a comprehensive review', *Pathol Res Pract,* 248, pp. 154631.

Jang, D. I., Lee, A. H., Shin, H. Y., Song, H. R., Park, J. H., Kang, T. B., Lee, S. R. and Yang, S. H. (2021) 'The Role of Tumor Necrosis Factor Alpha (TNF-α) in Autoimmune Disease and Current TNF-α Inhibitors in Therapeutics', *Int J Mol Sci,* 22(5).

Jardé, T., Chan, W. H., Rossello, F. J., Kaur Kahlon, T., Theocharous, M., Kurian Arackal, T., Flores, T., Giraud, M., Richards, E., Chan, E., Kerr, G., Engel, R. M., Prasko, M., Donoghue, J. F., Abe, S.-I., Phesse, T. J., Nefzger, C. M., Mcmurrick, P. J., Powell, D. R., ... and Abud, H. E. (2020) 'Mesenchymal Niche-Derived Neuregulin-1 Drives Intestinal Stem Cell Proliferation and Regeneration of Damaged Epithelium', *Cell Stem Cell,* 27(4), pp. 646-662.e7.

Jiang, S., Deng, T., Cheng, H., Liu, W., Shi, D., Yuan, J., He, Z., Wang, W., Chen, B., Ma, L., Zhang, X. and Gong, P. (2023) 'Macrophage-organoid co-culture model for identifying treatment strategies against macrophage-related gemcitabine resistance', *Journal of Experimental & Clinical Cancer Research,* 42(1).

Jiang, Y., Chen, J., Du, Y., Fan, M. and Shen, L. (2025) 'Immune modulation for the patterns of epithelial cell death in inflammatory bowel disease', *International Immunopharmacology,* 154, pp. 114462.

Jin, Y., Chen, Z., Liu, X. and Zhou, X. (2013) 'Evaluating the microRNA targeting sites by luciferase reporter gene assay', *Methods Mol Biol,* 936, pp. 117-27.

Johnnidis, J. B., Harris, M. H., Wheeler, R. T., Stehling-Sun, S., Lam, M. H., Kirak, O., Brummelkamp, T. R., Fleming, M. D. and Camargo, F. D. (2008) 'Regulation of progenitor cell proliferation and granulocyte function by microRNA-223', *Nature,* 451(7182), pp. 1125-1129.

Joly Condette, C., Khorsi-Cauet, H., Morlière, P., Zabijak, L., Reygner, J., Bach, V. and Gay-Quéheillard, J. (2014) 'Increased Gut Permeability and Bacterial Translocation after Chronic Chlorpyrifos Exposure in Rats', *PLoS ONE,* 9(7), pp. e102217.

Jubb, A. M., Chalasani, S., Frantz, G. D., Smits, R., Grabsch, H. I., Kavi, V., Maughan, N. J., Hillan, K. J., Quirke, P. and Koeppen, H. (2006) 'Achaete-scute like 2 (ascl2) is a target of Wnt signalling and is upregulated in intestinal neoplasia', *Oncogene,* 25(24), pp. 3445-57.

Jung, K. B., Kwon, O., Lee, M. O., Lee, H., Son, Y. S., Habib, O., Oh, J. H., Cho, H. S., Jung, C. R., Kim, J. and Son, M. Y. (2019) 'Blockade of STAT3 Causes Severe In Vitro and In Vivo Maturation Defects in Intestinal Organoids Derived from Human Embryonic Stem Cells', *J Clin Med,* 8(7).

Kaiser, G. C., Yan, F. and Polk, D. B. (1999) 'Mesalamine blocks tumor necrosis factor growth inhibition and nuclear factor kappaB activation in mouse colonocytes', *Gastroenterology,* 116(3), pp. 602-9.

Kamada, N., Hisamatsu, T., Okamoto, S., Chinen, H., Kobayashi, T., Sato, T., Sakuraba, A., Kitazume, M. T., Sugita, A., Koganei, K., Akagawa, K. S. and Hibi, T. (2008) 'Unique CD14+ intestinal macrophages contribute to the pathogenesis of Crohn disease via IL-23/IFN-γ axis', *Journal of Clinical Investigation*.

Kang, B., Alvarado, L. J., Kim, T., Lehmann, M. L., Cho, H., He, J., Li, P., Kim, B. H., Larochelle, A. and Kelsall, B. L. (2020) 'Commensal microbiota drive the

functional diversification of colon macrophages', *Mucosal Immunol,* 13(2), pp. 216-229.

Kaplan, G. G. (2015) 'The global burden of IBD: from 2015 to 2025', *Nat Rev Gastroenterol Hepatol,* 12(12), pp. 720-7.

Kaplan, G. G., Hubbard, J., Korzenik, J., Sands, B. E., Panaccione, R., Ghosh, S., Wheeler, A. J. and Villeneuve, P. J. (2010) 'The inflammatory bowel diseases and ambient air pollution: a novel association', *Am J Gastroenterol,* 105(11), pp. 2412-9.

Kaplan, G. G. and Ng, S. C. (2017) 'Understanding and Preventing the Global Increase of Inflammatory Bowel Disease', *Gastroenterology,* 152(2), pp. 313-321.e2.

Karin, M. and Clevers, H. (2016) 'Reparative inflammation takes charge of tissue regeneration', *Nature,* 529(7586), pp. 307-315.

Karo-Atar, D., Ouladan, S., Javkar, T., Joumier, L., Matheson, M. K., Merritt, S., Westfall, S., Rochette, A., Gentile, M. E., Fontes, G., Fonseca, G. J., Parisien, M., Diatchenko, L., von Moltke, J., Malleshaiah, M., Gregorieff, A. and King, I. L. (2022) 'Helminth-induced reprogramming of the stem cell compartment inhibits type 2 immunity', *J Exp Med,* 219(9).

Katkar, G. and Ghosh, P. (2023) 'Macrophage states: there's a method in the madness', *Trends in Immunology,* 44(12), pp. 954-964.

Kaz, A. M. and Venu, N. (2025) 'Diagnostic Methods and Biomarkers in Inflammatory Bowel Disease', *Diagnostics*, 15(11), pp. 1303. DOI: 10.3390/diagnostics15111303.

Kazemifard, N., Golestani, N., Jahankhani, K., Farmani, M. and Ghavami, S. B. (2025) 'Ulcerative colitis: the healing power of macrophages', *Tissue Barriers,* 13(2).

Khatana, U. F., Qamar, A. and Ashfaq, M. B. (2021) 'Infliximab-Associated Acneiform Eruption in a Patient With Inflammatory Bowel Disease', *Cureus,* 13(9), pp. e18213.

Kim, S. Y. and Nair, M. G. (2019) 'Macrophages in wound healing: activation and plasticity', *Immunology & Cell Biology,* 97(3), pp. 258-267.

Kim, T. I. (2015) 'The Role of Barrier Dysfunction and Change of Claudin Expression in Inflammatory Bowel Disease', *Gut Liver: Vol. 6*. Korea (South), pp. 699-700.

Konicek, B. W., Stephens, J. R., McNulty, A. M., Robichaud, N., Peery, R. B., Dumstorf, C. A., Dowless, M. S., Iversen, P. W., Parsons, S., Ellis, K. E., McCann, D. J., Pelletier, J., Furic, L., Yingling, J. M., Stancato, L. F., Sonenberg, N. and Graff, J. R. (2011) 'Therapeutic inhibition of MAP kinase interacting kinase blocks eukaryotic initiation factor 4E phosphorylation and suppresses outgrowth of experimental lung metastases', *Cancer Res,* 71(5), pp. 1849-57.

Koralov, S. B., Muljo, S. A., Galler, G. R., Krek, A., Chakraborty, T., Kanellopoulou, C., Jensen, K., Cobb, B. S., Merkenschlager, M., Rajewsky, N. and Rajewsky, K. (2008) 'Dicer ablation affects antibody diversity and cell survival in the B lymphocyte lineage', *Cell,* 132(5), pp. 860-74.

Kornbluth, A., Sachar, D. B. and The Practice Parameters Committee of the American College of Gastroenterology (2010) 'Ulcerative Colitis Practice Guidelines in Adults: American College of Gastroenterology, Practice Parameters Committee', *Official journal of the American College of Gastroenterology | ACG,* 105(3).

Kou, R., Guo, Y., Qin, Z., Xu, X., Liu, Y., Wei, W., Chen, Y., Jian, Z. and Lan, B. (2025) 'Systemic dysregulation of the gut microenvironment plays a pivotal role in the onset and progression of inflammatory bowel disease', *Front Immunol,* 16, pp. 1661386.

Koukos, G., Polytarchou, C., Kaplan, J. L., Morley-Fletcher, A., Gras-Miralles, B., Kokkotou, E., Baril-Dore, M., Pothoulakis, C., Winter, H. S. and Iliopoulos, D. (2013) 'MicroRNA-124 regulates STAT3 expression and is down-regulated in colon tissues of pediatric patients with ulcerative colitis', *Gastroenterology,* 145(4), pp. 842-52.e2.

Kromann, E. H., Cearra, A. P. and Neves, J. F. (2024) 'Organoids as a tool to study homeostatic and pathological immune–epithelial interactions in the gut', *Clinical and Experimental Immunology,* 218(1), pp. 28-39.

Kuenzig, M. E., Fung, S. G., Marderfeld, L., Mak, J. W. Y., Kaplan, G. G., Ng, S. C., Wilson, D. C., Cameron, F., Henderson, P., Kotze, P. G., Bhatti, J., Fang, V., Gerber, S., Guay, E., Kotteduwa Jayawarden, S., Kadota, L., Maldonado, D. F., Osei, J. A., Sandarage, R., ... and Benchimol, E. I. (2022) 'Twenty-first Century Trends in the Global Epidemiology of Pediatric-Onset Inflammatory Bowel Disease: Systematic Review', *Gastroenterology,* 162(4), pp. 1147-1159.e4.

Kuhn, K. A., Manieri, N. A., Liu, T.-C. and Stappenbeck, T. S. (2014) 'IL-6 Stimulates Intestinal Epithelial Proliferation and Repair after Injury', *PLoS ONE,* 9(12), pp. e114195.

Kumar, M., Garand, M. and Al Khodor, S. (2019) 'Integrating omics for a better understanding of Inflammatory Bowel Disease: a step towards personalized medicine', *J Transl Med,* 17(1), pp. 419.

Kushwaha, P., Qureshi, R., Khan, N. and Mukhopadhyay, S. (2026) 'Revolutionizing IBD therapy: Insights into contemporary treatment strategies', *International Reviews of Immunology,* 45(1), pp. 1-25.

Lagos-Quintana, M., Rauhut, R., Lendeckel, W. and Tuschl, T. (2001) 'Identification of novel genes coding for small expressed RNAs', *Science,* 294(5543), pp. 853-8.

Lan, H., Zhang, L. Y., He, W., Li, W. Y., Zeng, Z., Qian, B., Wang, C. and Song, J. L. (2021) 'Sinapic Acid Alleviated Inflammation-Induced Intestinal Epithelial Barrier Dysfunction in Lipopolysaccharide- (LPS-) Treated Caco-2 Cells', *Mediators Inflamm,* 2021, pp. 5514075.

Lapaquette, P., Bringer, M.-A. and Darfeuille-Michaud, A. (2012) 'Defects in autophagy favour adherent-invasive Escherichia coli persistence within macrophages leading to increased pro-inflammatory response', *Cellular Microbiology,* 14(6), pp. 791-807.

Lapaquette, P., Glasser, A.-L., Huett, A., Xavier, R. J. and Darfeuille-Michaud, A. (2010) 'Crohn's disease-associated adherent-invasiveE.â□□coliare selectively favoured by impaired autophagy to replicate intracellularly', *Cellular Microbiology,* 12(1), pp. 99-113.

Lau, N. C., Lim, L. P., Weinstein, E. G. and Bartel, D. P. (2001) 'An abundant class of tiny RNAs with probable regulatory roles in Caenorhabditis elegans', *Science,* 294(5543), pp. 858-62.

Lavelle, A. and Sokol, H. (2020) 'Gut microbiota-derived metabolites as key actors in inflammatory bowel disease', *Nat Rev Gastroenterol Hepatol,* 17(4), pp. 223-237.

Lazarov, T., Juarez-Carreño, S., Cox, N. and Geissmann, F. (2023) 'Physiology and diseases of tissue-resident macrophages', *Nature,* 618(7966), pp. 698-707.

Lee, R. C. and Ambros, V. (2001) 'An extensive class of small RNAs in Caenorhabditis elegans', *Science,* 294(5543), pp. 862-4.

Lee, R. C., Feinbaum, R. L. and Ambros, V. (1993) 'The C. elegans heterochronic gene lin-4 encodes small RNAs with antisense complementarity to lin-14', *Cell,* 75(5), pp. 843-54.

Lemaitre, M., Kirchgesner, J., Rudnichi, A., Carrat, F., Zureik, M., Carbonnel, F. and Dray-Spira, R. (2017) 'Association Between Use of Thiopurines or Tumor Necrosis Factor Antagonists Alone or in Combination and Risk of Lymphoma in Patients With Inflammatory Bowel Disease', *JAMA,* 318(17), pp. 1679.

Levin, A. D., Wildenberg, M. E. and van den Brink, G. R. (2016) 'Mechanism of Action of Anti-TNF Therapy in Inflammatory Bowel Disease', *J Crohns Colitis,* 10(8), pp. 989-97.

Li, C., Xu, Y., Gao, T., Zhang, S., Lin, Z., Gu, S., Fang, Y., Yuan, X., Yu, S., Jiang, Q., Lou, Z., Zhang, X., Zhang, J., Wu, Q., Gu, M., Ding, X., Sun, J. and Chen, Y. (2023) 'Ruxolitinib Alleviates Inflammation, Apoptosis, and Intestinal Barrier Leakage in Ulcerative Colitis via STAT3', *Inflamm Bowel Dis,* 29(8), pp. 1191-1201.

Li, D., Liu, L., Du, X., Ma, W., Zhang, J. and Piao, W. (2022) 'MiRNA-374b-5p and miRNA-106a-5p are related to inflammatory bowel disease via regulating IL-10 and STAT3 signaling pathways', *BMC Gastroenterol,* 22(1), pp. 492.

Li, L., Cheng, R., Wu, Y., Lin, H., Gan, H. and Zhang, H. (2024) 'Diagnosis and management of inflammatory bowel disease', *Journal of Evidence-Based Medicine,* 17(2), pp. 409-433.

Li, N., Xu, X., Xiao, B., Zhu, E. D., Li, B. S., Liu, Z., Tang, B., Zou, Q. M., Liang, H. P. and Mao, X. H. (2012) 'H. pylori related proinflammatory cytokines contribute to the induction of miR-146a in human gastric epithelial cells', *Mol Biol Rep,* 39(4), pp. 4655-61.

Li, T., Qiu, Y., Yang, H. S., Li, M. Y., Zhuang, X. J., Zhang, S. H., Feng, R., Chen, B. L., He, Y., Zeng, Z. R. and Chen, M. H. (2020) 'Systematic review and meta-analysis: Association of a pre-illness Western dietary pattern with the risk of developing inflammatory bowel disease', *J Dig Dis,* 21(7), pp. 362-371.

Li, Y., de Haar, C., Chen, M., Deuring, J., Gerrits, M. M., Smits, R., Xia, B., Kuipers, E. J. and van der Woude, C. J. (2010) 'Disease-related expression of the IL6/STAT3/SOCS3 signalling pathway in ulcerative colitis and ulcerative colitis-related carcinogenesis', *Gut,* 59(2), pp. 227-35.

Liao, T.-L., Chen, Y.-M., Tang, K.-T., Chen, P.-K., Liu, H.-J. and Chen, D.-Y. (2021) 'MicroRNA-223 inhibits neutrophil extracellular traps formation through regulating calcium influx and small extracellular vesicles transmission', *Scientific Reports,* 11(1), pp. 15676.

Lin, D., Jin, Y., Shao, X., Xu, Y., Ma, G., Jiang, Y., Xu, Y., Jiang, Y. and Hu, D. (2024) 'Global, regional, and national burden of inflammatory bowel disease, 1990–2021: Insights from the global burden of disease 2021', *International Journal of Colorectal Disease,* 39(1), pp. 139.

Lin, X. T., Zheng, X. B., Fan, D. J., Yao, Q. Q., Hu, J. C., Lian, L., Wu, X. J., Lan, P. and He, X. S. (2018) 'MicroRNA-143 Targets ATG2B to Inhibit Autophagy and Increase Inflammatory Responses in Crohn's Disease', *Inflamm Bowel Dis,* 24(4), pp. 781-791.

Lindemans, C. A., Calafiore, M., O'Connor, M., Mertelsmann, A., van den Brink, M. R. M. and Hanash, A. M. (2016) 'Interleukin-22 Treatment Promotes Intestinal Stem Cell-Mediated Epithelial Regeneration Via Stat3 Activation and Reduces GI Gvhd', *Biology of Blood and Marrow Transplantation,* 22(3, Supplement), pp. S56-S57.

Little, M. C., Hurst, R. J. M. and Else, K. J. (2014) 'Dynamic Changes in Macrophage Activation and Proliferation during the Development and Resolution of Intestinal Inflammation', *The Journal of Immunology,* 193(9), pp. 4684-4695.

Liu, J., Teng, P.-Y., Kim, W. K. and Applegate, T. J. (2021) 'Assay considerations for fluorescein isothiocyanate-dextran (FITC-d): an indicator of intestinal permeability in broiler chickens', *Poultry Science,* 100(7), pp. 101202.

Liu, T.-C., Naito, T., Liu, Z., VanDussen, K. L., Haritunians, T., Li, D., Endo, K., Kawai, Y., Nagasaki, M., Kinouchi, Y., McGovern, D. P., Shimosegawa, T., Kakuta, Y. and Stappenbeck, T. S. (2017) 'LRRK2 but not ATG16L1 is associated with Paneth cell defect in Japanese Crohn's disease patients', *JCI insight*, 2(6), pp. e91917. PubMed. DOI: 10.1172/jci.insight.91917 (Accessed 2017/03//).

Liu, Z., Xiao, B., Tang, B., Li, B., Li, N., Zhu, E., Guo, G., Gu, J., Zhuang, Y., Liu, X., Ding, H., Zhao, X., Guo, H., Mao, X. and Zou, Q. (2010) 'Up-regulated microRNA-146a negatively modulate Helicobacter pylori-induced inflammatory response in human gastric epithelial cells', *Microbes Infect,* 12(11), pp. 854-63.

Loddo, I. and Romano, C. (2015) 'Inflammatory Bowel Disease: Genetics, Epigenetics, and Pathogenesis', *Front Immunol,* 6, pp. 551.

Logan, R. F. and Skelly, M. M. (2002) 'Maintenance infliximab delayed loss of response in active Crohn disease', *ACP J Club,* 137(3), pp. 92.

Lou, Y.-L., Xie, D.-L., Huang, X.-H., Zheng, M.-M., Chen, N. and Xu, J.-R. (2024) 'The role of MNK1-mTORC1 pathway in modulating macrophage responses to Vibrio vulnificus infection', *Microbiology Spectrum,* 12(8), pp. e03340-23.

Lu, L., Mccurdy, S., Huang, S., Zhu, X., Peplowska, K., Tiirikainen, M., Boisvert, W. A. and Garmire, L. X. (2016) 'Time Series miRNA-mRNA integrated analysis

reveals critical miRNAs and targets in macrophage polarization', *Scientific Reports,* 6(1), pp. 37446.

Ma, L., Yu, J., Zhang, H., Zhao, B., Zhang, J., Yang, D., Luo, F., Wang, B., Jin, B. and Liu, J. (2022) 'Effects of Immune Cells on Intestinal Stem Cells: Prospects for Therapeutic Targets', *Stem Cell Reviews and Reports,* 18(7), pp. 2296-2314.

Macfarlane, L. A. and Murphy, P. R. (2010) 'MicroRNA: Biogenesis, Function and Role in Cancer', *Curr Genomics,* 11(7), pp. 537-61.

Maciag, G., Hansen, S. L., Krizic, K., Kellermann, L., Inventor Zøylner, M. J., Ulyanchenko, S., Maimets, M., Baattrup, A. M., Riis, L. B., Khodosevich, K., Sato, T., Bressan, R. B., Nielsen, O. H. and Jensen, K. B. (2024) 'JAK/STAT signaling promotes the emergence of unique cell states in ulcerative colitis', *Stem Cell Reports,* 19(8), pp. 1172-1188.

Magro, F., Langner, C., Driessen, A., Ensari, A., Geboes, K., Mantzaris, G. J., Villanacci, V., Becheanu, G., Nunes, P. B., Cathomas, G., Fries, W., Jouret-Mourin, A., Mescoli, C., de Petris, G., Rubio, C. A., Shepherd, N. A., Vieth, M., Eliakim, R. and on behalf of the European Society of Pathology and the European Crohn's and Colitis, O. (2013) 'European consensus on the histopathology of inflammatory bowel disease☆', *Journal of Crohn's and Colitis,* 7(10), pp. 827-851.

Mahid, S. S., Minor, K. S., Soto, R. E., Hornung, C. A. and Galandiuk, S. (2006) 'Smoking and inflammatory bowel disease: a meta-analysis', *Mayo Clin Proc,* 81(11), pp. 1462-71.

Mallon, K., Doherty, G. and Burns, R. (2024) 'P1152 Health-related quality of life among Irish Inflammatory Bowel Disease patients: a cross-sectional survey using the EQ-5D-5L', *Journal of Crohn's and Colitis,* 18(Supplement_1), pp. i2047-i2047.

Martin, J. C., Chang, C., Boschetti, G., Ungaro, R., Giri, M., Grout, J. A., Gettler, K., Chuang, L. S., Nayar, S., Greenstein, A. J., Dubinsky, M., Walker, L., Leader, A., Fine, J. S., Whitehurst, C. E., Mbow, M. L., Kugathasan, S., Denson, L. A., Hyams, J. S., ... and Kenigsberg, E. (2019) 'Single-Cell Analysis of Crohn's Disease Lesions Identifies a Pathogenic Cellular Module Associated with Resistance to Anti-TNF Therapy', *Cell,* 178(6), pp. 1493-1508.e20.

Martin-Rodriguez, O., Gauthier, T., Bonnefoy, F., Couturier, M., Daoui, A., Chagué, C., Valmary-Degano, S., Gay, C., Saas, P. and Perruche, S. (2021) 'Pro-Resolving Factors Released by Macrophages After Efferocytosis Promote Mucosal Wound Healing in Inflammatory Bowel Disease', *Frontiers in Immunology,* Volume 12 - 2021.

Matheis, F., Muller, P. A., Graves, C. L., Gabanyi, I., Kerner, Z. J., Costa-Borges, D., Ahrends, T., Rosenstiel, P. and Mucida, D. (2020) 'Adrenergic Signaling in Muscularis Macrophages Limits Infection-Induced Neuronal Loss', *Cell,* 180(1), pp. 64-78.e16.

Matusiak, M., Hickey, J. W., Luca, B., Lu, G., Kidziński, L., Zhu, S., Colburg, D. R. C., Phillips, D. J., Brubaker, S. W., Charville, G. W., Shen, J., Nolan, G. P., Newman, A. M., West, R. B. and van de Rijn, M. (2023) 'A spatial map of human macrophage niches reveals context-dependent macrophage functions in colon and breast cancer', *Res Sq*.

Mazumder, A., Bose, M., Chakraborty, A., Chakrabarti, S. and Bhattacharyya, S. N. (2013) 'A transient reversal of miRNA-mediated repression controls macrophage activation', *EMBO reports,* 14(11), pp. 1008-1016.

McGovern, D. P., Kugathasan, S. and Cho, J. H. (2015) 'Genetics of Inflammatory Bowel Diseases', *Gastroenterology,* 149(5), pp. 1163-1176.e2.

Melo, S. A. and Esteller, M. (2011) 'Dysregulation of microRNAs in cancer: playing with fire', *FEBS Lett,* 585(13), pp. 2087-99.

Meyer, A. R., Brown, M. E., Mcgrath, P. S. and Dempsey, P. J. (2022) 'Injury-Induced Cellular Plasticity Drives Intestinal Regeneration', *Cellular and Molecular Gastroenterology and Hepatology,* 13(3), pp. 843-856.

Milajerdi, A., Ebrahimi-Daryani, N., Dieleman, L. A., Larijani, B. and Esmaillzadeh, A. (2021) 'Association of Dietary Fiber, Fruit, and Vegetable Consumption with Risk of Inflammatory Bowel Disease: A Systematic Review and Meta-Analysis', *Adv Nutr,* 12(3), pp. 735-743.

Mills, C. D., Kincaid, K., Alt, J. M., Heilman, M. J. and Hill, A. M. (2000) 'M-1/M-2 Macrophages and the Th1/Th2 Paradigm1', *The Journal of Immunology,* 164(12), pp. 6166-6173.

Mizoguchi, E., Low, D., Ezaki, Y. and Okada, T. (2020) 'Recent updates on the basic mechanisms and pathogenesis of inflammatory bowel diseases in experimental animal models', *Intest Res,* 18(2), pp. 151-167.

Molodecky, N. A., Soon, I. S., Rabi, D. M., Ghali, W. A., Ferris, M., Chernoff, G., Benchimol, E. I., Panaccione, R., Ghosh, S., Barkema, H. W. and Kaplan, G. G. (2012) 'Increasing incidence and prevalence of the inflammatory bowel diseases with time, based on systematic review', *Gastroenterology,* 142(1), pp. 46-54.e42; quiz e30.

Montgomery, R. K., Carlone, D. L., Richmond, C. A., Farilla, L., Kranendonk, M. E., Henderson, D. E., Baffour-Awuah, N. Y., Ambruzs, D. M., Fogli, L. K., Algra, S. and Breault, D. T. (2011) 'Mouse telomerase reverse transcriptase (mTert) expression marks slowly cycling intestinal stem cells', *Proc Natl Acad Sci U S A,* 108(1), pp. 179-84.

Mousa, R. S., Invernizzi, P. and Mousa, H. S. (2024) 'Innate immune cells in the pathogenesis of inflammatory bowel disease - from microbial metabolites to immune modulation', *Frontiers in Gastroenterology,* Volume 3 - 2024.

Mowat, A. M. and Agace, W. W. (2014) 'Regional specialization within the intestinal immune system', *Nature Reviews Immunology,* 14(10), pp. 667-685.

Mozammel, N., Amini, M., Baradaran, B., Mahdavi, S. Z. B., Hosseini, S. S. and Mokhtarzadeh, A. (2023) 'The function of miR-145 in colorectal cancer progression; an updated review on related signaling pathways', *Pathol Res Pract,* 242, pp. 154290.

Muller, P. A., Koscsó, B., Rajani, G. M., Stevanovic, K., Berres, M. L., Hashimoto, D., Mortha, A., Leboeuf, M., Li, X. M., Mucida, D., Stanley, E. R., Dahan, S., Margolis, K. G., Gershon, M. D., Merad, M. and Bogunovic, M. (2014) 'Crosstalk between muscularis macrophages and enteric neurons regulates gastrointestinal motility', *Cell,* 158(2), pp. 300-313.

Murata, K., Jadhav, U., Madha, S., Van Es, J., Dean, J., Cavazza, A., Wucherpfennig, K., Michor, F., Clevers, H. and Shivdasani, R. A. (2020) 'Ascl2-Dependent Cell Dedifferentiation Drives Regeneration of Ablated Intestinal Stem Cells', *Cell Stem Cell,* 26(3), pp. 377-390.e6.

Muro, P., Zhang, L., Li, S., Zhao, Z., Jin, T., Mao, F. and Mao, Z. (2024) 'The emerging role of oxidative stress in inflammatory bowel disease', *Front Endocrinol (Lausanne),* 15, pp. 1390351.

Murray, Peter J., Allen, Judith E., Biswas, Subhra K., Fisher, Edward A., Gilroy, Derek W., Goerdt, S., Gordon, S., Hamilton, John A., Ivashkiv, Lionel B., Lawrence, T., Locati, M., Mantovani, A., Martinez, Fernando O., Mege, J.-L., Mosser, David M., Natoli, G., Saeij, Jeroen P., Schultze, Joachim L., Shirey, Kari A., ... and Wynn, Thomas A. (2014) 'Macrophage Activation and Polarization: Nomenclature and Experimental Guidelines', *Immunity,* 41(1), pp. 14-20.

Murray, P. J. and Wynn, T. A. (2011) 'Protective and pathogenic functions of macrophage subsets', *Nature Reviews Immunology,* 11(11), pp. 723-737.

Mustata, C., Roxana, Vasile, G., Fernandez-Vallone, V., Strollo, S., Lefort, A., Libert, F., Monteyne, D., Pérez-Morga, D., Vassart, G. and Garcia, M.-I. (2013) 'Identification of Lgr5-Independent Spheroid-Generating Progenitors of the Mouse Fetal Intestinal Epithelium', *Cell Reports,* 5(2), pp. 421-432.

Na, Y. R., Kim, S. W. and Seok, S. H. (2023) 'A new era of macrophage-based cell therapy', *Experimental & Molecular Medicine,* 55(9), pp. 1945-1954.

Na, Y. R., Stakenborg, M., Seok, S. H. and Matteoli, G. (2019) 'Macrophages in intestinal inflammation and resolution: a potential therapeutic target in IBD', *Nature Reviews Gastroenterology & Hepatology,* 16(9), pp. 531-543.

Nagaraj, S., Stankiewicz-Drogon, A., Darzynkiewicz, E., Wojda, U. and Grzela, R. (2024) 'miR-483-5p orchestrates the initiation of protein synthesis by facilitating the decrease in phosphorylated Ser209eIF4E and 4E-BP1 levels', *Scientific Reports,* 14(1), pp. 4237.

Naher, L., Kiyoshima, T., Kobayashi, I., Wada, H., Nagata, K., Fujiwara, H., Ookuma, Y. F., Ozeki, S., Nakamura, S. and Sakai, H. (2012) 'STAT3 signal transduction through interleukin-22 in oral squamous cell carcinoma', *Int J Oncol,* 41(5), pp. 1577-86.

Namour, F., Anderson, K., Nelson, C. and Tasset, C. (2022) 'Filgotinib: A Clinical Pharmacology Review', *Clin Pharmacokinet,* 61(6), pp. 819-832.

Neudecker, V., Brodsky, K. S., Clambey, E. T., Schmidt, E. P., Packard, T. A., Davenport, B., Standiford, T. J., Weng, T., Fletcher, A. A., Barthel, L., Masterson, J. C., Furuta, G. T., Cai, C., Blackburn, M. R., Ginde, A. A., Graner, M. W., Janssen, W. J., Zemans, R. L., Evans, C. M., ... and Eltzschig, H. K. (2017a) 'Neutrophil transfer of miR-223 to lung epithelial cells dampens acute lung injury in mice', *Sci Transl Med,* 9(408).

Neudecker, V., Haneklaus, M., Jensen, O., Khailova, L., Masterson, J. C., Tye, H., Biette, K., Jedlicka, P., Brodsky, K. S., Gerich, M. E., Mack, M., Robertson, A. A. B., Cooper, M. A., Furuta, G. T., Dinarello, C. A., O'Neill, L. A., Eltzschig, H. K., Masters, S. L. and McNamee, E. N. (2017b) 'Myeloid-derived miR-223 regulates intestinal inflammation via repression of the NLRP3 inflammasome', *J Exp Med,* 214(6), pp. 1737-1752.

Neurath, M. F. (2014) 'New targets for mucosal healing and therapy in inflammatory bowel diseases', *Mucosal Immunology,* 7(1), pp. 6-19.

Neurath, M. F. (2019) 'Targeting immune cell circuits and trafficking in inflammatory bowel disease', *Nat Immunol,* 20(8), pp. 970-979.

Ng, S. C., Bernstein, C. N., Vatn, M. H., Lakatos, P. L., Loftus, E. V., Jr., Tysk, C., O'Morain, C., Moum, B. and Colombel, J. F. (2013) 'Geographical variability and environmental risk factors in inflammatory bowel disease', *Gut,* 62(4), pp. 630-49.

Ng, S. C., Shi, H. Y., Hamidi, N., Underwood, F. E., Tang, W., Benchimol, E. I., Panaccione, R., Ghosh, S., Wu, J. C. Y., Chan, F. K. L., Sung, J. J. Y. and Kaplan, G. G. (2017) 'Worldwide incidence and prevalence of inflammatory bowel disease in the 21st century: a systematic review of population-based studies', *Lancet,* 390(10114), pp. 2769-2778.

Nguyen, P. M., Putoczki, T. L. and Ernst, M. (2015) 'STAT3-Activating Cytokines: A Therapeutic Opportunity for Inflammatory Bowel Disease?', *Journal of Interferon & Cytokine Research,* 35(5), pp. 340-350.

Niewiadomski, O., Studd, C., Wilson, J., Williams, J., Hair, C., Knight, R., Prewett, E., Dabkowski, P., Alexander, S., Allen, B., Dowling, D., Connell, W., Desmond, P. and Bell, S. (2016) 'Influence of food and lifestyle on the risk of developing inflammatory bowel disease', *Intern Med J,* 46(6), pp. 669-76.

Nissen, R. M. and Yamamoto, K. R. (2000) 'The glucocorticoid receptor inhibits NFkappaB by interfering with serine-2 phosphorylation of the RNA polymerase II carboxy-terminal domain', *Genes Dev,* 14(18), pp. 2314-29.

Nusse, Y. M., Savage, A. K., Marangoni, P., Rosendahl-Huber, A. K. M., Landman, T. A., De Sauvage, F. J., Locksley, R. M. and Klein, O. D. (2018) 'Parasitic helminths induce fetal-like reversion in the intestinal stem cell niche', *Nature,* 559(7712), pp. 109-113.

Núñez F, P., Krugliak Cleveland, N., Quera, R. and Rubin, D. T. (2021) 'Evolving role of endoscopy in inflammatory bowel disease: Going beyond diagnosis', *World Journal of Gastroenterology,* 27(20), pp. 2521-2530.

O'Brien, J., Hayder, H., Zayed, Y. and Peng, C. (2018) 'Overview of MicroRNA Biogenesis, Mechanisms of Actions, and Circulation', *Front Endocrinol (Lausanne),* 9, pp. 402.

O'Connell, R. M., Zhao, J. L. and Rao, D. S. (2011) 'MicroRNA function in myeloid biology', *Blood,* 118(11), pp. 2960-2969.

Odze, R. D. (2015) 'A contemporary and critical appraisal of ‘indeterminate colitis’', *Modern Pathology,* 28(1), pp. S30-S46.

Oh-Oka, K., Kojima, Y., Uchida, K., Yoda, K., Ishimaru, K., Nakajima, S., Hemmi, J., Kano, H., Fujii-Kuriyama, Y., Katoh, R., Ito, H. and Nakao, A. (2017) 'Induction of Colonic Regulatory T Cells by Mesalamine by Activating the Aryl Hydrocarbon Receptor', *Cell Mol Gastroenterol Hepatol,* 4(1), pp. 135-151.

Orazi, A., Du, X., Yang, Z., Kashai, M. and Williams, D. A. (1996) 'Interleukin-11 prevents apoptosis and accelerates recovery of small intestinal mucosa in mice treated with combined chemotherapy and radiation', *Lab Invest,* 75(1), pp. 33-42.

Ouimet, M., Ediriweera, H. N., Gundra, U. M., Sheedy, F. J., Ramkhelawon, B., Hutchison, S. B., Rinehold, K., van Solingen, C., Fullerton, M. D., Cecchini, K., Rayner, K. J., Steinberg, G. R., Zamore, P. D., Fisher, E. A., Loke, P. and Moore, K. J. (2015) 'MicroRNA-33-dependent regulation of macrophage metabolism directs immune cell polarization in atherosclerosis', *J Clin Invest,* 125(12), pp. 4334-48.

Ozel, I., Sha, G., Będzińska, A., Pylaeva, E., Naumova, Y., Thiel, I., Antczak, J., Squire, A., Gunzer, M., Zelinskyy, G., Kürten, C., Lang, S., Silvestre-Roig, C., Kortylewski, M., Granot, Z. and Jablonska, J. (2025) 'Neutrophil-specific targeting of STAT3 impairs tumor progression via the expansion of cytotoxic CD8+ T cells', *Signal Transduction and Targeted Therapy,* 10(1), pp. 279.

O'Carroll, D., Mecklenbrauker, I., Das, P. P., Santana, A., Koenig, U., Enright, A. J., Miska, E. A. and Tarakhovsky, A. (2007) 'A Slicer-independent role for Argonaute 2 in hematopoiesis and the microRNA pathway', *Genes & Development,* 21(16), pp. 1999-2004.

Palnaes Hansen, C., Hegnhøj, J., Møller, A., Brauer, C., Hage, E. and Jarnum, S. (1990) 'Ulcerative colitis and Crohn's disease of the colon. Is there a macroscopic difference?', *Ann Chir Gynaecol,* 79(2), pp. 78-81.

Parian, A. M., Obi, M., Fleshner, P. and Schwartz, D. A. (2023) 'Management of Perianal Crohn's Disease', *Official journal of the American College of Gastroenterology | ACG,* 118(8).

Parigi, T. L., Solitano, V., Armuzzi, A., Barreiro de Acosta, M., Begun, J., Ben-Horin, S., Biedermann, L., Colombel, J.-F., Dignass, A., Fumery, M., Ghosh, S., Kobayashi, T., Louis, E., Magro, F., Panaccione, R., Rausch, A., Reinisch, W., Selinger, C., Jairath, V., ... and Peyrin-Biroulet, L. (2024) 'Defining mucosal healing in randomized controlled trials of inflammatory bowel disease: A systematic review and future perspective', *United European Gastroenterology Journal,* 12(9), pp. 1266-1279.

Park, M. D., Silvin, A., Ginhoux, F. and Merad, M. (2022) 'Macrophages in health and disease', *Cell,* 185(23), pp. 4259-4279.

Pemmaraju, N., Bose, P., Rampal, R., Gerds, A. T., Fleischman, A. and Verstovsek, S. (2023) 'Ten years after ruxolitinib approval for myelofibrosis: a review of clinical efficacy', *Leuk Lymphoma,* 64(6), pp. 1063-1081.

Pham, T. N. D., Spaulding, C., Shields, M. A., Metropulos, A. E., Shah, D. N., Khalafalla, M. G., Principe, D. R., Bentrem, D. J. and Munshi, H. G. (2022) 'Inhibition of MNKs promotes macrophage immunosuppressive phenotype to limit CD8+ T cell antitumor immunity', *JCI Insight,* 7(9).

Pickert, G., Neufert, C., Leppkes, M., Zheng, Y., Wittkopf, N., Warntjen, M., Lehr, H.-A., Hirth, S., Weigmann, B., Wirtz, S., Ouyang, W., Neurath, M. F. and Becker, C. (2009) 'STAT3 links IL-22 signaling in intestinal epithelial cells to mucosal wound healing', *Journal of Experimental Medicine,* 206(7), pp. 1465-1472.

Platt, A. M., Bain, C. C., Bordon, Y., Sester, D. P. and Mowat, A. M. (2010) 'An Independent Subset of TLR Expressing CCR2-Dependent Macrophages Promotes Colonic Inflammation', *The Journal of Immunology,* 184(12), pp. 6843-6854.

Poggioli, G., Laureti, S., Campieri, M., Pierangeli, F., Gionchetti, P., Ugolini, F., Gentilini, L., Bazzi, P., Rizzello, F. and Coscia, M. (2007) 'Infliximab in the treatment of Crohn's disease', *Ther Clin Risk Manag,* 3(2), pp. 301-8.

Powell, A. E., Wang, Y., Li, Y., Poulin, E. J., Means, A. L., Washington, M. K., Higginbotham, J. N., Juchheim, A., Prasad, N., Levy, S. E., Guo, Y., Shyr, Y., Aronow, B. J., Haigis, K. M., Franklin, J. L. and Coffey, R. J. (2012) 'The pan-ErbB negative regulator Lrig1 is an intestinal stem cell marker that functions as a tumor suppressor', *Cell,* 149(1), pp. 146-58.

Pull, S. L., Doherty, J. M., Mills, J. C., Gordon, J. I. and Stappenbeck, T. S. (2005) 'Activated macrophages are an adaptive element of the colonic epithelial progenitor niche necessary for regenerative responses to injury', *Proc Natl Acad Sci U S A,* 102(1), pp. 99-104.

Qiu, W., Wu, B., Wang, X., Buchanan, M. E., Regueiro, M. D., Hartman, D. J., Schoen, R. E., Yu, J. and Zhang, L. (2011) 'PUMA-mediated intestinal epithelial apoptosis contributes to ulcerative colitis in humans and mice', *J Clin Invest,* 121(5), pp. 1722-32.

Rani, R., Smulian, A. G., Greaves, D. R., Hogan, S. P. and Herbert, D. R. (2011) 'TGF-β limits IL-33 production and promotes the resolution of colitis through regulation of macrophage function', *Eur J Immunol,* 41(7), pp. 2000-9.

Reed, J., Walczak, W. J., Petzold, O. N. and Gimzewski, J. K. (2009) 'In situ mechanical interferometry of matrigel films', *Langmuir,* 25(1), pp. 36-9.

Remke, M., Groll, T., Metzler, T., Urbauer, E., Kövilein, J., Schnalzger, T., Ruland, J., Haller, D. and Steiger, K. (2024) 'Histomorphological scoring of murine colitis models: A practical guide for the evaluation of colitis and colitis-associated cancer', *Experimental and Molecular Pathology,* 140, pp. 104938.

Richards, C. D. and Botelho, F. (2019) 'Oncostatin M in the Regulation of Connective Tissue Cells and Macrophages in Pulmonary Disease', *Biomedicines,* 7(4).

Rieder, F., Karrasch, T., Ben-Horin, S., Schirbel, A., Ehehalt, R., Wehkamp, J., de Haar, C., Velin, D., Latella, G., Scaldaferri, F., Rogler, G., Higgins, P. and Sans, M. (2012) 'Results of the 2nd scientific workshop of the ECCO (III): basic mechanisms of intestinal healing', *J Crohns Colitis,* 6(3), pp. 373-85.

Robichaud, N., del Rincon, S. V., Huor, B., Alain, T., Petruccelli, L. A., Hearnden, J., Goncalves, C., Grotegut, S., Spruck, C. H., Furic, L., Larsson, O., Muller, W. J., Miller, W. H. and Sonenberg, N. (2015) 'Phosphorylation of eIF4E promotes EMT and metastasis via translational control of SNAIL and MMP-3', *Oncogene,* 34(16), pp. 2032-42.

Robichaud, N., Hsu, B. E., Istomine, R., Alvarez, F., Blagih, J., Ma, E. H., Morales, S. V., Dai, D. L., Li, G., Souleimanova, M., Guo, Q., del Rincon, S. V., Miller, W. H., Ramón y Cajal, S., Park, M., Jones, R. G., Piccirillo, C. A., Siegel, P. M. and Sonenberg, N. (2018) 'Translational control in the tumor microenvironment promotes lung metastasis: Phosphorylation of eIF4E in neutrophils', *Proceedings of the National Academy of Sciences,* 115(10), pp. E2202-E2209.

Robinson, P., Italia, Z., Italia, Z., Hoang, T., Rodriguez, E., Eckols, T. K., Kasembeli, M., Zorrilla, L. H., Soto, L. M., Mahalingam, R. and Tweardy, D. J. (2025) 'STAT3 Inhibition to Treat Ulcerative Colitis-Associated Colorectal Cancer', *International Journal of Molecular Sciences*, 26(21), pp. 10808. DOI: 10.3390/ijms262110808.

Robinson, P., Montoya, K., Magness, E., Rodriguez, E., Villalobos, V., Engineer, N., Yang, P., Bharadwaj, U., Eckols, T. K. and Tweardy, D. J. (2023) 'Therapeutic Potential of a Small-Molecule STAT3 Inhibitor in a Mouse Model of Colitis', *Cancers*, 15(11), pp. 2977. DOI: 10.3390/cancers15112977.

Roda, G., Jharap, B., Neeraj, N. and Colombel, J. F. (2016) 'Loss of Response to Anti-TNFs: Definition, Epidemiology, and Management', *Clin Transl Gastroenterol,* 7(1), pp. e135.

Rodriguez-Bores, L., Fonseca, G. C., Villeda, M. A. and Yamamoto-Furusho, J. K. (2007) 'Novel genetic markers in inflammatory bowel disease', *World J Gastroenterol,* 13(42), pp. 5560-70.

Rogoz, A., Reis, B. S., Karssemeijer, R. A. and Mucida, D. (2015) 'A 3-D enteroid-based model to study T-cell and epithelial cell interaction', *J Immunol Methods,* 421, pp. 89-95.

Rousseaux, C., Lefebvre, B., Dubuquoy, L., Lefebvre, P., Romano, O., Auwerx, J., Metzger, D., Wahli, W., Desvergne, B., Naccari, G. C., Chavatte, P., Farce, A., Bulois, P., Cortot, A., Colombel, J. F. and Desreumaux, P. (2005) 'Intestinal antiinflammatory effect of 5-aminosalicylic acid is dependent on peroxisome proliferator-activated receptor-gamma', *J Exp Med,* 201(8), pp. 1205-15.

Rudick, R. A. and Sandrock, A. (2004) 'Natalizumab: alpha 4-integrin antagonist selective adhesion molecule inhibitors for MS', *Expert Rev Neurother,* 4(4), pp. 571-80.

Rupaimoole, R. and Slack, F. J. (2017) 'MicroRNA therapeutics: towards a new era for the management of cancer and other diseases', *Nat Rev Drug Discov,* 16(3), pp. 203-222.

Saez, A., Herrero-Fernandez, B., Gomez-Bris, R., Sánchez-Martinez, H. and Gonzalez-Granado, J. M. (2023) 'Pathophysiology of Inflammatory Bowel Disease: Innate Immune System', *Int J Mol Sci,* 24(2).

Saha, S., Aranda, E., Hayakawa, Y., Bhanja, P., Atay, S., Brodin, N. P., Li, J., Asfaha, S., Liu, L., Tailor, Y., Zhang, J., Godwin, A. K., Tome, W. A., Wang, T. C., Guha, C. and Pollard, J. W. (2016) 'Macrophage-derived extracellular vesicle-packaged WNTs rescue intestinal stem cells and enhance survival after radiation injury', *Nature Communications,* 7(1), pp. 13096.

Sairenji, T., Collins, K. L. and Evans, D. V. (2017) 'An Update on Inflammatory Bowel Disease', *Primary Care: Clinics in Office Practice,* 44(4), pp. 673-692.

Sajjadi-Dokht, M., Merza Mohamad, T. A., Sulaiman Rahman, H., Suliman Maashi, M., Danshina, S., Shomali, N., Solali, S., Marofi, F., Zeinalzadeh, E., Akbari, M., Adili, A., Aslaminabad, R., Farshdousti Hagh, M. and Jarahian, M. (2022) 'MicroRNAs and JAK/STAT3 signaling: A new promising therapeutic axis in blood cancers', *Genes Dis,* 9(4), pp. 849-867.

Salas, A., Hernandez-Rocha, C., Duijvestein, M., Faubion, W., McGovern, D., Vermeire, S., Vetrano, S. and Vande Casteele, N. (2020) 'JAK–STAT pathway targeting for the treatment of inflammatory bowel disease', *Nature Reviews Gastroenterology & Hepatology,* 17(6), pp. 323-337.

Samad, M. A., Ahmad, I., Hasan, A., Alhashmi, M. H., Ayub, A., Al-Abbasi, F. A., Kumer, A. and Tabrez, S. (2025) 'STAT3 Signaling Pathway in Health and Disease', *MedComm,* 6(4).

Sandborn, W. J., Colombel, J. F., Enns, R., Feagan, B. G., Hanauer, S. B., Lawrance, I. C., Panaccione, R., Sanders, M., Schreiber, S., Targan, S., van Deventer, S., Goldblum, R., Despain, D., Hogge, G. S. and Rutgeerts, P. (2005) 'Natalizumab induction and maintenance therapy for Crohn's disease', *N Engl J Med,* 353(18), pp. 1912-25.

Sandborn, W. J., Nguyen, D. D., Beattie, D. T., Brassil, P., Krey, W., Woo, J., Situ, E., Sana, R., Sandvik, E., Pulido-Rios, M. T., Bhandari, R., Leighton, J. A., Ganeshappa, R., Boyle, D. L., Abhyankar, B., Kleinschek, M. A., Graham, R. A. and Panes, J. (2020) 'Development of Gut-Selective Pan-Janus Kinase Inhibitor

TD-1473 for Ulcerative Colitis: A Translational Medicine Programme', *Journal of Crohn's and Colitis,* 14(9), pp. 1202-1213.

Sandborn, W. J., Panés, J., D'Haens, G. R., Sands, B. E., Su, C., Moscariello, M., Jones, T., Pedersen, R., Friedman, G. S., Lawendy, N. and Chan, G. (2019) 'Safety of Tofacitinib for Treatment of Ulcerative Colitis, Based on 4.4 Years of Data From Global Clinical Trials', *Clin Gastroenterol Hepatol,* 17(8), pp. 1541-1550.

Sandborn, W. J., Su, C., Sands, B. E., D'Haens, G. R., Vermeire, S., Schreiber, S., Danese, S., Feagan, B. G., Reinisch, W., Niezychowski, W., Friedman, G., Lawendy, N., Yu, D., Woodworth, D., Mukherjee, A., Zhang, H., Healey, P. and Panés, J. (2017) 'Tofacitinib as Induction and Maintenance Therapy for Ulcerative Colitis', *N Engl J Med,* 376(18), pp. 1723-1736.

Sands, B. E., Anderson, F. H., Bernstein, C. N., Chey, W. Y., Feagan, B. G., Fedorak, R. N., Kamm, M. A., Korzenik, J. R., Lashner, B. A., Onken, J. E., Rachmilewitz, D., Rutgeerts, P., Wild, G., Wolf, D. C., Marsters, P. A., Travers, S. B., Blank, M. A. and van Deventer, S. J. (2004) 'Infliximab maintenance therapy for fistulizing Crohn's disease', *N Engl J Med,* 350(9), pp. 876-85.

Santos, A. J. M., Lo, Y.-H., Mah, A. T. and Kuo, C. J. (2018) 'The Intestinal Stem Cell Niche: Homeostasis and Adaptations', *Trends in Cell Biology,* 28(12), pp. 1062-1078.

Schmitt, M., Schewe, M., Sacchetti, A., Feijtel, D., van de Geer, W. S., Teeuwssen, M., Sleddens, H. F., Joosten, R., van Royen, M. E., van de Werken, H. J. G., van Es, J., Clevers, H. and Fodde, R. (2018) 'Paneth Cells Respond to Inflammation and Contribute to Tissue Regeneration by Acquiring Stem-like Features through SCF/c-Kit Signaling', *Cell Rep,* 24(9), pp. 2312-2328.e7.

Schott, J., Reitter, S., Philipp, J., Haneke, K., Schäfer, H. and Stoecklin, G. (2014) 'Translational Regulation of Specific mRNAs Controls Feedback Inhibition and Survival during Macrophage Activation', *PLOS Genetics,* 10(6), pp. e1004368.

Sehgal, A., Donaldson, D. S., Pridans, C., Sauter, K. A., Hume, D. A. and Mabbott, N. A. (2018) 'The role of CSF1R-dependent macrophages in control of the intestinal stem-cell niche', *Nature Communications,* 9(1).

Selinger, C. P., Rosiou, K. and Lenti, M. V. (2024) 'Biological therapy for inflammatory bowel disease: cyclical rather than lifelong treatment?', *BMJ Open Gastroenterology,* 11(1), pp. e001225.

Sender, R., Weiss, Y., Navon, Y., Milo, I., Azulay, N., Keren, L., Fuchs, S., Ben-Zvi, D., Noor, E. and Milo, R. (2023) 'The total mass, number, and distribution of immune cells in the human body', *Proceedings of the National Academy of Sciences,* 120(44).

Seto, A. G., Beatty, X., Lynch, J. M., Hermreck, M., Tetzlaff, M., Duvic, M. and Jackson, A. L. (2018) 'Cobomarsen, an oligonucleotide inhibitor of miR-155, co-ordinately regulates multiple survival pathways to reduce cellular proliferation and survival in cutaneous T-cell lymphoma', *British Journal of Haematology,* 183(3), pp. 428-444.

Shahini, A. (2023) 'Role of interleukin-6-mediated inflammation in the pathogenesis of inflammatory bowel disease: focus on the available therapeutic approaches and gut microbiome', *J Cell Commun Signal,* 17(1), pp. 55-74.

Shang, R., Lee, S., Senavirathne, G. and Lai, E. C. (2023) 'microRNAs in action: biogenesis, function and regulation', *Nature Reviews Genetics,* 24(12), pp. 816-833.

Sharma, B., Agriantonis, G., Twelker, K., Ebelle, D., Kiernan, S., Siddiqui, M., Soni, A., Cheerasarn, S., Simon, W., Jiang, W., Cardona, A., Chapelet, J., Agathis, A. Z., Gamboa, A., Dave, J., Mestre, J., Bhatia, N. D., Shaefee, Z. and Whittington, J. (2025) 'Gut Microbiota Serves as a Crucial Independent Biomarker in Inflammatory Bowel Disease (IBD)', *Int J Mol Sci,* 26(6).

Sheedy, F. J., Palsson-McDermott, E., Hennessy, E. J., Martin, C., O'Leary, J. J., Ruan, Q., Johnson, D. S., Chen, Y. and O'Neill, L. A. J. (2010) 'Negative regulation of TLR4 via targeting of the proinflammatory tumor suppressor PDCD4 by the microRNA miR-21', *Nature Immunology,* 11(2), pp. 141-147.

Shen, B., Abreu, M. T., Cohen, E. R., Farraye, F. A., Fischer, M., Feuerstadt, P., Kapur, S., Ko, H. M., Kochhar, G. S., Liu, X., Mahadevan, U., McBride, D. L., Navaneethan, U., Regueiro, M., Ritter, T., Sharma, P. and Lichtenstein, G. R. (2025) 'Endoscopic diagnosis and management of adult inflammatory bowel

disease: a consensus document from the American Society for Gastrointestinal Endoscopy IBD Endoscopy Consensus Panel', *Gastrointestinal Endoscopy,* 101(2), pp. 295-314.

Silva, F. A., Rodrigues, B. L., Ayrizono, M. L. and Leal, R. F. (2016) 'The Immunological Basis of Inflammatory Bowel Disease', *Gastroenterol Res Pract,* 2016, pp. 2097274.

Siminovitch, K. A. (2006) 'Advances in the molecular dissection of inflammatory bowel disease', *Semin Immunol,* 18(4), pp. 244-53.

Simpson, P. and Papadakis, K. A. (2008) 'Endoscopic evaluation of patients with inflammatory bowel disease', *Inflammatory Bowel Diseases,* 14(9), pp. 1287-1297.

Soler, D., Chapman, T., Yang, L. L., Wyant, T., Egan, R. and Fedyk, E. R. (2009) 'The binding specificity and selective antagonism of vedolizumab, an anti-alpha4beta7 integrin therapeutic antibody in development for inflammatory bowel diseases', *J Pharmacol Exp Ther,* 330(3), pp. 864-75.

Sommer, K., Wiendl, M., Müller, T. M., Heidbreder, K., Voskens, C., Neurath, M. F. and Zundler, S. (2021) 'Intestinal Mucosal Wound Healing and Barrier Integrity in IBD–Crosstalk and Trafficking of Cellular Players', *Frontiers in Medicine,* 8.

Sonenberg, N. and Hinnebusch, A. G. (2009) 'Regulation of translation initiation in eukaryotes: mechanisms and biological targets', *Cell,* 136(4), pp. 731-45.

Sorrentino, D., Nguyen, V. Q. and Chitnavis, M. V. (2019) 'Capturing the Biologic Onset of Inflammatory Bowel Diseases: Impact on Translational and Clinical Science', *Cells*, 8(6), pp. 548. DOI: 10.3390/cells8060548.

Spurlock, C. F., 3rd, Aune, Z. T., Tossberg, J. T., Collins, P. L., Aune, J. P., Huston, J. W., 3rd, Crooke, P. S., Olsen, N. J. and Aune, T. M. (2011) 'Increased sensitivity to apoptosis induced by methotrexate is mediated by JNK', *Arthritis Rheum,* 63(9), pp. 2606-16.

Stein, M., Keshav, S., Harris, N. and Gordon, S. (1992) 'Interleukin 4 potently enhances murine macrophage mannose receptor activity: a marker of alternative

immunologic macrophage activation', *Journal of Experimental Medicine,* 176(1), pp. 287-292.

Stewart, C. J., Ajami, N. J., O'Brien, J. L., Hutchinson, D. S., Smith, D. P., Wong, M. C., Ross, M. C., Lloyd, R. E., Doddapaneni, H., Metcalf, G. A., Muzny, D., Gibbs, R. A., Vatanen, T., Huttenhower, C., Xavier, R. J., Rewers, M., Hagopian, W., Toppari, J., Ziegler, A.-G., ... and Petrosino, J. F. (2018) 'Temporal development of the gut microbiome in early childhood from the TEDDY study', *Nature,* 562(7728), pp. 583-588.

Stuhlmann-Laeisz, C., Lang, S., Chalaris, A., Krzysztof, P., Enge, S., Eichler, J., Klingmüller, U., Samuel, M., Ernst, M., Rose-John, S. and Scheller, J. (2006) 'Forced dimerization of gp130 leads to constitutive STAT3 activation, cytokine-independent growth, and blockade of differentiation of embryonic stem cells', *Mol Biol Cell,* 17(7), pp. 2986-95.

Su, S., Zhao, Q., He, C., Huang, D., Liu, J., Chen, F., Chen, J., Liao, J.-Y., Cui, X., Zeng, Y., Yao, H., Su, F., Liu, Q., Jiang, S. and Song, E. (2015a) 'miR-142-5p and miR-130a-3p are regulated by IL-4 and IL-13 and control profibrogenic macrophage program', *Nature Communications,* 6(1), pp. 8523.

Su, X., Yu, Y., Zhong, Y., Giannopoulou, E. G., Hu, X., Liu, H., Cross, J. R., Rätsch, G., Rice, C. M. and Ivashkiv, L. B. (2015b) 'Interferon-γ regulates cellular metabolism and mRNA translation to potentiate macrophage activation', *Nat Immunol,* 16(8), pp. 838-849.

Sultan, S., El-Mowafy, M., Elgaml, A., Ahmed, T. A. E., Hassan, H. and Mottawea, W. (2021) 'Metabolic Influences of Gut Microbiota Dysbiosis on Inflammatory Bowel Disease', *Front Physiol,* 12, pp. 715506.

Sökmen, O., Göçmen, R. and Tuncer, A. (2022) 'Multiple Sclerosis - Like Demyelinating Lesions During Adalimumab Treatment in a Case with Crohn's Disease', *Noro Psikiyatr Ars,* 59(4), pp. 342-344.

Takeda, N., Jain, R., LeBoeuf, M. R., Wang, Q., Lu, M. M. and Epstein, J. A. (2011) 'Interconversion between intestinal stem cell populations in distinct niches', *Science,* 334(6061), pp. 1420-4.

Talebi, S., Zeraattalab-Motlagh, S., Rahimlou, M., Naeini, F., Ranjbar, M., Talebi, A. and Mohammadi, H. (2023) 'The Association between Total Protein, Animal Protein, and Animal Protein Sources with Risk of Inflammatory Bowel Diseases: A Systematic Review and Meta-Analysis of Cohort Studies', *Adv Nutr,* 14(4), pp. 752-761.

Tamoutounour, S., Henri, S., Lelouard, H., De Bovis, B., De Haar, C., Van Der Woude, C. J., Woltman, A. M., Reyal, Y., Bonnet, D., Sichien, D., Bain, C. C., Mowat, A. M., Reis E Sousa, C., Poulin, L. F., Malissen, B. and Guilliams, M. (2012) 'CD64 distinguishes macrophages from dendritic cells in the gut and reveals the Th1-inducing role of mesenteric lymph node macrophages during colitis', *European Journal of Immunology,* 42(12), pp. 3150-3166.

Tebbutt, N. C., Giraud, A. S., Inglese, M., Jenkins, B., Waring, P., Clay, F. J., Malki, S., Alderman, B. M., Grail, D., Hollande, F., Heath, J. K. and Ernst, M. (2002) 'Reciprocal regulation of gastrointestinal homeostasis by SHP2 and STAT-mediated trefoil gene activation in gp130 mutant mice', *Nat Med,* 8(10), pp. 1089-97.

Tessner, T. G., Muhale, F., Riehl, T. E., Anant, S. and Stenson, W. F. (2004) 'Prostaglandin E2 reduces radiation-induced epithelial apoptosis through a mechanism involving AKT activation and bax translocation', *Journal of Clinical Investigation,* 114(11), pp. 1676-1685.

Tetteh, P. W., Basak, O., Farin, H. F., Wiebrands, K., Kretzschmar, K., Begthel, H., van den Born, M., Korving, J., de Sauvage, F., van Es, J. H., van Oudenaarden, A. and Clevers, H. (2016) 'Replacement of Lost Lgr5-Positive Stem Cells through Plasticity of Their Enterocyte-Lineage Daughters', *Cell Stem Cell,* 18(2), pp. 203-13.

Tian, C.-M., Yang, M.-F., Xu, H.-M., Zhu, M.-Z., Yue, N.-N., Zhang, Y., Shi, R.-Y., Yao, J., Wang, L.-S., Liang, Y.-J. and Li, D.-F. (2023) 'Stem cell-derived intestinal organoids: a novel modality for IBD', *Cell Death Discovery,* 9(1).

Tian, H., Biehs, B., Warming, S., Leong, K. G., Rangell, L., Klein, O. D. and de Sauvage, F. J. (2011) 'A reserve stem cell population in small intestine renders Lgr5-positive cells dispensable', *Nature,* 478(7368), pp. 255-259.

Tomic, G., Morrissey, E., Kozar, S., Ben-Moshe, S., Hoyle, A., Azzarelli, R., Kemp, R., Chilamakuri, C. S. R., Itzkovitz, S., Philpott, A. and Winton, D. J. (2018) 'Phospho-regulation of ATOH1 Is Required for Plasticity of Secretory Progenitors and Tissue Regeneration', *Cell Stem Cell,* 23(3), pp. 436-443.e7.

Torrence, A. E., Brabb, T., Viney, J. L., Bielefeldt-Ohmann, H., Treuting, P., Seamons, A., Drivdahl, R., Zeng, W. and Maggio-Price, L. (2008) 'Serum biomarkers in a mouse model of bacterial-induced inflammatory bowel disease', *Inflamm Bowel Dis,* 14(4), pp. 480-90.

Torres, J., Mehandru, S., Colombel, J.-F. and Peyrin-Biroulet, L. (2017) 'Crohn's disease', *The Lancet,* 389(10080), pp. 1741-1755.

Trifari, S., Pipkin, M. E., Bandukwala, H. S., Äijö, T., Bassein, J., Chen, R., Martinez, G. J. and Rao, A. (2013) 'MicroRNA-directed program of cytotoxic CD8+ T-cell differentiation', *Proceedings of the National Academy of Sciences,* 110(46), pp. 18608-18613.

Trouplin, V., Boucherit, N., Gorvel, L., Conti, F., Mottola, G. and Ghigo, E. (2013) 'Bone marrow-derived macrophage production', *J Vis Exp,* (81), pp. e50966.

Tsimberidou, A. M., Vining, D. J., Arora, S. P., de Achaval, S., Larson, J., Kauh, J., Cartwright, C., Avritscher, R., Alibhai, I., Tweardy, D. J. and Kaseb, A. O. (2025) 'Phase I Trial of TTI-101, a First-in-Class Oral Inhibitor of STAT3, in Patients with Advanced Solid Tumors', *Clinical Cancer Research,* 31(6), pp. 965-974.

Tüfekci, K. U., Meuwissen, R. L. and Genç, S. (2014) 'The role of microRNAs in biological processes', *Methods Mol Biol,* 1107, pp. 15-31.

Ueno, A., Jijon, H., Traves, S., Chan, R., Ford, K., Beck, P. L., Iacucci, M., Fort Gasia, M., Barkema, H. W., Panaccione, R., Kaplan, G. G., Proud, D. and Ghosh, S. (2014) 'Opposing effects of smoking in ulcerative colitis and Crohn's disease may be explained by differential effects on dendritic cells', *Inflamm Bowel Dis,* 20(5), pp. 800-10.

Ungaro, R., Mehandru, S., Allen, P. B., Peyrin-Biroulet, L. and Colombel, J.-F. (2017) 'Ulcerative colitis', *The Lancet,* 389(10080), pp. 1756-1770.

Van Assche, G., Van Ranst, M., Sciot, R., Dubois, B., Vermeire, S., Noman, M., Verbeeck, J., Geboes, K., Robberecht, W. and Rutgeerts, P. (2005) 'Progressive multifocal leukoencephalopathy after natalizumab therapy for Crohn's disease', *N Engl J Med,* 353(4), pp. 362-8.

van der Flier, L. G. and Clevers, H. (2009) 'Stem cells, self-renewal, and differentiation in the intestinal epithelium', *Annu Rev Physiol,* 71, pp. 241-60.

van der Flier, L. G., van Gijn, M. E., Hatzis, P., Kujala, P., Haegebarth, A., Stange, D. E., Begthel, H., van den Born, M., Guryev, V., Oving, I., van Es, J. H., Barker, N., Peters, P. J., van de Wetering, M. and Clevers, H. (2009) 'Transcription factor achaete scute-like 2 controls intestinal stem cell fate', *Cell,* 136(5), pp. 903-12.

van Deventer, S. J. (1999) 'Anti-TNF antibody treatment of Crohn's disease', *Ann Rheum Dis,* 58 Suppl 1(Suppl 1), pp. I114-20.

Vavricka, S. R., Brun, L., Ballabeni, P., Pittet, V., Vavricka, B. M. P., Zeitz, J., Rogler, G., Schoepfer, A. M. and and the Swiss, I. B. D. C. S. G. (2011) 'Frequency and Risk Factors for Extraintestinal Manifestations in the Swiss Inflammatory Bowel Disease Cohort', *Official journal of the American College of Gastroenterology | ACG,* 106(1).

Veauthier, B. and Hornecker, J. R. (2018) 'Crohn's Disease: Diagnosis and Management', *Am Fam Physician,* 98(11), pp. 661-669.

Verstockt, S., Verstockt, B. and Vermeire, S. (2019) 'Oncostatin M as a new diagnostic, prognostic and therapeutic target in inflammatory bowel disease (IBD)', *Expert Opinion on Therapeutic Targets,* 23(11), pp. 943-954.

Vidal-Lletjós, S., Andriamihaja, M., Blais, A., Grauso, M., Lepage, P., Davila, A. M., Gaudichon, C., Leclerc, M., Blachier, F. and Lan, A. (2019) 'Mucosal healing progression after acute colitis in mice', *World J Gastroenterol,* 25(27), pp. 3572-3589.

Villablanca, E. J., Selin, K. and Hedin, C. R. H. (2022) 'Mechanisms of mucosal healing: treating inflammatory bowel disease without immunosuppression?', *Nature Reviews Gastroenterology & Hepatology,* 19(8), pp. 493-507.

Viola, M. F. and Boeckxstaens, G. (2021) 'Niche-specific functional heterogeneity of intestinal resident macrophages', *Gut,* 70(7), pp. 1383-1395.

Viragova, S., Li, D. and Klein, O. D. (2024) 'Activation of fetal-like molecular programs during regeneration in the intestine and beyond', *Cell Stem Cell,* 31(7), pp. 949-960.

Vitale, I., Shema, E., Loi, S. and Galluzzi, L. (2021) 'Intratumoral heterogeneity in cancer progression and response to immunotherapy', *Nature Medicine,* 27(2), pp. 212-224.

Voetmann, L. M., Rolin, B., Kirk, R. K., Pyke, C. and Hansen, A. K. (2023) 'The intestinal permeability marker FITC-dextran 4kDa should be dosed according to lean body mass in obese mice', *Nutrition & Diabetes,* 13(1).

Vos, A. C., Wildenberg, M. E., Arijs, I., Duijvestein, M., Verhaar, A. P., de Hertogh, G., Vermeire, S., Rutgeerts, P., van den Brink, G. R. and Hommes, D. W. (2012) 'Regulatory macrophages induced by infliximab are involved in healing in vivo and in vitro', *Inflamm Bowel Dis,* 18(3), pp. 401-8.

Vos, A. C. W., Wildenberg, M. E., Duijvestein, M., Verhaar, A. P., Van Den Brink, G. R. and Hommes, D. W. (2011) 'Anti–Tumor Necrosis Factor-α Antibodies Induce Regulatory Macrophages in an Fc Region-Dependent Manner', *Gastroenterology,* 140(1), pp. 221-230.e3.

Vos, T., Lim, S. S., Abbafati, C., Abbas, K. M., Abbasi, M., Abbasifard, M., Abbasi-Kangevari, M., Abbastabar, H., Abd-Allah, F., Abdelalim, A., Abdollahi, M., Abdollahpour, I., Abolhassani, H., Aboyans, V., Abrams, E. M., Abreu, L. G., Abrigo, M. R. M., Abu-Raddad, L. J., Abushouk, A. I., ... and Murray, C. J. L. (2020) 'Global burden of 369 diseases and injuries in 204 countries and territories, 1990–2019: a systematic analysis for the Global Burden of Disease Study 2019', *The Lancet,* 396(10258), pp. 1204-1222.

Vulliemoz, M., Brand, S., Juillerat, P., Mottet, C., Ben-Horin, S. and Michetti, P. (2020) 'TNF-Alpha Blockers in Inflammatory Bowel Diseases: Practical Recommendations and a User's Guide: An Update', *Digestion,* 101 Suppl 1, pp. 16-26.

Wang, H., Ning, X., Zhao, F., Zhao, H. and Li, D. (2024) 'Human organoids-on-chips for biomedical research and applications', *Theranostics,* 14(2), pp. 788-818.

Wang, H., Wang, J., Zhao, Y., Zhang, X., Liu, J., Zhang, C., Haffty, B., Verzi, M., Zhang, L., Gao, N., Feng, Z. and Hu, W. (2020) 'LIF is essential for ISC function and protects against radiation-induced gastrointestinal syndrome', *Cell Death & Disease,* 11(7), pp. 588.

Wang, H., Zhang, S., Yu, Q., Yang, G., Guo, J., Li, M., Zeng, Z., He, Y., Chen, B. and Chen, M. (2016) 'Circulating MicroRNA223 is a New Biomarker for Inflammatory Bowel Disease', *Medicine (Baltimore),* 95(5), pp. e2703.

Wang, J., Chang, C.-Y., Yang, X., Zhou, F., Liu, J., Feng, Z. and Hu, W. (2023) 'Leukemia inhibitory factor, a double-edged sword with therapeutic implications in human diseases', *Molecular Therapy,* 31(2), pp. 331-343.

Wang, L., Llorente, C., Hartmann, P., Yang, A. M., Chen, P. and Schnabl, B. (2015) 'Methods to determine intestinal permeability and bacterial translocation during liver disease', *J Immunol Methods,* 421, pp. 44-53.

Wang, N., Zheng, J., Chen, Z., Liu, Y., Dura, B., Kwak, M., Xavier-Ferrucio, J., Lu, Y.-C., Zhang, M., Roden, C., Cheng, J., Krause, D. S., Ding, Y., Fan, R. and Lu, J. (2019) 'Single-cell microRNA-mRNA co-sequencing reveals non-genetic heterogeneity and mechanisms of microRNA regulation', *Nature Communications,* 10(1), pp. 95.

Wang, Q., Yuan, F., Zuo, X. and Li, M. (2025) 'Breakthroughs and challenges of organoid models for assessing cancer immunotherapy: a cutting-edge tool for advancing personalised treatments', *Cell Death Discovery,* 11(1).

Weischenfeldt, J. and Porse, B. (2008) 'Bone Marrow-Derived Macrophages (BMM): Isolation and Applications', *CSH Protoc,* 2008, pp. pdb.prot5080.

West, N. R., Owens, B. M. J. and Hegazy, A. N. (2018) 'The oncostatin M-stromal cell axis in health and disease', *Scand J Immunol,* 88(3), pp. e12694.

Westphalen, C. B., Asfaha, S., Hayakawa, Y., Takemoto, Y., Lukin, D. J., Nuber, A. H., Brandtner, A., Setlik, W., Remotti, H., Muley, A., Chen, X., May, R., Houchen, C. W., Fox, J. G., Gershon, M. D., Quante, M. and Wang, T. C. (2014)

'Long-lived intestinal tuft cells serve as colon cancer-initiating cells', *J Clin Invest,* 124(3), pp. 1283-95.

'What will it take to get miRNA therapies to market?', (2024) *Nature Biotechnology,* 42(11), pp. 1623-1624.

Wightman, B., Ha, I. and Ruvkun, G. (1993) 'Posttranscriptional regulation of the heterochronic gene lin-14 by lin-4 mediates temporal pattern formation in C. elegans', *Cell,* 75(5), pp. 855-62.

William, M., Leroux, L. P., Chaparro, V., Graber, T. E., Alain, T. and Jaramillo, M. (2019) 'Translational repression of Ccl5 and Cxcl10 by 4E-BP1 and 4E-BP2 restrains the ability of mouse macrophages to induce migration of activated T cells', *Eur J Immunol,* 49(8), pp. 1200-1212.

Wittkopf, N., Pickert, G., Billmeier, U., Mahapatro, M., Wirtz, S., Martini, E., Leppkes, M., Neurath, M. F. and Becker, C. (2015) 'Activation of Intestinal Epithelial Stat3 Orchestrates Tissue Defense during Gastrointestinal Infection', *PLOS ONE,* 10(3), pp. e0118401.

Woting, A. and Blaut, M. (2018) 'Small Intestinal Permeability and Gut-Transit Time Determined with Low and High Molecular Weight Fluorescein Isothiocyanate-Dextrans in C3H Mice', *Nutrients,* 10(6).

Wright, P. B., Mcdonald, E., Bravo-Blas, A., Baer, H. M., Heawood, A., Bain, C. C., Mowat, A. M., Clay, S. L., Robertson, E. V., Morton, F., Nijjar, J. S., Ijaz, U. Z., Milling, S. W. F. and Gaya, D. R. (2021) 'The mannose receptor (CD206) identifies a population of colonic macrophages in health and inflammatory bowel disease', *Scientific Reports,* 11(1).

Wu, J., Zhu, Y., Liu, D., Cong, Q. and Bai, C. (2024) 'Biological functions and potential mechanisms of miR-143-3p in cancers (Review)', *Oncol Rep,* 52(3).

Xavier, R. J. and Podolsky, D. K. (2007) 'Unravelling the pathogenesis of inflammatory bowel disease', *Nature,* 448(7152), pp. 427-434.

Xing, Z., Li, X., He, J., Chen, Y., Zhu, L., Zhang, X., Huang, Z., Tang, J., Guo, Y. and He, Y. (2024) 'OLFM4 modulates intestinal inflammation by promoting IL-22+ILC3 in the gut', *Communications Biology,* 7(1).

Xu, H., Zhu, J., Smith, S., Foldi, J., Zhao, B., Chung, A. Y., Outtz, H., Kitajewski, J., Shi, C., Weber, S., Saftig, P., Li, Y., Ozato, K., Blobel, C. P., Ivashkiv, L. B. and Hu, X. (2012) 'Notch-RBP-J signaling regulates the transcription factor IRF8 to promote inflammatory macrophage polarization', *Nat Immunol,* 13(7), pp. 642-50.

Xu, X. R., Liu, C. Q., Feng, B. S. and Liu, Z. J. (2014) 'Dysregulation of mucosal immune response in pathogenesis of inflammatory bowel disease', *World J Gastroenterol,* 20(12), pp. 3255-64.

Xue, M., Leibovitzh, H., Jingcheng, S., Neustaeter, A., Dong, M., Xu, W., Espin-Garcia, O., Griffiths, A. M., Steinhart, A. H., Turner, D., Huynh, H. Q., Dieleman, L. A., Panaccione, R., Aumais, G., Bressler, B., Bitton, A., Murthy, S., Marshall, J. K., Hyams, J. S., ... and Croitoru, K. (2024) 'Environmental Factors Associated With Risk of Crohn's Disease Development in the Crohn's and Colitis Canada - Genetic, Environmental, Microbial Project', *Clin Gastroenterol Hepatol,* 22(9), pp. 1889-1897.e12.

Yan, K. S., Gevaert, O., Zheng, G. X. Y., Anchang, B., Probert, C. S., Larkin, K. A., Davies, P. S., Cheng, Z.-F., Kaddis, J. S., Han, A., Roelf, K., Calderon, R. I., Cynn, E., Hu, X., Mandleywala, K., Wilhelmy, J., Grimes, S. M., Corney, D. C., Boutet, S. C., ... and Kuo, C. J. (2017) 'Intestinal Enteroendocrine Lineage Cells Possess Homeostatic and Injury-Inducible Stem Cell Activity', *Cell stem cell,* 21(1), pp. 78-90.e6.

Yan, Y., Kolachala, V., Dalmasso, G., Nguyen, H., Laroui, H., Sitaraman, S. V. and Merlin, D. (2009) 'Temporal and Spatial Analysis of Clinical and Molecular Parameters in Dextran Sodium Sulfate Induced Colitis', *PLoS ONE,* 4(6), pp. e6073.

Yang, C. and Merlin, D. (2024) 'Unveiling Colitis: A Journey through the Dextran Sodium Sulfate-induced Model', *Inflamm Bowel Dis,* 30(5), pp. 844-853.

Yang, X., Guo, H. and Zou, M. (2026) 'Inflammatory bowel diseases: pathological mechanisms and therapeutic perspectives', *Molecular Biomedicine,* 7(1), pp. 2.

Yang, Y., Ma, Y., Shi, C., Chen, H., Zhang, H., Chen, N., Zhang, P., Wang, F., Yang, J., Zhu, Q., Liang, Y., Wu, W., Gao, R., Yang, Z., Zou, Y. and Qin, H. (2013)

'Overexpression of miR-21 in patients with ulcerative colitis impairs intestinal epithelial barrier function through targeting the Rho GTPase RhoB', *Biochem Biophys Res Commun,* 434(4), pp. 746-52.

Yashima, K., Kurumi, H., Yamaguchi, N. and Isomoto, H. (2025) 'Progressing advanced therapies for inflammatory bowel disease: Current status including dual biologic therapy and discontinuation of biologics', *Expert Review of Gastroenterology & Hepatology,* 19(3), pp. 291-310.

Yeshi, K., Jamtsho, T. and Wangchuk, P. (2024) 'Current Treatments, Emerging Therapeutics, and Natural Remedies for Inflammatory Bowel Disease', *Molecules,* 29(16), pp. 3954.

You, Z., Shen, J., Ahuja, V., Watermeyer, G., Steinwurz, F., Shapina, M., Fiocchi, C. and Ran, Z. (2025) 'Gastroenterologists' attitudes and challenges toward treat-to-target strategies in inflammatory bowel disease: a multinational survey', *Therapeutic Advances in Gastroenterology,* 18, pp. 17562848251383792.

Yuan, X., Berg, N., Lee, J. W., Le, T.-T., Neudecker, V., Jing, N. and Eltzschig, H. (2018) 'MicroRNA miR-223 as regulator of innate immunity', *Journal of Leukocyte Biology,* 104(3), pp. 515-524.

Yui, S., Azzolin, L., Maimets, M., Pedersen, M. T., Fordham, R. P., Hansen, S. L., Larsen, H. L., Guiu, J., Alves, M. R. P., Rundsten, C. F., Johansen, J. V., Li, Y., Madsen, C. D., Nakamura, T., Watanabe, M., Nielsen, O. H., Schweiger, P. J., Piccolo, S. and Jensen, K. B. (2018) 'YAP/TAZ-Dependent Reprogramming of Colonic Epithelium Links ECM Remodeling to Tissue Regeneration', *Cell Stem Cell,* 22(1), pp. 35-49.e7.

Zhan, Y., Guo, J., Yang, W., Goncalves, C., Rzymski, T., Dreas, A., Żyłkiewicz, E., Mikulski, M., Brzózka, K., Golas, A., Kong, Y., Ma, M., Huang, F., Huor, B., Guo, Q., da Silva, S. D., Torres, J., Cai, Y., Topisirovic, I., ... and Del Rincón, S. V. (2017) 'MNK1/2 inhibition limits oncogenicity and metastasis of KIT-mutant melanoma', *J Clin Invest,* 127(11), pp. 4179-4192.

Zhang, C., Ouyang, Y. W., He, H. X., Su, P. Z. and Li, Z. T. (2025) 'The Emerging Role of CCL17 in the Immunologic Regulation of Inflammatory Bowel Disease', *Journal of Gastroenterology and Hepatology,* 40(10), pp. 2425-2434.

Zhang, J., Wang, C., Guo, Z., Da, B., Zhu, W. and Li, Q. (2021a) 'miR-223 improves intestinal inflammation through inhibiting the IL-6/STAT3 signaling pathway in dextran sodium sulfate-induced experimental colitis', *Immun Inflamm Dis,* 9(1), pp. 319-327.

Zhang, M.-W., Shen, Y.-J., Shi, J. and Yu, J.-G. (2021b) 'MiR-223-3p in Cardiovascular Diseases: A Biomarker and Potential Therapeutic Target', *Frontiers in Cardiovascular Medicine,* 7.

Zhang, T., Yu, J., Zhang, Y., Li, L., Chen, Y., Li, D., Liu, F., Zhang, C. Y., Gu, H. and Zen, K. (2014) 'Salmonella enterica serovar enteritidis modulates intestinal epithelial miR-128 levels to decrease macrophage recruitment via macrophage colony-stimulating factor', *J Infect Dis,* 209(12), pp. 2000-11.

Zhang, T., Zhang, R., Liu, W., Qi, Y., Wang, H., Zhang, H., Xiao, Z., Pandol, S. J., Han, Y. P. and Zheng, X. (2024) 'Transcription factor EB modulates the homeostasis of reactive oxygen species in intestinal epithelial cells to alleviate inflammatory bowel disease', *Biochim Biophys Acta Mol Basis Dis,* 1870(5), pp. 167065.

Zhang, X., Liu, C., Li, H. and Guo, L. (2020) 'Effects of miR-21 on proliferation and apoptosis of WT cells via PTEN/Akt pathway', *Exp Ther Med,* 19(3), pp. 2155-2160.

Zhang, Y., Zhang, M., Zhong, M., Suo, Q. and Lv, K. (2013) 'Expression profiles of miRNAs in polarized macrophages', *Int J Mol Med,* 31(4), pp. 797-802.

Zhang, Y. Z. and Li, Y. Y. (2014) 'Inflammatory bowel disease: pathogenesis', *World J Gastroenterol,* 20(1), pp. 91-9.

Zhao, M., Feng, R., Ben-Horin, S., Zhuang, X., Tian, Z., Li, X., Ma, R., Mao, R., Qiu, Y. and Chen, M. (2022) 'Systematic review with meta-analysis: environmental and dietary differences of inflammatory bowel disease in Eastern and Western populations', *Aliment Pharmacol Ther,* 55(3), pp. 266-276.

Zheng, L. and Duan, S. L. (2023) 'Molecular regulation mechanism of intestinal stem cells in mucosal injury and repair in ulcerative colitis', *World J Gastroenterol,* 29(16), pp. 2380-2396.

Zhou, H., Xiao, J., Wu, N., Liu, C., Xu, J., Liu, F. and Wu, L. (2015) 'MicroRNA-223 Regulates the Differentiation and Function of Intestinal Dendritic Cells and Macrophages by Targeting C/EBPbeta', *Cell Rep,* 13(6), pp. 1149-1160.

Zhou, H., Zhang, J., Eyers, F., Xiang, Y., Herbert, C., Tay, H. L., Foster, P. S. and Yang, M. (2016) 'Identification of the microRNA networks contributing to macrophage differentiation and function', *Oncotarget,* 7(20), pp. 28806-28820.

Zhou, Q. M. and Zheng, L. (2023) 'Research progress on the relationship between Paneth cells-susceptibility genes, intestinal microecology and inflammatory bowel disease', *World J Clin Cases,* 11(34), pp. 8111-8125.

Zhuang, G., Meng, C., Guo, X., Cheruku, P. S., Shi, L., Xu, H., Li, H., Wang, G., Evans, A. R., Safe, S., Wu, C. and Zhou, B. (2012) 'A Novel Regulator of Macrophage Activation', *Circulation,* 125(23), pp. 2892-2903.

Zigmond, E., Varol, C., Farache, J., Elmaliah, E., Satpathy, A. T., Friedlander, G., Mack, M., Shpigel, N., Boneca, I. G., Murphy, K. M., Shakhar, G., Halpern, Z. and Jung, S. (2012) 'Ly6C hi monocytes in the inflamed colon give rise to proinflammatory effector cells and migratory antigen-presenting cells', *Immunity,* 37(6), pp. 1076-90.